

Inaugural dissertation  
for  
Obtaining the doctoral degree  
of the  
Combined Faculty of Mathematics, Engineering and Natural  
Sciences  
Of the  
Ruprecht – Karls – University  
Heidelberg

Presented by  
MSc Irene Garcés Lázaro  
Born in: Zaragoza, Spain  
Oral examination: 20th February 2024



# **Restoring NK cells function against cancer**

Referees:

Prof. Dr. med. Alexander Dalpke

Prof. Dr. Adelheid Cerwenka



# 1 Table of Contents

---

<b>2</b>	<b>ZUSAMMENFASSUNG</b> .....	<b>3</b>
<b>3</b>	<b>SUMMARY</b> .....	<b>5</b>
<b>4</b>	<b>INTRODUCTION</b> .....	<b>7</b>
4.1	THE IMMUNE SYSTEM .....	7
4.1.1	<i>Innate immunity</i> .....	8
4.1.2	<i>Adaptive immunity</i> .....	10
4.2	INNATE LYMPHOID CELLS .....	14
4.2.1	<i>ILC1, ILC2 and ILC3</i> .....	14
4.2.2	<i>NK cells</i> .....	15
4.3	TUMOR MICROENVIRONMENT .....	20
4.3.1	<i>Neoangiogenesis</i> .....	21
4.3.2	<i>Tumor microenvironment and immune cells</i> .....	21
4.3.3	<i>Patient-derived organoids: A precision model for investigating the tumor microenvironment in vitro</i> .....	23
4.4	HYPOXIC ENVIRONMENTS: THE IMPACT OF OXYGEN CONCENTRATION ON NK CELLS.....	23
4.4.1	<i>Hypoxia inducible factors</i> .....	24
4.4.2	<i>Immune cells exposed to hypoxia</i> .....	26
4.5	NEW IMMUNOTHERAPIES .....	27
4.5.1	<i>Adoptive cell therapies: Chimeric Antigen Receptor cells</i> .....	27
4.6	NK CELLS ENGAGERS .....	31
<b>5</b>	<b>AIMS OF THE STUDY</b> .....	<b>34</b>
<b>6</b>	<b>MATERIAL AND METHODS</b> .....	<b>35</b>
6.1	CELL CULTURE MEDIA, REAGENTS AND BUFFERS .....	35
6.2	CHEMICALS .....	36
6.3	CELL LINES, PRIMARY CELLS AND BACTERIA STRAIN .....	38
6.4	BUFFERS AND MEDIA.....	39
6.5	KITS .....	40
6.6	ANTIBODIES AND FUSION PROTEINS .....	41
6.7	PLASMID AND OLIGONUCLEOTIDES .....	43
6.8	PLASTIC WARE AND CONSUMABLES.....	44
6.9	LABORATORY EQUIPMENT .....	45
6.10	SOFTWARES .....	46
<b>7</b>	<b>METHODS</b> .....	<b>47</b>
7.1	CELL CULTURE METHODS .....	47
7.1.1	<i>Freezing and thawing cells</i> .....	47
7.1.2	<i>Passaging of cell lines</i> .....	47
7.1.3	<i>Counting of cells with Trypan blue</i> .....	47
7.1.4	<i>Human primary NK cells isolation</i> .....	47
7.1.5	<i>Human primary NK cells culture</i> .....	48
7.1.6	<i>Cytokine-induced memory-like NK cells</i> .....	48
7.1.7	<i>Feeder cells expansion</i> .....	48
7.1.8	<i>Patient derived organoids cell lines culture</i> .....	48
7.1.9	<i>Spheroid generation and culture</i> .....	49

7.2	FUNCTIONAL NK CELL ASSAYS.....	49
7.2.1	<i>Tumor co-cultures and cytokine PMA/Ionomycin stimulation (degranulation assay).....</i>	49
7.2.2	<i>Tumor cell confluency assay.....</i>	49
7.2.3	<i>Organoid coculture with NK cells in IncuCyte.....</i>	50
7.3	FLUORESCENCE-ACTIVATED CELL SORTING (FACS).....	50
7.4	FACS SORTING.....	50
7.5	VIRUS TRANSDUCTION OF NK CELLS.....	51
7.5.1	<i>Lentivirus production.....</i>	51
7.5.2	<i>Lentivirus titration.....</i>	51
7.5.3	<i>Lentiviral transduction of human NK cells.....</i>	51
7.6	TRANSFECTION OF NK CELLS BY ELECTROPORATION.....	52
7.7	TRANSFECTION OF CELL LINES BY ELECTROPORATION.....	53
7.8	REAL TIME METABOLITES MEASUREMENT.....	53
7.9	PLASMIDS PURIFICATION AND SEQUENCING.....	53
7.9.1	<i>Transformation of bacteria.....</i>	53
7.9.2	<i>Colony expansion.....</i>	54
7.9.3	<i>Sequencing.....</i>	54
7.10	SOLUBLE FACTOR MEASUREMENT.....	54
7.11	IMAGING OF NK CELL MIGRATION INTO TUMOR SPHEROIDS.....	54
7.12	STATISTICAL ANALYSIS.....	55
<b>8</b>	<b>RESULTS.....</b>	<b>57</b>
8.1	EFFECT OF HYPOXIA ON NK CELLS <i>IN VITRO</i> IN COMBINATION WITH IMMUNOTHERAPY.....	57
8.1.1	<i>Surface protein expression, IFN<math>\gamma</math> production and degranulation of NK cells exposed to hypoxia.....</i>	57
8.1.2	<i>Decreased proliferation of NK cells exposed to seven days hypoxia.....</i>	60
8.1.3	<i>Decreased metabolism of human NK cells exposed to hypoxia.....</i>	61
8.1.4	<i>HIF-1<math>\alpha</math> genetic disruption in human NK cells unleashes IFN<math>\gamma</math> production under hypoxia.....</i>	63
8.1.5	<i>HIF-1 <math>\alpha</math> targeted NK cells react to patient derived organoids in a patient specific manner.....</i>	65
8.1.6	<i>HER-2-CAR NK cell function is negatively affected by hypoxia.....</i>	71
8.1.7	<i>CRISPR/Cas9-targeted edition of HIF-1<math>\alpha</math> in HER-2 CAR NK cells enhances killing of patient-derived colorectal adenocarcinoma organoids.....</i>	78
8.1.8	<i>Improved infiltration of HER-2-CAR, HIF-1<math>\alpha</math> CRISPR/Cas9-targeted NK cells in HT-29 spheroids.....</i>	82
8.2	CYTOKINE-INDUCED MEMORY-LIKE NK CELL CYTOKINE PRODUCTION AND SURFACE PROTEIN EXPRESSION UNDER HYPOXIA.....	84
8.2.1	<i>Cytokine-induced memory-like NK cells exposed to hypoxia reduce IFN<math>\gamma</math> production upon IL-12/18 stimuli.....</i>	85
8.2.2	<i>CML NK cells alter surface markers after seven days of hypoxia exposure.....</i>	86
8.3	OPTIMIZATION OF CRISPR/CAS9 ELECTROPORATION PROTOCOL FOR GENERATING DOUBLE AND TRIPLE KNOCKOUTS IN HUMAN NK CELLS.....	87
8.3.1	<i>Generation of single KOs in human primary NK cells.....</i>	87
8.3.2	<i>Production of double and triple KOs in human primary NK cells.....</i>	90
8.3.3	<i>Functional evaluation of unsorted KO NK cells shows cell line and ligand dependency.....</i>	91
<b>9</b>	<b>DISCUSSION.....</b>	<b>93</b>
9.1	OPTIMIZING IMMUNOTHERAPIES TARGETING HYPOXIC SOLID TUMORS THROUGH NK CELL MODULATION.....	94
9.1.1	<i>Altered surface expression of human NK cell markers and receptors after seven days hypoxia.....</i>	94
9.1.2	<i>Reduced soluble factor production, proliferation and OXPHOS in NK cells exposed to hypoxia.....</i>	96
9.1.3	<i>HIF-1 alpha targeted NK cells: A promising candidate for alleviating the effects of hypoxia exposure.....</i>	98
9.1.4	<i>HIF-1 <math>\alpha</math> targeted NK Cells exhibit line-dependent efficacy against patient derived organoids.....</i>	100
9.1.5	<i>HER-2 CAR NK cells efficacy is hampered by hypoxia exposure.....</i>	102
9.1.6	<i>Targeting HIF-1 alpha to enhance HER-2 CAR NK cell cytotoxicity against PDO lines.....</i>	104
9.1.7	<i>Enhanced infiltration of HER-2 CAR HIF-1<math>\alpha</math> targeted NK Cells into HT-29 spheroids.....</i>	106

9.1.8	<i>Surface receptors, soluble factor production and proliferation alterations in hypoxia-exposed cytokine-induced memory-like NK Cells.....</i>	<i>107</i>
9.2	ENHANCING CRISPR/CAS9-BASED GENE EDITING IN HUMAN PRIMARY NK CELLS.....	108
9.2.1	<i>CRISPR/Cas9 electroporation has high efficacy for single KOs.....</i>	<i>108</i>
<b>10</b>	<b>CONCLUSIONS .....</b>	<b>111</b>
<b>11</b>	<b>REFERENCES .....</b>	<b>113</b>
<b>12</b>	<b>ABBREVIATIONS .....</b>	<b>142</b>
<b>13</b>	<b>ACKNOWLEDGMENTS.....</b>	<b>144</b>

## 2 ZUSAMMENFASSUNG

---

Umweltbedingungen beeinflussen signifikant das Erscheinungsbild und die Funktionalität von Immunzellen. Insbesondere hypoxische Bedingungen (Sauerstoffkonzentration unter 5 %), die in Geweben und Organen vorherrschen, beeinflussen sowohl das adaptive als auch das angeborene Immunsystem. Der Transkriptionsfaktor Hypoxia-inducible Factor 1-alpha (HIF-1 $\alpha$ ) spielt eine entscheidende Rolle bei der Regulation der Anpassung von Immunzellen an Hypoxie. Natürliche Killerzellen (NK-Zellen) sind bei der Tumorerkennung unerlässlich, da sie Tumorzellen durch die Produktion von Zytokinen, Chemokinen und zytolytischen Granula angreifen. Dennoch verlieren NK-Zellen, die in stark hypoxischen soliden Tumoren eindringen, oft ihre Funktionalität. Menschliche primäre NK-Zellen stellen eine Herausforderung für klassische Transduktions- und Transfektionsmethoden dar, was die Erforschung und Generierung verbesserter NK-Zellen für Immuntherapien erschwert.

In dieser Studie untersuchte ich die Auswirkungen von Hypoxie und HIF-1 $\alpha$  auf menschliche NK-Zellen. Meine Ergebnisse zeigten, dass NK-Zellen, die Hypoxie ausgesetzt waren (1 % Sauerstoff), im Vergleich zu NK-Zellen unter Normoxie (21 % Sauerstoff) eine reduzierte Produktion von IFN $\gamma$ , eine verminderte Degranulation als Reaktion auf Zytokinstimulation und Tumorzellen sowie eine beeinträchtigte Proliferation aufwiesen. Ich erforschte die Möglichkeit, die Funktionalität menschlicher NK-Zellen unter Hypoxie durch das genetische Targeting von *HIF1A* mithilfe der CRISPR/Cas9-Ribonukleoprotein-basierten Transfektion zu korrigieren. HIF-1 $\alpha$ -deletierte NK-Zellen konnten unter Hypoxie die IFN $\gamma$ -Produktion nach Stimulation mit IL-12/18 im Vergleich zu Kontrollzellen wiederherstellen.

Um die praktische Anwendbarkeit von HIF-1 $\alpha$ -deletierten NK-Zellen zu bewerten, verwendete ich organoidbasierte Zelllinien von Patienten mit kolorektalem Adenokarzinom. Die Ergebnisse zeigten eine gesteigerte Zytotoxizität von HIF-1 $\alpha$ -deletierten NK-Zellen gegenüber bestimmten organoidbasierten Zielstrukturen, insbesondere in Kombination mit der Ausrichtung des Chimären Antigenrezeptors (CAR) gegen HER-2.

Zusätzlich untersuchte ich die Auswirkungen von Hypoxie auf zytokininduzierte „memory like“ (CML) NK-Zellen. CML-NK-Zellen, die sieben Tage lang Hypoxie ausgesetzt waren, zeigten eine reduzierte IFN $\gamma$ -Produktion nach Stimulation mit IL-12/18 im Vergleich zu normoxischen Kontrollen. Die Degranulation und die Zytokinproduktion nach der Kokultur mit K562 Tumorzellen blieben jedoch unverändert. Diese Ergebnisse legen nahe, dass CML-NK-Zellen empfindlich auf Sauerstoff reagieren, was möglicherweise durch HIF-1 $\alpha$  reguliert wird und weitere Untersuchungen erfordert.

Darüber hinaus entwickelte ich ein effizientes Transfektionsprotokoll für menschliche primäre NK-Zellen unter Verwendung von Elektroporation und CRISPR/Cas9-Ribonukleoprotein mit farbmarkierten sgRNAs. Dies ermöglichte die erfolgreiche Deletion von Oberflächenmolekülen wie TRAIL, NKG2A, TIGIT, CD112R, DNAM-1 und CD96 und die Sortierung von doppelten und dreifachen Knockout-Populationen von NK-Zellen.

Zusammenfassend betont meine Studie die Bedeutung der Sauerstoffkonzentration für menschliche primäre NK-Zellen und stellt ein zytotoxisches NK-Zellprodukt vor: HER-2 CAR HIF-1 $\alpha$  NK-Zellen, das für CML-NK-Zellen vielversprechend sein könnte. Darüber hinaus habe ich ein effektives Transfektionssystem für menschliche primäre NK-Zellen entwickelt, um die Bekämpfung von Tumorzellen zu verbessern.

### 3 SUMMARY

---

Environmental conditions significantly influence the phenotype and functionality of immune cells. Specifically, hypoxic conditions (oxygen concentration below 1%) prevalent in tissues and organs impact both the adaptive and innate immune systems. The transcription factor hypoxia-inducible factor 1-alpha (HIF-1 $\alpha$ ) plays a pivotal role in regulating immune cell adaptation to hypoxia. Natural killer (NK) cells are essential in tumor surveillance, as they target tumor cells by producing cytokines, chemokines, and cytolytic granules. Nevertheless, NK cells infiltrating solid tumors with hypoxic environments often lose their functionality. In addition, the high sensitivity of human primary NK cells to *in vitro* culturing conditions poses a challenge for classical transduction and transfection methods, hindering the study and generation of improved NK cells for immunotherapies.

In this study, I investigated the effects of hypoxia and HIF-1 $\alpha$  on human NK cells. My findings indicate that NK cells exposed to hypoxia (1 % oxygen) exhibited reduced IFN $\gamma$  production, diminished degranulation response to cytokine stimuli and tumor targets, and impaired proliferation compared to NK cells exposed to normoxia (21 % oxygen). I explored the potential rescue of human NK cell functionality under hypoxia by genetically targeting *HIF1A* using CRISPR/Cas9 ribonucleoprotein-based transfection. HIF-1 $\alpha$ -targeted NK cells, under hypoxia, restored IFN $\gamma$  production upon IL-12/18 stimulation compared to mock control cells.

To assess the practical applicability of HIF-1 $\alpha$ -targeted NK cells, I employed patient-derived organoid lines from colorectal adenocarcinoma patients. The results revealed an enhanced cytotoxicity in HIF-1 $\alpha$ -targeted NK cells against specific patient-derived organoids, particularly when combining Chimeric Antigen Receptor (CAR) targeting HER-2 with HIF-1 $\alpha$  targeting.

Additionally, I investigated the impact of hypoxia on cytokine-induced memory-like (CML) NK cells. CML NK cells exposed to hypoxia for seven days displayed a reduced IFN $\gamma$  production upon IL-12/18 stimulation compared to normoxic controls. However, degranulation and cytokine production during K562 co-culture remained unaffected. These results suggest an oxygen sensitivity in CML NK cells, potentially regulated by HIF-1 $\alpha$ , which warrants further investigation.

Furthermore, I developed an efficient transfection protocol for human primary NK cells using electroporation and CRISPR/Cas9 ribonucleoprotein with dye-labelled sgRNAs. This allowed successful targeting of surface molecules such as TRAIL, NKG2A, TIGIT, CD112R, DNAM-1, and CD96, enabling the sorting of double and triple knockout populations of NK cells.

In summary, my study highlights the importance of oxygen concentrations for human primary NK cells and introduces a cytotoxic NK cell product: HER-2 CAR HIF-1 $\alpha$  NK cells, which may hold promise for CML NK cells. Moreover, I established an effective transfection system for human primary NK cells, facilitating the generation of gene edited NK cells to enhance tumor target killing.



## 4 INTRODUCTION

### 4.1 THE IMMUNE SYSTEM

The immune system is the group of protection mechanisms within an organism against a potential hazard. The immune system's major task is to maintain the homeostasis in the organism, providing defense against foreign (e.g. viruses, bacteria or polluting agents) and internal hazards (e.g. cancer cells). In order to maintain the correct balance of the organism and survive to jeopardy, the immune system must be correctly tuned. When there is a dysfunction, health issues may occur, such as autoimmune diseases (e.g. lupus) or immunodeficiency diseases (e.g. chronic granulomatous disease or AIDS).

For this reason, immunology is fundamental for biomedical research, with a worldwide impact and a broad focus, such as on cancer therapy, vaccines or congenital diseases. Immunology was developed in the XIX century, with the research work of Elie Metchnikoff (1845–1916) elucidating phagocytosis and Emil Behring (1854–1917) and Paul Ehrlich (1854–1915) who described antibodies by first time (Behring, 1890; Behring & Kitasato, 1890; Kaufmann, 2019). These discoveries provided the first hint about a division in the immune system, cellular and humoral defense (Figure 4.1).

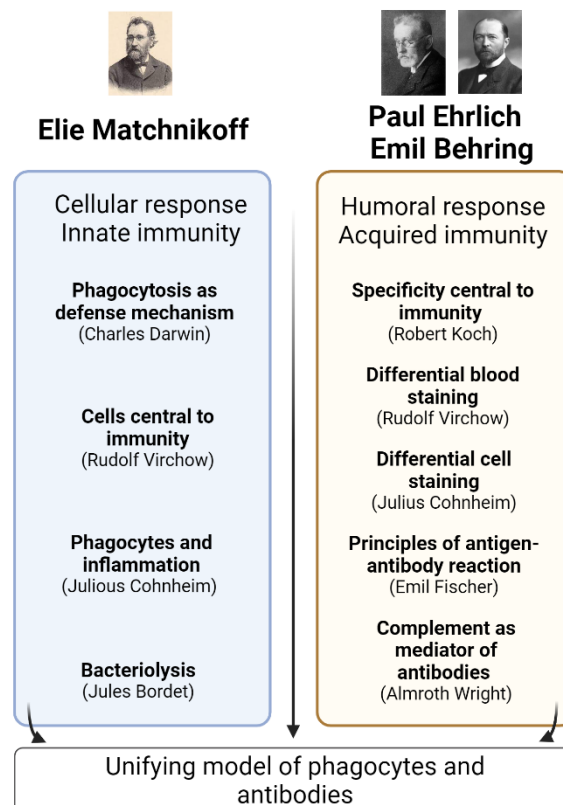


**Figure 4.1:** History of immunology foundation. Metchnikoff, Ehrlich and Behring's work summarized with mentors and collaborators between brackets. Adapted from (Kaufmann, 2008). Created in Biorender.com.

In the XX century, another division was defined above the humoral and cellular clusters: innate and adaptive immunity (Kaufmann, 2008) (Figure 4.2). Innate immunity is the immediate defense against the hazard, and comprises cellular (e.g. phagocytes and natural killer) and physical protection (such as skin or mucosal barrier). On the other hand, adaptive immunity is the long-term response to the hazard. It is conformed by lymphocytes (e.g. CD8<sup>+</sup> T cells) that have been sensitized to certain antigens and are capable to generate memory against it.

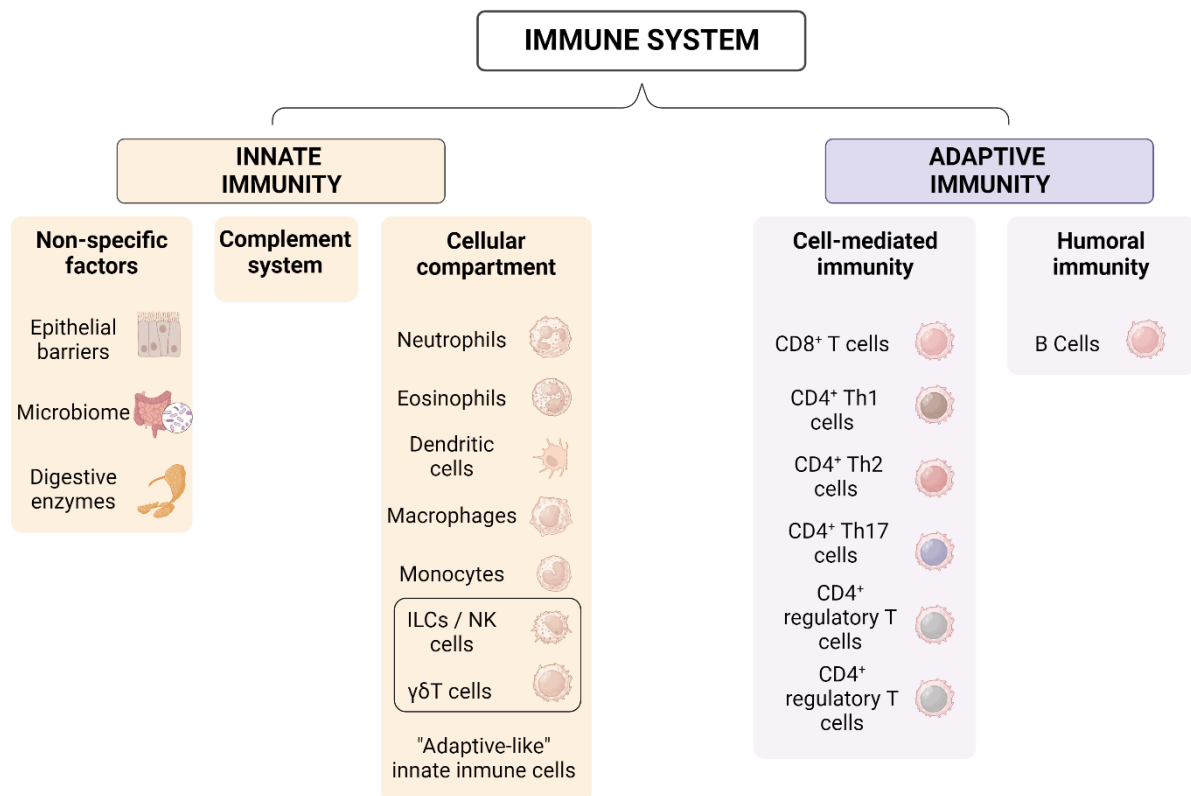


**Figure 4.2:** Summary of the immune system according to innate and adaptive immunity. Created in Biorender.com.

#### 4.1.1 Innate immunity

Innate immunity is the first response that an organism counts with against the hazard. It is not only present in jaw vertebrates (such as mammals), but also in invertebrates, plants and prokaryotes (Litman et al., 2005; Nürnberger et al., 2004). One of the common mechanisms is the physical barrier, which is a protection layer shared among all the organisms. For example, the skin barrier and tight junctions in epithelial cells that protect animals from external agents have a similar function as the wax layer and rigid cell wall in plants (Nürnberger et al., 2004). However, physical protection is not enough for certain jeopardies, which might require a chemical and microbial protection. These are the combination of mucosal barrier (for instance, the saliva containing enzymes able to disrupt bacterial membranes or the eye mucosa protection), acid pH in the stomach secretions or the symbiotic microbiome in the intestinal tract (Turner, 2009).

When these protective barriers are compromised, harmful agents can gain entry into the organism. In such circumstances, the innate immune system deploys additional defense mechanisms. The first line of defense is the humoral response, which involves the complement system. As previously mentioned, the complement system represents one of the earliest documented immune responses, dating back to 1890 (Nesargikar et al., 2012). This system consists of a cascade of proteins, with activation occurring through three primary pathways: the alternative, lectin, and classical pathways (Mayer, 1973).

The alternative pathway's activation is mediated by foreign structures composed of carbohydrates, lipids, and proteins. In contrast, the lectin pathway is triggered when circulating mannose-binding lectin (MBL) or ficolin binds to pathogen surfaces, such as viruses or bacteria (Matsushita, 1996). This binding initiates the formation of a protein aggregate that attracts other complement proteins, thereby enhancing the protein cascade. The classical pathway, on the other hand, is activated when IgG and IgM antibodies bind to foreign pathogens. The complement proteins initiating the classical pathway recognize the Fc portion of these immunoglobulins (Sarma & Ward, 2011). All three pathways converge in their response by forming a membrane attack complex (MAC) that creates pores in the pathogen's membrane, leading to its lysis.

Nevertheless, the complement system is not an entirely isolated defense mechanism, it interacts with myeloid and non-myeloid cells that also produce complement proteins (e.g. liver parenchymal cells) (Wetsel, 1995). The complement system is also connected to adaptive immunity, it interacts with the B cell receptor and creates an activation loop with T cells, in a DAF and C3/5aR dependent manner (Carroll, 2004; Heeger et al., 2005).

Over time, a hazard may become resistant to all the previously described defense mechanisms. Therefore, a more sophisticated line of innate response has evolved, known as the cellular response. The cellular response comprises a group of innate immune cells, including myeloid cells (neutrophils, eosinophils, mast cells, basophils, monocytes, dendritic cells, and macrophages) and lymphocytic cells (innate lymphoid cells (ILCs) and  $\gamma\delta$ T cells).

Within the cellular response, various types of phagocytes, including macrophages, monocytes, dendritic cells (DCs), mast cells, and neutrophils, play a crucial role in processing and eliminating cellular debris and apoptotic cells resulting from pathogen attacks. For instance, macrophages employ phagocytosis to remove debris and apoptotic cells. They process these materials by enclosing them in vesicles through the fusion of lysosomal or endosomal compartments. These vesicles are referred to as phagolysosomes. As they mature, phagolysosomes gradually become more acidic, which facilitates the digestion of the enclosed hazardous material (Berón et al., 1995; H Allen & Aderem, 1996).

To identify potential threats, biological barcoding signals activate innate immune cells, often referred to as "signal o." Microorganisms possess pathogen-associated molecular pattern molecules (PAMPs), while cells within the organism release damage-associated molecular pattern molecules (DAMPs), as seen in ischemic processes, for instance. Innate immune cells are equipped with pattern recognition receptors (PRRs) that bind to these ligands. Among PRRs, various receptor subtypes have evolved, including Toll-like receptors (TLRs), IG-I-like

receptors, nucleotide oligomerization detection-like receptors (NOD-like), receptors for advanced glycation end products (RAGE), and absent-in-melanoma (AIM)<sub>2</sub>-like receptors (Litman et al., 2005; Tang et al., 2012).

The binding of these receptors to their ligands not only initiates autophagy and inflammation through the activation of interferon regulatory factors (IRF) and the nuclear factor kappa B (NF $\kappa$ B) pathway but also promotes crosstalk among immune cells by enhancing the migration of dendritic cells, activating NK cells, and stimulating T-cells activation (Tang et al., 2012). One example is the activation of TLR<sub>1</sub>, 2, or 4, depending on the ligand (such as double-stranded released DNA, heat shock proteins, or LPS). This activation leads to the triggering of the myeloid differentiation primary response gene 88 (MyD88) or TIR-containing adapter inducing IFN $\beta$  (TRIF) pathway, both of which result in cytokine production, including type I interferons or IL-12 (Kawai & Akira, 2009).

While DAMPs and PAMPs recognition may involve some common pattern recognition receptors (PRRs), they are subject to specific regulation. For example, the recognition of the HMGB<sub>1</sub> protein by PRRs (TLR<sub>4</sub>, 2, RAGE, and triggering receptor expressed on myeloid cells-1 (TREM-1)) includes a "safety break" in myeloid cells provided by CD24 homodimers, which restrains the response to DAMPs but not PAMPs (G. Y. Chen et al., 2009). In addition to inflammation, antigen-presenting cells (APCs) are also activated by PAMPs or DAMPs to stimulate naïve T cells. APCs present major histocompatibility complex II to sensitize T cells to the hapten, ensuring the proper activation of T cells (Cosgrove et al., 1991). Therefore, the innate immune system plays a crucial role in orchestrating adaptive immunity.

#### 4.1.2 Adaptive immunity

When a threat eludes the innate defenses, adaptive immunity steps in to counteract it with a specific response against an antigen. The history of adaptive immunity is intricately intertwined with the discoveries in innate immunity, encompassing both humoral and cellular components.

Initially, there was a trend theory suggesting that serum antibodies were excised receptors, but Tiselius demonstrated that they were  $\gamma$  immunoglobulins (Behring, 1890; Behring & Kitasato, 1890; Tiselius & Kabat, 1938). Fagraeus, in 1947, showed that serum antibody levels increased due to plasma cells (Fagraeus, 1947). However, the cells responsible for producing these antibodies and the nature of the molecules involved remained unclear.

Miller reported the presence of a specific lymphocyte population in the thymus (J. F. A. P. Miller, 1962). Simultaneously, Cooper's work introduced a new cluster of antibody-producing cells in chickens, generated in the bursa of Fabricius. Cooper's research, which combined the removal of the thymus and bursa, revealed a lack of a specific response against threats, especially when the thymus was removed (M. D. Cooper, 2015; M. D. Cooper et al., 1965). Consequently, the cells responsible for antibody production were named B cells (referring to the bursa of Fabricius), while thymus cells were identified as responding to the antibodies and eliminating the threats, thus being called T cells (Kaufmann, 2019).

Plasma cells (matured B cells) produce different forms of immunoglobulins: IgM (secreted in heterodimers of five molecules, early immune response marker); IgG (“classic” antibody, found in peripheral blood and targets an antigen); IgE (triggers eosinophils by hapten recognition, induces allergy), IgA (in mucosae and maternal milk, protects against pathogens) and IgD (part of BCR, activates basophils and eosinophils) (K. Chen et al., 2020).

In the realm of adaptive immunity, lymphocytes can be classified into two main categories: B cells, equipped with B cell receptors (BCRs), and T cells, which possess T cell receptors (TCRs). The generation of diversity in TCRs and BCRs is orchestrated through recombination processes involving variable (V), diversity (D), and joining (J) segments within germ-line DNA sequences, as elucidated by Tonogawa (Sakano et al., 1980) (Figure 4.3). Specifically, TCRs exhibit VDJ recombination in the  $\beta/\delta$  subunit, while the  $\alpha/\gamma$  subunit involves only VJ recombination. In contrast, BCRs feature two heavy chains (VDJ) and two light chains (VJ,  $\lambda$ , and  $\kappa$ ). Subsequently, somatic cloning processes come into play, facilitating both the elimination of self-reactive B and T cells through negative selection and the promotion of cells responsive to antigens via positive selection (Goodnow et al., 1989; Jenkinson et al., 1992).

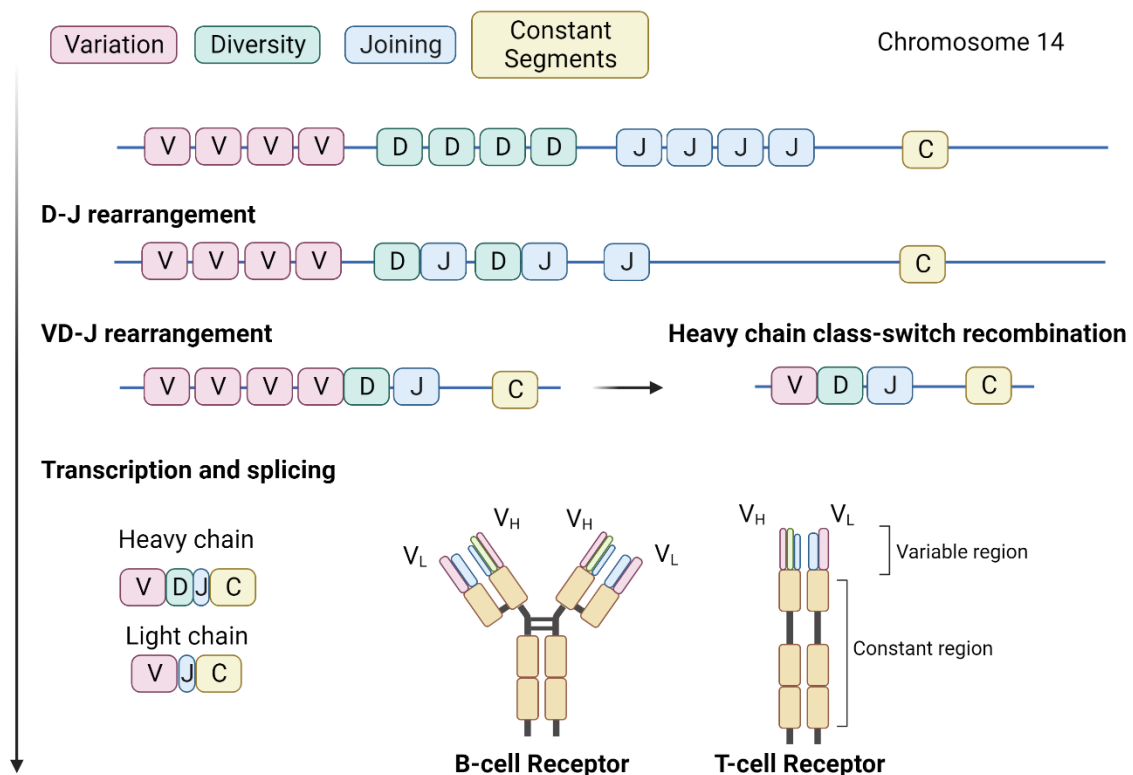


**Figure 4.3:** Scheme of VDJ recombination, BCR and TCR structure. Figure created in Biorender.com.

Nonetheless, it was the Nobel Prize awarded Doherty and Zinkernagel that elucidated the role of T cells as cytolytic cells primed through antigen recognition by MHC molecules (Zinkernagel & Doherty, 1979). Zinkernagel and Doherty observed that lymphocytes isolated from LCMV-infected mice were reactive against targets that shared H-2 molecules (Cantor & Boyse, 1975). The H-2 recognition led to a huge interest in the characterization of the TCR structure, which was characterized simultaneously by different groups, and led to the

discovery of variable and constant regions (Hedrick et al., 1982). As the field of immunology continued to expand, new discoveries revealed that T cells could be categorized into two primary subgroups: CD4<sup>+</sup> (helper) engaging with MHC-II and CD8<sup>+</sup> (cytotoxic) T cells interacting with MHC-I (Bjorkman et al., 1987; Cantor & Boyse, 1975). Additionally, there is a third subgroup characterized by the presence of  $\gamma\delta$  TCR chains, commonly referred to as  $\gamma\delta$  T cells.

CD4<sup>+</sup> T cells are activated by antigen-presenting cells (APCs) through MHC-II interactions and play a crucial role in communicating with other immune cells, including macrophages, B cells, and CD8<sup>+</sup> T cells. Because of their involvement in supporting and coordinating immune responses, this group of T cells is aptly named "helper T cells", divided in TH0, TH2, TH17 and Treg groups (Harrington et al., 2005; Mosmann et al., 1986; Sakaguchi et al., 1995) (see Figure 4.4). Helper T cells can be further categorized into subgroups based on the specific cytokines they are exposed to and the transcription factors they activate. When a naïve helper T cell (TH0) encounters MHC-II stimuli binding to the T cell receptor (TCR) and is exposed to IL-12, it triggers STAT-4 and T-bet, resulting in its differentiation into a T helper 1 (TH1) cell. TH1 cells, in turn, activate macrophages and cytotoxic T cells (CD8<sup>+</sup>) by producing IL-2, TNF $\alpha$ , and IFN $\gamma$  (Murphy & Reiner, 2002).

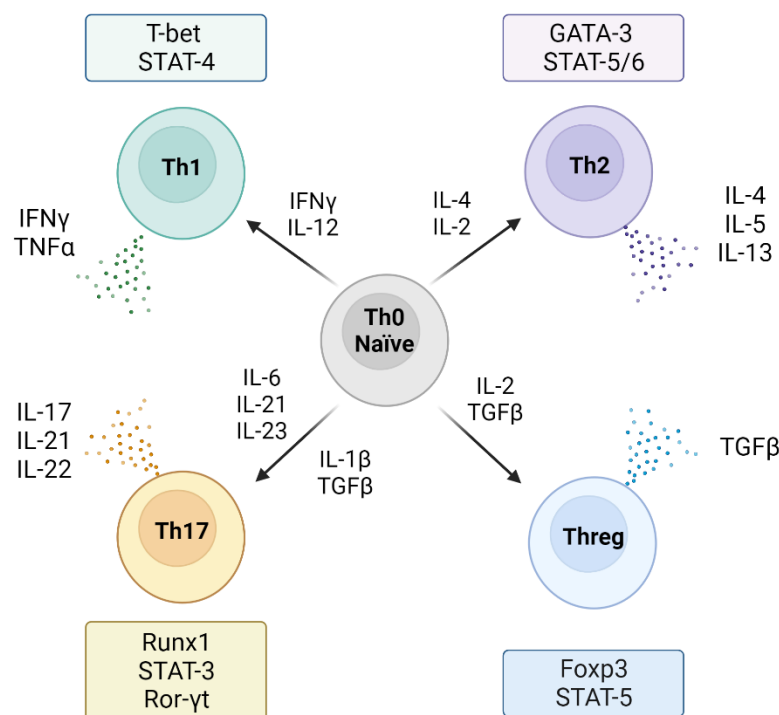


**Figure 4.4:** Th CD4<sup>+</sup> T cell populations stratified by transcription factor expression and cytokine pre-stimulation and production. Figure created in Biorender.com.

TH1 and TH2 cells have the capacity to regulate each other through a negative feedback loop. TH1 cells, producing IFN $\gamma$ , stimulate the STAT-1 pathway, which increases IL-12R (maintaining their responsiveness to IL-12) and inhibits GATA-3. Similarly, TH0 cells, when stimulated by IL-2 and IL-4, enhance STAT-5/6 and trigger GATA-3, inhibiting STAT-1. Consequently, TH2 priming inhibits TH1 and vice versa (Mosmann et al., 1986; W. Zheng &

Flavell, 1995). If the balance between TH<sub>1</sub> and TH<sub>2</sub> responses is disrupted, it can lead to immune diseases, such as organ-specific autoimmunity when TH<sub>1</sub> responses predominate (e.g. inflammatory bowel disease), or conditions like asthma and allergies when TH<sub>2</sub> responses are dominant.

The third group was discovered through the observation of an abundance of IL-17 in TH<sub>1</sub>-related diseases, where the absence of IFN $\gamma$ /IL-12 effector cells exacerbated the symptoms. This novel TH cluster was designated as TH<sub>17</sub> (Harrington et al., 2005). TH<sub>17</sub> cells are generated when naïve helper cells are stimulated with IL-23, IL-21 and IL-6, leading to the activation of Runx1 and ROR $\gamma$ c, which subsequently enhances ROR $\gamma$ t expression, inducing the secretion of IL-17 and IL-23. Intriguingly, T-bet stimulation inhibits the maturation of TH<sub>17</sub> cells, implying a delicate balance among helper T cell subsets (Lazarevic et al., 2011).

However, not all T helper cells contribute to immune defense. Upon stimulation with IL-2 and TGF $\beta$ , TH<sub>0</sub> cells differentiate into regulatory T cells (Treg), characterized by the overexpression of Foxp3 and the secretion of IL-10 and TGF $\beta$ . The primary function of Treg cells is to regulate autoimmunity, serving as a crucial internal control mechanism. However, in the context of cancer, Tregs can have detrimental effects as they inhibit surrounding immune cells (Reiner, 2007; Sakaguchi et al., 1995).

CD8<sup>+</sup> T cells, also known as cytotoxic T cells, exhibit MHC-I restriction through their T cell receptors (TCR) (Cantor & Boyse, 1975). The TCRs of cytotoxic T cells are associated with two scaffold molecules: CD3 co-receptor subunits ( $\zeta$ ,  $\gamma$ , and  $\epsilon$ ), which contain ITAM (Immunoreceptor Tyrosine-based Activation Motif) activatory domains, and the CD8 co-receptor, which activates Zap70 and dimerizes with the CD45 receptor (Raskov et al., 2021).

CD8<sup>+</sup> T cells are attracted by chemokine and integrin gradients on antigen-presenting cells or target cells, leading to the formation of an immune synapse. Antigen-presenting cells (APCs) and target cells present antigen peptides on their surfaces via the MHC-I complex, which are recognized by the TCR/CD3 complex and CD8 co-receptor on the surface of cytotoxic T cells (Bjorkman et al., 1987). Following TCR priming, cytotoxic T cells require the binding of the CD28 co-receptor with CD80/86, which triggers the activation of the cytotoxic machinery (Raskov et al., 2021; Shiku et al., 1975).

Once cytotoxic T cells are primed, they orchestrate the cell death of the target cell expressing the antigen to which they have been sensitized. CD8<sup>+</sup> T cells induce cell lysis through the creation of mechanical pores in the target cell membrane, achieved by the secretion of perforin, granzymes, or granulysin (Basu et al., 2016). Furthermore, the interaction of receptors with death domains triggers apoptosis in tumor cells (Fu et al., 2016). However, in the absence of activating signals and the presence of inhibitory stimuli (such as PD1-PDL1 binding), T cells become exhausted and lose their ability to mount an effective response against the pathogen.

## 4.2 INNATE LYMPHOID CELLS

Innate lymphoid cells (ILCs) are immune cells that produce cytokines and, unlike adaptive immune cells that possess BCR and TCRs, they have the ability to lyse target cells without the activation of antigen specific receptors. Among ILCs there is a division in subgroups depending on the expression of transcription factors and function: ILC1s, ILC2s, ILC3s and Natural Killer cells (the main interest of this dissertation)(refer to Figure 4.5).

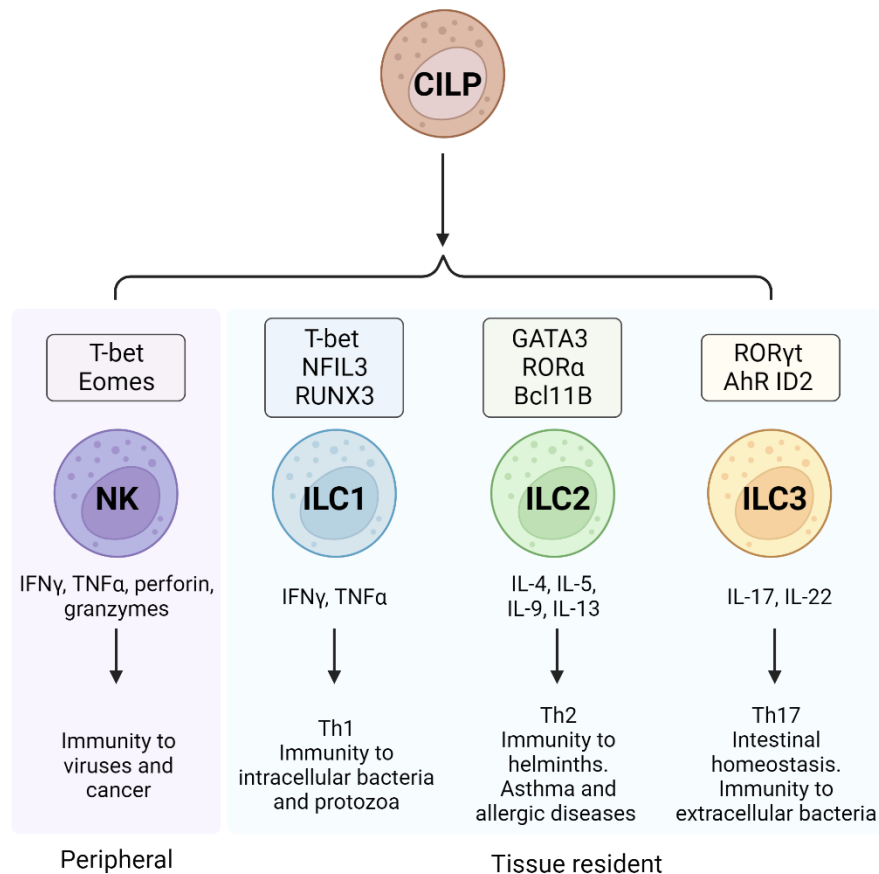


**Figure 4.5:** Summary of innate lymphoid cells. Figure created with Biorender.com.

### 4.2.1 ILC1, ILC2 and ILC3

During ILC development, the common innate lymphoid progenitors (CILPs) diverges in NK progenitor or in common helper innate lymphoid progenitors (CHILPs). CHILPs express GATA3 and further differentiate either to innate lymphoid cell precursors (ILCPs) by expressing promyelocytic leukemia zinc finger (PLZF) or lymphoid tissue inducer progenitors (LTiPs). ILCP further promote to ILC1s (by T-bet, NFIL3, RUNX3 expression), ILC2s (driven by ROR $\alpha$ , Bcl11B, GATA3 and GFl1) and ILC3s (expressing ROR $\gamma$ T, AhR and ID2) (Spits et al., 2013; Vivier et al., 2018).

ILCs are tissue-resident cells, resting in the peripheral organs, such as mesenteric lymph nodes (ILC1, 2 and 3), lungs (ILC2s), small intestine (ILC1, 2 and 3) or liver (ILC2) (Gasteiger et al., 2015; Mchedlidze et al., 2013). ILCs are divided by function in a similar way as Th1, 2 and 17 cells. ILC1s display a mirroring function as Th1 cells, reacting to internal microbes, cancer cells and virus. ILC1s produce cytolytic granules containing granzyme and perforin, but also

IFN $\gamma$ , activating macrophages and displaying low cytotoxic capability (compared to CD8<sup>+</sup> T cells or NK cells). ILC2s are mirroring Th2, they detect allergens and parasites (e. g. helminths) and produce IL-4, IL-5, IL-9, IL-13 and AREG expression (Gasteiger et al., 2015; Vivier et al., 2018). ILC3s are located in mucosae, regulating the intestinal commensals and detecting extracellular microbes. ILC3s secrete IL-22, IL-17, GM-CSF and lymphotoxin. They induce intestinal stem cell differentiation and activate Th17 cell responses. Moreover, recent findings show the promising role of human ILC3s as responders to cancer, producing IFN $\gamma$  and triggering cancer cell line lysis by TRAIL apoptosis pathway (Siegler et al., 2022).

#### 4.2.2 NK cells

In 1975, Kiessling and colleagues introduced a novel class of splenic lymphocytes exhibiting cytotoxic activity against Moloney leukemia cells, coining the term "Natural Killers" (Kiessling, Klein, Pross, et al., 1975). NK cells uniqueness relies on the variety of surface receptors, which creates a balance between the activating and inhibiting signals, determining how NK cells respond to a target cell (e. g tumor cells or virus-infected cells) (Chiossone et al., 2018)(see Figure 4.6).

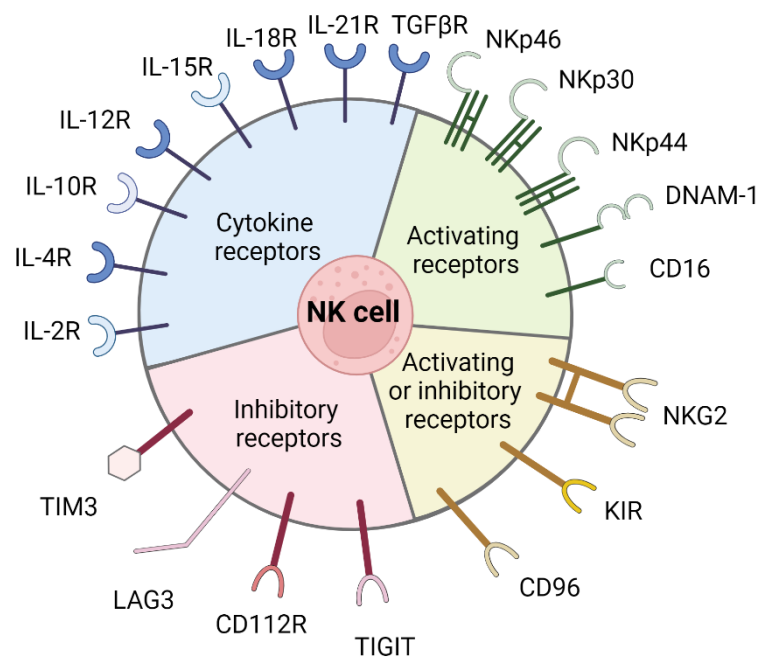


**Figure 4.6:** Surface receptors of NK cells clustered by function. Figure adapted from Chiossone et al (Chiossone et al., 2018). Figure created in Biorender.com.

##### 4.2.2.1 Soluble factors and granules

In part, NK cell cytotoxicity is mediated by the secretion of soluble factors and cytokines, including IFN $\gamma$ , TNF $\alpha$ , and various Granzymes, such as Granzyme B. The historical context of early observations in the 19th century regarding the reduction of tumors in patients with concurrent bacterial infections is highly relevant (Coley, 1909). Subsequent research milestones have significantly contributed to our understanding of NK cell function.

In the mid-20th century, Wheelock's discovery of interferon-like virus inhibitor (later named Interferon  $\gamma$ ) and its role in controlling viral infections added crucial insights to the field

(Wheelock, 1965; Young & Hardy, 1995). Subsequently, independent studies conducted by the Rosenberg group and the Old group provided evidence that IFN $\gamma$  governs immunosurveillance mediated by CD8<sup>+</sup> T cells and depletion of IFN $\gamma$  is associated with enhanced tumor growth (Barth et al., 1991; Kaplan et al., 1998). The 1990s witnessed pivotal research by Trinchieri, which established the link between IFN $\gamma$  and NK cells. This work demonstrated how the stimulation of NK cells through cytokines, such as IL-12 (commonly referred to as natural killer cell stimulatory factor), resulted in the production of IFN $\gamma$ . IFN $\gamma$  played a vital role in controlling infections like MCMV independently of B and T lymphocytes (Orange et al., 1995).

However, the discovery of necrosis within tumors remained elusive until 1975 when Old's group isolated an endotoxin, naming it tumor necrosis factor (Carswell et al., 1975). Subsequently, the production of TNF- $\alpha$  by NK cells was associated with stimulation induced by viral infections or cancerous cells (Kashii et al., 1999; Orange & Biron, 1996). In addition, the secretion of TNF- $\alpha$  and IFN $\gamma$  by the type 1 immune response (cytotoxic T cells, NK cells and ILC1s) arrest tumor cells in G<sub>1</sub>/Go, inducing senescence and controlling tumor growth (Braumüller et al., 2013).

Furthermore, studies revealed that the susceptibility of NK cells to various stimuli was genotype-dependent among mice, with no cross-reaction observed in mice of the same genotype (Kiessling, Klein, & Wigzell, 1975). These findings laid the groundwork for exploring the specificity of NK cells and the role of major histocompatibility complex (MHC) molecules. It became evident that NK cells possessed a defense mechanism that targets MHC-lacking tumor cells, while MHC-I-expressing cells could evade immune recognition (Klein et al., 1978; Ljunggren & Kärre, 1990; Storkus et al., 1989).

#### 4.2.2.2 *Killer Ig-Like Receptors (KIRs)*

Nevertheless, the identity of receptors binding to MHC-I molecules remained elusive. Yokoyama's group made a significant breakthrough by demonstrating that Ly-49A<sup>+</sup> NK cells could not lyse H-2D-expressing mice (being H-2D a MHC-I molecule), in contrast to Ly-49A<sup>-</sup> NK cells, which exhibited efficient cytotoxicity (Daniels et al., 1994). Therefore, Ly-49A<sup>+</sup> triggering inhibited the recognition of NK cells to the cell target, protected by the expression of the MHC-I molecule. Subsequently, multiple Ly-49 receptors, including Ly-49D and Ly-49G.2, were unveiled (Lanier & Phillips, 1996).

In the case of human MHC-I receptors, Alessandro Moretta and colleagues played a pivotal role by proposing the analogous function of Ly-49 and p58 receptors (Wagtman, Biassoni, et al., 1995). However, p58 receptors differed from Ly-49A in their C-Lectin independence, a distinction later clarified with the introduction of Killer Ig-like Receptors (KIRs). KIRs were characterized as three distinct p58 receptors featuring an immunoglobulin-like structure, along with an immune receptor tyrosine-based activation motif (ITAM) in short-tail KIRs and an inhibitory function (ITIM) in long-tail KIRs (Wagtman, Rajagopalan, et al., 1995). KIRs recognize a range of HLA-A, HLA-B, and HLA-C allotypes, thus dictating MHC-I inhibition in humans, in contrast to mice where C-lectin-based receptors govern this process.

#### 4.2.2.3 *C-type lectin receptors: NKG2 family*

Nonetheless, NK cells do not exclusively engage with MHC-I through KIRs. Bach's group made a significant contribution by employing hybridization techniques and cDNA extraction to identify 12 distinct groups of NK cell sequences, encompassing both NK cells. Within the NK cells group 2 (NKG2), they identified sequences encoding type II membrane proteins (Houchins et al., 1991). The NKG2 receptors were further characterized, and they were categorized into four transcripts: A, B, C, and D. Among these, A, B, and C exhibited high sequence similarity, whereas D displayed only a 21 % similarity with the other family members (Houchins et al., 1991). Despite their individual characteristics, NKG2 receptors share membership in the lectin family group with Ly49 receptors, known as C-type lectin-like receptors (CTLR) (Bartel et al., 2013).

However, the mechanisms by which NKG2 receptors initiated signaling and their specific ligands remained unknown. Lanier et al. made a groundbreaking discovery, revealing that human NKG2D binds to the DNAX adaptor protein 10 (DAP10). This interaction activates the Src homology 2 (SH2) binding domain, leading to the activation of the PI3K cascade through the binding of its p85 subunit (Wu et al., 1999).

Bauer et al. also made significant contributions by demonstrating that human NKG2D binds to the non-classical MHC-I molecules MICA and MICB. This interaction triggers the cytolytic activity of both NK and T cells (Bauer et al., 1998). Furthermore, other MHC-I related molecules, such as UL16 binding protein transcripts 1 and 2 (ULBP1 and 2), were identified as ligands for human NKG2D (Cosman et al., 2001).

In the context of murine ligands, Cerwenka and colleagues reported that the retinoic acid early inducible molecule (RAE-1) and H60 served as ligands of NKG2D. Simultaneously, Diefenbach's and Yokoyama's groups identified the murine ULBP transcript-like (MULT1) as an additional ligand (Carayannopoulos et al., 2002; Cerwenka et al., 2000; Diefenbach et al., 2003; Nausch & Cerwenka, 2008). The pivotal role of NKG2D in tumor surveillance was established through the work of Guerra's team, who demonstrated that a murine model lacking NKG2D expression exhibited poor survival outcomes in the presence of a tumor burden (Guerra et al., 2008).

NKG2A, NKG2B, and NKG2C were concurrently described alongside NKG2D, all belonging to the NKG2 family (Houchins et al., 1991). NKG2A/B forms heterodimers with CD94 and binds to HLA-E, exerting an inhibitory effect through its immunoreceptor tyrosine-based inhibitory motif (ITIM) domain (Lazetic et al., 1996). Notably, HLA-E engages not only with NKG2A/B (inhibitory) but also with NKG2C (activating) receptors. The activation of NKG2C, also necessitates the formation of a heterodimer with CD94 (Lee et al., 1998; M. Braud et al., 1998).

In contrast to NKG2A/B, NKG2C lacks the ITIM domain. Instead, it associates with DAP12, triggering the phosphoinositide 3-kinase (PI3K) cascade (Lanier et al., 1998). Depending on the presence of NKG2A/B or NKG2C, HLA-E binding can either enhance cytotoxicity or inhibit it. This leads to distinct NK cell populations that either degranulate against their targets or are restrained in their response.

#### 4.2.2.4 CD16

One of the earliest receptors to be characterized was CD16, serving as the low-affinity receptor for the FcR type III portion of IgG antibodies. It initiates antibody-dependent cellular cytotoxicity (ADCC) through its intracellular immunoreceptor tyrosine-based activation motif (ITAM). The research by Lanier and colleagues revealed a clear distinction among NK cells, defining two primary NK cell populations: CD56<sup>bright</sup>/CD16<sup>+/-</sup> and CD56<sup>dim</sup>/CD16<sup>++</sup> (M. A. Cooper et al., 2001; Lanier et al., 1986). Functionally, CD56<sup>dim</sup> cells exhibit enhanced cytotoxicity. However, it was initially unclear which receptors were associated with each of these populations. The same research group reported that NK cells, along with a small fraction of T cells, possess a distinct form of CD16 that triggers their response to anti-CD16 antibodies, whereas other granulocytes lack such an active CD16 (Lanier et al., 1988; Perussia et al., 1984).

The main regulator of CD16 surface expression is ADAM17, a metalloprotease-17. ADAM17 becomes activated following NK cell stimulation, which can occur through exposure to cytokines or target cells, and this activation leads to CD16 shedding (Romee et al., 2013). The presence or absence of CD16 holds significant relevance for immunotherapies, as opsonized antigens by IgG antibodies can activate ADCC. Consequently, monoclonal antibody therapies can be amplified through ADCC in CD16<sup>+</sup> NK cells.

Currently, clinical approaches are exploring engineered T cells expressing a chimeric antigen receptor with a high-affinity form of CD16. This approach aims to combine CD8<sup>+</sup> T cells with CD16 ADCC for enhanced therapeutic effect (ClinicalTrials.gov Identifier: NCT03189836) (Rataj et al., 2019). Similarly, NK cells engineered to produce non-cleavable CD16 for targeting B-cell lymphoma have exhibited increased tumor cell lysis when combined with monoclonal antibodies. This underscores the broad impact and potential of CD16 engineering (H. Zhu et al., 2020).

#### 4.2.2.5 Natural cytotoxicity receptors: NKp46, NKp44, NKp30, NKp80 and NKp65

In the 1990s, a significant breakthrough occurred with the characterization of the Natural Killer cell protein receptors, including NKp46, NKp44, NKp30, and NKp80. NKp46 was the first to be described by the Moretta siblings' group. Their studies identified a unique NK protein with a molecular weight of 46 kDa, expressed in all CD56<sup>+</sup> cells but not in all CD16<sup>+</sup> cells, thus marking it as a novel NK cell marker (Pessino et al., 1998). Activation of NKp46 with an antibody was shown to enhance the cytolytic activity of NK cells through the release of Ca<sup>2+</sup>, confirming its activating function (Sivori et al., 1999).

Subsequently, three more receptors from the same family were characterized with molecular weights of 44 kDa, 30 kDa, and 80 kDa, named NKp44, NKp30, and NKp80, respectively. NKp44 was associated with IL-2-activated NK cells but not with resting NK cells. Conversely, NKp30 was identified as an activating receptor in both resting and activated NK cells (Pende et al., 1999). Over the following years, extensive research into this receptor family led to the identification of their corresponding coding genes: NCR1 (NKp46), NCR2 (NKp44), and NCR3 (NKp30) (Kruse et al., 2014). In contrast, the NKp80 receptor was found in both CD3<sup>+</sup> and CD3<sup>-</sup> cells, with the coding gene KLRF1, highlighting the heterogeneity of receptors within this family (Vitale et al., 2001). Regarding their ligands, NKp46 and NKp44 ligands are

believed to be abundant in bacteria, viruses, and tumor cells. However, the identities of these ligands remain to be clearly understood. The stress molecule B7H6, expressed in certain tumors, was identified as a ligand for NKp30. Additionally, Aicl (Clec2B) was discovered as a ligand for NKp80, and KACL (CLEC2A) for NKp65, another member of the NCR family (Bartel et al., 2013).

#### 4.2.2.6 *NECTIN pathway receptors: DNAM-1, TIGIT, CD96 and CD112R*

During the 1990s, a surge of discoveries in the realm of immune receptors emerged. This era saw the characterization of the DNAX accessory molecule-1 (DNAM-1) receptor by Lanier and his colleagues (Shibuya et al., 1996). DNAM-1 was identified in both T and NK cells. However, its ligands, CD155 (PVR) and Nectin-2 (CD112), were not uncovered until years later by Moretta's group (Bottino et al., 2003). Both of these ligands are found in tumor cells and are associated with stress responses.

DNAM-1 plays a pivotal role in activating NK and T cells, resulting in the production of cytokines and the induction of cytotoxicity. Its activation mechanism involves a tyrosine- and asparagine-based motif, often referred to as the Immunoreceptor tyrosine tail ITT-like motif. This motif initiates phosphorylation by Src kinases, ultimately triggering calcium fluxes (Zhang et al., 2015). A decade later, the discovery of an antagonist for DNAM-1, known as T cell Ig and ITIM domain (TIGIT), added a new layer to the picture. TIGIT interacts with CD155, CD112, and CD113 but exerts an inhibitory influence through its ITIM domain (Stanietsky et al., 2009; Yu et al., 2009).

While DNAM-1 and TIGIT engage in a dynamic interplay for their ligands, there was another enigmatic receptor cloned in the 1990s in T cells: CD96 (P. L. Wang et al., 1992) Colonna and colleagues shed light on CD96 (also known as Tactile), which recognizes CD155 and promotes NK cell adhesion via  $\beta$ 2 Integrin (Fuchs et al., 2004) Intriguingly, CD96 was reported to enhance NK cell cytotoxicity against tumors expressing CD155. However, Blake and colleagues demonstrated a contrasting effect of CD96 in tumor metastases (Blake et al., 2016). As of now, a clear consensus on the role of CD96 in NK cells remains elusive, and its functionality appears to be dichotomous.

Adding to the complexity of this receptor network is the recent introduction of CD112R (also known as PVRIG). Initially described in T cells, CD112R exclusively interacts with CD112 as its ligand (Y. Zhu et al., 2016). Notably, studies have shown that blocking CD112R leads to enhanced tumor elimination in both solid tumors and leukemias (J. Li et al., 2021; Y. Li et al., 2021). Overall, it is noteworthy to highlight the complexity of the described pathway, which consists of two inhibitory receptors (TIGIT and CD112R), one activating receptor (DNAM-1) and a final receptor with ambiguous functionality (CD96).

In summary, this receptor network is characterized by two inhibitory receptors (TIGIT and CD112R), one activating receptor (DNAM-1), and an additional receptor, CD96, with a dual nature and ambiguous functionality. The intricate web of interactions among these receptors adds depth to our understanding of immune responses.

### 4.3 TUMOR MICROENVIRONMENT

Throughout history, cancer has been an enduring companion of mankind. Despite our increased understanding of its origins, characteristics, and spread, the fundamental nature of this disease has persisted since ancient times. The earliest recorded evidence of tumors dates back to the Inca civilization. Antique mummies bearing neoplastic bone injuries and ceramics depicting surgical procedures (around 2400 BCE) provide some of the first historical clues (Sarria et al., 2018; Urteaga B. & Pack, 1966).

Further historical records come from ancient Egypt, with the Edwin Smith and the Ebers Papyrus (circa 1600 BCE). These documents describe "bulging masses" and methods for cauterization, hinting at the presence of tumor diseases (Urteaga B. & Pack, 1966). It wasn't until ancient Greece that a specific term was coined for tumors. The word "cancer," or "krakinos" in ancient Greek, was first used by Hippocrates (460-370 BCE) to describe what we now refer to as tumors. Hippocrates drew an analogy between tumors and crabs, from a central mass extending into radial protrusions (Papavramidou et al., 2010). Each "crab paw" represented metastasis, while the central "head" symbolized the primary tumor.

As society progressed and life expectancy increased, modern medicine emerged. The contemporary view of cancer involves cells that have undergone genetic alterations, evading normal regulatory mechanisms and eluding control checkpoints. The global incidence of cancer has been on the rise, prompting the urgent need for a deeper understanding of the disease and the development of effective treatments (Parkin & Parkin, 2001).

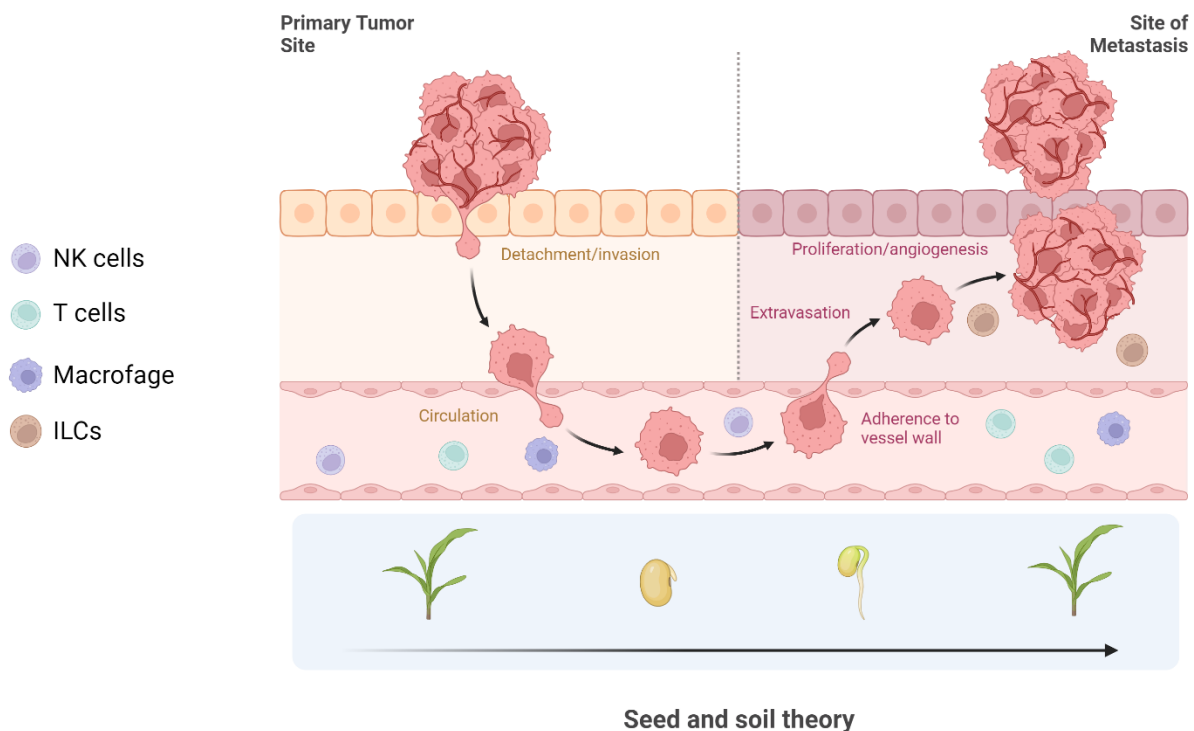


**Figure 4.7:** Tumor progression from primary tumor site to the site of metastasis according to the soil and seed theory. Figure created in Biorender.com.

A fundamental concept in cancer biology is the ability of tumor cells to invade neighboring tissues, a phenomenon known as metastasis. This process was originally conceptualized by Paget in the 1880s, as he observed a non-random distribution among breast cancer patients with metastases. He introduced the "seed and soil" theory (Langley & Fidler, 2011; Paget, 1889). Paget drew a parallel between the biological process of a seed finding fertile ground to grow. Just as a seed, a tumor cell can spread in all directions, but only when it reaches the suitable tissue (the right "soil") with the necessary conditions for survival and growth, can it develop into a new tumor (or "plant"). This analogy portrays cancer as a farmer, seeking the perfect soil for its seeds (Figure 4.7).

Based on Paget's theory, the concept of the tumor microenvironment (TME) emerged to describe the "soil." Research in this area branched into two main directions: angiogenesis and immunology (Witz, 2009).

#### 4.3.1 Neoangiogenesis

Judah Folkman led the research regarding TME vascularization and angiogenesis, which started by the early observation of the presence of angiogenic factors in tumor tissues and tumor antiangiogenesis factors (TAFs) (Ran et al., 1976; Ran & Witz, 1972). Among them, the vascular endothelial growing factor (VEGF), erythropoietin (EPO) or platelet derived growing factor (PDGF) support the growth and irrigation of the tumor. These factors recruit pericytes in the tumor site, which is related to neoangiogenesis. The concept of neoangiogenesis is introduced as the generation of new blood vessels, characterized by an incomplete and fenestrated construction within the tumor (Roberts & Palade, 1997). Thus, it impedes immune cell infiltration, reduces oxygen concentration, and hinders drug supply. Therefore, a research branch became focused on preventing tumor vascularization: the anti-angiogenesis (Folkman, 1972). To date, there are several therapies orientated towards angiogenesis, such as the monoclonal antibody targeting VEGF (Bevacizumab), which showed promising results for different solid tumors including lung, colorectal, liver and renal cell carcinomas (Allegra et al., 2011; Fulgenzi et al., 2022; McDermott et al., 2018).

#### 4.3.2 Tumor microenvironment and immune cells

In parallel to the angiogenesis, there was another early observation about the TME: the infiltration of immune cells, among them, cytotoxic T cells, macrophages and NK cells (Brubaker & Whiteside, 1977; Hersh et al., 1976; Moore & Moore, 1979; Vose et al., 1977). The presence of infiltrating NK cells in the tumor niche is correlated with increased survival and reduced tumor burden (Nersesian et al., 2021).

Initially, the stages of tumor resolution were described in three main stages: elimination (where immune cells act as tumor suppressor); equilibrium (the immune system controls the expansion of carcinogenic cells); and escape (tumor cells mock the immune system and avoid the suppression and progress to clinically apparent cancers) (Koebel et al., 2007). During this process, the surrounding soluble factors have a determinant impact on the activity of infiltrating immune cells.

#### 4.3.2.1 *Pro-inflammatory cytokines*

In addition to the cellular compartment of the TME, there are also soluble factors, such as the tumor associated immunoglobulins (for ex. IgGs and IgM), and complement compounds (Ran et al., 1976; Ran & Witz, 1972; Witz, 2009). Another aspect to highlight is the presence of cytokines, which can play both a pro-inflammatory and an anti-inflammatory role. During the last century, IL-12 was described by Trinchieri's group, reporting IL-12 as a major Th1 skewing factor (Michiko Kobayashi et al., 1989). Few years later, IL-18 was reported by Okamura and colleagues. IL-18 triggers IFN $\gamma$  production in Th1 and Th2 in combination to IL-2 or IL-12 (Okamura et al., 1998). IL-12 and IL-18 are produced by professional antigen presenting cells (Kupffer cells in the liver, dendritic cells and macrophages) and surrounding cells (f. e. epithelial cells) (Michiko Kobayashi et al., 1989; Wolf et al., 1991).

Following the identification of IL-2 receptors, IL-15 was subsequently identified through the work of the Caligiuri group (Carson et al., 1994). It was soon linked to the development and activation of NK cells, and their reliance on IRF-1 activation for proper execution of their inflammatory function (Ogasawara et al., 1998). Within the TME, the presence of myeloid cells producing IL-15 is correlated with a reduction in tumor mass, attributed to immune system activity (Santana Carrero et al., 2019).

Another classical cytokine that was described in the 1980s was IL-6 (Kishimoto, 1989). Conversely, IL-6 supports tumor growth and guides the metastasis site by having a constitutive activation of the oncogene STAT3 in cancer cells, anti-apoptotic signalling and stabilizing p53 (Fisher et al., 2014; Rebouissou et al., 2009). Regarding the role of IL-6 in immunology, its trans signaling acts as a guide for the initiation of CD8<sup>+</sup> T and NK cells infiltration through the capillaries, assisting in bringing them closer to the tumor niche (Dejean et al., 2009; Pedersen et al., 2016).

#### 4.3.2.2 *Anti-inflammatory cytokines*

Despite the pro-inflammatory factors, tumor cells possess evasion mechanisms through the secretion of anti-inflammatory cytokines. Sporn and colleagues described TGF $\beta$  as a protein inducing platelet transformation (Assoians et al., 1983). Later, the work by Massagué reported the direct action of TGF $\beta$  in T cells by repressing cytolytic gene products (Perforin, Granzyme A and B, Fas ligand and IFN $\gamma$ ), which led to an increased tumor burden (Thomas & Massagué, 2005). It was also described how TGF $\beta$  induces the turnover of CD4<sup>+</sup> T cells to Treg phenotype, inducing immunosuppression (Moo-Young et al., 2009). Subsequently, the effect of TGF $\beta$  on NK cells was identified, indicating its role in repressing the gene expression of cytolytic factors (IFN $\gamma$ , TNF $\alpha$ , and GM-CSF) (Bellone et al., 1995). However, Lee group described the imprinting effect on NK cells mediated by TGF $\beta$ , which resulted in hypersecretion of IFN $\gamma$ , contradicting the previously explained inhibitory role (Foltz et al., 2018). Presently, there is still controversy regarding the true role of TGF $\beta$  in NK cells, and since blocking TGF $\beta$  has been associated with cardiac toxicity, there is currently no advanced therapy that inhibits TGF $\beta$  (Larson et al., 2020). Recently, the FDA approved the use of oncolytic adenovirus delivering a TGF $\beta$  neutralizing molecule, further insights are expected in the future (NCT04673942).

In the 1990s the work led by Moore and O'Garra showed a new cytokine: IL-10. It was identified as an inhibitor of cytokine production of Th1 cells by altering macrophages antigen-presentation but not B cells (Fiorentino et al., 1991; Fiorentino et al., 1991). IL-10 has immunosuppressive effects, which are therapeutically interesting for autoimmune diseases (such as graft versus host disease or colitis). On the contrary, it supports cancer growth by inhibiting immune cells (De Vries, 1995). Several approaches have been developed to target it, such as blocking antibodies or CAR-T cells, which have shown promising pre-clinical results (Sullivan et al., 2023).

#### 4.3.3 Patient-derived organoids: A precision model for investigating the tumor microenvironment *in vitro*

As a result of many years of biomedical research, there are many therapies available for the treatment of patients suffering of cancer diseases (e. g. surgery, chemotherapy and personalized therapy). Nevertheless, a subset of patients fails to respond to these therapies, experiencing aggressive relapses and disease progression. Therefore, one of the main challenges in the cancer research field is to match predictive therapies to each patient, allowing a personalized approach. In the recent decades, a novel *in vitro* approach has been developed: patient-derived organoids (PDOs) or tumoroids. The biopsies of the tumors of the patients are processed and stimulated to differentiate into a 3D structure (using matrigel or basal membrane extract as scaffold). PDOs maintain the stem-cell entities and self-renewal of the tumor growth in a 3D manner, keeping the genetic background of the patients (Sato et al., 2011; Weeber et al., 2015). Currently, there are many studies assessing the use of PDOs platforms to test new therapies, such as chemotherapeutical agents or monoclonal antibodies (Betge et al., 2022; Ooft et al., 2019).

### 4.4 HYPOXIC ENVIRONMENTS: THE IMPACT OF OXYGEN CONCENTRATION ON NK CELLS

The concentration of oxygen and the process of aerobic respiration have played a pivotal role in the development of life on our planet. Since prehistoric times, when oxygen concentration stabilized at 21 % in Earth's atmosphere, these percentages have remained relatively constant. However, there are other "atmospheres" present in our planet: various biological compartments, including organs and blood vessels have their own gas composition. Among them, in the human body, a variety of oxygen percentages exists depending on its gas exchange between cells (Carreau et al., 2011)(refer to Figure 4.8). Solid tumors show reduced oxygen percentages (< 1 %), which is induced by the fast-metabolism of tumor cells (known as the Warburg effect) and the lack of a healthy vascular net (Garcés-Lázaro et al., 2022).

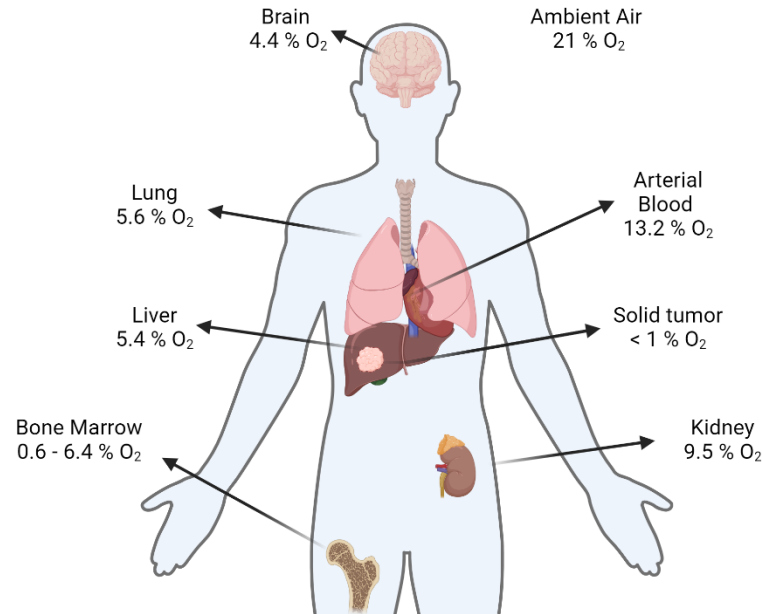


**Figure 4.8:** Concentration of oxygen distributed within tissue compartments. Figure adapted from Carreau et al. (Carreau et al., 2011). Figure created in Biorender.com.

#### 4.4.1 Hypoxia inducible factors

As a swimming fish that gets out of the sea and starts seeking for water and having spasms, cells also activate a specific pathway when oxygen concentration drops. The nobel Prize awarded scientists Kaelin, Ratcliffe, and Semenza dedicated their careers explaining how and why the activation of hypoxia-specific pathways are regulated. Semenza reported the existence of certain proteins, which were present only under hypoxia (1 % oxygen), naming them as hypoxia-inducible factors (HIFs). He described HIF-1 $\alpha$  as oxygen sensitive and ARNT (HIF-1 $\beta$ ) as oxygen independent, which later was correlated with angiogenesis gene triggering and embryonic development (Semenza, 2000; G. L. Wang & Semenzas, 1993). Later on, two additional HIFs were described: HIF-2 $\alpha$ , HIF-3 $\alpha$ , and HIF-1 $\beta$  (Masoud & Li, 2015). While HIF-1 $\alpha$ , HIF-2 $\alpha$ , and HIF-1 $\beta$  are expressed in nearly all tissues, HIF-3 $\alpha$  is primarily found in corneal epithelium and functions as a negative regulator of HIF-1 $\alpha$  and HIF-2 $\alpha$ .

The exact regulation of the factors was unraveled by Kalein and Ratcliff, who discovered Von Hippel Lindau protein (VHL) (Hon et al., 2002; Stebbins et al., 1999). VHL, an ubiquitin ligase, becomes activated by -OH groups on specific proline residues of HIF-1/2 $\alpha$  (Pro-402 and Pro-564 for HIF-1 $\alpha$ , Pro-405 and Pro-531 for HIF-2 $\alpha$ ) (Hon et al., 2002; Ratcliffe, 2007). VHL subsequently recruits the elongin-C/elongin-B/cullin-2 E<sub>3</sub> ubiquitin ligase complex, leading to the degradation of HIF-1/2 $\alpha$  by the 26S proteasome (Ivan MKondo et al., 2001; Stebbins et al., 1999).

In addition, there are more HIFs regulators, such as the factor inhibiting HIFs (FIH). FIH, an asparagine hydroxylase, interacts with asparagine residues in HIF-1 $\alpha$  (Asn-803) and HIF-2 $\alpha$  (Asn-851), inhibiting their interaction with p300 and thereby repressing translational activation of HIF-1/2 $\alpha$  (Hewitson et al., 2002; Mahon et al., 2001).

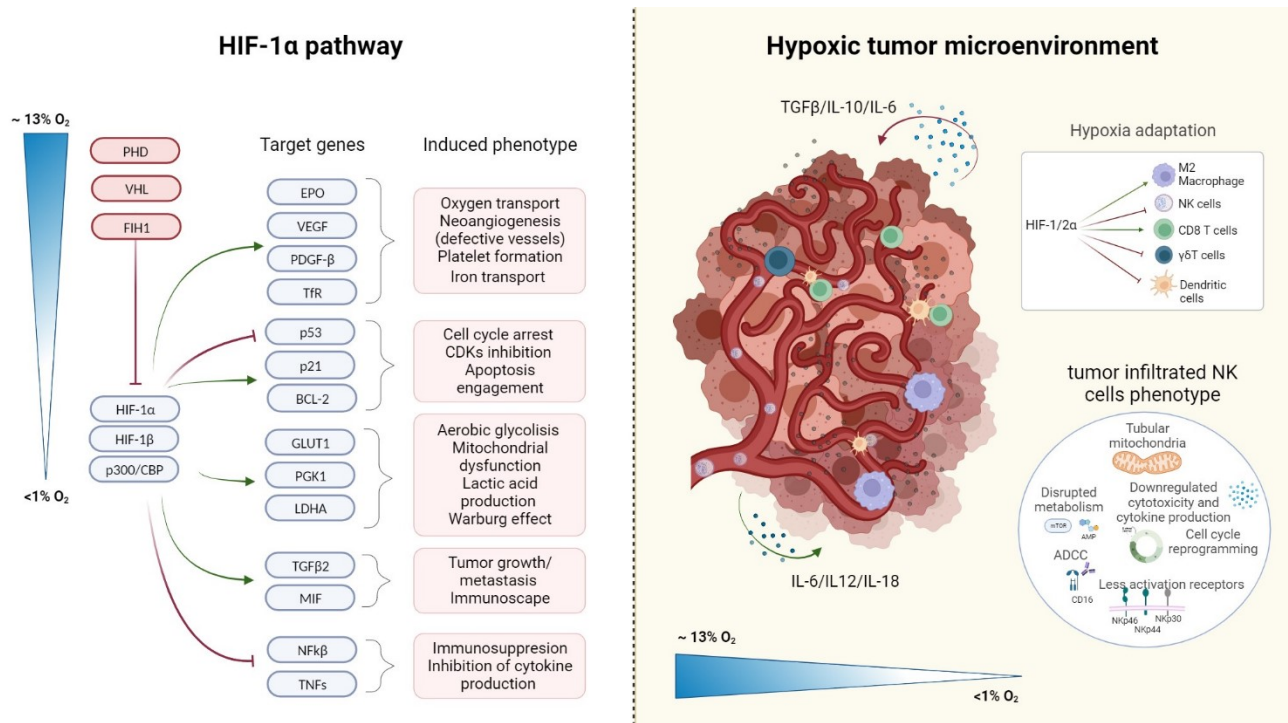


**Figure 4.9:** HIF-1 $\alpha$  pathway genes and HIFs influence in tumor infiltrating immune cells. Adapted from (Garcés-Lázaro et al., 2022). Created in Biorender.com.

Additionally, there are oxygen-independent mechanisms involved in the regulation of HIFs, exemplified by the hypoxia-associated factor (HAF). HAF, an E<sub>3</sub> ubiquitin ligase, binds to HIF-1 $\alpha$  within amino acids 296-400 region of HIF-1 $\alpha$  and marks it for ubiquitination, subsequently triggering proteasome-dependent degradation of HIF-1 $\alpha$  protein (Hewitson et al., 2002). Another regulator of HIF-1 $\alpha$  reported in literature is the heat shock protein 90 (Hsp90). Hsp90 interacts with HIF-1 $\alpha$  and activates E<sub>3</sub> ubiquitin ligases, promoting HIF-1 $\alpha$  degradation both in normoxia and hypoxia (Ehrlich et al., 2008). Furthermore, Prof. Yeh and colleagues showed that the VHL-mediated degradation of HIF-1/2 $\alpha$  is also sensitive to SUMOylation, enabling VHL binding to HIF-1/2 $\alpha$  without hydroxyproline. This process can be reversed by SENP1, which inhibits SUMOylation and induces HIF-1 $\alpha$  stabilization (Cheng et al., 2007; Yeh, 2009).

In normoxic conditions, HIF-1/2 $\alpha$  factors are primarily degraded or remain inactive. In contrast, under hypoxic conditions, the inhibition of HIF-1/2 $\alpha$  protein stabilization is less pronounced than in normoxia. As a result, HIF-1/2 $\alpha$  forms complexes with HIF-1 $\beta$  and p300/CBP coactivators, translocates to the nucleus, and initiates the transcription of target genes. These target genes include those involved in: cell cycle regulation (CDKN1A and CDKN1B); anaerobic metabolism, lactic acid production, and mitochondrial dysfunction (GLUT1, PGK1, and LDHA); oxygen transport, neoangiogenesis, and platelet formation (EPO,

VEGF, ARNT, CITED2, TGF- $\beta$ , and Tfr) and tumor growth, immunosuppression, and cell migration (TGFB2) (Garcés-Lázaro et al., 2022) (Figure 2).

#### 4.4.2 Immune cells exposed to hypoxia

The study of the effects of hypoxia or hypoxia-inducible factors (HIFs) in immune cells has flourished in recent decades, providing deeper insights into how immune cells respond to the tumor microenvironment. Two recent studies shed light on the impact of HIFs, and presumably hypoxia, on CD8<sup>+</sup> T cells. Palazon et al. demonstrated that genetic depletion of HIF-1 $\alpha$  in cytotoxic T cells led to a reduction in the production of soluble factors and infiltration into melanoma tumors (Palazon et al., 2017). In a separate study, researchers, led by Prof. Johnson, genetically engineered human CD19 CAR-T cells to ectopically express HIF-2 $\alpha$ , resulting in improved tumor clearance. Interestingly, overexpression of HIF-1 $\alpha$  had no discernible effect on CD8<sup>+</sup> T cells (Veliça et al., 2021).

While HIFs appear to provide substantial support for the response of CD8<sup>+</sup> T cells to tumors, regulatory T cells (Tregs) exhibit a different phenotype. Moo-Yong and colleagues reported that HIF-1 $\alpha$  activation induced Tregs to adopt an immunosuppressive role, driven by IL-6 cytokine within the tumor microenvironment. HIF-1 $\alpha$  exhibited a cooperative effect with TGF $\beta$ , promoting Foxp3 transcription while simultaneously inducing ROR $\gamma$ t and IL-17 production at the transcriptional level (Miska et al., 2019).

In the context of NK cells, exposure to hypoxia resulted in reduced cytokine secretion, although the CXCR4 marker was upregulated, correlating with increased migration (Fiegl et al., 2009; Parodi et al., 2018). Conversely, hypoxia exposure led to the downregulation of Nkp44, Nkp46, Nkp30, and NKG2D protein and RNA expression, while leaving CD16 and antibody-dependent cell-mediated cytotoxicity (ADCC) activity unaltered (Balsamo et al., 2013).

Another investigation revealed that murine NK cells lacking HIF-1 $\alpha$ , due to Ncr1-Cre-mediated knockout, contributed to non-productive angiogenesis within the tumor microenvironment. This was associated with a noticeable decrease in the infiltration of HIF-1 $\alpha$ -deficient NK cells expressing the angiostatic soluble VEGFR-1 within the tumor, resulting in elevated VEGF levels in the tumor milieu. Despite a reduction in primary tumor size, these tumors displayed compromised vascularization, leading to increased tumor metastasis and a decrease in immune cell presence (Krzywinska et al., 2017).

Our group reported the role of HIF-1 $\alpha$  as an immune checkpoint in murine NK cells. HIF-1 $\alpha$ -deficient NK cells exhibited enhanced control of tumor burden compared to control NK cells. Tumor-infiltrating NK cells from the HIF-1 $\alpha$ -deficient group showed increased transcriptional expression of IFN $\gamma$  and NF $\kappa$ B at the single-cell level. Our group unraveled a mechanism linking IL-12/18 to IL-18 receptor and NF $\kappa$ B activation, which in turn triggers IFN $\gamma$  production. HIF-1 $\alpha$  acts as a negative regulator of this pathway, inhibiting IFN $\gamma$  production and thus blunting the immune response against tumor cells (Ni et al., 2020).

Interestingly, HIF-1 $\alpha$ 's role in NK cells extends to other pathological contexts, such as wound healing or cytomegalovirus (CMV) infection. Prof. Stockmann's group reported worsened

bacterial infection outcomes in skin wounds when using mice with a deficiency of HIF-1 $\alpha$  in NKp46<sup>+</sup> cells, while the opposite phenotype was observed in a mouse line with VHL-deficient NK cells (Sobecki et al., 2021). Additionally, Prof. Yokoyama's group highlighted the significance of HIF-1 $\alpha$  in regulating the metabolic reprogramming of NK cells to facilitate antiviral responses against MCMV infection (Victorino et al., 2021). Nevertheless, the use of HIF-1 $\alpha$  for therapy in human NK cells holds promise but is not yet completely understood.

## 4.5 NEW IMMUNOTHERAPIES

In the last decades, there have been many discoveries that improve the biomedical therapies. For example, the last laureates for the Nobel Prize in Physiology or Medicine, Karikó and Weissman settled the ground for the mRNA-based vaccines, which lead the herd immunity against COVID-19 in the past years (Karikó et al., 2005, 2008). For a scientist in 1990s, an mRNA vaccine would seem impossible. However, the engine that keeps translational science in motion is the application of “old concepts” (such as mRNA) into new therapies (such as COVID-19 vaccines).

Much like the global COVID-19 pandemic, which has seen a total of 696 million cases to date, was ameliorated through vaccination, cancer patients can likewise gain advantages from the integration of cutting-edge technologies into oncological treatments, aimed at diminishing mortality rates.

### 4.5.1 Adoptive cell therapies: Chimeric Antigen Receptor cells

In a scenario akin to how a Roman warrior would need to adapt their strategies when facing an elephant or even an army of legionnaires encountering 50 elephants, the need for an adjustment in the battle against tumor cells becomes apparent. Just as Scipio devised an unconventional strategy to defeat Hannibal's elephants by using trumpet and drum music to scare the animals into retreat, we face an analogous challenge in the world of immunology.

In our immune system, the patrolling army consists of natural killer (NK) and T cells, which are adept at handling typical threats. However, tumor cells, being massive and abnormal cell masses, pose an unusual challenge when juxtaposed with a healthy cell. Scientists like Zsch and Gross proposed a novel “weapon” to harness immune cells specifically against tumor cells, laying the groundwork for Chimeric Antigen Receptor cells (CAR cells) (Eshhar et al., 1993; Gross et al., 1989; Gross & Eshhar, 2016).

Zsch, alongside colleagues, observed that although tumor-specific lymphocytes were scarce, and tumors had their own immune evasion mechanisms, there were patented antibodies with strong binding affinity to tumor ligands. They ingeniously combined the variable regions of these antibodies with the constant regions of the T-cell receptor (TCR). This innovation ensured the preservation of the natural cytotoxicity triggered by the TCR-activated pathway, but with the flexibility to target a variety of antigens depending on the linked antibody (Eshhar et al., 1993; Gross et al., 1989). In this way, the development of CAR cells mirrors Scipio's adaptation to confront an unconventional adversary, using innovative strategies to combat an extraordinary challenge within the field of immunotherapy.

In the early 2000s, it became evident that the Chimeric Antigen Receptor (CAR) constructs, comprising only the antibody and T-cell receptor (TCR) components, was insufficient to elicit a sustained anti-tumor response. To address this limitation, the introduction of a co-stimulatory domain into the genetic sequence was proposed as a solution. The first co-stimulatory domain explored was CD28, a co-stimulatory activation domain used by professional APCs cells to activate T cells. Second-generation CARs using CD28 as co-stimulatory domain were tested in murine naïve T cells against the 2,4,6-trinitrophenyl (TNP) skin antigen (Friedmann-Morvinski et al., 2005). CAR T cells equipped with the CD28 co-stimulatory domain exhibit enhanced functionality when compared to the first-generation CAR constructs.

This approach has gained widespread adoption, especially when combined with CD19-targeted T cells designed to combat leukemia tumor cells (Kowolik et al., 2006). The work led by Campana suggested that second-generation constructs were not limited to the CD28 co-stimulatory domain, but instead, they pointed to 4-1BB (CD137) as an activating intracellular domain. They engineered anti-CD19-4-1BB-CD3 $\zeta$  T cells, which exhibited improved tumor responses compared to the first-generation anti-CD19-CD3 $\zeta$  T cells (Imai et al., 2004). A comparison between the 4-1BB and CD28 as co-stimulatory domains emerged years later, demonstrating that both constructs efficiently induced complete remission in patients. However, the CD28 construct cohort exhibited a higher incidence of cytokine-release syndrome and neuroinflammation disorders, leading to the conclusion that the usage of 4-1BB as a co-stimulatory domain in CAR-T cells might be more beneficial (Ying et al., 2019). To date, 944 clinical trials are ongoing worldwide using CAR-T therapies being 70 of them developed in Europe (Clinicaltrials.gov). The European Medicines Agency has approved a total of 5 CAR-T cell therapies (Table 1) (Committee for Medicinal Products for Human Use, 2022; European Cancer Patient Coalition, 2022; European Medicines Agency, 2021a, 2021b). On the other hand, there are currently 39 clinical trials assessing CAR-NK cells therapy in USA and China (Clinicaltrials.gov).

APPROVED CAR-T CELL THERAPIES IN EUROPE			
Product	Target	Co-stimulatory domain	Company
Abecma® Idecabtagene Vicleucel	BCMA Myeloma cells	CD8a, 41-BB	BMS
Breyanzi® Lisocabtagene maraleucel	CD-19 <sup>+</sup> B cells	CD28, 41-BB	BMS
Carvykti® Ciltacabtagene autoleucel	BCMA- myeloma B cells	CD8a, 41-BB	Janssen Biotech
Kymria® Tisagenlecleucel	CD-19 <sup>+</sup> B cells	41-BB	Novartis
Yescarta® Axicabtagene ciloleucel	CD-19 <sup>+</sup> B cells	CD28	Kite/Gilead

**Table 4.1:** Approved CAR-T cell therapies in Europe (2022).

#### 4.5.1.1 New CAR generations

To date, CAR generations have continued to evolve, culminating in the development of fourth-generation CARs (Chmielewski & Abken, 2020). Fourth-generation CARs encompass an additional gene modification, in addition to the co-stimulatory domains and the tumor antigen recognition domain, with the aim of fine-tuning the CAR immune cells (see Figure 4.10).

Nearly a decade ago, Stasi, Tey, and colleagues reported a novel "suicide cassette" added to a construct targeting CD19 (anti-CD19 CAR T cells), which effectively prevented host-versus-graft disease (Stasi et al., 2011). The control of cell death was achieved by modifying the caspase 9 domain, known as iCasp9, which lacks dimerizing capacity but contains a binding domain for the drug AP1903. The addition of AP1903 induced the formation of iCasp9 homodimers, triggering apoptosis, while in the absence of AP1903, the CD19-CAR T cells retained their cytotoxic capacity. As of today, this approach has undergone Phase I clinical trials targeting B cell malignancies (X. Zhou et al., 2020). By incorporating the suicide chemical switch, strict antigen selection can be expanded, as seen in the case of FLT3, which is expressed in melanoma cells and hematopoietic progenitor cells.

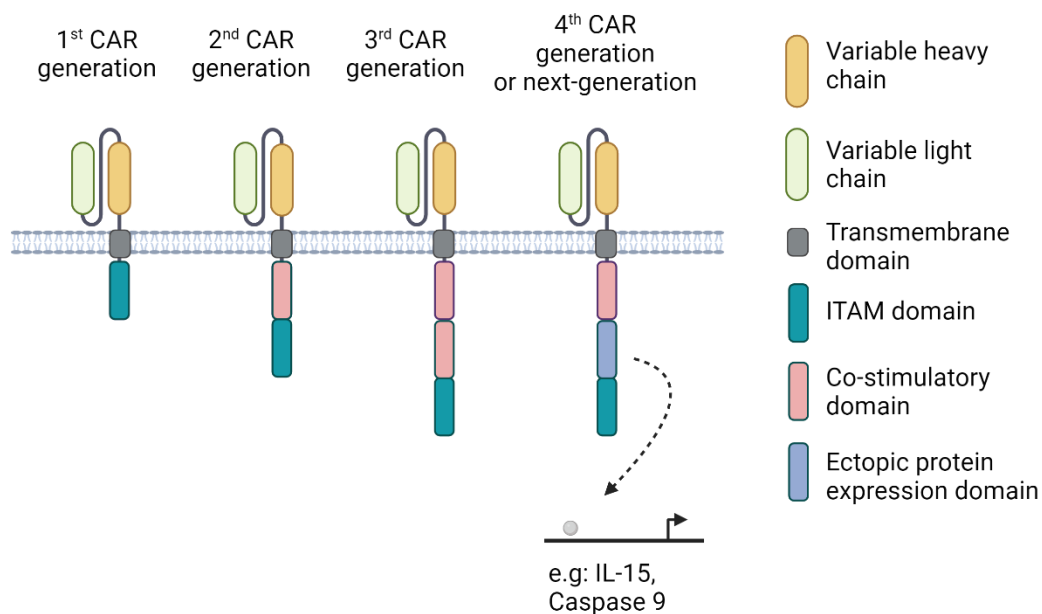


**Figure 4.10:** Generations of CAR constructs and structure. Created in Biorender.com.

While CAR-T cell therapies hold promise as a clinical approach for treating B-cell malignancies, there are challenges that hinder their applicability to a broader range of tumor types. One of the primary obstacles is the development of cytokine release syndrome (CRS) and immune effector cell-associated neurotoxicity syndrome (ICANS), which not only prolong the patient's medical care but also increase the associated economic costs. Another limitation is the reliance on autologous T cells, which are often unresponsive in cancer patients. Although allogeneic T-cell CAR-T cells can be produced, they require further

editing of the T-cell receptor (TCR) to prevent TCR-mediated graft-versus-host disease (GVHD). In this regard, natural killer (NK) cells emerge as a promising alternative due to their variety of tumor-sensitive receptors and their potential as an off-the-shelf cellular therapy (Daher & Rezvani, 2021).

Pre-clinical results using anti-FLT3 CAR NK-92 cells carrying iCasp9 suggest effective control of the CAR NK-92 cells, minimizing off-target responses and preventing the killing of progenitor cells (Oelsner et al., 2019). Although there was an ongoing Phase I/II clinical trial testing CD-19-CD28-iCasp9-IL-15 transduced cord blood NK cells in patients with B cell lymphoma, the trial was withdrawn in 2020 due to lack of funding (NCT03579927). Rezvani's group proposed a combined approach, involving the transduction of cord blood-derived NK cells with an anti-CD19 CAR construct and an autocrine production of IL-15. Additionally, CRISPR/Cas9-mediated targeting of the major inhibitor of the IL-15-triggered pathway, cytokine-inducible Src homology-2 containing protein (CISH), resulted in a sustained response for up to 7 months after the adoptive transfer of CD19-IL-15-CISHKO-NK cells into humanized mice with injected Raji tumor cells (CD19<sup>+</sup> B cells) (Daher et al., 2021). The constant updating of the CAR constructs indicates more clinical trials and therapies in the upcoming years, being specially promising for treating leukemias and lymphomas.

#### 4.5.1.2 *Targeting solid tumors: HER-2 tumor antigen*

In the history of science, there have been moments when the distinction between scientific audiences and the general public has blurred. This phenomenon was particularly evident when Charles Darwin famously asserted that 'man comes from the ape,' a statement that triggered significant public discourse. An iconic episode in this context was the renowned evolution debate between Wilberforce and Huxley in Oxford, symbolizing the societal division between anti-Darwinism (represented by Wilberforce) and pro-Darwinism (championed by Huxley) (Lucas, 1979).

Centuries later, public interest in debates has waned compared to the allure of films and social media. In 2008, the story of a significant tumor antigen discovery was brought to the big screen in the form of the movie 'Living Proof.' This film showcased the research of Dr. Slamon, a scientist who was seeking a cure for breast cancer in the 1980s. It elucidates how Slamon's work led to the identification of the Herceptin receptor 2 (HER-2), which was found to be constantly amplified in the gene *ErbB2* in 25-30 % of breast cancer patients (Slamon et al., 1987). Moreover, increased expression of HER-2 protein was linked to poorer survival outcomes. HER-2 belongs to the *ErbB* receptor family, which includes HER-1, HER-2, HER-3, and HER-4. HER-2 features a tyrosine kinase domain and forms heterodimers with its family members, triggering cell survival, proliferation, and cell cycle progression (Groenen et al., 1994).

Following Dr. Slamon's pioneering work, the use of monoclonal antibodies targeting HER-2 in breast cancer patients marked one of the initial successes in tumor-specific therapy, exemplified by Trastuzumab (Ennis S Lamon et al., 2001; Molina et al., 2001). Trastuzumab specifically targeted HER-2, preventing heterodimer formation and inhibiting the HER-2 pathway. Nevertheless, its specificity was not universally applicable, as some tumors had insufficient basal expression of HER-2 to respond to Trastuzumab. A second-generation HER-

2 monoclonal antibody, Pertuzumab, was developed, targeting a distinct epitope of HER-2 by directly binding to the dimerization domain. This enabled the treatment of patients with lower HER-2 surface expression compared to Trastuzumab (Clynes et al., 2000; Franklin et al., 2004; Swain et al., 2015). Today, the combination of Pertuzumab with Trastuzumab is used as a neoadjuvant therapy for breast cancer patients, leading to an 18-month increase in life expectancy compared to placebo treatment (Boix-Perales et al., 2014).

However, the use of monoclonal antibodies may trigger side effects through antibody-dependent cellular cytotoxicity (ADCC), which, when combined with a neoadjuvant application, results in a rather aggressive treatment (Franklin et al., 2004). Consequently, the field of CAR-engineered T and NK cells using HER-2 as a target ligand has become a prominent approach in the treatment of solid tumors. I had the opportunity to work on a project involving the transduction of HER-2 CAR T cells using a switchable system through an antibody bridge, which yielded successful pre-clinical results in humanized mice carrying patient-derived xenografts from pancreatic ductal adenocarcinoma (Raj et al., 2019). HER-2 CAR T cells have also been successfully employed in a case report involving a child with rhabdomyosarcoma (Hegde et al., 2020). A similar construct was utilized in the NK-92 cell line, demonstrating successful pre-clinical results (Nowakowska et al., 2018). Moreover, HER-2 targeted therapy has been shown to induce cardiac side effects, owing to the expression of HER-2 in cardiomyocytes. In this regard, there exist specific medical guidelines tailored to monitor cardiac effects in patients treated with monoclonal antibodies against HER-2 (Florido et al., 2017). In summary, HER-2 represents a promising candidate for the development of enhanced CAR-based therapies, which is one of the key findings from this study.

## 4.6 NK CELLS ENGAGERS

In the 1990s, the concept of immune checkpoints gained prominence. Allison's research team confirmed the existence of a T-cell-associated protein termed "cytotoxic T lymphocyte antigen 4" (CTLA-4) (Leach et al., 1996). Blocking CTLA-4 triggers an amplified T-cell response against tumor cells. Subsequently, in 2011, a CTLA-4 checkpoint inhibitor received approval for treating metastatic melanoma and is currently under investigation for other solid tumors, showing promising outcomes (Hammers et al., 2014; Weber et al., 2019).

Another significant checkpoint are PD-1 and PD-L1, whose therapeutic blockade has been evaluated in various solid tumors. PD-1 was initially identified in 1992 by Honjo and colleagues, following their observation of PD-1 overexpression in apoptotic CD8<sup>+</sup> T cells (Ishida et al., 1992). Shortly after, the ligand PD-L1 was characterized, elucidating the PD-1/PD-L1 inhibition axis (Freeman et al., 2000). Tumor cells expressing PD-L1 engage PD-1 on CD8<sup>+</sup> T cells, leading to their inhibition, thus promoting immune evasion.

Following the advent of first-generation inhibitors (ipilimumab for CTLA-4 and nivolumab/pembrolizumab for PD-L1), subsequent generations emerged, expanding the utility of checkpoint inhibitors in patient treatment. Presently, there are 1173 ongoing clinical trials employing PD-L1 inhibitors (499 in Europe) (clinicaltrials.gov). In summary, the

introduction of "classical" checkpoint inhibitors presented a novel approach to target tumor antigens, fostering ongoing exploration and advancement in the field.

The use of specific antibodies continued being applied to target various ligands, including EGFR (Cetuximab) and CD20 (Rituximab) (Chames & Baty, 2009; Perez et al., 1985; Staerz et al., 1985), in addition to the well-known HER-2 targeting antibodies and checkpoint inhibitors. However, in 1995, Mack and colleagues introduced a novel molecule structure that fused an anti-CD3 single-chain variable fragment (scFv) to an anti-EpCAM (tumor antigen), leading to the activation of peripheral T lymphocytes against EpCAM<sup>+</sup> tumor cells (Mack et al., 1995). This innovative approach of bridging immune cells with tumor cells using small molecules was further expanded, with significant contributions from the group led by Professor Bauerle.

The first bispecific T cell engager (BiTEs) to gain approval was Blinatumomab in 2009, which targeted the CD19 tumor antigen and demonstrated substantial efficacy in Phase I/II/III clinical trials for patients with B cell malignancies, while minimizing off-site cytotoxicity (Bargou et al., 2008; Dreier et al., 2003). Solitomab, an EpCAM-targeting engager, is currently undergoing clinical trials and has shown promising results in refractory solid tumors (Brischwein et al., 2006; Kebenko et al., 2018; Schlereth et al., 2005). In 2023, the European Medicines Agency approved the use of Glofitamab, an anti-CD20 engager, for the treatment of B cell malignancies (Hutchings et al., 2021).

In the context of NK cells, the field of engagers is primarily led by the groups of Miller in the USA and Vivier in the EU. The Miller group has developed a new generation of bispecific or trispecific killer cell engagers (BiKEs or TriKEs) that target the CD16 receptor on NK cells, which triggers antibody-dependent cellular cytotoxicity (ADCC), in addition to the desired tumor antigens. Notable examples include the CD16-CD33 BiKE, which elicited a specific NK cell response against myelodysplastic tumor cells *in vitro* and *in vivo*, with enhanced efficacy through ADAM17 inhibition (a protease that sheds CD16 from the cell surface) (Gleason et al., 2014; Wiernik et al., 2013). The CD16-CD19 BiKE was further equipped with a second tumor antigen target, CD22, becoming a TriKE (CD16-CD19-CD22), which demonstrated similar efficacy to Rituximab *in vitro* against human B cell leukemia (Gleason et al., 2012). Several TriKEs molecules are currently being tested, including those combining CD16-IL-15, such as the TriKE targeting mesothelin in lung cancer or TEM8, a pan-cancer tumor-specific antigen (Kaminski et al., 2022; Kennedy et al., 2023). The B7H3-targeted CD16-IL-15 TriKE has shown promising results in expanding and activating NK cells, with no observed off-target-cytotoxicity associated with recombinant human IL-15 infusion in patients (J. S. Miller et al., 2022). A planned clinical trial using this molecule is expected to commence in 2024.

The group led by Vivier (Innate Pharma CSO) has taken a similar approach and named their product "natural killer cell engager" (NKCE), now in its third generation (Demaria et al., 2021). Using Nkp46 or Nkp30-CD16 NKCE against three different tumor antigens, *in vitro* results have shown enhanced cytotoxicity of NK cells when compared to Obinutuzumab, Cetuximab, and Rituximab against CD20<sup>+</sup>, EGFR<sup>+</sup>, and CD19<sup>+</sup> tumor cell lines, respectively (Colomar-Carando et al., 2022; Gauthier et al., 2019). The NKCE molecule targeting CD123 in acute myeloid leukemia has demonstrated promising results *in vitro* and *in vivo*, supporting

future clinical testing (Gauthier et al., 2023). Another NK cell engager product is the tetraspecific antibody-based natural killer cell engager (ANKET), which stimulates NK cells using Nkp46-CD16-IL2R $\beta$  and targets the CD20 tumor antigen, effectively resolving B cell malignancies both *in vitro* and *in vivo* (Demaria et al., 2022).

In conclusion, modern immunotherapies encompass three main branches: monoclonal antibodies, CAR-T cells, and engagers.

## 5 AIMS OF THE STUDY

---

Environmental conditions significantly influence the phenotype and function of immune cells, particularly oxygen concentrations that exist within tissues and organs have been reported to affect both the adaptive and the innate immune system. Oxygen concentration below 1 % is prevalent in solid tumors as a result of the unhealthy vasculature and the high oxygen demands that fuel the fast metabolism of tumor cells. The transcription factor hypoxia-inducible factor 1- $\alpha$  (HIF-1 $\alpha$ ) plays a key role in immune cell adaptation to hypoxia.

Natural killer (NK) cells, crucial for tumor surveillance, often lose functionality in the hypoxic microenvironment of solid tumors, necessitating enhanced immunotherapies. However, human primary NK cells pose challenges for genetic modification.

This study posits that hypoxia and HIF-1 $\alpha$  activity influence how human primary NK cells respond to targets and cytokines. The study aims are as follows:

1. Major Aim: Investigate the effect of hypoxia on human NK cells and mitigate its negative effects by targeting HIF-1 $\alpha$  to develop primary human CAR-NK cells capable of efficiently targeting solid tumor cells.
2. Secondary Aims:
  - a. Assess the effects of hypoxia on cytokine-induced memory-like NK cells.
  - b. Develop a protocol to transfect human primary NK cells using the CRISPR/Cas9 ribonucleoprotein system.

This study aims to propose innovative immunotherapeutic approaches using human primary NK cells within the context of solid tumors with low oxygen concentration. Additionally, the developed transfection method could be applied to other immune cells and desired targets, facilitating the study of proteins and genes in primary immune cells.

## 6 MATERIAL AND METHODS

### 6.1 CELL CULTURE MEDIA, REAGENTS AND BUFFERS

CELL CULTURE MEDIA		
Media	Company	Catalogue no.
CellGenix® GMP SCGM Serum-free Stem Cell Growth Medium for Hematopoietic Stem and Progenitor Cells, NK Cells and CIK Cells	Cell Genix	20802-0500
Dulbecco's Modified Eagle's Medium (DMEM) with Glucose, L-glutamine, Sodium pyruvate, and Sodium bicarbonate	Sigma-Aldrich	D6459
Gibco™ Advanced DMEM/F-12	Thermo Fisher Scientific	12634010
Gibco™ Opti-MEM™ Reduced Serum Medium	GIBCO-Invitrogen	31985047
Gibco™ RPMI 1640 Medium	Fisher Scientific	11530586
McCoy's 5A (Modified) Medium	Thermo Fisher Scientific	16600082
NK MACS® Medium	Miltenyi Biotec	130-114-429
CELL CULTURE REAGENTS AND BUFFERS		
Reagent	Company	Catalogue no.
[Leu15]-Gastrin I human	Sigma-Aldrich	G9145-.1MG
A-83 01	Sigma-Aldrich	SML0788-5MG
Accutase cell detachment solution	Sigma	SCR005
BME	Bio- Techne	3433-010-R1
Dimethylsulphoxide Hybri Max™ (DMSO)	Sigma-Aldrich	D2650
Dulbecco's Phosphate Buffered Saline (PBS)	GIBCO-Invitrogen	14190
Fetal Bovine Serum, Origin: EU Approved 10270	GIBCO-Invitrogen	10270
Gibco™ B-27™ Supplement (50X), serum free	Gibco-Invitrogen	17504001
GlutaMAX™ Supplement	Thermo Fisher	35050061

	Scientific	
hEGF	Sigma-Aldrich	E9644-5X.2MG
HEPES (1M)	Gibco-Invitrogen	15630056
Horse Serum, heat inactivated, New Zealand origin	Thermo Fisher Scientific	26050088
Human Serum, sterile filtered	Pancoll-biotech	P30-2401
L-Glutamine 200 mM (100x)	GIBCO-Invitrogen	25030
N-Acetyl-L-cysteine	Sigma-Aldrich	A9165
Nicotinamide	Sigma-Aldrich	N0636
NOGGIN ( Cell Culture), recombinant Human	Peprtech	120-10C-20
Penicillin/Streptomycin Solution	GIBCO-Invitrogen	15140
Primocin®	Invivogen	ant-pm-05
Prostaglandin E2	Biomol	Cay14010-5
SB 202190	Biomol	Cay10010399
Seahorse™ XF 1.0 M Glucose Solution	Agilent	103577-100
Seahorse™ XF RPMI media & Calibrant	Agilent	103576-100
TrypLE Express Enzyme (1X)	Gibco-Invitrogen	2072325
Trypsin-EDTA (1x) HBSS, without Ca <sup>2+</sup> /Mg <sup>2+</sup> with EDTA	GIBCO-Invitrogen	25300
UltraPure™ 0,5M EDTA, pH 8	Invitrogen	15575020
Y-27632 (hydrochloride)	Biomol	Cay10005583
β-mercaptoethanol	GIBCO-Invitrogen	31350010

**Table 6.1:** Media and reagents used in cell culture.

## 6.2 CHEMICALS

CHEMICALS AND BIOLOGICAL REAGENTS		
Cell line	Company	Catalogue no.
7-AAD	BD Bioscience	15868458
Ampicillin	Sigma-Aldrich	A9518-25G
Aqua Zombie™	Biolegend	423102
BioCat Universal Agarose	BioCat	AGA500-BCAT

BioColl® 500	Bio&Sell	BS.L 6115
spCAS9 2NLS Nuclease	Synthego	S-M23584-01
Electrolytic Buffer E2	Thermo Fisher Scientific	MPK10096
GeneRuler DNA Ladder Mix-5x50 µg	Thermo Fisher	SM0331
GolgiPlug™ Protein Transport Inhibitor (containing Brefeldin A)	BD Bioscience	555029
GolgiStop™ Protein Transport Inhibitor (containing Monensin)	BD Bioscience	554724
Human IL-2	Hoffmann-La Roche	1104-0890
Human TruStain FcX™	Biologend	422302
Image-iT™ Green Hypoxia Reagent	Thermo Fisher	I14834
Incucyte Cytotox Red Dye	Sartorius	4632
Ionomycin	Sigma-Aldrich	I3909
LB Broth (Lennox)	Sigma-Aldrich	L3022-1KG
LB Broth with agar (Miller)	Sigma-Aldrich	L3147-250G
Midori Green Advance	Biozym Scientific	617004
Nuclease-free Water (not DEPC treated)	Ambion	AM9937
Percoll®	GE Health	17-0891-01
Phorbol-12-myristat-13-acetat (PMA)	Sigma-Aldrich	P1585
Poly-D-Lysine	Sigma	P6407
Protamine Sulfate	VWR International	SAFSP3369
Recombinant Human IL-12 p70 (CHO derived)	Peprtech	200-12
Recombinant human IL-15	PeprTech	200-15
Recombinant human IL-18	MBL	B003-5
Recombinant human IL-1β	Immunotools	11340013
Resuspension Buffer R	Thermo Fisher Scientific	MPK10096
Resuspension Buffer T	Thermo Fisher Scientific	MPK10096
TBK1/IKKε inhibitor (BX795)	Invivogen	1000424
β-mercaptoethanol	VWR chemicals	0482-100ML

**Table 6.2:** Chemicals and biological reagents used.

### 6.3 CELL LINES, PRIMARY CELLS AND BACTERIA STRAIN

CELL LINES CULTURE			
Cell line	Cell type	Medium	Provider/Reference
A-375	Human malignant melanoma (NRAS mutant)	RPMI	Prof. Michael Boutros (DKFZ, Heidelberg, Germany)
HEK293T	Human embryonic kidney line transformed with SV40 large T Ag	DMEM	Prof. Carsten Watzl (ifADO, Dortmund, Germany)
HT-29	Human colorectal adenocarcinoma	5X McCoy's	Purchased at DSMZ (AC299)
K562	Human chronic myelogenous leukemia	RPMI	Prof. Carsten Watzl (ifADO, Dortmund, Germany)
K562/4-1BB/mbIL-15/mbIL-21	Modified K62 with 4-1BBL, membrane bounded IL-15/18 and GFP/RFP	RPMI	Prof. Winfried S. Wels (Georg Speyer Haus, Frankfurt, Germany)
SKMel-37	Human amelanotic cutaneous melanoma of rectal tumor origin	DMEM	Prof. Helga Bernhard (Darmstadt clinic)
PRIMARY CELLS CULTURE			
Primary cells	Medium	Stimulation	
Cytokine-induced memory-like NKs	NK cells media (Miltenyi/Cell Genix)	ON 5 ng/ $\mu$ L hIL-12 (PeproTech), 10 ng/ $\mu$ L of hIL-15 (MBL), 1 $\mu$ L/mL of rhIL-18 (MBL) and 400 U/mL rhIL-2	
NKs	NK cells media (Miltenyi/Cell Genix)	400 U/mL rhIL-2	
Patient derived organoids (PDOs)	Complete ENA media	Described in Betge <i>et al</i> , Nature, 2022*	
BACTERIA STRAIN			
Designation	Description	Provider	
One Shot® Stbl3 Chemically Competent E. coli	Designed strain for cloning direct repeats in LV vectors	Thermo Fischer Scientific	

\*List of supplements and PDOs origin detailed in “1.1.8 Patient derived organoids cell lines culture”

**Table 6.3:** Cell lines, primary cells and bacteria strain.

## 6.4 BUFFERS AND MEDIA

MEDIA AND BUFFERS	
Solution	Supplements
Cell Lysis buffer for RNA Isolation	RLT buffer from Qiagen, 1% $\beta$ -mercaptoethanol
Cell-Freezing medium	FCS 10 % DMSO
Complete 5x McCoy's	5X McCoy's medium, 10 % FCS, 1 % P/S, 1 % L-Glutamine
Complete DMEM	DMEM medium, 10 % FCS, 1 % P/S, 1 % L-Glutamine
Complete NK	MACS NK/Cell Genix NK medium, 10 % Human Serum, 1 % P/S
Complete RPMI	RPMI medium, 10 % FCS, 1 % P/S, 1 % L-Glutamine
Complete $\alpha$ MEM	$\alpha$ MEM medium, 12.5% FCS, 12.5% Horse Serum, 1 % P/S, 0.01 % $\beta$ -mercaptoethanol
FACs buffer	0.5L PBS, 1 % FCS, 0.02 % $\text{NaN}_3$ , 2 mM EDTA
LB agar plates	1.5 % bacto-agar in LB medium, 0.1 % Ampicillin
Cell Lysis buffer for Western Blot	Cell Lysis buffer 10 X, SDS 10 X buffer, PMSF 100X
MACS buffer	PBS, 0.1% BSA, 2 mM EDTA
Perm buffer	1:10 Permeabilization buffer concentrate in distilled water
Red Cell Lysis buffer	For 0.5L water: 0.605 g TRIS base, 4.01 g Ammoniumchlorid, pH 7.2
SDS-PAGE buffer (10 X)	50 mM Tris-HCl pH 6.8, 10.28 % SDS, 36 % glycerol, 0.6 M dithiothreitol (DTT) bromphenol blue
SDS-PAGE Separating gel (12 %)	1.6 mL 30 % polyacrylamide, 1 mL 1.5 M Tris/HCl, pH 8.8, 40 $\mu$ L 10 % SDS and APS, 2.4 $\mu$ L TEMED and 4 mL $\text{H}_2\text{O}$
SDS-PAGE Stacking gel (6 %)	0.68 mL 30 % polyacrylamide, 0.5 mL 1 M Tris/HCl, pH 6.8, 40 $\mu$ L 10 % SDS and APS, 2.4 $\mu$ L TEMED and 4 mL $\text{H}_2\text{O}$
Sort buffer	PBS, 1 % FCS, 2 mM EDTA
TAE Buffer	40 mM Tris, 5 mM sodium acetate, 1 mM EDTA
Western blot antibody dilution buffer	0.05 % Tween-20, 5 % skimmed milk or BSA powder in PBS
Western blot blocking buffer	0.05 % Tween-20, 5 % skimmed milk in PBS

**Table 6.4:** Media and buffers used in this dissertation.

## 6.5 KITS

KITS		
Product	Company	Catalogue no.
Cytofix/Cytoperm™ buffer	BD	554714
CytoTox-Fluor™ Cytotoxicity Assay	Promega	G9260
Fixation/Permeabilization Solution Kit	BD	554714
FoxP3 Transcription factor staining buffer	eBioscience	00-5523-00
MACSPlex Cytotoxic T/NK Cell Kit, human	Miltenyi Biotec	130-125-800
Neon™ Transfection System 100 µL Kit	Invitrogen	MPK10096
NK Cell Isolation Kit, human	Miltenyi Biotec	130-092-657
OneTaq® 2X Master Mix	New England Biotechnology	M0482S
ProtoScript® II First Strand cDNA Synthesis Kit	New England Biotechnology	E6560S
PureLink™ HiPure Plasmid Maxiprep	Thermo Fisher Scientific	K210007
Q5® Site-Directed Mutagenesis Kit	New England Biotechnology	E0554S
QIAprep Spin Miniprep Kit	Qiagen	27106X4
Qubit™ dsDNA HS and BR Assay Kits	Invitrogen	Q32851
Qubit™ RNA High Sensitivity (HS), Broad Range (BR), and Extended Range (XR) Assay Kits	Invitrogen	Q32852
RNeasy® Mini Kit	Qiagen	74104
RT <sup>2</sup> SYBR Green qPCR Mastermix	Qiagen	330501
Seahorse™ XF Cell Mito Stress Test Kit	Agilent	103010-100
TransIT® Lentivirus System	Mirus	MIR6655
TURBO DNA-free™ kit	Ambion	AM1907
Western Bright Sirius	Advantas	K-12043-C20

**Table 6.5:** List of kits used in the study.

## 6.6 ANTIBODIES AND FUSION PROTEINS

ISOTYPES				
Specificity	Label	Clone	Company	Catalogue no.
Mouse IgG1, k	APC	MOPC-21	Biolegend	400122
Recombinant human	APC	REA293	Miltenyi Biotec	130-120-709
Mouse IgG1, k	BV421	MOPC-21	Biolegend	400158
Mouse IgG1, k	BV650	X40	Biolegend	563231
Mouse IgG1, k	BV785	MOPC-21	Biolegend	400170
Mouse IgG1, k	FTTC	MOPC-21	Biolegend	554679
Mouse IgG1, k	PB	MOPC-21	Biolegend	981812
Mouse IgG1, k	PE	MOPC-21	Biolegend	400112
Mouse IgG2b, kappa	PE	MPC-11	Biolegend	400312
Rat IgG2a, kappa	PE	RTK2758	Biolegend	407507
Mouse IgG1, k	PECy7	MOPC-21	Biolegend	400126

**Table 6.6.1:** Isotype controls.

EXTRACELLULAR PRIMARY ANTIBODIES FOR FLOW CYTOMETRY				
Specificity	Label	Clone	Company	Catalogue no.
Anti-Fc IgG1	APC	HP6017	Biolegend	409306
CD112	APC	TX31	Biolegend	337412 / 337411
CD155	APC	SKII.4	Biolegend	337617
CD45	APC	HI30	Biolegend	304011
CD56	APC	HCD56	Biolegend	318310
CD96	APC	NK92.39	Biolegend	338410
NKG2C	APC	REA205	Miltenyi Biotec	130-103-701
NKp80	APC	5D12	Biolegend	346707 / 346708
TIGIT	APC	MBSA43	Biolegend	17-9500-42
CD45	APCy7	HI30	Biolegend	304014
CD56	APCy7	HCD56	Biolegend	318331
CD69	BV421	FN50	Biolegend	310929 / 310930
FASL	BV421	MHM-88	Biolegend	314515

IL-21	BV421	3A3-N2.1	BD	564755
NKp46	BV421	9E2/Nkp46	Biolegend	331913
CD25	BV605	BC96	Biolegend	302631
NKp30	BV605	P30-15	Biolegend	563384
CD107a	BV650	H4A3	Biolegend	328637
NKG2D	BV650	1D11	Biolegend	563408
CD3	BV711	OK3	Biolegend	317327
CD56	BV785	5.1H11	Biolegend	362550
CD107a	FITC	MOPC-21	Biolegend	328606
CD3	FITC	HIT3a	Biolegend	300306
CD38	FITC	HIT2	Biolegend	303503
CD45	FITC	HI30	Biolegend	304005
DNAM-1	FITC	11A8	Biolegend	338303
CD45	Pacific Blue	30-F11	Biolegend	103125
CD112R	PE	W16216D	Biolegend	301504
CD96	PE	NK92.39	Biolegend	338405 / 338406
IL-18R	PE	H44	Biolegend	313808
NKG2A	PE	REA110	Miltenyi Biotec	130-098-814
TGFβ-R II	PE	W17055E	Biolegend	399703
TRAIL	PE	RIK-2	Biolegend	308205 / 308206
CD16	PECy7	3G8	Biolegend	302016
CD45	PeCy7	HI30	Biolegend	304015
HER-2	PeCy7	24D2	Biolegend	324413
NKp44	PE-Cy7	P44-8	Biolegend	325115 / 325116
CD45	PERP/Cy5	2D1	Biolegend	368503
<b>EXTRACELLULAR PRIMARY ANTIBODIES FOR FLOW CYTOMETRY</b>				
<b>Specificity</b>	<b>Label</b>	<b>Clone</b>	<b>Company</b>	<b>Catalogue no.</b>
Eomes	PE-Cy7	WD1928	Thermo Fisher Scientific	25-4877-41
Granzyme B	BV421	QA18A28	Biolegend	396413

IFN $\gamma$	APC	4S.B3	Biolegend	502511 / 502512
Ki67	PE	11F6	Biolegend	151209
T-bet	BV785	4B10	Biolegend	644835
TNF $\alpha$	PECy7	Mab11	Biolegend	502929
FUSION PROTEINS FOR FLOW CYTOMETRY				
Specificity	Label	Company	Catalogue no.	
rh ErbB2/Her2	Fc	R&D	1129-ER-050	

**Table 6.6.2:** Extracellular and intracellular antibodies and fusion protein used in flow cytometry.

ANTIBODIES FOR WESTERN BLOT			
Specificity	Label	Company	Catalogue no.
VHL Polyclonal Antibody	-	Thermo Fisher Scientific	PA5-13488
$\beta$ -Actin	-	Cell Signalling Technology	4967S
HIF-1 $\alpha$ Polyclonal Antibody	-	Novus Biologicals	NB-100-105
Rabbit IgG (H + L)	HRP	Cell Signalling Technology	7074

**Table 6.6.3:** Antibodies used for western blot.

## 6.7 PLASMID AND OLIGONUCLEOTIDES

DNA PLASMIDS			
Plasmid	Description	Insert (size)	Provider/Reference
pMD2.G	Lentivirus envelope plasmid	-	Addgene/92104
Ps-5.28.z-IEW	Lentivirus vector for ErbB2.FRP5-CAR expression	ErbB2.FRP5 (1515 bp)	Prof. Winfried Wels, Georg Speyer Haus, Frankfurt
psPAX2	Lentivirus packaging plasmid	-	Addgene/35002

**Table 6.7.1:** DNA plasmids.

crRNA OLIGONUCLEOTIDES			
Target gene	Sequence	Exon	Provider
CD226 (DNAM-1)	GT <sup>T</sup> AAGAGGTCGATCTGACG	3	IDT
CD226 (DNAM-1)	CGATGACGCTCCACCT <sup>T</sup> CCG	3	IDT
CD226 (DNAM-1)	GT <sup>T</sup> CAAGATCGGGACCCAGC	3	IDT
CD96	CGTGCAGATGCAATGGTCCA	3	IDT

ErbB2 (HER2)	GAGTCCATGCCCAATCCCGA	5	IDT
ErbB2 (HER2)	CAACTACCTTTCTACGGACG	6	IDT
HIF-1a	GAGCTCCCAATGTCGGAGTT	1	IDT
HIF-1a	GTTTTCCAAACCTCCGACAT	1	IDT
HIF-1a	TGTTTTCCAAACCTCCGACAT	1	IDT
KLRC1	TGAACAGGAAATAACCTATG	2	IDT
KLRC1	GGTCTGAGTAGATTACTCCT	2	IDT
PVRIG (CD112R)	CAGAACGTGGCATCCGGCAA	3	IDT
PVRIG (CD112R)	ATTGCCGGATGCCACGTTCT	3	IDT
PVRIG (CD112R)	GTGGGTTCAAGTTCGGATGG	3	IDT
TIGIT	ACCCTGATGGGACGTACACT	2	IDT
TIGIT	TATCGTTCACGGTCAGCGAC	2	IDT
TIGIT	TGGGGCCACTCGATCCTTGA	2	IDT
TNFSF10 (TRAIL)	GCACTTGAGGAATGGTGAAC	1	IDT
TNFSF10 (TRAIL)	CTACCTTTCTAACGAGCTGA	2	IDT
TNFSF10 (TRAIL)	GAAGATCACGATCAGCACGC	5	IDT
trcRNA			
Product	Provider	Catalogue no.	
Alt-R® CRISPR-Cas9 Negative Control crRNA #1	IDT	1072544	
Alt-R® CRISPR-Cas9 tracrRNA, ATTO™ 550	IDT	1075928	

**Table 6.7.2:** crRNA oligonucleotides and trcRNA.

## 6.8 PLASTIC WARE AND CONSUMABLES

PLASTIC WARE AND CONSUMABLES		
Product	Company	Catalogue no.
3D CoSeedis™ Chip880	ABC biopply	ABC-C880
Cryovial, 2 mL sterile	Greiner Bio-one	122263
Falcon® 6-well Clear Flat Bottom, not Treated Cell Culture Plate, Sterile	Corning	351146

Falcon® 24-well Polystyrene Clear Flat Bottom, not Treated Cell Culture Plate, Sterile	Corning	351147
MACS™ LS Columns	Miltenyi Biotec	130-042-401
RNase-free Microfuge Tubes (1.5 mL)	Thermofisher Ambion	AM12400
Serological pipette 5 ml, padded	Sarstedt AG & Co.	861253001
Serological pipette 10 ml, padded	Sarstedt AG & Co.	861254001
Serological pipette 25 ml, padded	Sarstedt AG & Co.	861685001
Seahorse™ XF HS Miniplate Kit	Agilent	103725-100
Tissue Culture Plate, Flat Bottom	Sarstedt AG & Co.	1000039
Tissue Culture Plate, Round Bottom	BD Bioscience	83.3924.300
TPP® tissue culture plates, 96 well plate, Round bottom, Polystyrene, Sterile	TPP	Z707899-162EA
Mini Cell Scrapers	Hözel	B-22003
Bundle pluriStrainer® Mini 40 µm and Flow Cytometry Tubes	Pluriselect	43-10040-46
SafeSeal Tips Professional 10 µl, 20 µl, 200 µl, 1000 µl	Biozym	770005, 770050, 770100, 770280, 770600
Trans-Blot Turbo Transfer Pack 0.2 µm Nitrocellulose	Biorad	1704159

**Table 6.8:** Plastic ware and consumables.

## 6.9 LABORATORY EQUIPMENT

LABORATORY EQUIPMENT	
Product	Company
200 Gel Imaging Workstation	Azure biosystem
C1000 Touch™ Thermal Cycler	Bio-Rad
ChemiDoc MP Imaging System	Bio-Rad
FACS Aria™ Fusion Cell Sorter	BD Biosciences
Heraeus Pico Centrifuge	Thermo Fisher Scientific
Incubator BD056	BINDER
LSR Fortessa™ Cell Analyzer	BD Biosciences
Multifuge™ X1 Centrifuge	Thermo Fisher Scientific

N2 Tank Biosafe smart 500	Biosafe
Neon™ Transfection System	Thermo Fisher Scientific
pH Meter Seven Compact	Zeiss
Plate reader Infinite 200 pro	Tecan
QuantStudio™ 5 Real-Time PCR System, 384-well	Applied Biosystems
Qubit 4 Fluorometer	Thermo Fisher Scientific
Seahorse™ XF HS Mini Analyzer	Agilent
Spark® Multimode Microplate Reader	TECAN
Trans-Blot Turbo Transfer System	Biorad
UltraMicroscope Blaze™	Miltenyi Biotec

**Table 6.9:** Laboratory equipment.

## 6.10 SOFTWARES

SOFTWARES	
Product	Company/Developers
Agilent Seahorse Analytics	Agilent
Biorender	Biorender
cBioportal for cancer genomics	Memorial Sloan Kettering Cancer Center
ChatGTP*	Open AI
CRISPR design tool	Synthego
Custom Alt-R® CRISPR-Cas9 guide RNA	IDT
Fiji ImageJ	Schindelin et al.
Flowjo	Flowjo
Graph Pad Prism 8	GraphPad Software Inc
IncuCyte Base Analysis and Plate Reader	Sartorius
MACs Quantify	Miltenyi
SnapGene viewer	SnapGene
Spark Control	TECAN

**Table 6.10:** Softwares for data analysis. \*ChatGTP software tool was used as a grammar correction tool (in the general text) and as a translation tool for “Zusammenfassung”.

## 7 METHODS

---

### 7.1 CELL CULTURE METHODS

#### 7.1.1 Freezing and thawing cells

Cells were counted and washed with room temperature PBS prior freezing. The frozen media used was FCS with 10% DMSO in sterile conditions, using a concentration range according to the cell type. Each cryovial contained 1-1.5 mL of media with cells, and was placed inside a MrFrosty box filled with isopropanol. After storage in -80°C for 3 days minimum, frozen cryovials were transferred to liquid nitrogen tank.

Thawing cells was performed by placing the cryovial in the waterbath at 37°C. Gently pipetting 1 mL pre-warmed complete media (accordingly to each cell type), cells were transferred to a 15 mL falcon tube with 13 mL of media. Then, a spin of 1500 rpm /9 acc./9 decc./RT was done in order to wash the cells. Then supernatant was aspirated and resuspended in pre-warmed complete media and seeded in the appropriate flask or well plate.

#### 7.1.2 Passaging of cell lines

All cell lines were regularly checked for contamination and over-growing. Suspension cell lines (K562, NK-92 and NK-92 CI) were spun down at 1500 rpm/ 9 acc./ 9 decc./ RT, counted and reseeded in a concentration of 2 million cells per 10 mL complete media. Adherent cell lines (A375, HEK, SKMel-37 and HT-9) seeded in 25 cm<sup>3</sup>, 75 cm<sup>3</sup> and 175 cm<sup>3</sup> flask were washed with 5 mL, 10 mL or 20 mL of room temperature PBS respectively. Washing PBS was aspirated and then 0.5 mL, 1 mL or 3 mL of Trypsin (regular passaging) or Accutase (passaging before experiment in order to not damage the haptens) were pipetted. Immediately after adding the de-attaching agents, cells were placed in 37°C incubator. Once cells were in suspension (10-15' incubation), they were splitted accordingly to the desired concentration. Media and origin is detailed in table 1.1.

#### 7.1.3 Counting of cells with Trypan blue

Cells were counted using Neubauer chamber. 10 µL of suspension or adherent cells were mixed with Trypan blue in a certain dilution. Thus, 10 µL of the mix was loaded in Neubauer chamber, distinguishing dead cells (dark) from live cells (bright) with 10X magnification.

$$\text{Cell number} = \frac{\text{dilution factor} \times 10^4 \times \text{counted cells}}{\text{wells}}$$

#### 7.1.4 Human primary NK cells isolation

Human primary NK cells were isolated from healthy donors from the blood bank from Medical Faculty Mannheim (UMM) in sterile conditions. Peripheral blood mononuclear cells (PBMCs) were isolated immediately after blood collection in the core facility. The blood from the buffy coat was transferred to a T75 Flask, and then room temperature PBS was added up to 140 mL. Then, in 50 mL Falcon tubes containing 15 mL of Percoll or Biocoll solution, the

mixture of blood and PBS was carefully loaded on top up to 50 mL, generating two phases dilution. A gradient density centrifugation was performed at 2000 rpm/ 3 acc./ 1 decc./ 10 ' /RT. After the centrifugation, different density compartments were observed: erythrocytes at the bottom, percoll, lymphocytic fraction and plasma. The lymphocytic fraction was collected using Pasteur pipette and transferred to a 50 mL Falcon tube, with a total ratio of 2 Falcons per buffy coat. The total volume was adjusted to 50 mL with RT PBS with the concomitant spinning at 800 rpm/ 9 acc./ 9 decc./10 ' / RT. Then, the supernatant was discarded and one wash with 50 mL RT PBS was performed, with 1500 rpm/ 9 acc./ 9 decc./10 ' / RT. In the meantime, red cell lysis buffer was warmed at 37°C in the water bath. PBMCs pellet was resuspended in 50 mL 37°C warmed red cell lysis buffer in one Falcon tube, and incubated for 15' at

37°C. After incubation, samples were centrifuged at 800 rpm/ 9 acc./ 9 decc./10 ' / RT with concomitant 2x RT PBS washes at 1500 rpm/ 9 acc./ 9 decc./10 ' / RT. Once PBMCs were counted, human NK cell isolation kit (Miltenyi) was used to negatively select NK cells by magnetic separation. The protocol for the kit was followed as described by manufacturer, with a concentration of 100 million PBMCs by LS column.

#### 7.1.5 Human primary NK cells culture

Human primary NK cells were cultured in specific media for NK cells by CellGenix (GMP SCGM medium) or by Miltenyi (MACs NK medium with supplements by manufacturer). For regular NK cells culture, both media were supplemented with 10% human serum (Novus biotec), 1% Penicillin/Streptomycin and 400 U/mL of recombinant human IL-2 (refer to Table 1.1). Culture concentration was kept in a range of 1-2 million cells per mL, with the according passaging.

#### 7.1.6 Cytokine-induced memory-like NK cells

In order to produce cytokine-induced memory-like NK cells, freshly isolated NK cells were stimulated with 5 ng/μL human IL-12 (PeproTech), 10 ng/μL of human IL-15 (MBL), 5 ng/μL of recombinant human IL-18 (MBL) and 400 U/mL recombinant human IL-2 for 16-18h in complete media as abovementioned (Table 1.1). After stimulation, NK cells were washed and resuspended in regular NK cells culture media with 400 U/mL IL-2.

#### 7.1.7 Feeder cells expansion

In order to expand NK cells, 41BB-IL-mbIL15/21 K562 feeder cells were used (kindly shared by Prof. Winfried S. Wels) (see Table 1.3). Feeder cells were cultured as reported previously and irradiated at 100 Grays (Oberoi et al., 2020). NK to feeder cells co-culture was performed in a 1:1 ratio. After 48h coculture cells were centrifuged 1500 rpm/ 9 acc./ 9decc./ 10' /RT and washed with PBS in order to remove dead cells. Afterwards, cells were resuspended at 2 million per mL concentration in complete NK media with 400 U/mL rhIL2.

#### 7.1.8 Patient derived organoids cell lines culture

Patient derived colorectal organoids (PDOs) were kindly shared by Dr. Elke Burguermeister and Prof. Matthias Ebert (Uniklinikum Mannheim) (refer to Table 1.3). Two PDOs cell lines were used, P22 and P7 (randomized by name). PDOs were cultured in solid matrix, basement

membrane extracts (BME) and supplemented as previously reported (Betge et al., 2022). In short, produced organoids were cultured in DMEM/F12 (Life technologies) medium with 1% Peniciline and Streptomine, Glutamax and HEPES. Further supplements were used as Nogging (PeproTech), B27 (Life technologies), n-acetyl cysteine, gastrin, hEGF and nicotinamide (Sigma-Aldrich), A83-01 (Biocat), SB-202190 prostaglandin E2 and Y-27632 (Biomol) and primocin (Invivogen). The described medium is named as ENA.

### 7.1.9 Spheroid generation and culture

HT-29 cell line was cultured in 3D to produce spheroids in collaboration with Dr. Med. José Alberto Villacorta Hidalgo (Miltenyi). Cells were seeded in low concentration in agarose gel matrix 3D CoSeedis™ Chip800 on a 6 well plate with the corresponding media. The culture process was performed following manufacturer's protocol until spheroids were growing at a steady rate.

## 7.2 FUNCTIONAL NK CELL ASSAYS

### 7.2.1 Tumor co-cultures and cytokine PMA/Ionomycin stimulation (degranulation assay)

Functional analysis of human NK cells response to tumor cells and cytokines was monitored by flow cytometry based analysis. All the assays were performed in a total duration of 4h, in which NK cells were stimulated either with tumor cells in the desired effector to target ratio or cytokine concentration. NK cells were seeded in p96 round bottom plates in combination with the target cells. For cytokine stimulation, hIL-12 (10 ng/mL) and rhIL-18 (100 ng/mL) or phorbol myristate acetate (PMA, 50 ng/mL)/Ionomycin (0.5  $\mu$ M) were added in a total volume of 200  $\mu$ L of media for 50.000 NK cells per well. In order to stain degranulation, CD107a surface protein expression was stained during the assay with anti-human CD107a IgG1k H4A3 clone (FITC), in a 1/20 total dilution in media. Cells were centrifuged at 1500 rpm/9 acc./ 9 dec./1' RT and incubated at 37°C in a cell culture incubator. After 30'-1h from stimulation, transporters inhibitors (GolgiPlug containing Brefeldin A/GolgiStop containing Monesin) were added in 1/1000 dilution without disturbing the cell pellet. Then, NK cells were stained and analysed by flow cytometry (described in next section). Cytokine and soluble factors production profile was detected by intracellular facs staining of IFN $\gamma$ , Granzyme B and TNF $\alpha$ .

### 7.2.2 Tumor cell confluency assay

The tumor confluency assay was performed by TECAN analysis, measuring the layer of adhered tumor cells to the bottom of the well plate. Adherent tumor cells were seeded in the desired ratio the day before the analysis, in a 70% confluency rate in 500  $\mu$ L appropriate media in p24 well plates. Once 90% confluency rate was reached, media was aspirated and changed by fresh media with NK cells in an effector to target ratio range of (2:1, 1:1 and 0.5:1). After the specified timing in each experiment, media was removed and 2x PBS washes were gently performed, without altering the cancer cells monolayer. Then, fresh media was added and the TECAN measurement was performed, reading the full well area density. In order to

get higher statistical power, all conditions were performed in duplicates, and a tumor cells seeded without NK cells was used as 100% confluency threshold value.

### 7.2.3 Organoid coculture with NK cells in IncuCyte

PDOs thawed at passage 7 were used for NK cells co-culture, in an effector to target ratio of 0.5 to 1. PDOs were resuspended in non-enzymatic cell dissociation buffer (Life Technologies) and incubated during 15' on ice. Afterwards, 2x PBS washes and centrifugation at 400 G/ 9 acc./ 9 decc./ 10'/ RT were performed. A fraction of resuspended PDOs were subtracted and completely digested in TrypLE (Thermo Fisher Scientific) at 37°C for 20' (with periodic resuspension every 4'). Single cell PDO dilution was counted in order to seed the desired E:T ratio, and cooled on ice. If needed, 2 µM Image IT Hypoxia dye (Thermo Fisher scientific) in complete advanced DMEM was used for 1 hour at 37°C in order to stain PDOs <5 % oxygen. NK cells were counted and washed in PBS and resuspended with or without PDOs in 3-5 µL BME. As controls, NK cells alone, PDOs alone and combination of stainings were used, as well as 5x replicates per condition in a 96 well plate. Cells were supplemented in 50% RPMI and 50% ENA Y-27632/nicotinamide-free media with 400 U/mL rhIL-2 and 0.001% CytotoxRed (Sartorius). Subsequently, the plate was inserted in IncuCyte to perform the measurements in periodic intervals ranging from 2 hours to 3 hours during 5 days.

## 7.3 FLUORESCENCE-ACTIVATED CELL SORTING (FACS)

Cells were prepared in suspension, and transferred to a 96 well plate with round bottom. All cells were washed with PBS in a total volume of 200 µL. All washes were performed with 1500 rpm/ 9 acc./9 dec./3'/4°C. If CD16 was not included as extracellular staining, TruStain Fc blocking was performed prior staining (15' at RT). Live/death cell staining was performed with AquaZombie staining in PBS, combined with primary/extracellular staining in the desired dilution in 50 µL per well (30'/4°C incubation protected from light). Alternatively, primary/extracellular antibody staining was done in FACS buffer (recipe described in materials section), and 7AAD live/death cell staining was added before measuring the samples in a 1:40 dilution. Then, 2x FACS buffer washes were performed in 200 µL total volume. If intracellular staining was required, FOXP3 Fix/Perm Buffer kit was used following manufacturer's instructions. Intracellular antibodies were diluted in permeabilization solution and staining was performed for 30' at 4°C in darkness. After 2x washes with permeabilization solution, cells were diluted in FACS buffer "in house" prepared (refer to Table 1.4).

## 7.4 FACS SORTING

If the stained cells were used for sorting, the staining procedure was performed in sterile conditions. Samples were suspended in PBS with 2% EDTA and filtered in a 5 mL round bottom tube with cell strainer. 7AAD death/alive marker dye was added immediately before the sorting process.

## 7.5 VIRUS TRANSDUCTION OF NK CELLS

### 7.5.1 Lentivirus production

Second generation lentivirus were produced in transfected HEK293 cells in order to infect NK cells. 5 million HEK cells were seeded in a 75 cm<sup>3</sup> flask in complete DMEM media on the day before the transfection (75-80% of confluency).

As envelope plasmid pMD2.G (VSVG envelope plasmid) was used, and psPAX2 (Gag, Pol, REV) as packaging plasmid in a 1 µg/µL concentration with a 1:1 ratio to transfer plasmid. Alternatively TransIT Lentivirus System by Mirus was used, with the manufacturer's produced packaging and envelope plasmids, in a concentration of 1:10 transfer plasmid (1 µg/µL concentration) to lentivirus packaging mix (0.1 µg/µL). Ps-5.28.z-IEW was used as expression plasmid to insert Erbb2.FRP5-CAR surface protein. The complex with plasmids was formed in free-serum OptiMem media and incubated for 10' at RT. The gene mixture was added dropwise to the HEK293 cells culture in S2 safety laboratory and placed in incubator. Supernatant was collected 48 h later and centrifuged at 1500 rpm/ 9 acc./ 9 decc./ 15' / 4°C, pellet was discarded and supernatant was stored in cryovials at -80C or used immediately for infection.

### 7.5.2 Lentivirus titration

Virus were titrated by flow cytometry in HEK293 cells, measuring GFP<sup>+</sup> % of cells. Virus supernatant was diluted in serial dilutions using serum free media as diluent. In order to calculate the volume to use in primary NK cells, a multiplicity of infection (MOI) of 6 was selected. TU/mL and volume were calculated with the according formulas:

$$\frac{\text{TU}}{\text{mL}} = \frac{\text{number of transduced cells} \cdot \% \text{ GFP}^+ \text{ of cells} \cdot \text{dilution factor}}{\text{virus volume in mL}}$$

$$\text{Volume of viral vector} = \left( \frac{\text{Number of cells}}{\text{Viral titer in TU/ mL}} \right) \cdot \text{MOI}$$

### 7.5.3 Lentiviral transduction of human NK cells

Human NK cells were stimulated with 2000 U/mL rhIL-1β, 400 U/mL rhIL-2 and 10 ng/mL hIL-15 in complete media after buffy coat isolation. Three days later, cells were washed with PBS at 1500 rpm/ 9 acc./ 9 decc./ 10' / RT, and resuspended in serum-free NK MACs complete media. Protamine sulfate (8 µg/mL) polycation was used as transduction enhancer, and BX785 (0.6 µg/mL) as inhibitor for noncanonical IκB kinases TANK-binding kinase 1 (TBK1), which regulates the response of NK cells towards virus. These chemical compounds were added to the described media, and incubated during 20' at room temperature with NK cells. Afterwards, NK cells were seeded in a p48 well plate in 150 µl or p24 well plate at 250 µL (4 million per mL density) and 32°C thawed virus supernatant was added at the desired MOI (usually in a total volume of 500-750 µL). A spinfection was performed 1500 rpm/ 9 acc./ 9 decc./ 90', with posterior overnight incubation at 37°C. Then, cells were centrifuged to

remove the remaining transduction reagents, newly prepared NK MACs complete media containing 400 U/mL of rhIL-2 was added

At day 5 post-transduction, 4x RT PBS washes were performed with the infected human NK cells (1500 rpm/ 9 acc./ 9 decc./ 10'/ RT). Transduced NK cells were transported in PBS solution to S1 safety facility, where they were seeded in complete NK MACs media supplemented with 400 U/mL rhIL-2 in a concentration of 1 million/mL. Transduction efficacy was tested by flow cytometry observing green fluorescent protein (GFP) expression.

## 7.6 TRANSFECTION OF NK CELLS BY ELECTROPORATION

Virus-free transfection of NK cells was performed with Neon Transfection System electroporation device (Thermo Fisher). Human NK cells isolated from PBMCs were expanded for 5 days with 400 U/mL IL-2, 10 ng/mL hIL-15 and 2000 U/mL IL-1 $\beta$ . In order to perform CRISPR/Cas9 gene edition, single guide RNA duplex was formed by CRISPR-RNA sequence (crRNA) and a trans-activating-CRISPR RNA sequence (tracrRNA) labelled with ATTO-550 dye (refer to Table 1.7.2). 90 pico mol of crRNA and tracrRNA were mixed up to 6  $\mu$ L with Duplex Buffer (IDT), and incubated for 5' at 95C. Afterwards, the duplex was cooled down for 10' at RT before incubating with Cas9 ribonucleoprotein (RNP) derived from *Streptococcus pyogenes* with 2 nuclear localization signals (NLS) from Synthego. 60 pico mol of Cas9 RNP per sample was prepared up to 6  $\mu$ L with Duplex Buffer, mixed with the duplex complex and incubated at RT from 20'-60'. During this time, NK cells were resuspended in a concentration of 1 M-2.5M per electroporation condition. Buffer T provided by Thermo Fisher was used to dilute NK cells immediately before electroporation. Neon Transfection System cuvette with 3 mL of Buffer E2 was used, as well as 100  $\mu$ L electroporation tips for each condition.

As parameters for the electroporation, the voltage pulse was 1900, pulse width was 20 milliseconds and one pulse number. After electroporating, cells were resuspended in 1 mL antibody free complete pre-warmed media, standing in horizontal positioned eppendorfs at 37 C during 90'. Cells were centrifuged at 1500 rpm / 5' / RT and resuspended in complete media with 400 U/mL rhIL-2 in 1 million cells per mL concentration. Extracellular targeted proteins KO efficacy was evaluated by flow cytometry from 72 hours after electroporation. Intracellular targeted proteins were sorted 18-24 hours according to their ATTO-550 dye expression.

## 7.7 TRANSFECTION OF CELL LINES BY ELECTROPORATION

NK-92 and HT-29 cell lines were electroporated in Buffer R at the described conditions in Table 6.1.

NEON TRANSFECTION SYSTEM ELECTROPORATION PARAMETERS		
Cell type	Buffer	Parameters
HT-29	R	1600 V/ 10 ms/ 3 pulses
NK-92	R	1250 V/ 10 ms/ 3 pulses
Primary NKs	T	1900 V/ 20 ms/ 1 pulse

**Table 7.7.1:** Electroporation parameters used for the different cell lines.

## 7.8 REAL TIME METABOLITES MEASUREMENT

In order to measure metabolites Seahorse XF HS Mini (Agilent) machine was used. The day before the assay, 8 wells cartridges were hydrated overnight at 37°C in CO<sub>2</sub>-free incubator in XF Calibrant. If the plates were not coated, Agilent Seahorse XG HS plates were coated with 20 µL poly-Lysine (100 mg/mL) for 1 hour at 37°C. Subsequently, the plate was washed twice with sterile water and air dried for 30'. Then, if used immediately cells could be added or stored sealed at 4°C.

On the day of the experiment, fresh calibrant was added at 37°C for 60' to the cartridge plate. The medium used for the assay was RPMI with 1% Glucose and L-Glutamine (all reagents provided by manufacturer) and kept at 37°C. Coated XF HS plates were warmed at 37°C prior use, for a minimum range of 1 hour. 30 µL of NK cells dilution was added per well, in a range of 50.000 to 150.000 cells per condition. All conditions were triplicated. In order to seed cells in monolayer, XF HS plates were centrifuged. If needed, silicone mask of the plate (coated by manufacturer) was removed. 150 µL of pre-warmed assay medium was added per well, and the plate was incubated at 37°C in CO<sub>2</sub> free incubator from 45' to 1 hour.

Cartridges were loaded with the kit's reagents (XFp Cell Mito Stress Test Kit); oligomycin, FCCP and rotenone/antimycin following manufacturer's instructions. After calibrating the cartridge, it was loaded in the plate with the seeded cells, and the measurement was performed. Data was analysed using Agilent Seahorse Analytics (<https://seahorseanalytics.agilent.com>).

## 7.9 PLASMIDS PURIFICATION AND SEQUENCING

### 7.9.1 Transformation of bacteria

In order to amplify the plasmids used (PAX2, PMSG.2 and Ps.58 Z IEW), 50 ng of DNA were integrated in 50 µL of One shot Stbl3 chemically competente E. coli prokaryotic cells (Table 1.3). They were incubated on ice during 30' with a concomitant heat shock at 42°C for 45' with

immediate incubation on ice for 10'. 950  $\mu$ L of LB broth media was added and shaken at 37°C at 200 rpm for 1 hour. 150  $\mu$ L of the bacteria culture was spreaded in agarose plates containing ampicillin as selection factor, and plates were incubated overnight at 37°C. Untransformed *E. coli* culture was used as negative control of spontaneous bacteria growth.

### 7.9.2 Colony expansion

Single colonies from transformed bacteria were collected and inserted in 15 mL of LB broth media containing ampicillin, and incubated for 24 hours at 400 rpm shaking at 37°C. Due to the bacteria expansion, the transparent solution turned turbid, as indication viable colonies. The DNA of the expanded bacteria was isolated using QIAprep Spin Miniprep Kit (Qiagen) following the manufacturer's instructions. Alternatively, a larger volume of bacteria was expanded, in a varying volume from 250 mL – 500 mL and incubated at the described conditions. DNA from > 250 mL bacteria preparation was isolated using QIAprep Spin Maxiprep Kit (Qiagen) according to the kit instructions. The quantity and purity of the isolated DNA was calculated by measuring the absorbance at 260 nm ( $A_{260}$ ) in TECAN. Pure DNA was estimated according to the  $A_{260}/A_{280}$  ratio, considering standard purity at 1.8 – 2.0 values. The desired colonies were immediately used or stored at -20°C.

### 7.9.3 Sequencing

Sanger sequencing in Eurofins (Tube seq service, <https://www.eurofinsgenomics.eu/en/home/>) was purchased in order to confirm plasmids sequence. Sequencing primers and DNA concentration was prepared according to manufacturer's guidance. Sanger data from sequencing was further analysed using SnapGene viewer software.

## 7.10 SOLUBLE FACTOR MEASUREMENT

Cytokines in culture were measured by MACsPlex cytotoxic T/NK kit, human (Miltenyi). Supernatants were spun at 2000 rpm / 9 acc./ 9 dec./ 10' and frozen at -80°C. After completely thawing, supernatants were centrifuged at 10.000 G / 9 acc./ 9 dec./ 10' / 4°C and diluted to the desired volume in MACSPlex Buffer. Soluble factors were stained following manufacturer's instructions, and samples were measured using a MACQuant X device. The software analysis and final quantification was performed using MACs Quantify Software version 2.13.1.

## 7.11 IMAGING OF NK CELL MIGRATION INTO TUMOR SPHEROIDS

NK cells were co-cultured with HT-29 generated spheroids for 2 hours at 37°C, at a ratio of 100.000 NK cells per tumor spheroid in technical replicates. 3X washes with PBS at RT were performed, aiming to remove the remaining culture media (300 G / 3' / RT). The fixation of the samples were performed using paraformaldehyde (PFA) at 4 % dilution in PBS, adding 1 mL of PFA per sample during 20' in rotating motion using MACs rotor at RT. Remaining PFA solution was removed performing 3X PBS washes as aforementioned. Permeabilization of the samples was performed using the Perm buffer provided in MACs Blaze kit, adding 0.5 mL per sample and incubating them in a MACs rotor overnight. Samples were spun 300 G / 3' / RT

and supernatant (permabilization buffer) was discarded. The staining buffer provided in the MACs Blaze kit was diluted at 1/10 in RT PBS. CD45-VioR667 antibody (Miltenyi) was used in 1/100 dilution in staining buffer. Staining was performed at 37°C during 24 hours in constant motion using MACs rotor. The excess of the antibody staining buffer was eliminated by performing 3X washes in the staining buffer diluted at 1/10. Samples were embedded in 1.5 % agarose in double distilled H<sub>2</sub>O in cassettes moulds which were polymerizing at RT for 20'. The size of each agarose-embedded sample was adjusted to blocks of 1 cm<sup>3</sup>. Blocks were dehydrated in 50 % ethanol (ETOH) in double distilled H<sub>2</sub>O and incubated during 2 hours at RT in rotation. Similarly, concomitant dehydration was performed in 70 % and 100 % ETOH dilutions during 2 hours and overnight (respectively). Sample blocks were cleared using ethyl cinnamate (ECI) clearing buffer during 3 hours in rotating motion at RT. Samples were stored in ECI buffer at RT. Spheroids with recruited NK cells were observed using light sheet Blaze microscope, sample blocks were immersed in the imaging solution found in the microscope chamber. Pictures were taken at 2 μM distance pictures in each spheroid sample, detecting NK cells using the red laser and GFP in the green laser. Fiji imaging software was used to build 3D images from the stacking pictures taken in each condition, and CD45-VioR667 red signal was used to quantify single NK cells recruited. This method was entirely performed at Miltenyi's installations in Bergisch Gladbach, as secondment partner from the MATURE NK cell consortium during which this study was conducted.

## 7.12 STATISTICAL ANALYSIS

Statistical analysis was performed using paired student's t-test, one-way ANOVA and Saphiro test was used for confirmation of normalization. If the spread was considered as normal, parametric analysis was performed (using non-parametric analysis for samples not-normally distributed). Statistical significance was determined by p-value of  $p < 0.05$  (\*),  $p < 0.01$  (\*\*),  $p < 0.001$  (\*\*\*) and  $p < 0.0001$  (\*\*\*\*). Not significance was considered if p-value  $> 0.05$ .



## 8 RESULTS

---

### 8.1 EFFECT OF HYPOXIA ON NK CELLS *IN VITRO* IN COMBINATION WITH IMMUNOTHERAPY

The solid tumor microenvironment is characterized by a notably low oxygen concentration (< 1 %), when compared to organs like the brain (< 4 %) or liver (5 % O<sub>2</sub>) (Benner et al., Barrier et al.). Furthermore, the impact of hypoxia on human NK cells has been reported, an increased migration capacity by CXCR<sub>4</sub> upregulation. This is accompanied by the downregulation of NK cell surface receptors like NKp46, NKp80, and NKp44, but without a significant effect on ADCC (Balsamo et al., 2013; Parodi et al., 2018). Additionally, both murine and human NK cells exposed to the hypoxic hepatocarcinoma microenvironment have shown fragmented mitochondria, with a reduction in OXPHOS metabolism and an increase in glycolysis. At the same time, NK cells extracted from hypoxic tumor cores display a reduction of cytotoxicity towards K562 cells and production of soluble factors IFN $\gamma$  and TNF $\alpha$ , when challenged *in vitro* with IL-12/18 and PMA/Ionomycin (X. Zheng et al., 2019).

The transcription factor HIF-1 $\alpha$  plays a pivotal role in regulating NK cells, as evidenced by studies involving HIF-1 $\alpha$ -/-/NKp46 murine cells, which demonstrated significantly better tumor burden control compared to wild-type controls (Krzywinska et al., 2017; Ni et al., 2020). However, the role of HIF-1 $\alpha$  on human NK cells as cytotoxic mediators towards solid tumors remains not completely understood.

In my study, I focused on describing the general effects of hypoxia on human NK cells, as well as the generation of human HIF-1 $\alpha$  knockout (KO) NK cells. This research aims to enhance NK-centered immunotherapies for solid tumors, including the development of CAR-NK cells.

#### 8.1.1 Surface protein expression, IFN $\gamma$ production and degranulation of NK cells exposed to hypoxia

With the aim of studying the effects of hypoxia on human NK cells *in vitro*, I began by designing an experimental model manipulating oxygen concentrations to generate normoxic or hypoxic culture conditions. I screened the response of NK cells to different stimuli that could be present in the tumor microenvironment (such as tumor cells and IL-12/18) as well as chemical compounds; oxygen consumption rate and extracellular acidification rate as metabolism indicators; proliferation and expression of surface molecules relevant for NK cell activation or inhibition.

I devised an experimental setup that enabled me to use flow cytometry to assess NK cells exposed to hypoxia (defined as 1 % O<sub>2</sub> in this study) over short-term (six hours) and long-term (seven days) periods, mirroring the newly recruited NK cells to the hypoxic niche and the tissue-resident/tumor-infiltrating NK cells respectively (Figure 8.1 A and B).

An initial indication of functional alterations was the diminished size of NK cells exposed to seven days of hypoxia compared to normoxia and 6 hours hypoxia exposed groups as judged from a reduction in forward scatter. (Figure 8.1 C).

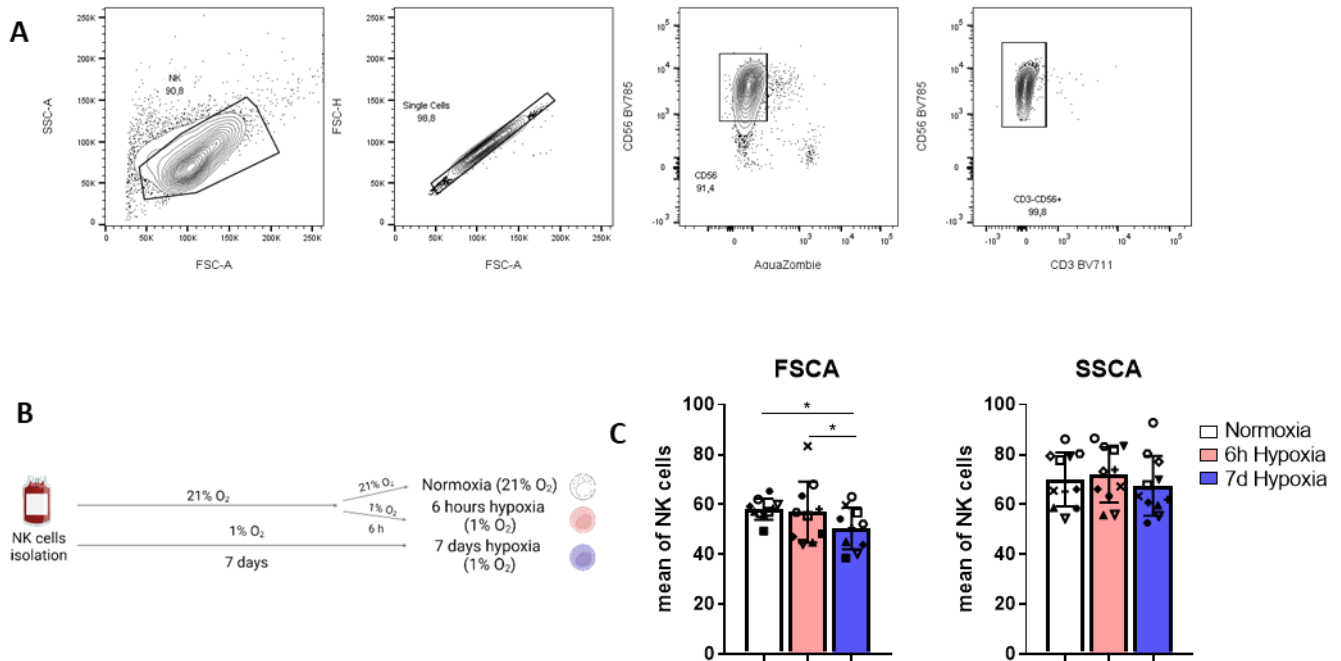


**Figure 8.1: Human NK cells exposed to hypoxia show a reduction in forward scatter.** (A) Representative contour plots showing gating strategy for flow cytometry analysis. (B) Scheme of experimental set up. Image created in Biorender.com. (C) Representative histogram (left) and mean (right) of FSC-A and SSC-A determined by flow cytometry (n = 10). p-value\* < 0.05; p-value\*\* < 0.01. Analysis done by Saphiro's normality test and one way ANOVA.

Prior research had already demonstrated that hypoxia can modulate the NK cell transcriptome, with over 179 genes significantly altered between 16 hours or 96 hours of 1% O<sub>2</sub> (Parodi et al., 2018). Hence, I contemplated whether sustained exposure to hypoxia influences surface receptors and ligands on NK cells that are relevant to cytotoxicity. I assembled a panel of fluorescently labelled antibodies for flow cytometry targeting activating and inhibitory receptors, cytokine receptors, and metabolism markers (refer to Figure 8.2). I noted a moderately decreased frequency after seven days hypoxia of NK cells with detectable levels of NKP44 (-21.7% reduction, p\*\* = 0.0012), NKG2A (-11.9%, p\*\*\* = 0.0008); whereas the number of NK cells expressing CD69 (+21.17 fluorescence mean intensity, p\* = 0.0205) and CD57 (+22.5 fluorescence mean intensity, p\*\* = 0.0099) were elevated (Figure 8.2). Most prominently, CD39-positive NK cells were virtually absent (2.6%, p\* = 0.0168) after long-term hypoxia, while common (48.4%) under normal oxygen exposure. In addition, surface expression levels of TRAIL (p\*\*\*\* < 0.0001), IL-18-receptor (p\*\*\* = 0.0012) and CD38 (p\*\*\*\* < 0.0001) were reduced in the total cell population as measured by mean fluorescence intensity.

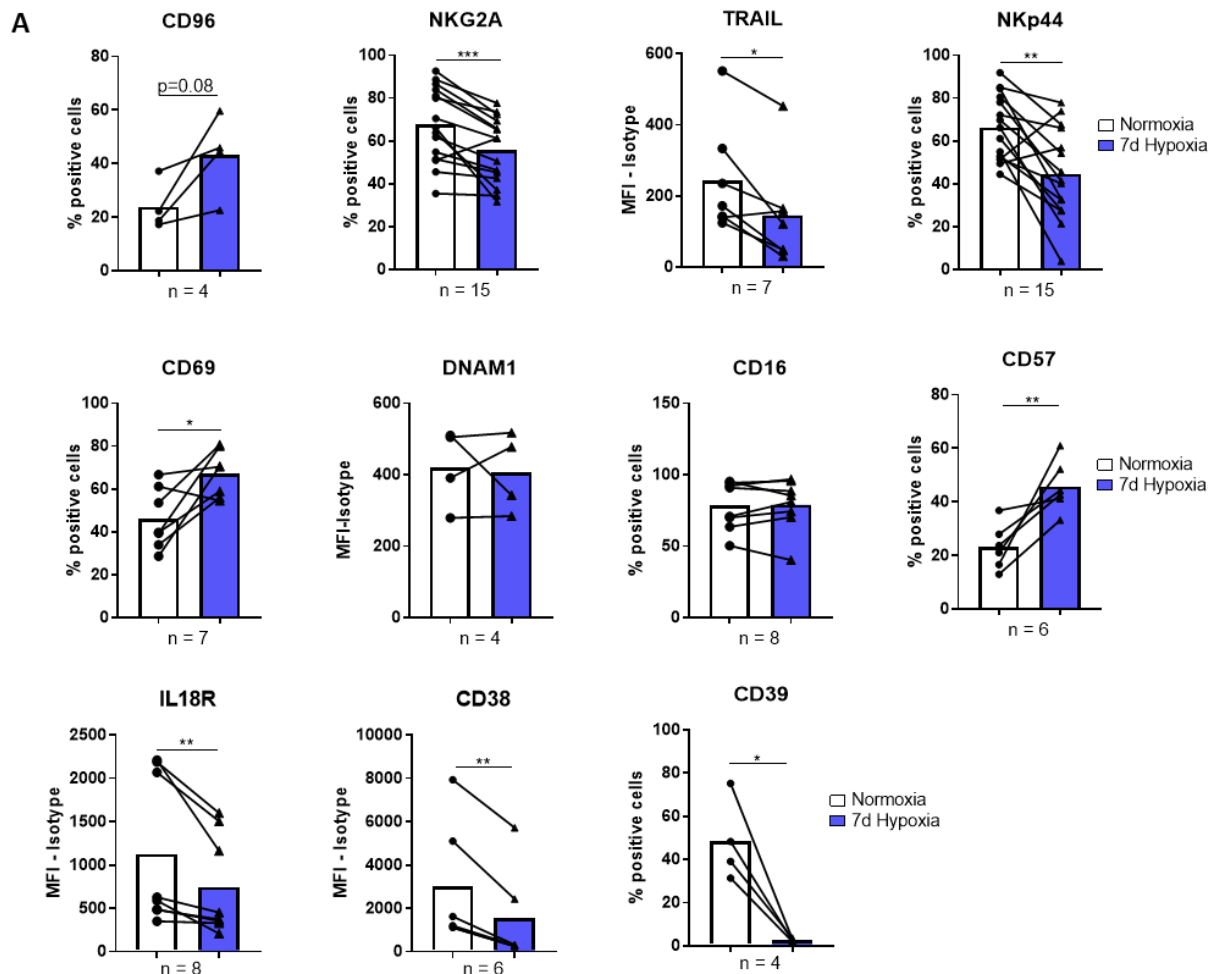


**Figure 8.2: Cell surface receptor expression on hypoxia and normoxia exposed NK cells.** (A) Expression of cell surface receptors on NK cells exposed seven days to normoxia or hypoxia in percentage or mean fluorescence intensity. p-value\* < 0.05; p-value\*\* < 0.01; p-value\*\*\* < 0.005. Analysis done by Saphiro's normality test and paired t-test.

To further examine whether exposure to hypoxia causes functional changes in NK cells, I evaluated their response to the chronic myeloid leukemia K562 cell line or cytokines that induce IFN $\gamma$  production (IL-12 and IL-18) (Figure 8.3 B and C). I assessed NK cell function using flow cytometry, observing intracellular IFN $\gamma$  in response to IL-12 and IL-18 or surface expression of CD107a as degranulation marker in response to co-culture with K562 cells. Long-term hypoxia significantly reduced NK cell responses, with a 46.8 % reduction degranulating cells ( $p^{***} = 0.0004$ ) and 35 % reduction in NK cells with detectible IFN $\gamma$  production ( $p^{**} = 0.001$ ). The negative impact of hypoxia on IFN $\gamma$  production (3.8 %,  $p^{**} = 0.0098$ ) and degranulation (12.8 %,  $p^* = 0.01$ ) was already apparent after six hours of hypoxia (Figure 8.3 B and C). Long-term hypoxia similarly diminished NK cell granulation in response to solid tumor cell lines of melanoma (A375, 10.7 %  $p^* = 0.0247$ ) and colorectal adenocarcinoma (HT-29, 9.6 %,  $p^* = 0.0166$ ) and chemical stimulation of NK cell degranulation with PMA+Ionomycin (28.1 %,  $p^{**} = 0.0024$ ) (Figure 8.3 D). Overall, sustained hypoxia leads to a reduction in NK cell size and impairs their capacity to respond to tumor cells, IL-12/18 cytokines, and PMA/Ionomycin chemicals.

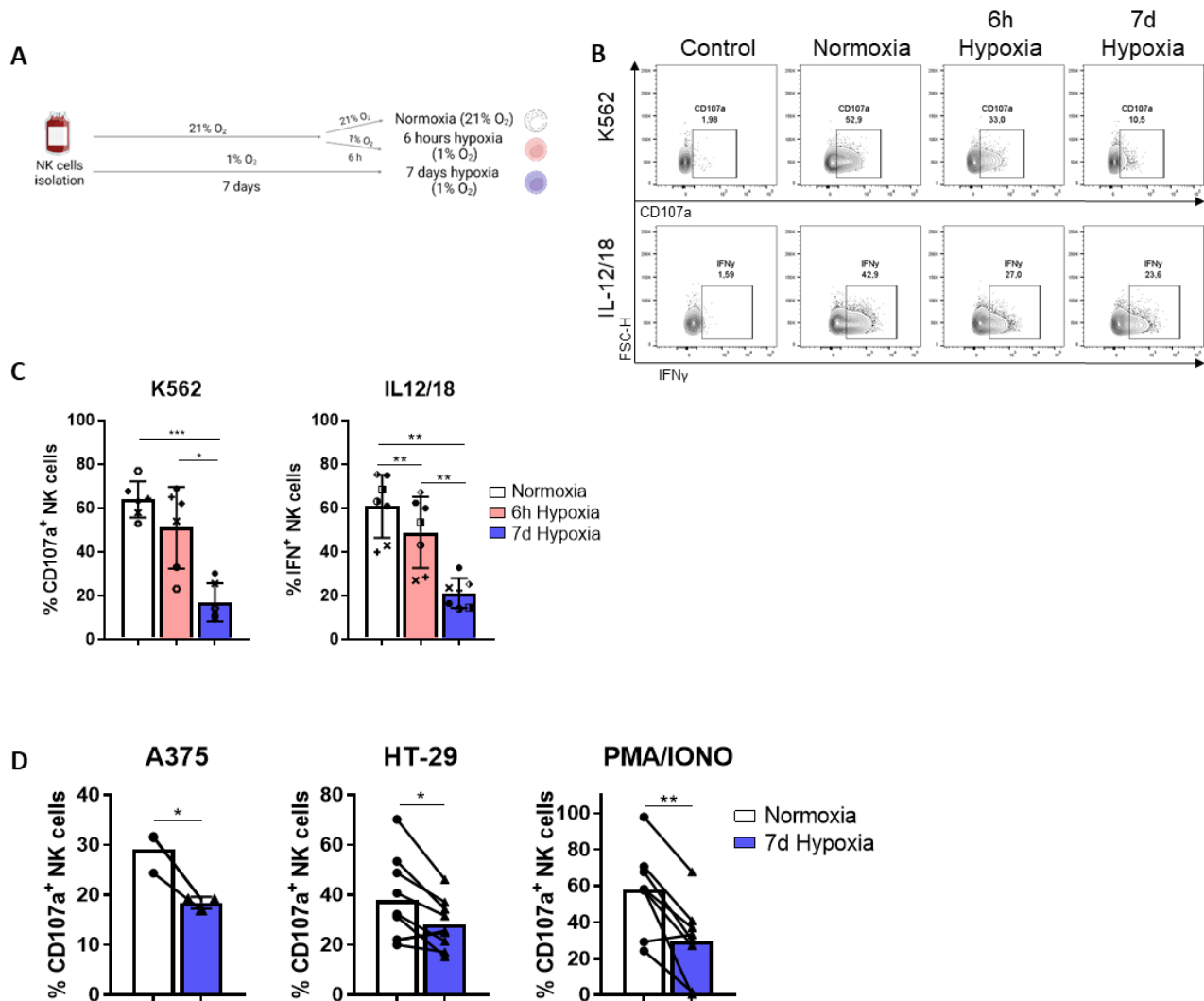


**Figure 8.3: Degranulation and IFN $\gamma$  production of human primary NK cells exposed to hypoxia are impaired.** (A) Scheme of experimental set up. Image created in Biorender.com. (B) CD107a expression upon co-culture with K562 and IFN $\gamma$  expression by flow cytometry after IL-12/18 stimulation, representative contour plot. (C) Summarized data (n = 7). (D) CD107a expression assessed by flow cytometry after stimulation with PMA/Ionomycin (n = 8), A375 coculture (n = 3) or HT-29 (n = 8) after 7d hypoxia or normoxia culture. p-value\* < 0.05; p-value\*\* < 0.01; p-value\*\*\* < 0.005. Analysis done by Saphiro's normality test, paired t-test (D) and one way ANOVA (C).

### 8.1.2 Decreased proliferation of NK cells exposed to seven days hypoxia

Efficient proliferation is often essential for effector cells to respond effectively to a threat. Given the fact that I have already observed reduced degranulation and IFN $\gamma$  production, I wondered whether exposure to hypoxia would also impact the proliferation of NK cells. I evaluated proliferation through intracellular staining of the Ki67 proliferative marker expressed in actively proliferating cells and labelling NK cells with the CFSE cell trace dye, which is quantitatively diluted upon cell division. While control IL2-stimulated NK cells harboured a majority (80.2 %, p\*\*\*\* < 0.0001) of actively cycling cells as determined by Ki67 expression, NK cells exposed to seven days of hypoxia were mostly non-cycling (41.3 %, p\*\* = 0.0035). Based on dilution of the CFSE dye during the seven days of culture, most NK cells

(57.7 %) had not divided at all once exposed to 1% oxygen. indicating a significant reduction in NK cell proliferation (see figure 8.4).

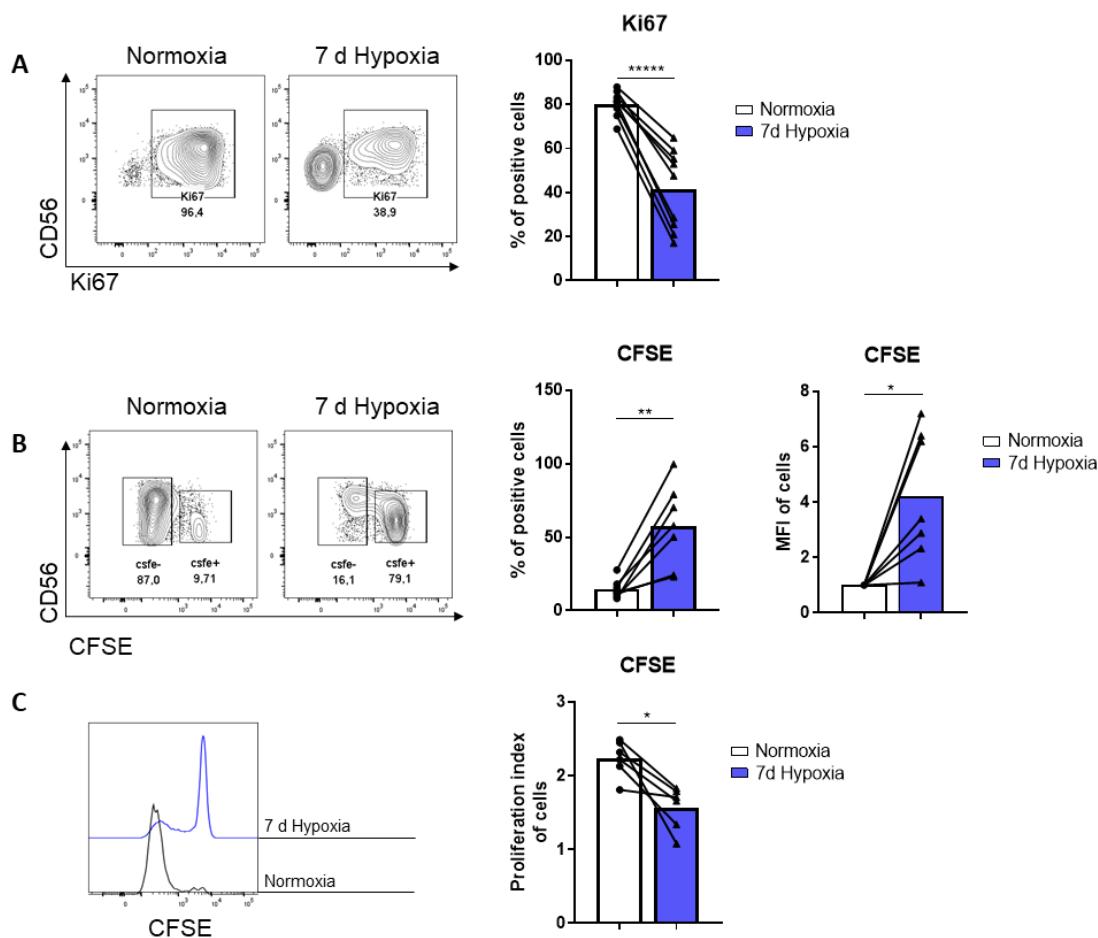


**Figure 8.4: Human primary NK cells exposed to hypoxia show reduced proliferation.** (A) Ki67 intracellular staining in NK cells. n=9 (B) CellTrace CFSE labelling in NK cells measured by flow cytometry in percentage of positive cells (left) and mean fluorescence intensity (right). n=7. (C) Proliferation index of NK cells calculated from CFSE staining. n=6. p-value\* < 0.05; p-value\*\* < 0.01; p-value\*\*\*\* < 0.0001. Analysis done by Shapiro's normality test, paired t-test.

### 8.1.3 Decreased metabolism of human NK cells exposed to hypoxia

Diminished oxygen concentration is associated with the reprogramming of metabolism through glycolysis, a process interlinked with NK cell activation and function (Terrén et al., 2019). Therefore, I explored the impact of hypoxia exposure on NK cells by quantifying their oxygen consumption rate (OCR) and extracellular acidification rate (ECAR) in microchambers on an Agilent Seahorse device. The measurement is based in the detection of proton exchange and oxygen concentration, which is linked to the proton transporters in the mitochondrial membrane as part of the mitochondrial respiration. After the basal measurement, the first injection of Oligomycin inhibits ATP synthase (complex V) and results in a reduction of the mitochondrial respiration, linked to ATP production. It continues by injection of carbonyl cyanide-4 (trifluoromethoxy) phenylhydrazone (FCCP) which is an uncoupling agent and induces the maximum capacity of oxygen consumption by the complex IV. It gives the information about the spare respiratory capacity, which results as

the difference between the maximal respiration and the basal respiration. Finally, the combined injection of Rotenone and antimycin A inhibits complex I and complex III respectively. It allows the calculation of the nonmitochondrial respiration from processes outside the mitochondria (Divakaruni et al., 2014).

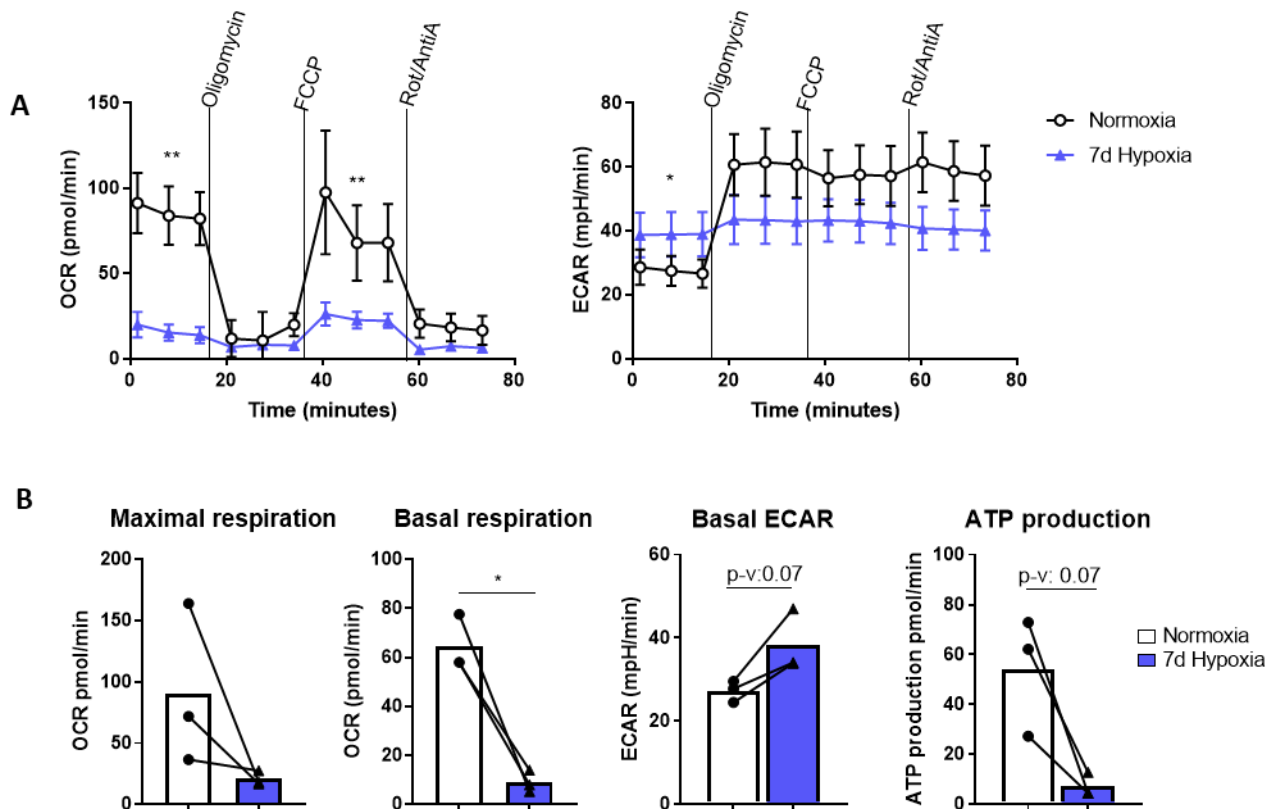


**Figure 8.5: Human primary NK cells exposed to hypoxia are metabolically impaired.** (A) Mitochondrial respiration and glycolysis were analyzed using Seahorse assays. Oxygen consumption rate (OCR) and extracellular acidification rate (ECAR) of NK cells are shown as the mean + SEM over time ( $n = 3$ ). (B) Maximal respiration, basal respiration, basal ECAR and ATP production were analyzed XF Cell Mito Stress test, analyzed with the online tool Seahorse analysis ( $n = 3$ ).  $p$ -value\* < 0.05;  $p$ -value\*\* < 0.01. Analysis performed by Saphiro's normality test and paired t-test.

NK cells subjected to seven days of hypoxia showed a significant OCR reduction of 54 pmol/min ( $p^{**} = 0.0013$ ) of normoxic controls, which were not increased by FCCP that uncouples the mitochondrial electron transfer chain from oxidative phosphorylation. In contrast, the ECAR values were increased by 9.6 mpH/min within the hypoxia-exposed group ( $p^* = 0.022$ ), remaining largely unaffected by perturbation of mitochondrial ATP production (Figure 8.5 A). Further analysis comparing normoxia and seven days hypoxia exposure NK cells encompassed: maximal respiration (-69.8 pmol/min); basal respiration (-55.2 pmol/min,  $p^* = 0.024$ ) and ATP production (-46.9 pmol/min,  $p = 0.07$ ), all of which exhibited marked reduction in NK cells exposed to seven days of hypoxia. Basal ECAR analysis showed an increase of 11.07 mpH/min ( $p = 0.07$ ) in NK cells exposed to seven days hypoxia (Figure 8.5 B). Taken together, these findings suggest compromised metabolism with reduced oxidative phosphorylation and increased reliance on anaerobic glycolysis in NK cells exposed to hypoxic conditions.

### 8.1.4 HIF-1 $\alpha$ genetic disruption in human NK cells unleashes IFN $\gamma$ production under hypoxia

One of the prominent regulators underpinning cellular responses to hypoxia is the sensor and transcription factor HIF-1 $\alpha$ , deletion of which in murine NK cells promotes inflammatory and anti-tumor responses in mouse models (Ni et al., 2020). With the aim to test whether genetic deletion of HIF-1 $\alpha$  can improve anti-tumor responses of human allogeneic NK cell therapies, I devised an electroporation strategy using CRISPR/Cas9 technology. I utilized CRISPR/Cas9 ribonucleotide protein, CRISPR/RNA, and trans-activating CRISPR/RNA labeled with ATTO-550 dye to efficiently disrupt the HIF-1 $\alpha$  exon 3 in primary NK cells, which have limited proliferative capacity and are largely refractory to transfection and lenti- or retroviral transduction (Bari et al., 2019).

24 hours after electroporation, I sorted successfully electroporated ATTO-550 positive cells (average of 82.2 % positive cells across the electroporated NK cells from independent donors) for validation of sgRNA efficiency and assessment of total protein quantification by western blot (Figure 8.6). Control or HIF-1 $\alpha$  targeted NK cells were cultured during 2 hours under 1 % O<sub>2</sub> and immediate cell lysis, loading a minimum of 180 000 cells per blot lane. Total protein KO was calculated after normalization of loading differences by  $\beta$ -Actin control, which gave a range of 30-70% of KO efficacy with the optimized electroporation method. This range suggests differences in the susceptibility of NK cells from certain donors to have a more or less successful HIF-1 $\alpha$  editing with final NK cell populations containing a mixture of cells with homozygous, heterozygous and possibly no disruption of *HIF1A* (refer to figure 8.6 C).

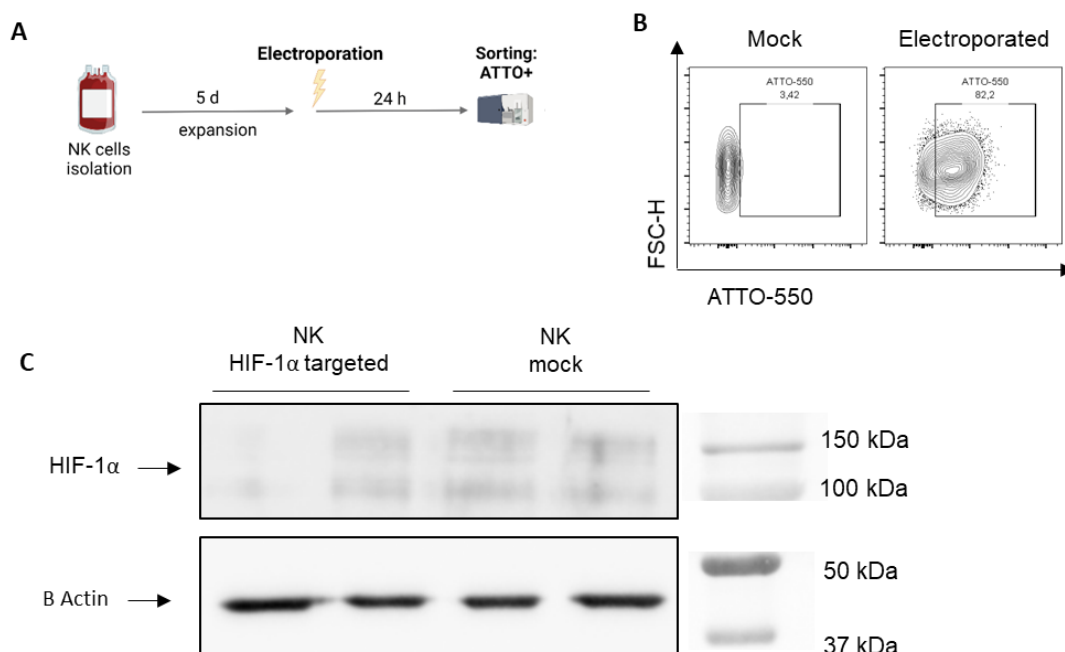


**Figure 8.6: Electroporation of NK cells with CRISPR/Cas9 RNP system targeting HIF-1 $\alpha$ .** (A) Scheme of the experimental design. (B) ATTO-550 frequency in NK cells after 24h electroporation with CRISPR/Cas9 RNP. (C) Western blot of NK cells targeted with sgRNA HIF-1 $\alpha$  or sgRNA mock control. Top membrane was used to stain HIF-1 $\alpha$  (130 kDa) and bottom membrane for  $\beta$  Actin (42 kDa), membranes were cut and revealed, protein plus ladder was used to locate each protein band.

Donors 1 and 2 were loaded in the same order in both membranes. Membranes were cut and revealed separately.

Post-sorting, the cells were allowed to rest overnight, followed by exposure to 24 hours of hypoxia coupled with concurrent IL-12/18 stimulation for 4 hours (Figure 8.7 A). 24 hours hypoxia was chosen as a pre-treatment based on the report showing strong HIF-1 $\alpha$  induction at this time point on human NK cells exposed to hypoxia (Balsamo et al., 2013).

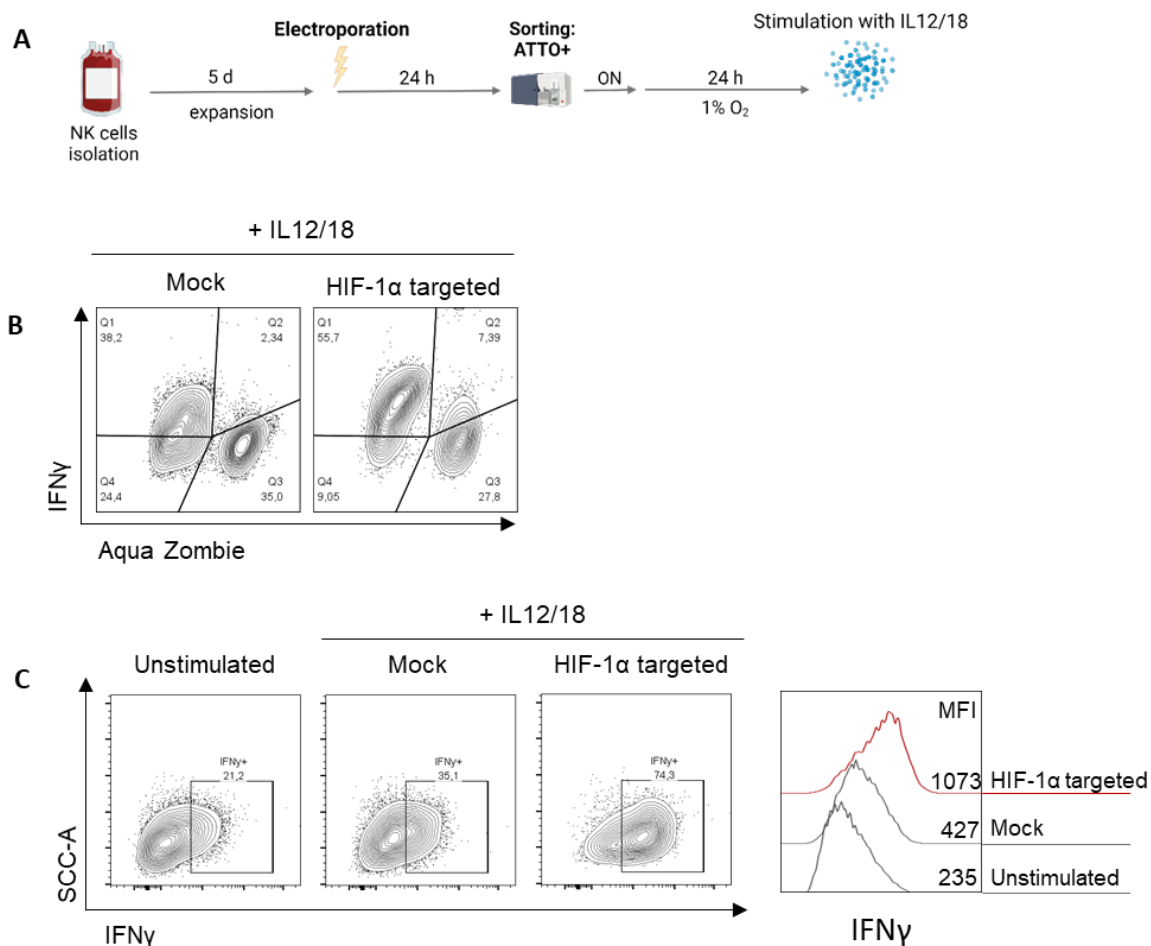


**Figure 8.7: HIF-1 $\alpha$  targeting unleashes NK cell reactivity upon cytokine stimulation.** (A) Experimental set up. NK cells isolated from PMBCs were expanded during 5 days in presence of IL-2/15/1 $\beta$ . The electroporation was performed using the Neon Transfection System and CRISPR/Cas9 RNP complex with sgRNA labelled with ATTO-550 dye. 24 hours later the NK cells were sorted according to ATTO-550 expression, and incubated overnight. Then, NK cells were exposed to 24 hours hypoxia and stimulated during 4 hours with IL-12/18. Image created with Biorender. (B) Cell death of electroporated NK cells 48 h after sorting. Last 24 h were under hypoxia and stimulated with IL-12/18 for 4 h. IFN $\gamma$  production and death (ZombieAqua dye) assessed by flow cytometry. (C) IFN $\gamma$  production depicted by flow cytometry staining upon IL-12/18 stimulation for 4 h. Frequency (left) and MFI (right) of IFN $\gamma$  intracellular staining in NK cells. p-value\* < 0.05; p-value\*\* < 0.01; p-value\*\*\* < 0.005. Analysis done by paired t-test.

To evaluate the functional impact of HIF-1 $\alpha$  gene disruption in NK cells, I examined intracellular IFN $\gamma$  after stimulation with pro-inflammatory cytokines IL-12 and IL-18. Both the

fraction of cells with detectible levels of intracellular IFN $\gamma$  as their individual expression levels of IFN $\gamma$  were increased after targeted deletion of HIF-1 $\alpha$  (40 % and 646 mean fluorescence intensity increase), without affecting cell survival (35 % and 27,8 % in control and HIF-1 $\alpha$  targeted NK cells respectively) (Figure 8.7 B and C).

Repetition of this experiment with NK cells obtained from independent donors exhibited a consistent increase in IFN $\gamma$  producing cells (93,3 % vs. 37,9 % for mock controls,  $p^* = 0,023$ ) after 24 hours of hypoxia, and a similar trend was observed after seven days of hypoxia (36,5 % vs. 22,8 % for mock controls,  $p = 0,066$ ) (refer to figure 8.8 A and B).

I explored the control of tumor growth by NK cells by measuring tumor cell confluency in TECAN, detecting the surface covered by the adherent tumor cells in presence or absence of effector cells (mock or HIF-1 $\alpha$  targeted NK cells). Percentage of tumor cells was calculated by normalizing to the measured surface covered by HT-29 cells lacking NK cells. NK cells were pre-exposed to hypoxia during 24 hours, further prolonged for additional 48 hours in co-culture with human colorectal adenocarcinoma HT-29 cells. During the first 24 hours, HT-29 cells co-cultured with HIF-1 $\alpha$  targeted NK cells showed a mean of 54 % of tumor cells confluency, compared to 80 % confluency in presence of mock NK cells. After 48 hours coculture, the presence of HIF-1 $\alpha$  targeted NK cells yielded 40 % of HT-29 cells confluency, compared to 70 % by mock NK cells co-culture (Figure 8.8 C).

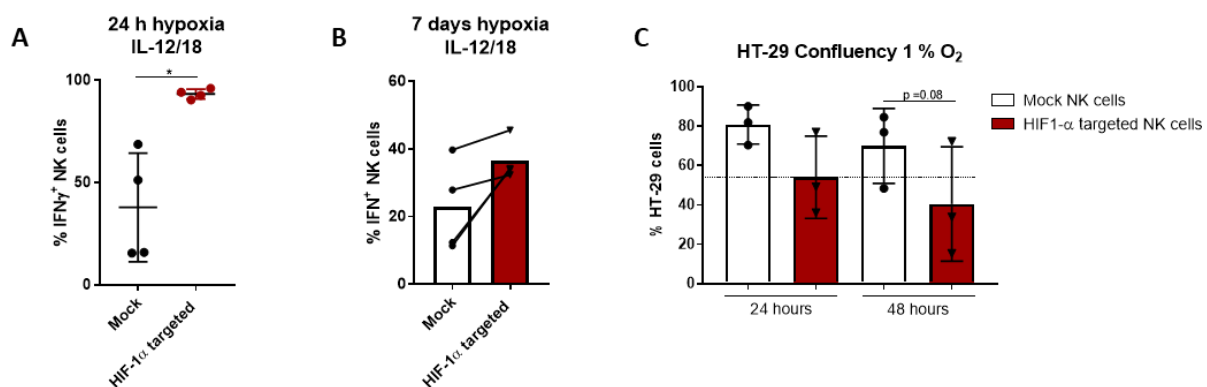


**Figure 8.8: HIF-1 $\alpha$  targeting triggers NK cell reactivity upon cytokine stimulation and tumor cells co-culture.** (A) NK cells targeted with mock sgRNA or HIF-1 $\alpha$  sgRNA after 24 hours exposure (A) or seven days (B) to hypoxia or normoxia and 4 hours of IL-12/18 stimulation. IFN $\gamma$  staining was performed intracellularly by flow cytometry. (C) NK cells targeted with mock sgRNA or HIF-1 $\alpha$  sgRNA expanded during seven days and pre-exposed to either 24 hours of hypoxia or normoxia prior HT-29 co-culture at a 1:1 effector to target ratio (under hypoxia or normoxia). Percentage of tumor cells calculated from confluency measurement by TECAN, using tumor cells alone as maximum confluency value.  $p$ -value\* < 0.05; Analysis done by Saphiro's normality test and paired t-test (A, B), and one-way ANOVA (C).

### 8.1.5 HIF-1 $\alpha$ targeted NK cells react to patient derived organoids in a patient specific manner

Despite the effectiveness of *in vitro* assays in simulating the low oxygen concentration typically found in the tumor microenvironment of solid tumors, the artificial exposure to 1 % oxygen concentration lacks the heterogeneity in gas diffusion, metabolites and the three-dimensional structure characteristic of a true tumor niche (Terrén et al., 2019). With this consideration, I opted for patient-derived organoids (PDO) of colorectal adenocarcinoma as a model, as they retain their physiological architecture and can replicate many aspects of the tumor microenvironment. Through collaboration with Prof. Dr. Ebert, Dr. Betge, and Dr. Burgermeister, I obtained a panel of four patient-derived organoids of colorectal adenocarcinoma, covering major driver mutations, such as *KRAS*, *APC*, *AKT1*, *SMAD4*, *PTEN*, *TP53* and *PIK3CA* (Figure 8.9)(Betge et al., 2022). PDO 7, 19 and 22 had a consensus molecular subtype 2, whereas PDO 30 was categorized as 3, while all the lines had stable microsatellite regions. Tumors encompassed distinct clinically relevant locations of colorectal cancer, with PDO 7 derived from the rectum and linked to familial adenomatous polyposis in stage III, PDO 19 derived from stage I sigmoid colon adenocarcinoma, and both PDO 22 and 30 derived from the ascending colon stage IV and II adenocarcinomas, respectively (Figure 8.9 B).

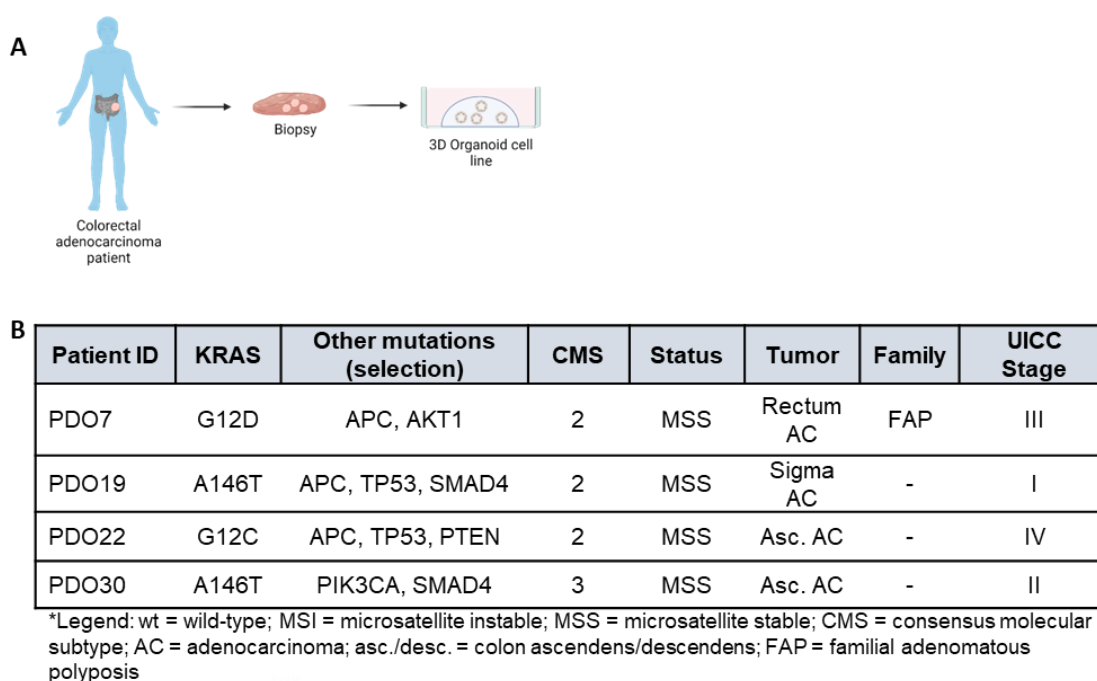


**Figure 8.9: Patient derived organoids from colon cancer patients (PDOs).** (A) Summary of organoid production. Biopsies from colorectal adenocarcinoma patients were differentiated into *in vitro* 3D organoid cell lines, which were generated by Prof. Burgermeister's group. Image created in Biorender.com. (B) Information adapted from published report from collaborators, whose PDO lines were used in this study (Betge et al., 2022).

To investigate the presence of hypoxia within the PDOs, I treated live cells with an enzymatically activatable dye (ImageIT Hypoxia Green dye), designed to activate its green fluorescence at oxygen concentrations below 5 % (Hoh et al., 2018). Initially, I evaluated PDO 7 and 22 organoid lines pre-exposed to 24h hypoxia or normoxia. I labelled them with ImageIT Hypoxia Green dye and captured 10x magnified images by IncuCyte, revealing

fluorescent cores within the organoids, suggesting the existence of areas deprived of oxygen even under normoxia, with the staining intensifying in the condition with reduced oxygen concentration in the incubator to 1% (Figure 8.10 A and B).

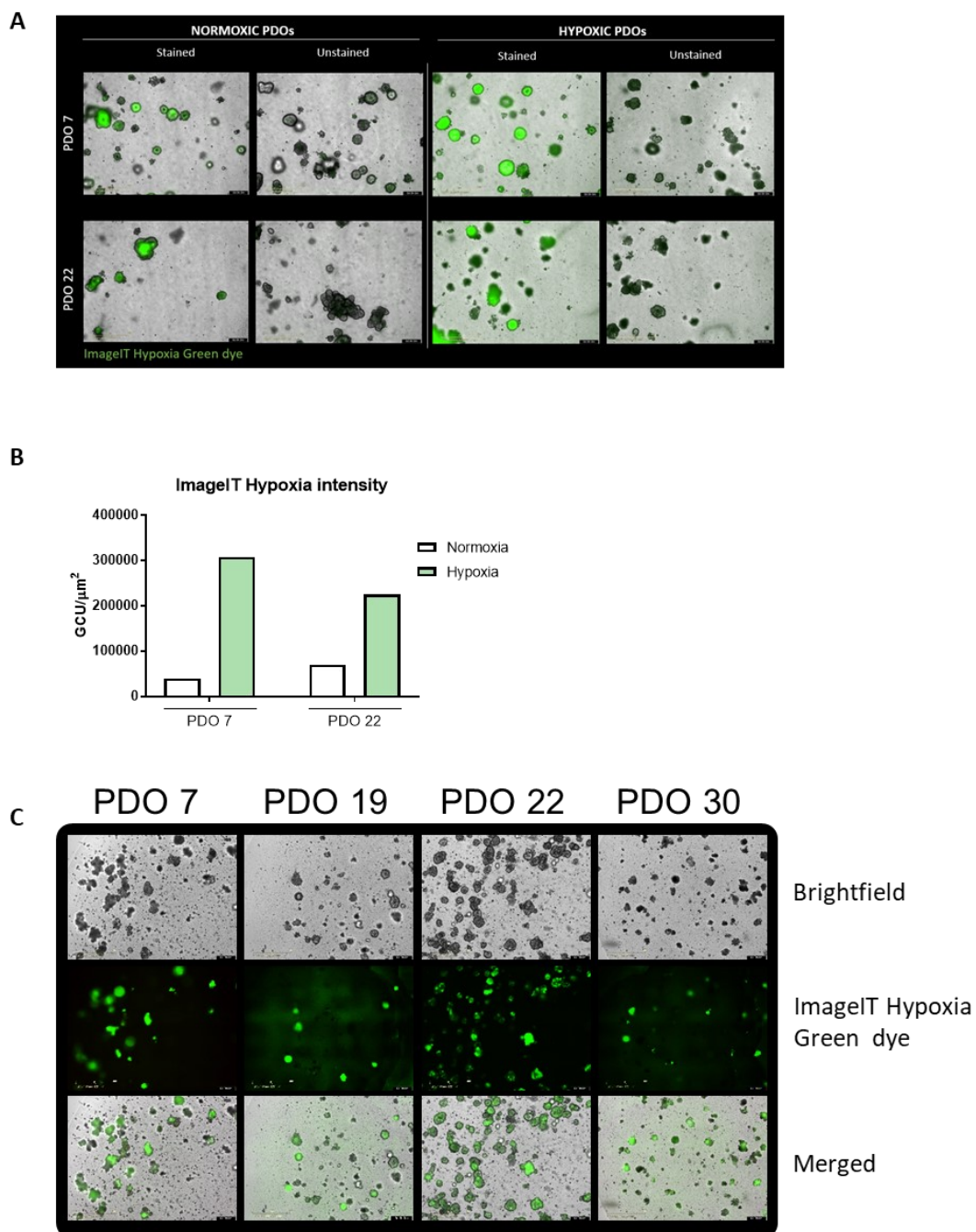


**Figure 8.10: Patient derived organoids from colon cancer patients (PDOs) display a hypoxic microenvironment.** (A) Patient derived organoids (PDOs) from colorectal adenocarcinoma stained with ImageIT Hypoxia Green dye (detecting < 5% O<sub>2</sub> concentrations) under normoxia or hypoxia (24 h). Images of IncuCyte (10 X) displaying brightfield and green fluorescence. (B) Quantification of ImageIT Hypoxia Green dye fluorescence by green integrated intensity (GCU) per μm<sup>2</sup> measured by IncuCyte. (C) Images at 10 X taken with IncuCyte microscope analyser of PDO lines 7, 19, 22 and 30 after six hours of staining with ImageIT Hypoxia Green dye (green) and brightfield.

Quantification of the intensity of the green fluorescence signal obtained from IncuCyte measurements confirmed responsiveness of the dye to hypoxia with elevated dye intensity in PDOs exposed to 24 hours of 1 % O<sub>2</sub>. Importantly, PDOs cultured with standard (21 %) oxygen concentrations still showed detectable dye activation when compared to unstained PDOs under normoxia (Figure 8.10 B). I confirmed the presence of detectable hypoxia (<5 % oxygen) after six hours of staining with ImageIT Hypoxia Green dye in PDO lines 7, 19, 22 and 30 without pre-exposure of 1 % oxygen, indicating the generation of a hypoxic gradient in the 3D PDO cultures (Figure 8.10 C).

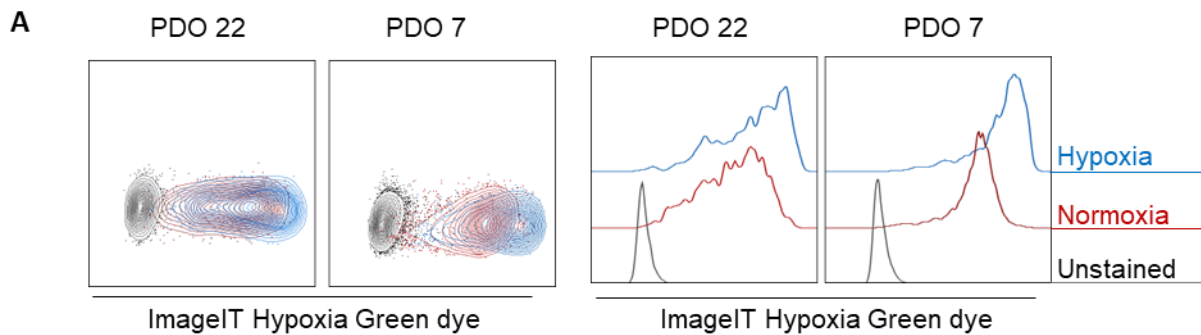


**Figure 8.11: Single cell detection of ImageIT Hypoxia Green dye in PDO lines.** (A) Analysis comparing single cell PDOs unstained and stained with ImageIT Hypoxia Green dye under normoxia or hypoxia.

After IncuCyte measuring, I then proceeded to analyse the PDO 7 and 22 samples as representative of the PDO lines through flow cytometry by digesting the 3D structures into single-cell suspension by enzymatic digestion, allowing me to quantify the intensity of ImageIT Hypoxia Green dye within the cells (see Figure 8.11.A). Individual cells dissociated from the two PDOs under standard culturing conditions showed wide distributions in the dye fluorescence intensity, which partially overlapped with populations derived from hypoxia-treated PDOs. This further supported the notion that PDOs indeed possess portions with a hypoxic microenvironment even under *in vitro* culture conditions with 21 % oxygen concentration.

To assess the ability of HIF-1 $\alpha$  CRISPR/Cas9 targeting NK cells to exert cytotoxicity towards PDO lines, I evaluated a method for expanding NK cells, generating a sufficient cell count for the ensuing experiments without altering NK receptor surface expression. In collaboration with Prof. Wels (Goethe Institut, Frankfurt), I acquired K562-41BBL-mbIL-15-mbIL-21 feeder cells, and confirmed their surface expression of membrane-bound growth factors IL-15 and IL-21, as well as the co-stimulatory ligand 4-1BBL using flow cytometry (Figure 8.12 A) (Oberoi et al., 2020). Upon evaluating the efficacy of proliferation-inactivated feeder cells by 100 Gy  $\gamma$ -irradiation in promoting NK cell expansion, I found them capable of stimulating the engineered NK cells to expand up to 15-fold in seven days, whereas IL-2 stimulation failed to induce any cellular expansion (Figure 8.12 B).

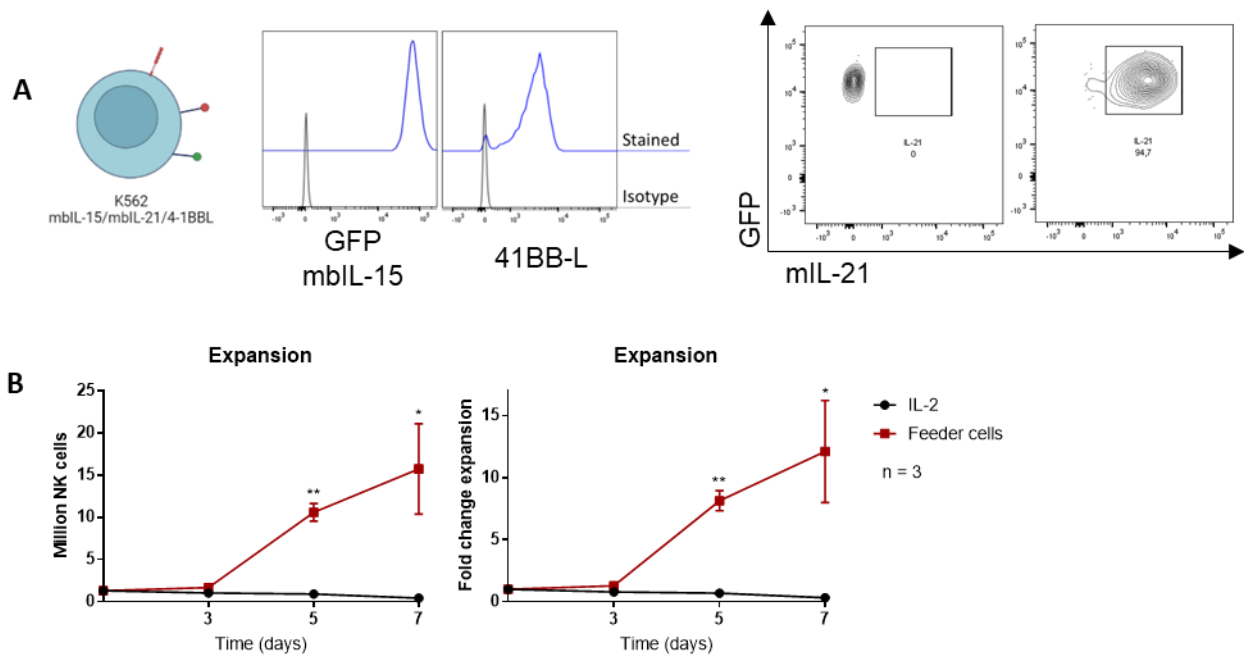


**Figure 8.12: K562-41BBL-mbIL-15-mbIL-21 feeder cells successfully expand human primary NK cells.** (A) Expression of K562-mbIL-15/21-41BBL feeder cells of GFP (membrane bound IL-15, 4-1BBL and IL-21). (B) Expansion of NK cells with K562-mbIL-15/21-41BBL feeder cells for one week. p-value\* < 0.05; p-value\*\* < 0.01. Analysis done by Saphiro's normality test and paired t-test.

I expanded both mock-targeted and HIF-1 $\alpha$  targeted NK cells for a week in co-culture with the irradiated feeder cells. Afterwards, I stimulated the NK cells with the PDO lines in a 5-day co-culture. I included the CytotoxRed dye in the culture medium, which enable monitoring cell death by acquiring fluorescence microscopy images within a humidified CO<sub>2</sub>- and temperature-controlled incubator with built-in automated microscope (IncuCyte) throughout a 5-day co-culture period (Figure 8.13).

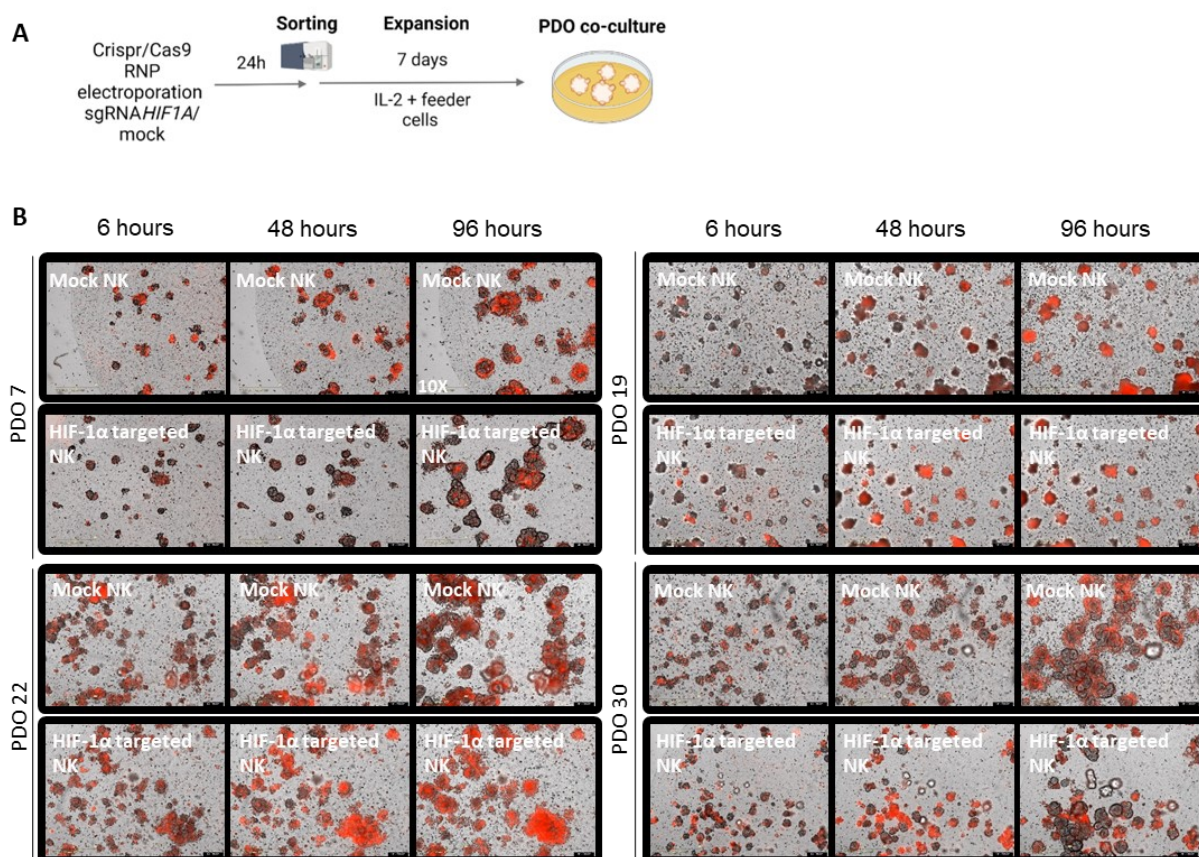


**Figure 8.13: HIF-1 $\alpha$  targeted NK cells cytotoxicity against target is PDO dependent.** (A) Summary of experimental set up. Human NK cells were electroporated with sgRNA targeting HIF-1 $\alpha$  or mock control, as explained previously. After seven days of expansion with feeder cells, NK cells were co-cultured with the four PDO lines during 5 days. Image created with Biorender.com. (B) Culture of POD 7, 19, 22 and 30 without or with expanded HIF-1 $\alpha$  targeted or mock NK cells in a 0.5 to 1 effector to target ratio. Images show CytotoxRed dye present in the media during coculture, images taken by IncuCyte at 10 X (representative images of 4 donors with 5 technical replicates).

When exposed to mock-targeted NK cells, PDO7 cultures displayed an 8.9-fold increase in CytotoxRed fluorescence within 24 hours, with limited increases in the following four days, suggesting an immediate cytotoxic response by NK cells. PDO 19 co-cultures displayed an early-response to NK cell mediated killing, having an average of 3-fold increase in dead cells compared to baseline, reaching a maximum of 7-fold increase at the last timepoint. PDO22 co-cultures, on the other hand, showed limited cell death (under 2-fold increase over baseline), indicative of relative resistance to NK-mediated cytotoxicity. Finally, PDO 30 co-culture showed an exponential NK-cell mediated PDO killing, arriving to a maximum of 13-fold increased dead cells in co-culture with both HIF-1 $\alpha$  targeted NK cells and mock control NK cells (Figure 8.14).

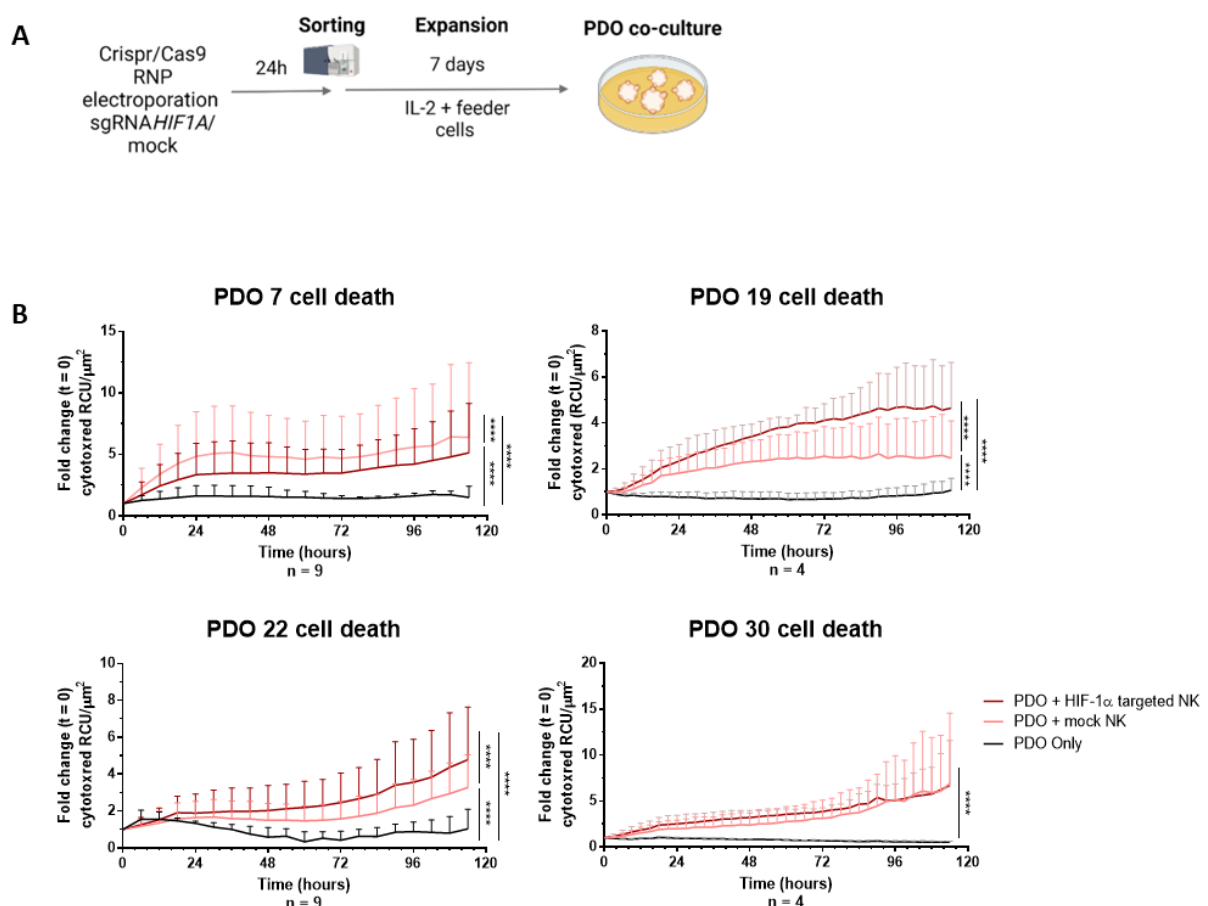


**Figure 8.14: Kinetics of HIF-1 $\alpha$  targeted NK cells mediated killing against target is PDO dependent.** (A) Summary of experimental set up as explained in 8.13. Image created in Biorender.com. (B) Co-culture of POD7 (n = 9), 19 (n = 4), 22 (n = 9) and 30 (n = 4) without or with expanded HIF-1 $\alpha$  targeted or mock NK cells in a 0.5 to 1 effector to target ratio. Quantification of

cytotoxicity dye by fluorescence intensity. (n=5) p-value<sup>\*\*\*</sup> < 0.005, p-value<sup>\*\*\*\*</sup> < 0.001. Analysis done by area under the curve and one way ANOVA.

Targeted disruption of HIF-1 $\alpha$  in NK cells diminished NK-mediated killing of PDO7 in the first 24 hours (4-fold increase in CytotoxRed). For PDO 19, HIF-1 $\alpha$  targeted NK cells showed an increased killing by 3-fold change, which maintained a tendency of enhanced killing during the co-culture. In contrast, PDO22 co-cultures with HIF1 $\alpha$ -targeted NK cells remained unaffected in the first 48 hours, but started to display a higher proportion of dead cells (CytotoxRed) from the third day of the experiment onwards. On the other hand, HIF-1 $\alpha$  targeting did not affect the kinetics of the intensity of the dead cell marker in PDO 30 co-cultures (Figure 8.14). However, individual analysis of 96-hour timepoint scored as statistically significant comparing HIF-1 $\alpha$  targeted and mock NK cells (refer to 8.15).

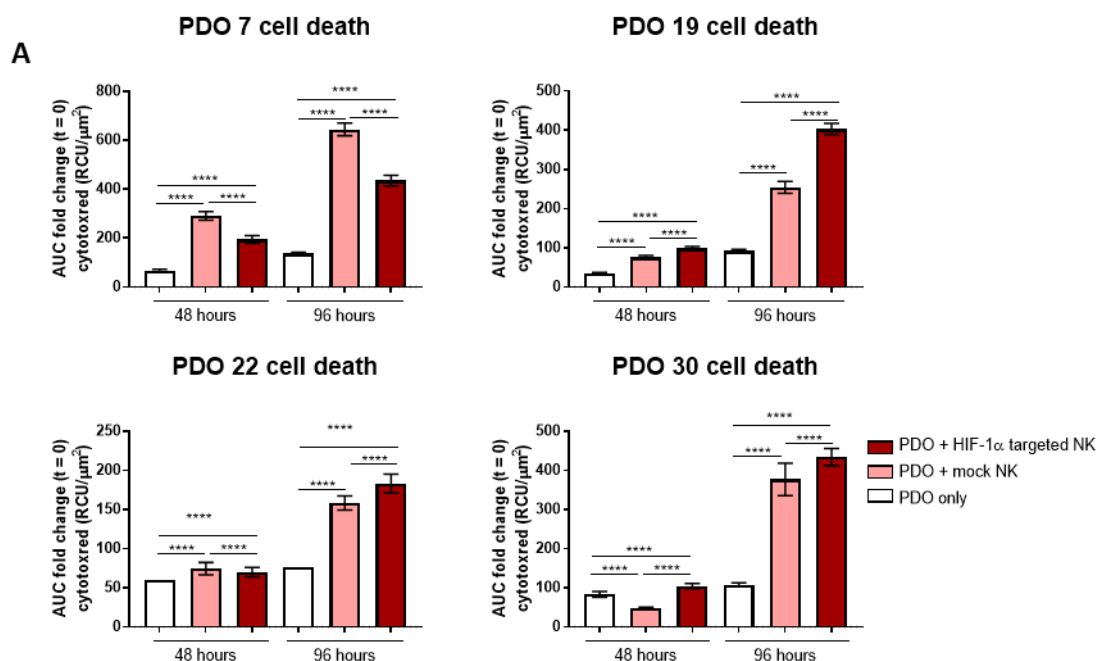


**Figure 8.15: HIF-1 $\alpha$  targeted NK cells cytotoxicity against target is PDO dependent.** (A) Quantification of cytotoxicity dye by fluorescence intensity at timepoints 48 hours and 96 hours. PDO 7 (n = 9), 19 (n = 4), 22 (n = 9) and 30 (n = 4). p-value<sup>\*\*\*</sup> < 0.005, p-value<sup>\*\*\*\*</sup> < 0.001. Analysis done area under the curve and one-way ANOVA.

These data underscore the substantial variability among colorectal cancers and their patient-derived organoids, alongside the potential effect of HIF-1 $\alpha$  targeting in NK cells in promoting or preventing killing of these tumor cells (Figure 8.14 and 8.15).

### 8.1.6 HER-2-CAR NK cell function is negatively affected by hypoxia

Current experimental clinical approaches for NK cancer therapy employ artificial chimeric antigen receptors or bi- or trispesific engager proteins to direct NK cell cytotoxicity towards tumor antigens (Albinger et al., 2021; Gauthier et al., 2019; Nowakowska et al., 2018). I therefore explored whether NK cells equipped with a chimeric antigen receptor directed against the epidermal growth factor receptor 2 (HER-2) constitute a therapeutic approach to eliminate solid tumors such as colorectal adenocarcinoma, with the objective of enhancing their performance within a hypoxic milieu by disruption of HIF-1 $\alpha$ . In collaboration with

Professor Wels, I generated primary NK cells lentivirally transduced to express a chimeric antigen receptor (5.28.z) consisting of single-chain Fv adaptation of the FRP5 antibody against HER-2 and two co-stimulatory domains, CD28 and CD3 $\zeta$ , (Figure 8.16 A).

To assess the efficacy of lentiviral transductions, fluorescence from an enhanced green fluorescent protein (EGFP) expressed from an internal ribosome entry site (IRES) in the CAR construct was measured by flow cytometry. After titration of the transduction units per mL, the multiplicity of infection (MOI) value selected was 8, using 450  $\mu$ L of virus supernatant per 250.000 primary human NK cells. Independent transductions of primary NK cells from multiple donors consistently showed 11-18 % GFP-positive cells, corresponding to an average transduction efficacy of 15 % (Figure 8.16 B). Subsequently, through fluorescence-activated cell sorting, GFP<sup>+</sup> and GFP<sup>-</sup> transduced NK cells were isolated, and the specific recognition of HER-2 by the GFP-positive population only was confirmed by flow cytometry, detecting the binding of a chimeric HER-2 protein labelled with human Fc, which was subsequently stained with anti-Fc APC-labelled antibody (Figure 8.16 C).

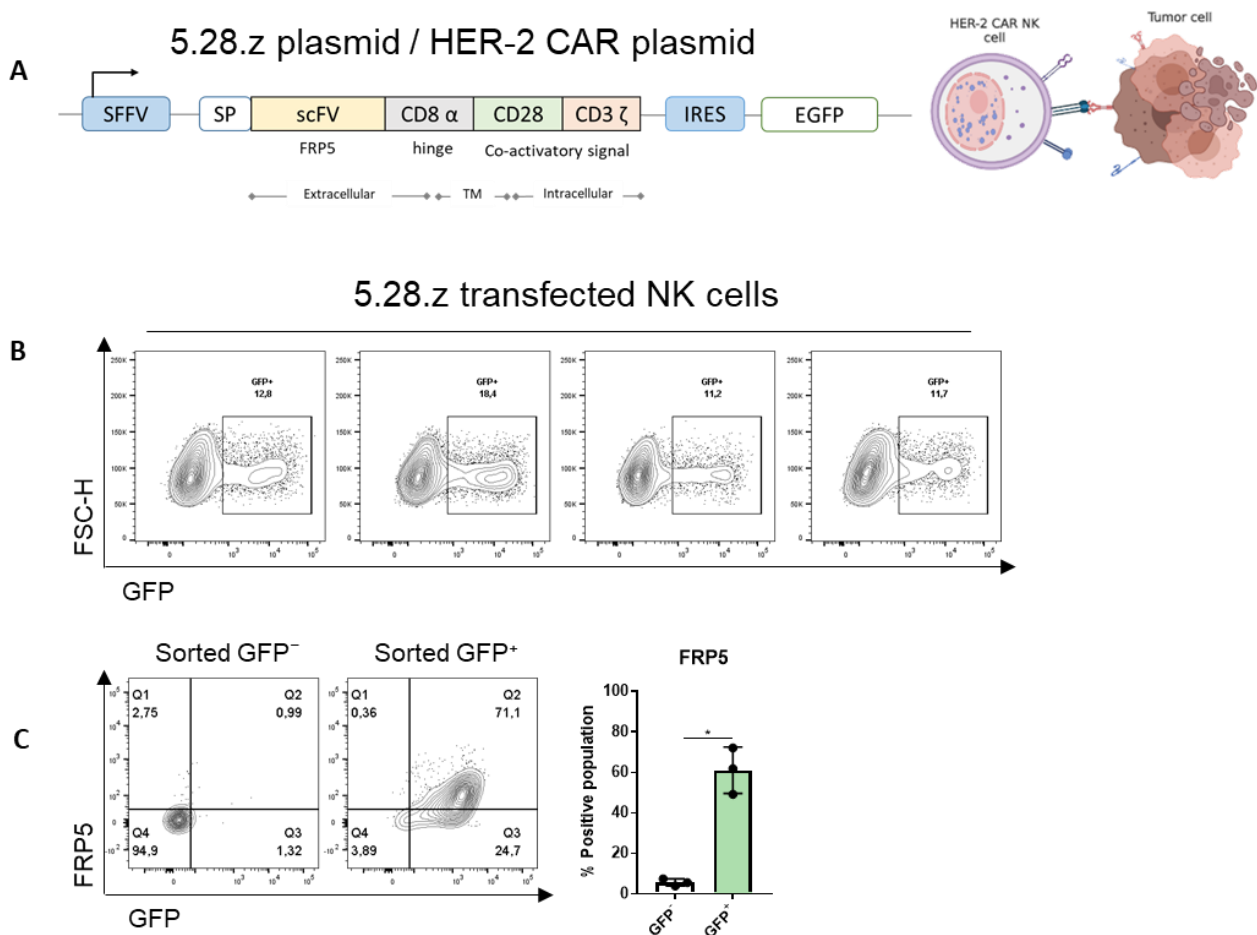


**Figure 8.16: HER-2 CAR NK generation by lentiviral transduction.** (A) 5.28.z plasmid structure, also named HER-2 CAR plasmid. (B) Contour plot of GFP frequency in NK cells seven days post-transduction (n=4, one plot per donor). (C) Contour plot of purity of CAR expression on NK cells after sorting and expansion. Surface FRP5 CAR expression depicted by staining with chimeric HER-2 protein truncated with artificial Fc binding and anti-Fc secondary antibody. Summary of FRP5 CAR purity surface expression in sorted GFP<sup>+</sup> and GFP<sup>-</sup> CAR transduced NK cells (right). p-value\* < 0.05, statistics analysis performed with Spahiro's normality test and paired t-test.

The cytotoxic efficacy of the generated HER-2 CAR NK cells was assessed in co-culture with SKMel-37 melanoma cells, which were confirmed to express HER-2 by flow cytometry (Figure 4.16 A). Upon four hours of co-culture, induction of intracellular TNF- $\alpha$  and IFN $\gamma$  production can be detected in 25.5 % and 21 % of NK cells, respectively. The fraction of responding cells appeared moderately higher in the HER-2 CAR NK cell population with 38.8 % and 28.1 % compared to GFP-/FRP5<sup>-</sup> NK control cells. An assessment of tumor cell control was executed via a confluency assay, which measures cell occupancy of a surface with adherent cells after 24 hours of co-culture. All the calculations were performed using tumor control only conditions (exposed to hypoxia or normoxia in the corresponding groups), whose confluency measure was normalized to 100 %. At a 1:1 ratio of NK to SKMel-37 tumor cells, confluency of the monolayer was reduced by 26 % by non-transgenic NK cells, whereas HER-2 CAR NK cells reduced confluency further with 46 %. Improved anti-tumor activity of NK cells equipped with a HER-2 CAR was also seen with 2:1 and 1:1 ratio (65 % and 28 % confluency reduction respectively). Collectively, these data show that allogeneic NK cells can mount inflammatory and cytotoxic responses towards SKMel-37 tumor cells, which are enhanced when NK cells possess the CAR directed against HER-2.

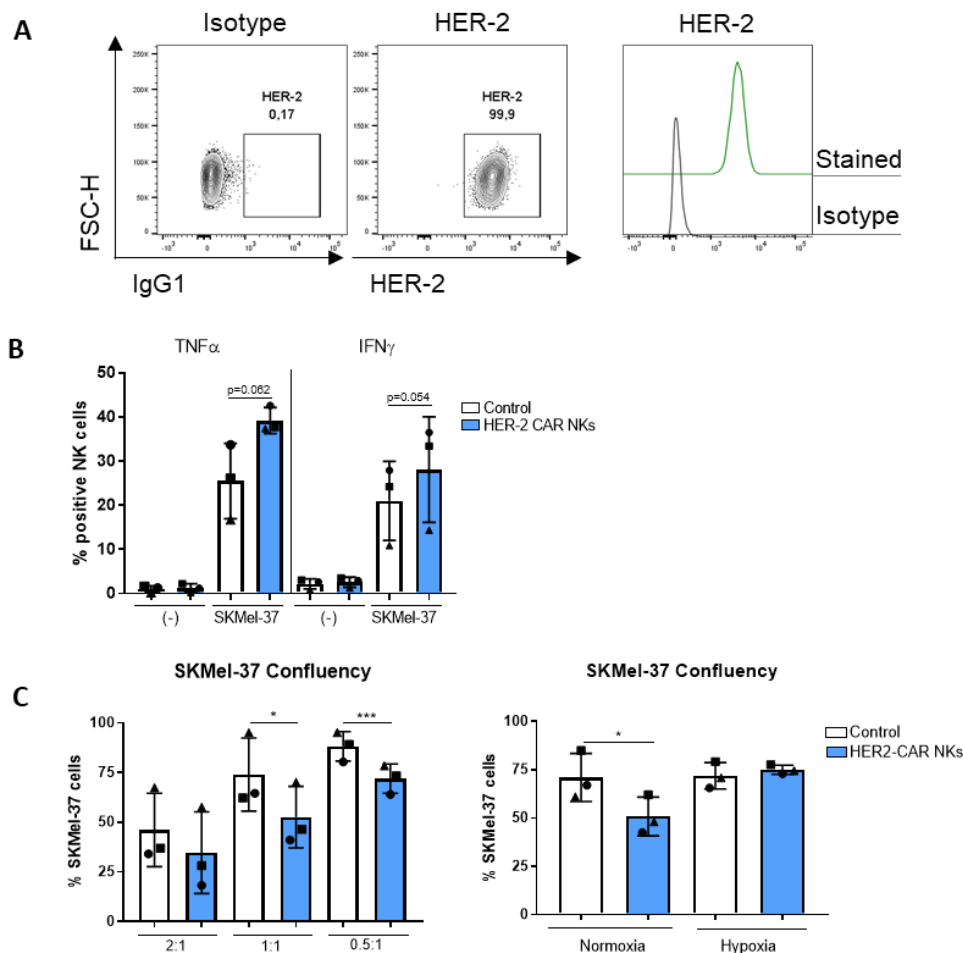


**Figure 4.17: HER2-CAR NK anti-tumor activity is impaired upon hypoxia exposure.** (A) HER-2 expression of SKMel-37 melanoma cells. (B) TNF $\alpha$  and IFN $\gamma$  expression in co-cultures of CAR-NK cells or control gated for live, CD3 $\epsilon$ <sup>-</sup> CD56<sup>+</sup> cells with or without SKMel-37 in 4 hours co-cultures measured by intracellular staining. Control group defined as GFP-/CAR<sup>-</sup> NK cells. (C) Confluency assay with SKMel-37 target cells and GFP-/CAR<sup>-</sup> control NK cells or HER-2 CAR NK cells at an effector to target

ratios of 2:1, 1:1 or 0.5:1 (left) or 1:1 (right). NK cells were pre-treated with 24 hours of exposure to 21 % (normoxia) or 1 % (hypoxia) oxygen with concomitant co-culture with SKMel-37 cells during 24 hours under normoxia or hypoxia.  $p$ -value\* < 0.05,  $p$ -value\*\*\* < 0.005 statistics analysis performed with Saphiro's normality test and paired t-test.

Then, I repeated this experiment at a 1 % oxygen concentration to gauge the potential impact of the hypoxic tumor microenvironment on the cytotoxic activity of HER-2 CAR NK cells. NK cells were pre-exposed to 24 hours of hypoxia or normoxia before co-culturing them with the SKMel-37 cell line (also under 21 % or 1 % oxygen concentrations). Then, I performed the co-cultures either under hypoxia or normoxia during 24 hours. Co-cultures exposed to hypoxia displayed a tumor cell confluency reduction of 28 % comparable to control experiments with 21 % oxygen concentrations. However, presence of HER-2 CAR on the NK cells no longer improved the anti-tumor response with similar confluency reductions measured (24 %) as for the non-transgenic control group (Figure 8.17). This data suggests that hypoxia might interfere with CAR-mediated cytotoxic responses in NK cells.

To pin down whether all CAR-mediated anti-tumor activity is lost in hypoxia-exposed HER-2 CAR NK cells, I generated HER-2 knockouts (HER-2 KO) by electroporating CRISPR/Cas9 nucleoproteins with sgRNAs targeting exon 6 of *ERBB2* in the colorectal adenocarcinoma line HT-29 (Figure 8.18 A and B). In normoxia, 48-hour co-cultures of HT-29 and HER-2 CAR NK cells demonstrated a reduction of tumor cell confluency in the monolayer of 52 %, which was largely lost in the HER-2 KO HT-29 cell line (28 % reduction in confluency). Cognate binding of the CAR ligand thus makes a substantial contribution to the anti-tumor response of the HER-2 CAR NK cells. Interestingly, under hypoxia, these differences were absent, showing a reduction of confluency of 33 % in HER-2 KO and HER-2<sup>+</sup> HT-29 cells (Figure 8.18 C and D). The surface expression of HER-2 protein in the HT-29 surface was not altered upon normoxia or hypoxia exposure (Figure 8.18 E). This data indicates that HER-2 CAR NK cells under hypoxia do not discriminate ligand expression, negatively affecting their cytotoxicity against target cells.

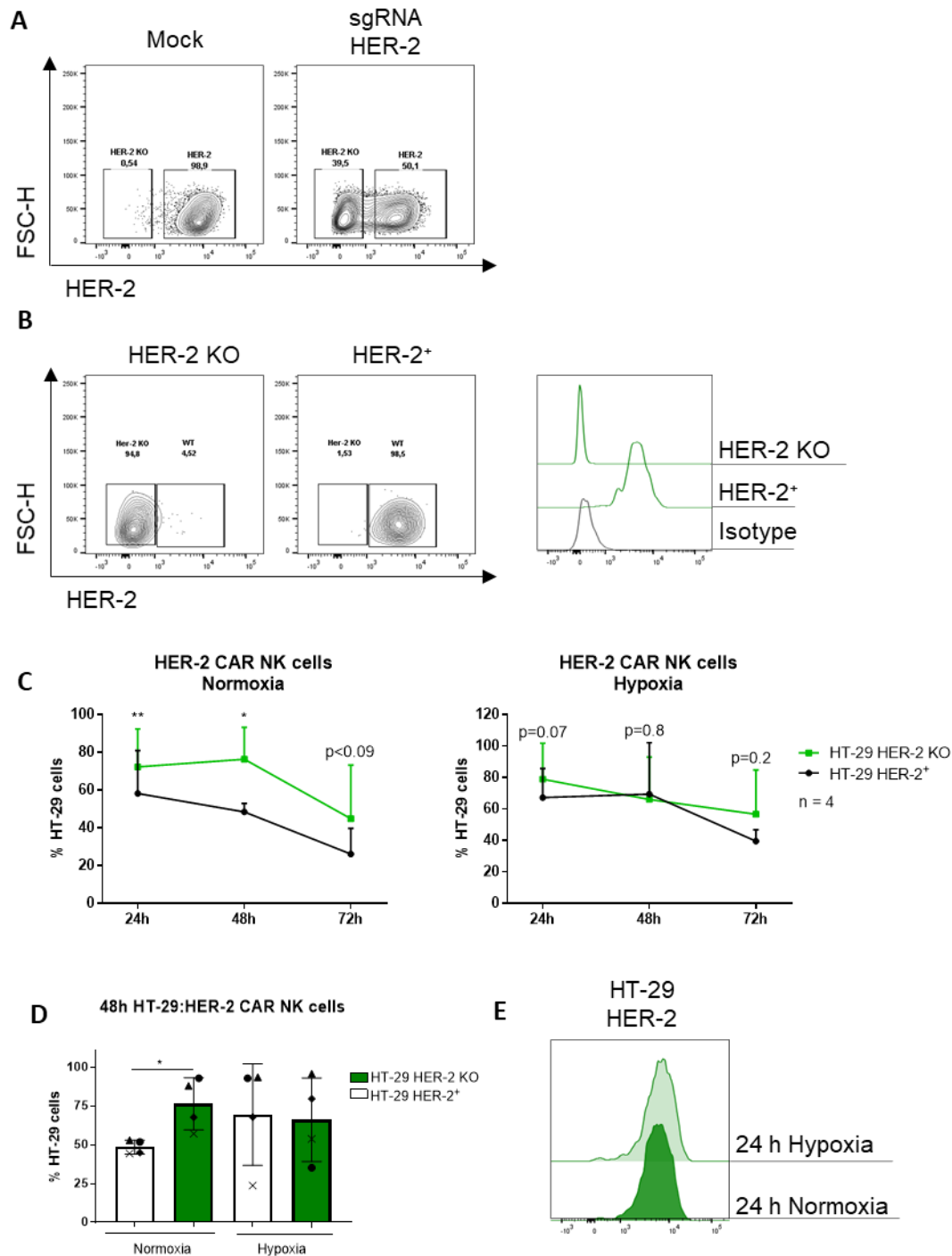


**Figure 4.18: Hypoxia impairs the efficacy of HER-2<sup>+</sup> CAR NK cells against HER-2<sup>+</sup> HT-29 tumor cells while leaving HER-2 KO HT-29 tumor cells unaffected.** (A) Surface staining of HER-2 in HT-29 cells after transfection with sgRNA targeting HER-2. (B) HER-2 expression of HT-29 cells after sorting HER-2<sup>+</sup> and HER-2 KO. (C) Confluency assay at 1 to 1 effector to target ratio at the indicated time points of HER-2 CAR NK cells and HT-29 HER-2<sup>+</sup> or HT-29 HER-2 KO cells under hypoxia or normoxia. HER-2 CAR NK cells were pre-exposed to 24 hours of hypoxia or normoxia prior the tumor cells exposure (n = 4). (D) Quantification of tumor cells in monolayer after 48 hours of coculture in the conditions previously described. (E) HER-2 surface staining of HT-29 cells after 24 hours of exposure to 1 % (hypoxia) or 21 % (normoxia) oxygen. P-value\*\* < 0.005, p-value\* < 0.05, statistics analysis performed with Spahiro's normality test and paired t-test.

Subsequently, I hypothesized that, similar to other tumor entities such as breast cancer, patients with colorectal cancer exhibit HER-2 expression. To assess this, I utilized the database available on cbioportal.com from the study published by Roelands and colleagues (Roelands et al., 2023), stratifying a cohort of 348 patients based on their mRNA expression standardized by Z-score of *ERBB2* (HER-2). Evaluating their progression-free survival over 140 months, I observed a distinct trend between the cohort of 174 patients with *ERBB2* high (0.11 to 7) and low (-5.3 to 0.1) mRNA expression. At 40 months, a 12% difference was already apparent, with more patients in the HER-2 high group (75%) showing no recurrence compared to the *ERBB2* low group (Figure 8.19.A). Regarding disease-specific survival, in an analysis of 160 patients per cohort, a similar trend is observed, with a higher probability for the 10 % of patients in the *ERBB2* low group to succumb directly to causes related to colorectal cancer. Therefore, there is an existent patient population with colorectal adenocarcinoma that may benefit from HER-2 targeted immunotherapies, such as HER-2 CAR NK cells.

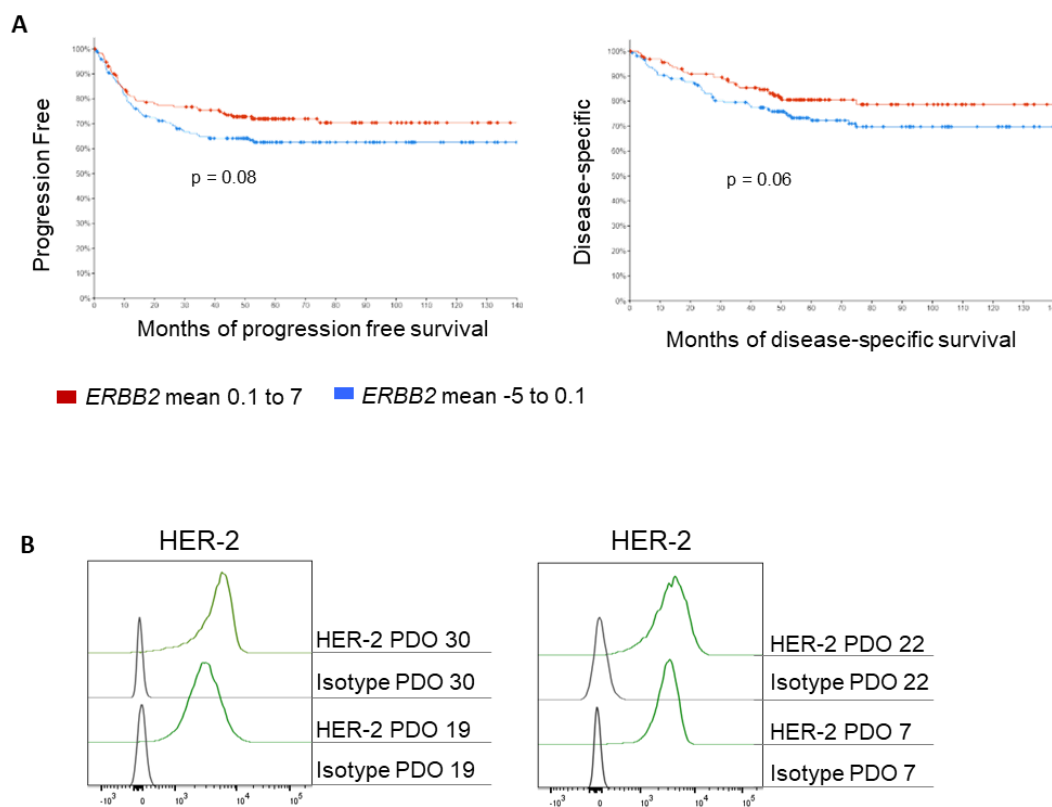


**Figure 8.19: HER-2 expression is detectable in colorectal adenocarcinoma patient cohorts and PDO lines.** (A) Analysis performed from available database of colorectal cancer patients stratifying the cohorts by their *ERBB2* mRNA expression (normalized by Z scored) (REF). *ERBB2* in red represents patients with a mean of 0.1 to 7 and *ERBB2* in blue a mean of -5 to 0.1. Progression free survival was calculated of 174 patient cohorts in each group, and disease-specific survival in 160 patient cohorts. Analysis performed at cbioportal.com. (B) HER-2 surface expression in PDO lines 30, 19, 22, and 7.

I was able to confirm that all the available PDO lines in our laboratory exhibited detectable levels of HER-2 by flow cytometry (Figure 8.19 B), potentially rendering them susceptible to targeting by HER-2 CARs.

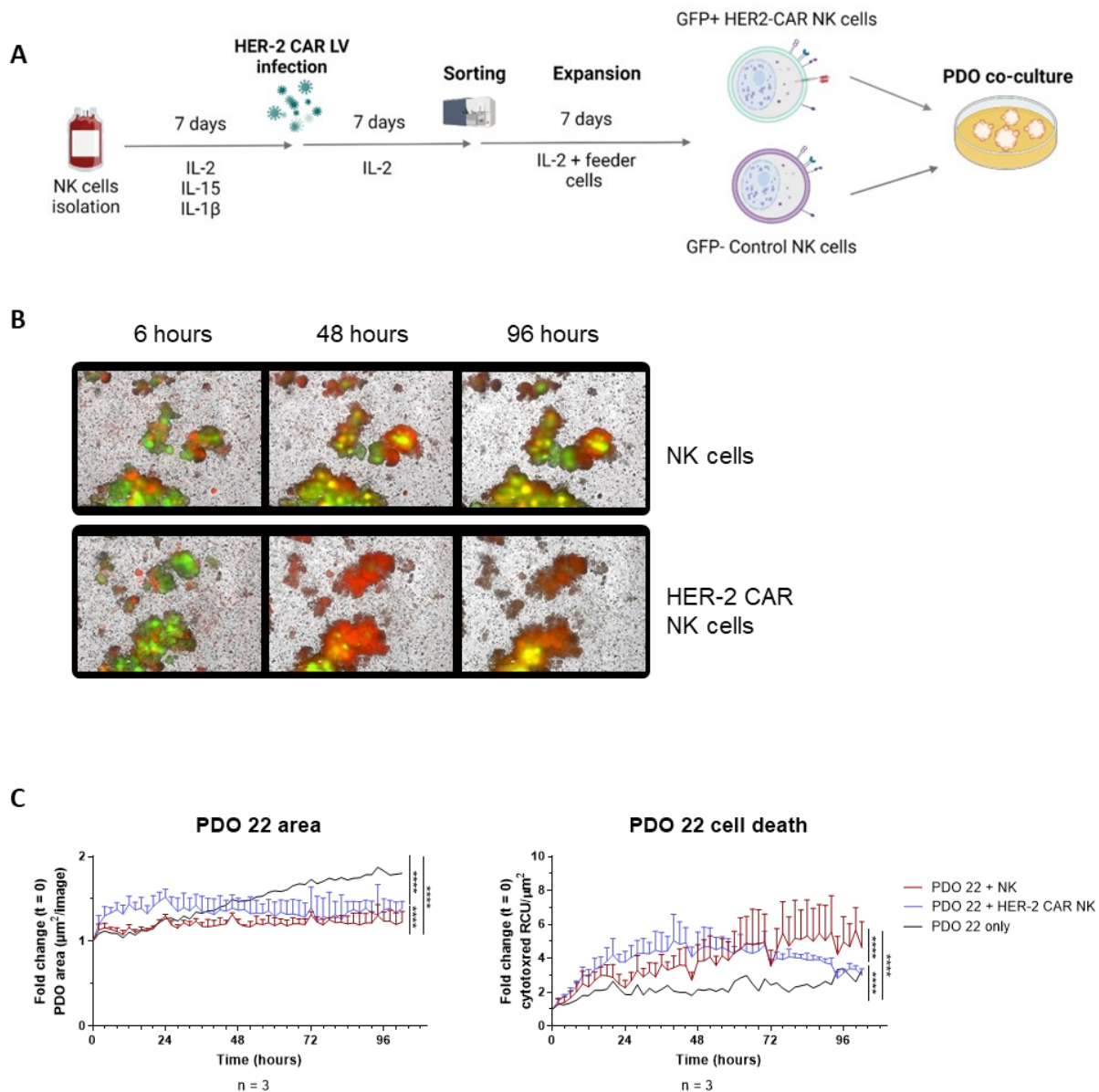


**Figure 8.20: HER-2 CAR NK cells display an early killing kinetic against PDO lines.** (A) Experimental setup: NK cells from healthy donors were expanded, HER-2 CAR lentivirus-infected, sorted for GFP<sup>+</sup> and Frp5 CAR surface expression, and co-cultured with feeder cells. Subsequently, HER-2 CAR NK cells or GFP<sup>-</sup> (non-transgenic) control NK cells were co-cultured with PDO line 22 for 5 days in presence of IL-2. Image created using Biorender. (B) Incucyte fluorescent images (10X objective) of PDO line 22 co-cultured with non-transgenic NK cells or HER-2 CAR NK cells at a 1:1 effector-to-target ratio. Images feature brightfield, red laser (CytotoxRed dye), and green laser (ImageIT Green Hypoxia dye). (C) PDO 22 area and intensity of Cytotoxred dye detected in the co-culture of PDO 22 with non-transgenic NK cells or HER-2 CAR NK cells. Co-culture performed at 1 to 1 effector to target ratio in presence of CytotoxRed dye and 400 U/mL of rhIL-2 (n= 3). p-value<sup>\*\*\*</sup> < 0.001, statistics analysis performed with area under the curve and one-way ANOVA.

Considering the intrinsic hypoxia of the PDOs (Figure 8.10 and 8.11), it is conceivable that the PDOs are refractory to killing by HER-2 CAR NK cells despite expression of the antigen. To evaluate the efficacy of the HER-2 CAR to direct NK cells against PDOs of colorectal adenocarcinoma, I selected PDO22 for co-cultures, as it is relatively resistant to killing by non-transgenic NK cells (Figure 8.13 and 8.14). As before, I co-cultured organoids and NK cells for five days while acquiring fluorescence micrographs in the presence of reporter dyes monitoring cell death (CytotoxRed) and hypoxia (ImageIT Hypoxia Green dye). The captured images illustrate the rapid killing ability within 48 hours of HER-2 CAR NK cells (4-fold change increased cell death compared to  $t = 0$ ) in comparison to the non-transgenic NK cells (2.8-fold change increase compared to  $t = 0$ ), with almost complete staining of organoid structures with CytotoxRed and granular debris on the edges detected in brightfield (Figure 8.20 A and B). In terms of kinetics, maximal PDO cell death was reached earlier by HER-2 CAR NK cells at approximately 36 hours than by non-transgenic NK cells, which exhibited a delayed response towards the end of the assay (from 72 hours onwards) (Figure 8.20 C). Expansion of the organoids as measured by the area occupied in the brightfield over time is repressed by NK cells both with and without HER-2 CAR NK cells. Taken together, these findings underscore the potential of HER-2 CAR NK cells as a therapeutic approach to confront HER-2-expressing solid tumors.

### 8.1.7 CRISPR/Cas9-targeted edition of HIF-1 $\alpha$ in HER-2 CAR NK cells enhances killing of patient-derived colorectal adenocarcinoma organoids

Targeted genetic disruption of HIF-1 $\alpha$  in NK cells rescued the repression of IFN $\gamma$  production under hypoxic conditions. As hypoxia eliminated HER-2-dependent anti-tumor activity of HER-2 CAR NK cells (Figure 8.18), I postulated that genetic targeting of HIF-1 $\alpha$  may similarly rescue anti-tumor activity of HER-2 CAR NK cells, which could be relevant in the intrinsically hypoxic regions of the colorectal adenocarcinoma PDOs. I targeted the HIF-1 $\alpha$  gene (*HIF1A*) for disruption by electroporation of CRISPR/Cas9 ribonucleoprotein complexes into HER-2 CAR NK cells. After expansion, I challenged the electroporated cells with HER-2<sup>+</sup> PDO lines of colorectal adenocarcinoma. Images generated by brightfield and CytotoxRed dye staining show a tendency of a rapid killing of PDO 7, 19 and 30 by HER-2 CAR HIF-1 $\alpha$  targeted NK cells (48 hours) compared to HER-2 CAR NK cells (96 hours) (Figure 8.21). In contrast, the killing of PDO 22 was present at a later timepoint, observing a sustained CytotoxRed signal after 96 hours for both NK cells conditions.

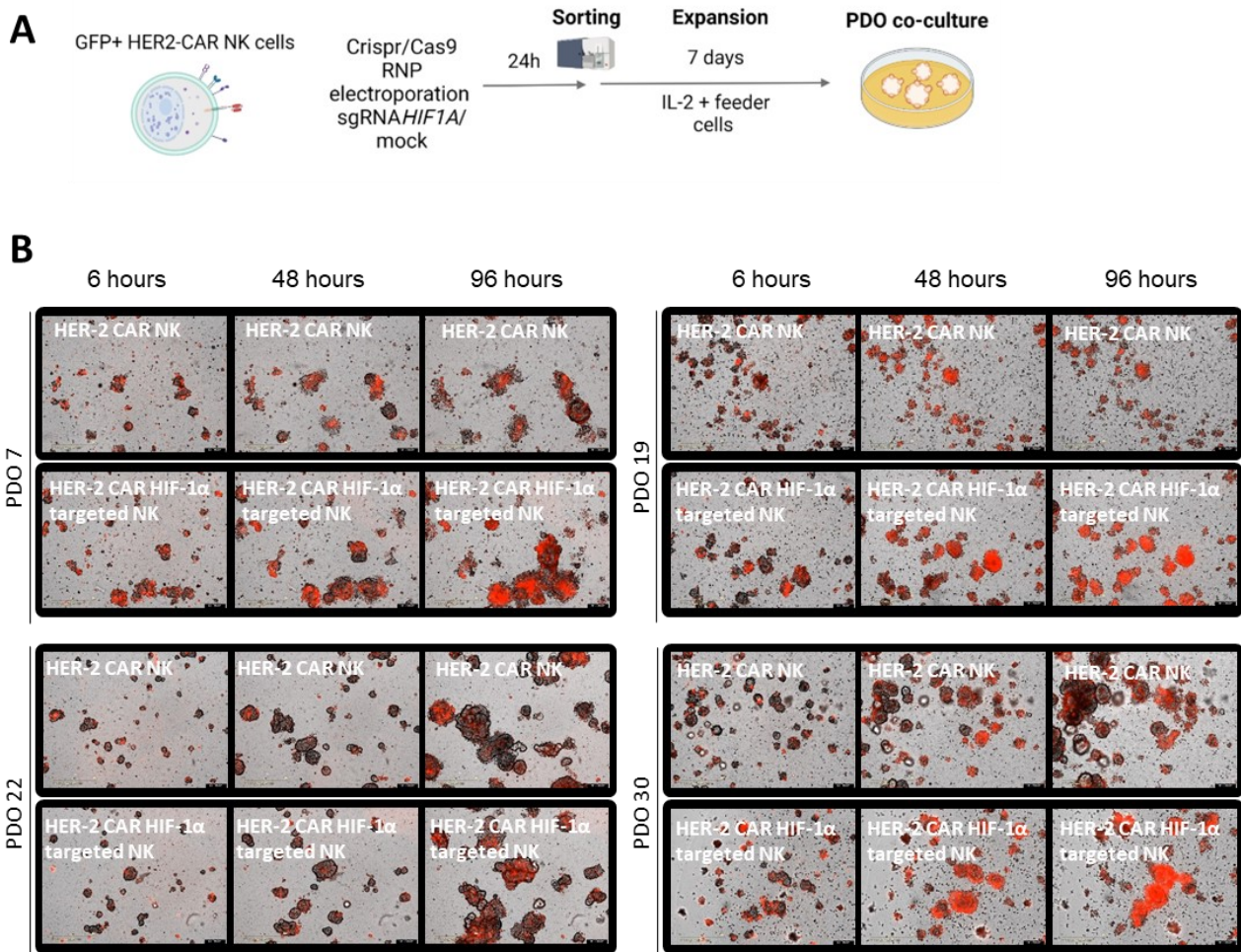


**Figure 8.21: HER-2 CAR HIF-1 $\alpha$  targeted NK cells kill PDO lines rapidly.** (A) Summary of experimental set up. HER-2 NK cells and control NK cells were electroporated with CRISPR/Cas9 RNP sgRNA-dye labelled against HIF-1 $\alpha$  gene or with mock control. 24h after cells were sorted according to dye expression and cultured for seven days in coculture with 41BBL-mbIL-15/21-K562 feeder cells. Then, 5 days PDO coculture in IncuCyte was performed. Figure created with Biorender.com. (B) Pictures from IncuCyte at 10X from day 0, day 2 and day 5 of coculture of HER-2 NK cells or HER-2 CAR HIF-1 $\alpha$  KO NK cells. Image-iT hypoxia (Green) and cytotox-red dyes (red) displayed respectively.

Upon analyzing PDO area from the area as measure of tumor growth, I found that inclusion of NK cells reduced (PDO 7, PDO 30) or prevented (PDO 19) outgrowth altogether (Figure 8.22 A). There was no discernible improvement attributable to genetic disruption of *HIF1A* in NK cells. Instead, both HER-2 CAR NK groups exhibited similar control over PDO growth (Figure 8.22).

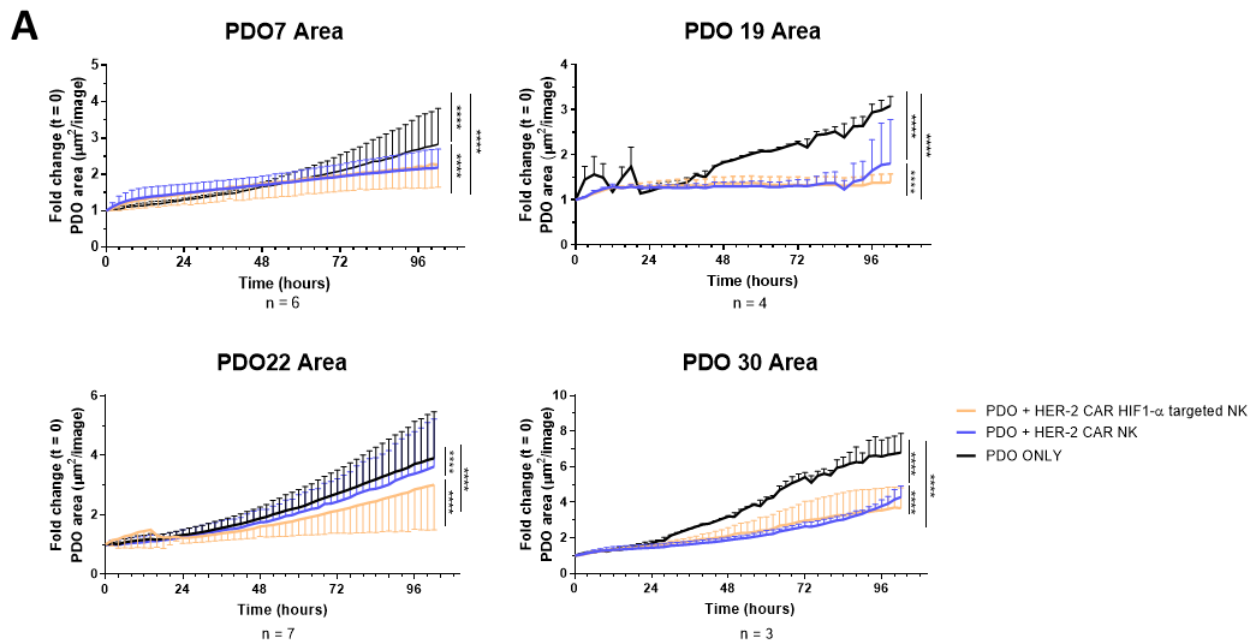


**Figure 8.22: HER-2 CAR HIF-1 $\alpha$  targeted NK cells and HER-2 CAR NK cells control PDOs growing in comparison to PDOs only.** (A) Fold change of the detected area in brightfield of PDOs ( $\mu\text{m}^2/\text{image}$ ) in coculture with HER-2 CAR NK cells or HER-2 CAR HIF-1 $\alpha$  targeted NK cells. Co-cultured performed during 102 hours with PDO lines 7 (n = 6), 19 (n = 3), 22 (n = 7), and 30 (n = 3). p-value\*\*\* < 0.005, p-value\*\*\*\* < 0.001, statistic analysis performed with area under the curve analysis and one-way paired ANOVA.

Nonetheless, I utilized CytotoxRed fluorescence as a marker for dead cells, aiming for a more sensitive measure of cytotoxicity displayed by HER-2 CAR or HER-2 HIF-1 $\alpha$  targeted NK cells against PDOs (as shown in Figure 8.23). After 48 hours of co-culture with PDO 7, the intensity of CytotoxRed dye reached a maximum of a 7-fold increase when using HER-2 CAR HIF-1 $\alpha$  targeted NK cells, while co-culture with HER-2 CAR NK cells resulted in a 5-fold increase.

The kinetics of PDO 19 cell death staining showed a decrease after 48 hours, resulting in a 4-fold increase with HER-2 CAR HIF-1 $\alpha$  targeted NK cells and a 2-fold increase with HER-2 CAR NK cells, respectively. For PDO 22, the intensity of CytotoxRed staining displayed an 8-fold increase after 96 hours of co-culture with HER-2 HIF-1 $\alpha$  targeted CAR NK cells, while HER-2 CAR NK cells yielded a 5-fold increase by the end of the co-culture. Lastly, PDO 30 exhibited a similar intensity of cell death staining during the first 48 hours. However, between 48 and 96 hours of co-culture, HER-2 CAR HIF-1 $\alpha$  targeted NK cells demonstrated an average 7-fold increase, whereas HER-2 CAR NK cells maintained a 4-fold increase in cytotoxicity from 48 hours to 96 hours. In conclusion, it is evident that HER-2 CAR HIF-1 $\alpha$  targeted NK cells exhibit enhanced cytotoxicity across all PDO samples.

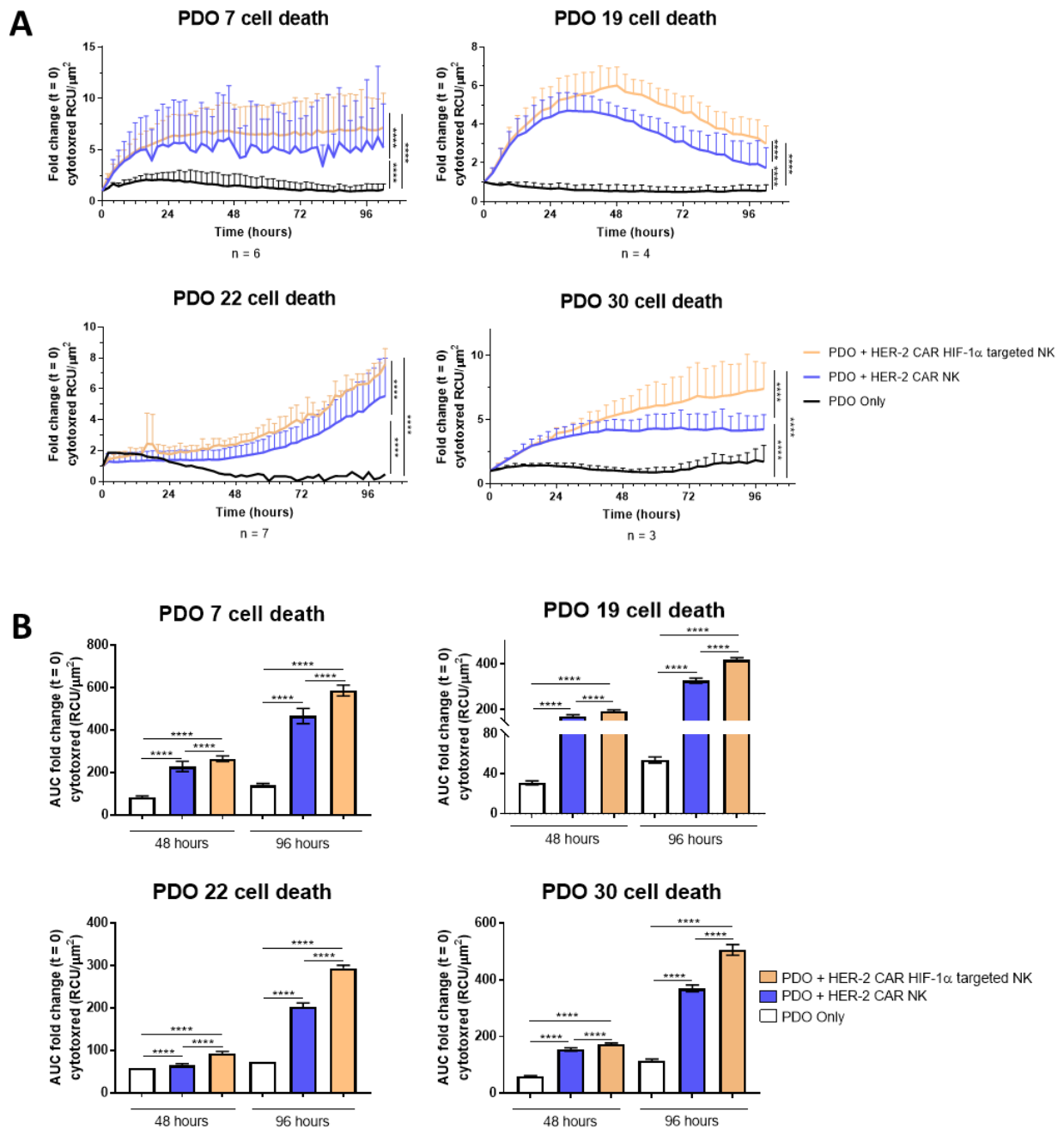


**Figure 8.23: HER-2 CAR HIF-1 $\alpha$  targeted NK cells show enhanced cytotoxicity against PDO lines.** (A) Quantification of the fluorescence intensity of CytotoxRed dye compared to timepoint 0 of co-cultures described in Figure 22. PDO 7 (n = 7), 19 (n = 3), 22 (n = 7) and 30 (n = 4). (B) Cell death of each PDO lines after 48 hours and 96 hours of co-culture with HER-2 CAR NK cells or HER-2 CAR HIF-1 $\alpha$  targeted NK cells calculated from CytotoxRed dye fluorescence intensity compared to timepoint 0. p-value<sup>\*\*\*</sup> < 0.005, p-value<sup>\*\*\*\*</sup> < 0.001, statistic analysis performed with area under the curve and one-way paired ANOVA.

Activation of NK cell effector functions induces the production of lytic vesicles containing Granzymes and Perforin or secretion of cytokines such as IFN $\gamma$  and granulocyte/macrophage-stimulating growth factor (GM-CSF). I collected the supernatant after 5 days of PDO 7 and 22 co-cultures with HER-2 CAR NK cells or HER-2 CAR HIF-1 $\alpha$  targeted NK cells. Quantification of IFN $\gamma$ , GM-CSF, Perforin and Granzyme B (pico grams per millilitre) produced by NK cells by flow cytometry-based multiplex immunoassays (MACs Plex) revealed no distinct differences between NK with or without targeted disruption of *HIF1A* (Figure 8.24).

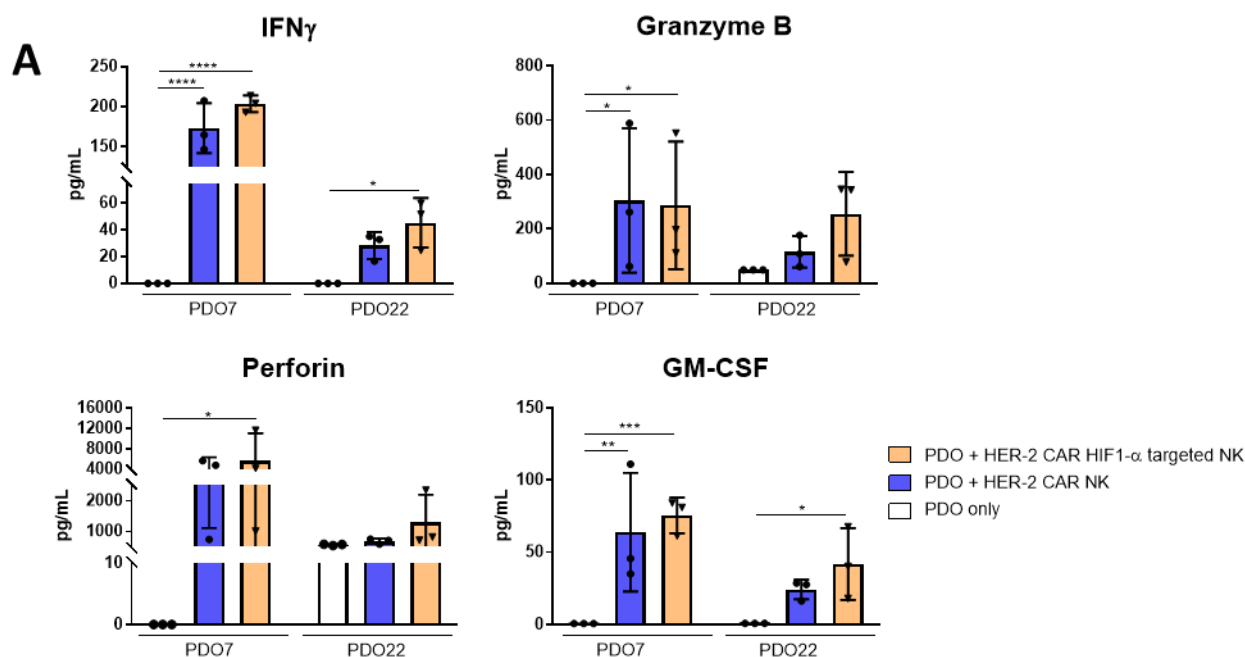


**Figure 8.24: HER-2 CAR HIF-1 $\alpha$  targeted NK cells produce similar soluble factors in coculture with PDOs.** (A) Cytokine quantification from PDO and NK cells coculture (timepoint = 5 days), detecting IFN $\gamma$ , GMCSF, Perforin and Granzyme B. (n = 3). p-value\*\*\* < 0.005, p-value\*\*\*\* < 0.001, statistic analysis performed with one-way paired ANOVA.

### 8.1.8 Improved infiltration of HER-2-CAR, HIF-1 $\alpha$ CRISPR/Cas9-targeted NK cells in HT-29 spheroids

To evaluate the potential of HER-2 CAR NK cells to penetrate solid tumors, spheroids were generated from the colorectal adenocarcinoma cell line HT-29 that naturally expresses the CAR antigen HER-2 (HER-2<sup>+</sup>) and a derived cell line in which the gene encoding HER-2 was disrupted by CRISPR/Cas9 (HER-2 KO; Figure 8.17). Experiments were performed at Miltenyi in collaboration with Dr. Möker, Dr. Zhang, and Dr. Villacorta on a Blaze light sheet microscope to visualize the infiltration of NK cells into tumor spheroids. Spheroids grown in an agarose matrix containing size-labelled wells were incubated with ImageIT Hypoxia Green dye to detect reduced oxygen availability within the entire spheroid volume (Figure 8.24 A and B). Subsequent co-culture with NK cells for 24 hours resulted in extensive cell debris visible around the spheroid core, suggesting that both HER-2 KO and HER-2<sup>+</sup> HT-29 spheroids were sensitive to NK cell-mediated elimination (Figure 8.24 C).

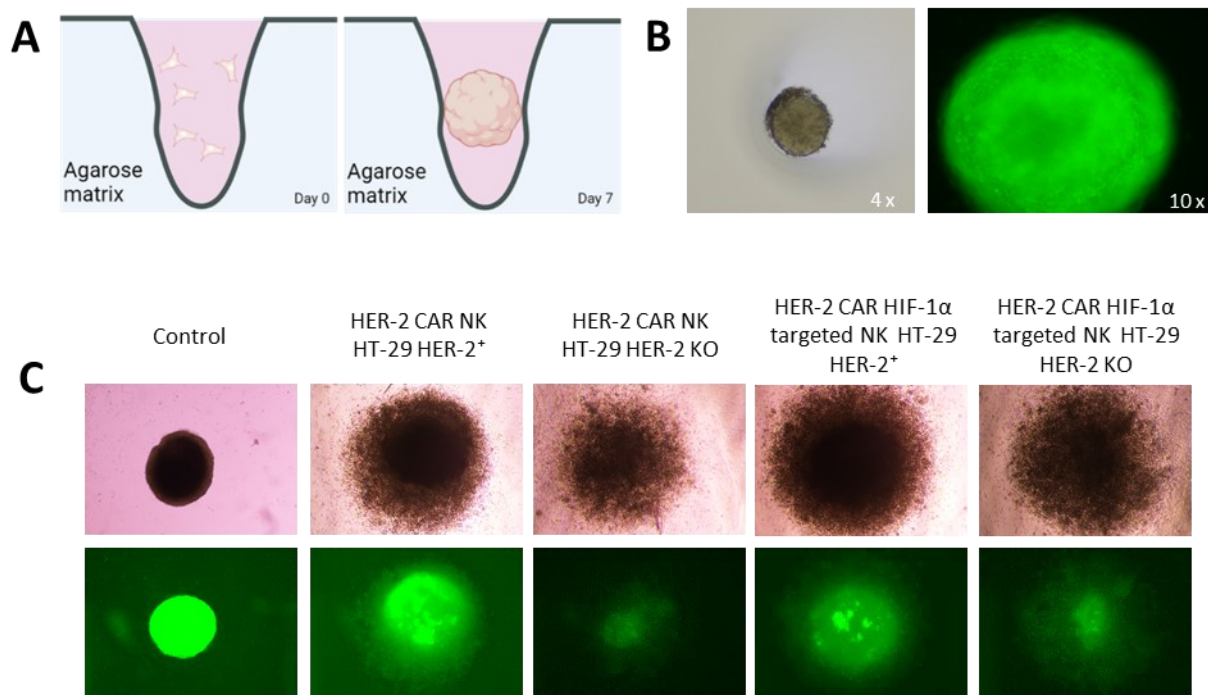


**Figure 8.25: NK cells disrupt HT-29 spheroids displaying hypoxia.** (A) Summary of HT-29 spheroid generation by agarose matrix from ABCbiotech. (B) Imaging of HT-29 spheroid on the matrix and with ImageIT Hypoxia Green dye after 30 minutes of staining. Brightfield images taken at 4 X magnification and green fluorescence pictures at 10 X magnification. (C) 24 h coculture of HT-29 spheroids HER-2 KO and HER-2<sup>+</sup> with HER-2 CAR NK cells or HER-2 HIF-1 $\alpha$  targeted NK cells at 4 X magnification. Green fluorescence displaying ImageIT Hypoxia Green dye intensity and GFP signal from HER-2 CAR NK cells and HER-2 CAR HIF-1 $\alpha$  targeted NK cells (n = 1).

With the intent to detect the NK cell infiltration preceding cytotoxic effects, I acquired 3D light sheet images of the samples after a 2-hour cultivation interval. Spheroids were fixed, permeabilized and stained with antibodies targeting the immune cell epitope CD45 present on NK cells, but absent on the HT-29 cancer cells. In the reconstructed three-dimensional representations, GFP fluorescence of CAR-transduced NK cells (Figure 8.15 and 8.26 A) overlapped with CD45-immunostained cells encapsulating the spheroid surface. The number of recruited NK cells ranged between 177-336 cells per spheroid and appeared largely independent from the presence of the HER-2 antigen on cancer cells (Figure 8.26 B and C).

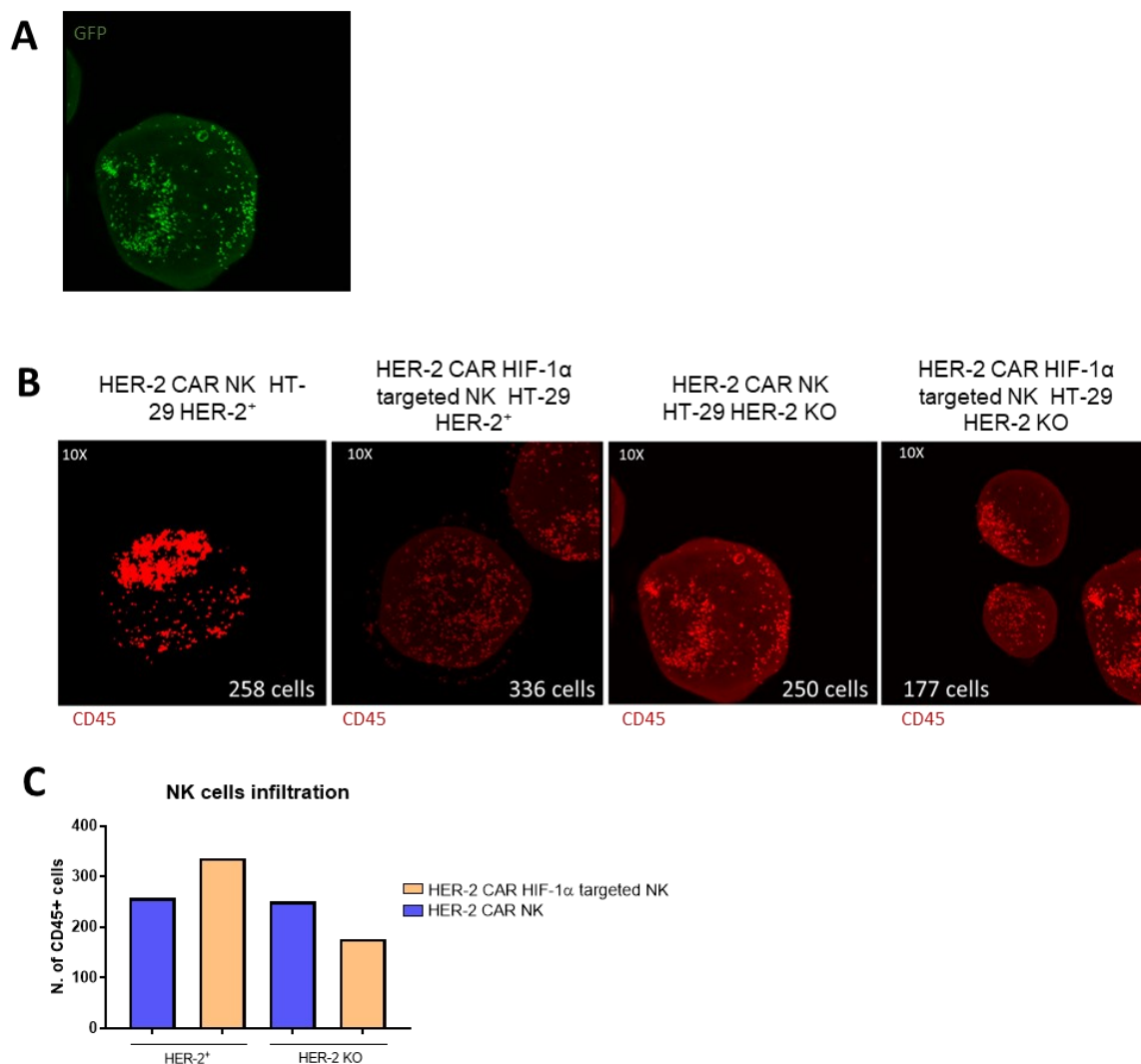


**Figure 8.26: Preliminary data suggests an increased NK cell recruitment of HER-2 CAR HIF-1 $\alpha$  targeted NK cells in HT-29 spheroids.** (A) 10 X magnification picture of a HT-29 spheroid displaying GFP fluorescence. (B) Imaging of HER-2<sup>+</sup> or HER-2 KO HT-29 spheroids after 2 hours coculture with HER-2 CAR or HER-2 CAR HIF-1 $\alpha$  targeted NK cells. CD45-VioR667 staining displayed in red. NK cells counting performed with ImageJ 3D analysis. (C) Quantification of cells per condition. (n = 1, 3 spheroids per condition as technical replicates).

## 8.2 CYTOKINE-INDUCED MEMORY-LIKE NK CELL CYTOKINE PRODUCTION AND SURFACE PROTEIN EXPRESSION UNDER HYPOXIA

Even though NK cells generally act non-adaptively as naïve effector cells, enhanced responses by NK cell subsets have been reported after exposure to certain haptens, viral infections or cytokine combinations (M. A. Cooper et al., 2009). Combined stimulation of NK cells with the cytokines IL-12, IL-18, and IL15, augments IFN $\gamma$  production and cytotoxicity upon

subsequent challenge of these cytokine-induced memory-like (CML) NK cells (Horenstein et al., 2018; Leong et al., 2014; Romee et al., 2016; Uppendahl et al., 2019). I hypothesized that hypoxia might interfere with the acquisition of memory-like recall responses of NK cells within the tumor microenvironment.

### 8.2.1 Cytokine-induced memory-like NK cells exposed to hypoxia reduce IFN $\gamma$ production upon IL-12/18 stimuli

To test my hypothesis, I generated CML NK cells as described (Leong et al., 2014) and examined the effect of sustained hypoxia (1 % O<sub>2</sub>) exposure during seven days on degranulation and cytokine production (Ni et al., 2020). As expected, when co-cultured with K562 cells, a larger proportion of CML NK cells (38.4 %) responded by IFN $\gamma$  production detected by flow cytometry, as compared to NK cells maintained under IL-2 and IL-15 stimulation alone (11.8 %). Hypoxia exposure did not alter the production of this cytokine in response to K562 target cells (33.3 % for CML NK cells and 8.7 % for IL-2/15 NK cells). However, seven days of hypoxia exposure suppressed IFN $\gamma$  production in response to stimulation with cytokines IL-12 and IL-18 in both CML NK cells (34 % under hypoxia vs 64.9 % under normoxia) and control NK cells (18.9 % after hypoxia and 48.8 % after normoxia), with approximately half of the population losing the production of IFN $\gamma$  (Figure 8.27 A and B). I evaluated CD107a marker in CML NK cells under normoxia or hypoxia after 4 hours of stimulation with K562, but no differences emerged (Figure 8.27 C).

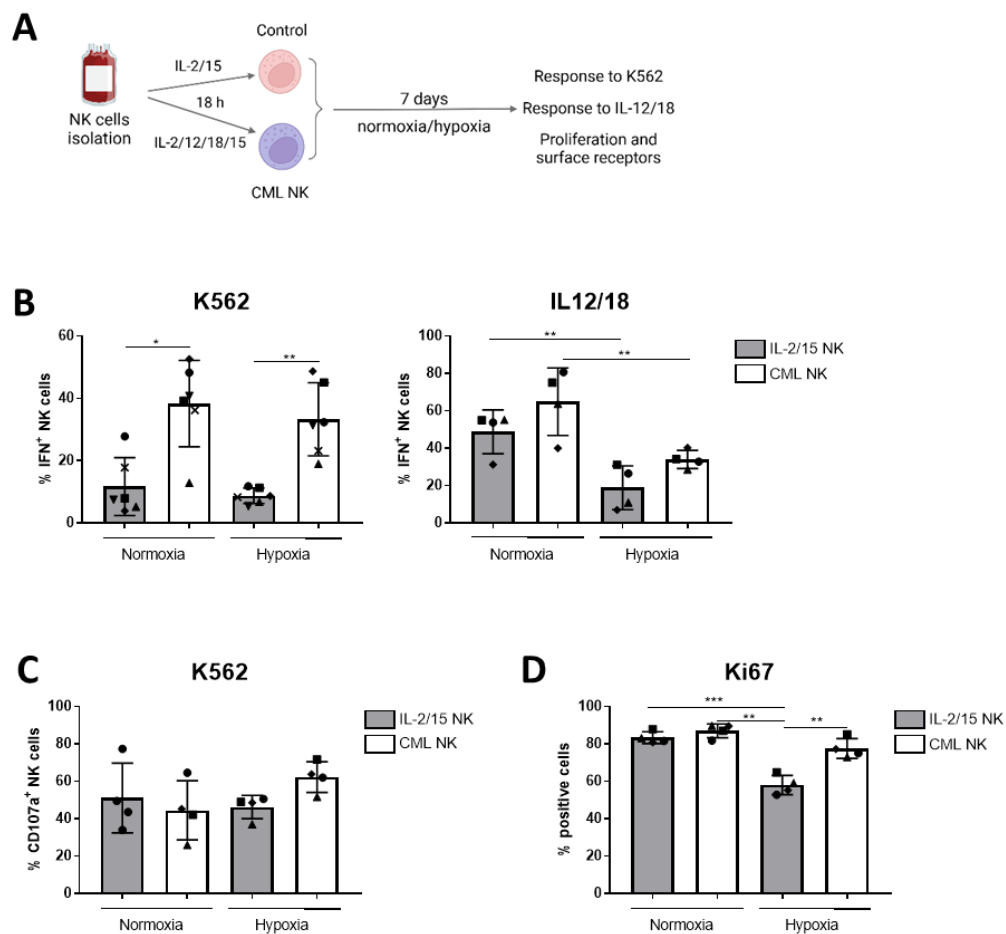


**Figure 8.27: Cytokine induced memory-like NK cells response to IL-12/18 is impaired, while proliferation and degranulation upon target exposure remain unaltered after hypoxia exposure**

(A) Summary of the experimental set up. Human primary NK cells were isolated from PBMCs and stimulated for 18 hours with cytokines. Control group was stimulated with IL-2/15 and cytokine induced memory-like NK (CML NK) cells were stimulated with IL-2/12/18/15. Afterwards, cells were cultured with IL-2/15 for seven days under hypoxia or normoxia for further testing of response to K562, IL-12/18, proliferation and surface receptor detection. Figure created in Biorender.com. (B) IFN $\gamma$  production stained in control NK cells or cytokine induced memory-like NK cells after coculture with K562 leukemia cells (n = 6) or stimulated with IL-12/18 for 4 hours under normoxia or hypoxia (n = 4). (C) CD107a frequency in NK cells cocultured with K562 leukemia cells as described in B. (n = 4). (D) Ki67 intracellular of control NK cells or cytokine induced memory-like NK cells under normoxia or hypoxia. (n = 4). p-value\* < 0.05; p-value\*\* < 0.01; p-value\*\*\* < 0.005. Analysis done by Saphiro's normality test and one way ANOVA.

Moreover, the proliferation marker Ki67 showed no difference in CML NK group after hypoxia exposition (Figure 8.27 D), whereas NK cells stimulated with IL-2/15 showed a reduction of Ki67 staining, as expected from previous data (Figure 8.4). Altogether, this data reports a different hypoxia effect in IFN $\gamma$  production and proliferation of CML NK cells when compared to IL-2/15 stimulated NK cells, where IL-12/18 stimulation was not sufficient to trigger IFN $\gamma$  production. I could conclude that CML NK cells maintain their efficacy after K562 co-culture, as well as proliferation independently of hypoxia exposure.

### 8.2.2 CML NK cells alter surface markers after seven days of hypoxia exposure

With the aim of conducting an examination of CML NK cells, I scrutinized a panel of markers associated with CML NK cells subsequent to their exposure to hypoxia (Leong et al., 2014). NKG2A frequency after hypoxia exposure showed a 30 % increase in CML NK cells (87.5 %) compared to IL-2/15 exposed NK cells (53.4 %). I observed a moderate increase of CD25 (IL-2 high-affinity receptor) in CML NK cells (24 %, p\* = 0.01) when compared to IL-2/15 NK cells group (7 %), without a detectable change between hypoxia and normoxia exposure. The frequency of NKP44 surface expressing cells was reduced in CML NK cells (38.3 %) compared to 73.5 % in IL-2/15 NK cells under normoxia (p = 0.08), detecting similar percentage between both NK cells groups of positive cells after hypoxia exposure (average of 66 %). CML NK cells exposed to hypoxia showed a moderate increase of NKP44 frequency when compared to normoxia pre-exposed group (p\* = 0.03). I noted an increase of CD127 (IL-7Ra) percentage of positive cells was increased in all NK cells pre-exposed to hypoxia (24.7 %, p\* = 0.03 IL-2/15 NK cells and 29 %, p = 0.07 CML NK cells), with a barely detectable staining under normoxia (2 %). TRAIL-positive IL-2/15 stimulated NK cells were reduced under hypoxia by half, whereas CML NK cells remained with a frequency of 40 % independently of the oxygen concentration. The increased frequency of TRAIL by CML NK cells was notable compared to IL-2/15 NK cells after hypoxia exposure (p\*\* = 0.008). I observed a threefold-decrease of the expression of NKP80 in CML NK cells when compared to IL-2/15 NK cells (p = 0.09), which was maintained after hypoxia exposure (p\* = 0.04) (Figure 8.28). On the other hand, CD16 frequency of surface expressing cells and CD96 mean fluorescence intensity expression was not altered between IL-2/15 stimulated NK cells and CML NK cells (without detectable changes upon hypoxia exposure). This data suggests that while certain markers associated

with CML NK cells remain stable (such as CD25 or Trail), others are perturbed (NKp44), potentially indicating a hypoxia-dependent change in the cells, in terms of soluble factor production, proliferation and receptor expression.

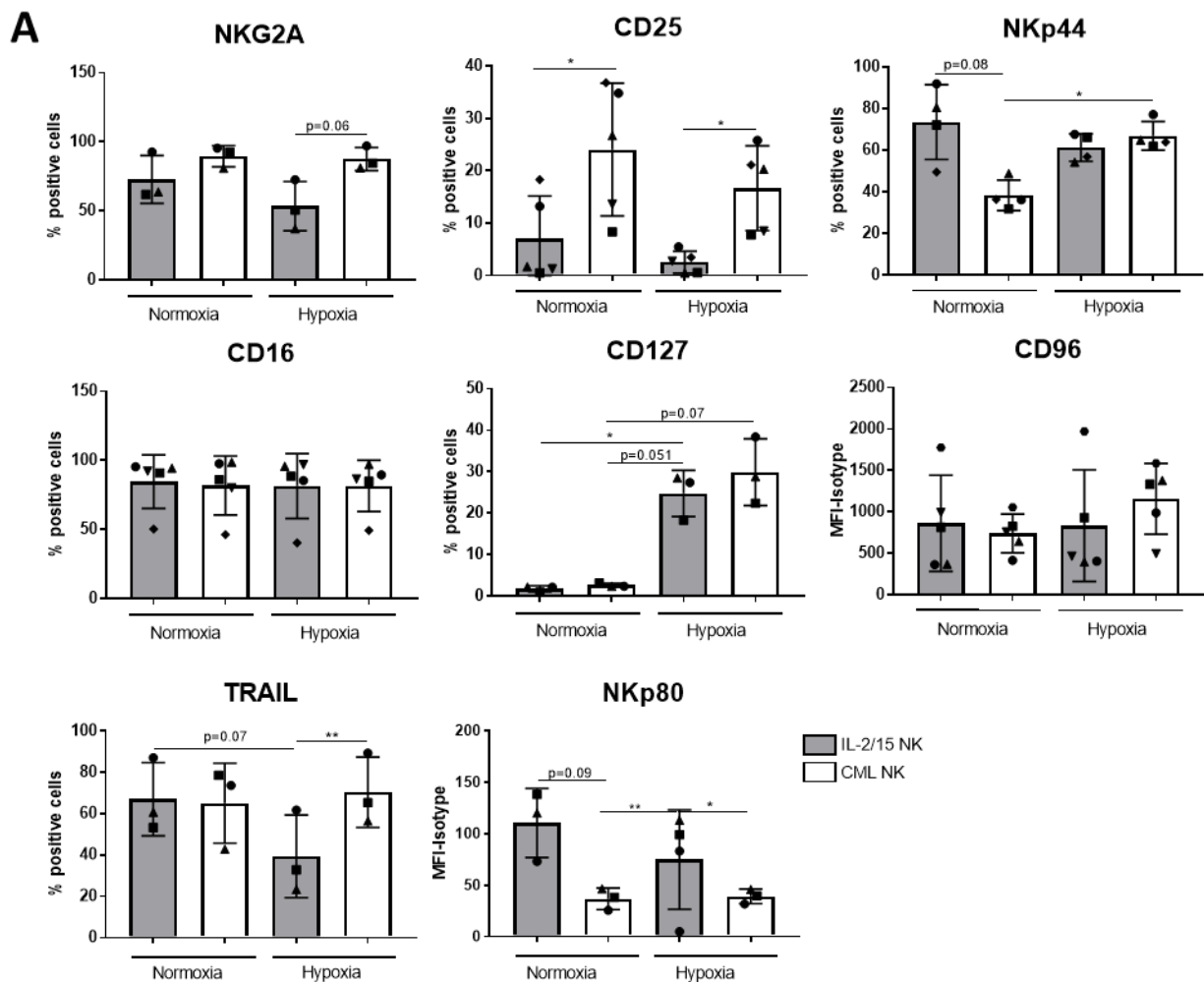


**Figure 8.28: Cytokine induced memory-like NK cells display a unique phenotype under hypoxia compared to control NK cells:** (A) Expression and frequency of cell surface markers detected by flow cytometry on cytokine induced memory-like NK cells (CML NK) or IL-2/15 stimulated NK cells after seven days under normoxia or hypoxia. p-value\* < 0.05; p-value\*\* < 0.01. Analysis done by Saphiro's normality test and one way ANOVA.

### 8.3 OPTIMIZATION OF CRISPR/CAS9 ELECTROPORATION PROTOCOL FOR GENERATING DOUBLE AND TRIPLE KNOCKOUTS IN HUMAN NK CELLS

Gene edition of primary human NK cells is specially challenging due to their resistance to lentivirus infection and low transfection efficacy (Bari et al., 2019). I aimed to optimize a CRISPR/Cas9 protocol in order to perform single, double and triple KOs in surface receptors, allowing a pathway-directed examination in human NK cells.

#### 8.3.1 Generation of single KOs in human primary NK cells

I initiated the process by adjusting the expansion duration of NK cells, extending it up to 5 days using IL-2/15/1 $\beta$  cytokines, reported previously as efficient expansion protocol prior to transduction (Bari et al., 2019). After the expansion, I performed an electroporation employing CRISPR/Cas9 ribonucleoprotein system as a user under S<sub>1</sub> biosecurity level conditions transfection system, using a duplex of CRISPR-RNA guide targeting the desired gene with trans-activating RNA ATTO-550 labelled. I performed the electroporation in absence of antibiotics (which can penetrate through the membrane of electroporated cells and reduce their survival) using Neon Transfection System technology at 1900 volts during 3 milliseconds and 1 pulse. Then, I expanded the transfected NK cells for a minimum of 5 days to a maximum of seven days prior sorting according to the surface staining of the targeted molecule (Figure 8.29 A).

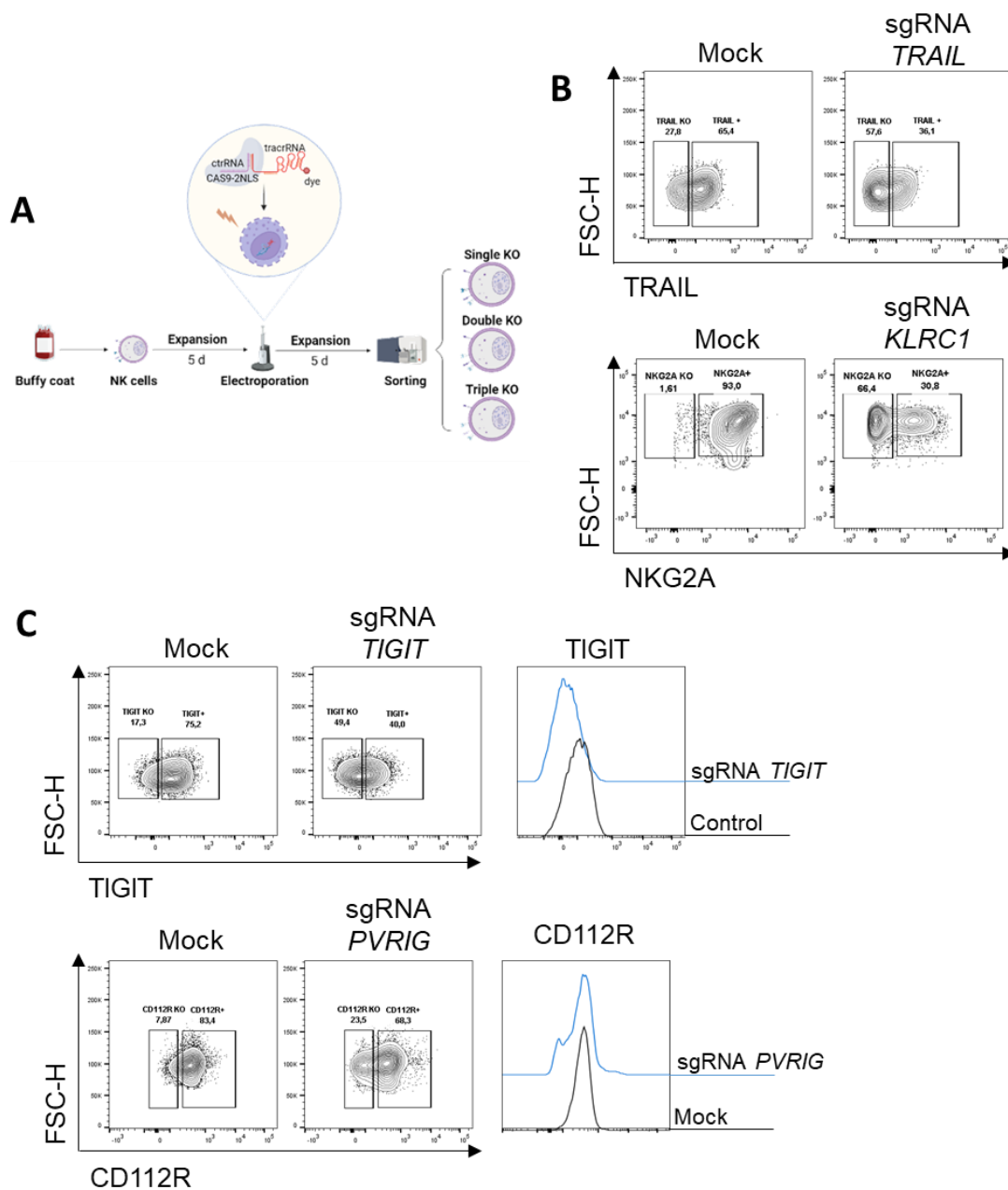


**Figure 8.29: CRISPR/Cas9 RNP technology is effective in human primary NK cells in surface receptors:** (A) Summary of the experimental set up. Human NK cells were isolated from PBMCs and

expanded during 5 days with an initial stimulation of IL-2/15/1 $\beta$  cytokines at day 0. Basal medium contained IL-2. On day 5, NK cells were electroporated using crRNA/tcrRNA system and CAS9 2NLS protein in the Neon Transfection electroporator. After electroporation, NK cells were expanded for a minimum time of 72 hours and sorted. Representative surface staining displaying the efficiency of the system after 5 days post-electroporation expansion of the receptors TRAIL and NKG2A (B), and receptors TIGIT and CD112R recognizing nectins.

I started choosing TRAIL and NKG2A (*KLRC1*) receptors as first targets, molecules notably expressed on the surface of isolated human NK cells. The transfection yielded 57 % (*TRAIL*, exon 2) and 66.4 % (*KLRC1*, exon 2) knockout efficacy after 5 days post-electroporation (Figure 8.28 B). I proceeded to examine the nectin pathway receptors, related to the stress-induced ligands CD112, CD155 and CD111, present in tumor cells (Bottino et al., 2003; Fuchs et al., 2004). The first molecules, TIGIT (exon 1) and CD112R (*PVRIG*, exon 3), achieved knockout rates of 32.1 % and 23.5 %, respectively (Figure 8.28 C). I optimized the protocol using CD96 (exon 1) and DNAM-1 (*CD226*, exon 1) receptors, achieving consistent and thorough knockouts after one week of expansion. I detected a reduced frequency of the targeted receptors in DNAM-1 and CD96 targeted NK cells (55.37 % reduction of DNAM-1 and 64.9 % of reduced CD96) as well as protein expression (976 to 61 mean fluorescence intensity in mock and DNAM-1 targeted NK cells; 874 to 91 mean fluorescence intensity in mock and CD96 targeted NK cells) (Figure 8.30). Collectively, the data indicates a robust protocol applicable to a range of surface receptors, regardless of their initial surface frequency.

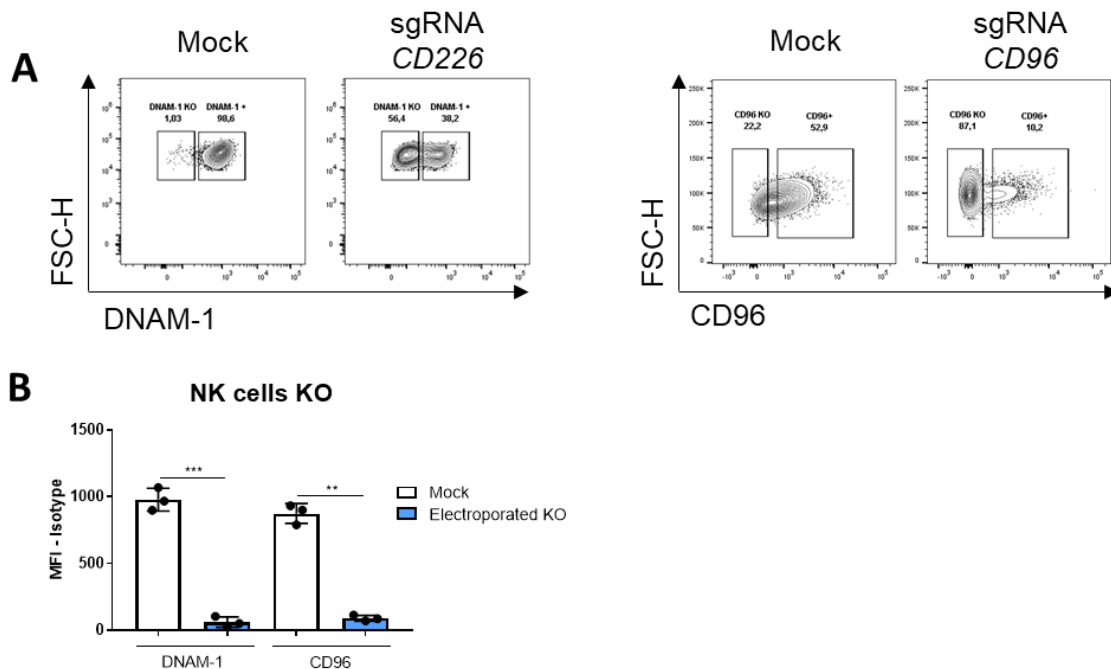


**Figure 8.30: Electroporation for surface markers DNAM-1 and CD96.** (A) Surface staining of DNAM-1 and CD96 receptors 3 days post-electroporation. (B) Compilation of donors seven days post-electroporation with sgRNA targeting DNAM-1 and CD96. p-value\*\* < 0.01, p-value\*\*\* < 0.005. Analysis done by Shapiro's normality test and paired t-test.

### 8.3.2 Production of double and triple KO in human primary NK cells

I postulated that same protocol should be suitable for combining different surface receptors, I chose the receptors recognizing nectin molecules: DNAM-1, TIGIT and CD112R. I performed double KO of the combination of receptors and triple sgRNAs, where I could detect a clean DNAM-1 depletion, whereas CD112R and TIGIT showed a minor reduction suitable for posterior sorting (Figure 8.30 A-C). After sorting each condition (single, double or triple targeting), I evaluated the KO stability 72 hours post-sorting, showing pure negative protein expression the corresponding sgRNA combinations; including the combination of three sgRNAs. In summary, in the conditions where I had targeted the surface receptors I could observe an alteration in mean fluorescence intensity (MFI-isotype): CD112R from 161 in mock to average 26 in targeted NK cells; TIGIT from 281 in mock to average 48 in targeted NK cells; and DNAM-1 from 223 in mock to 47.6 in targeted NK cells (Figure 8.31 D). I concluded that the generated protocol allows sorting the desired KO and further expand the NK cells in the receptors recognizing nectin ligands.

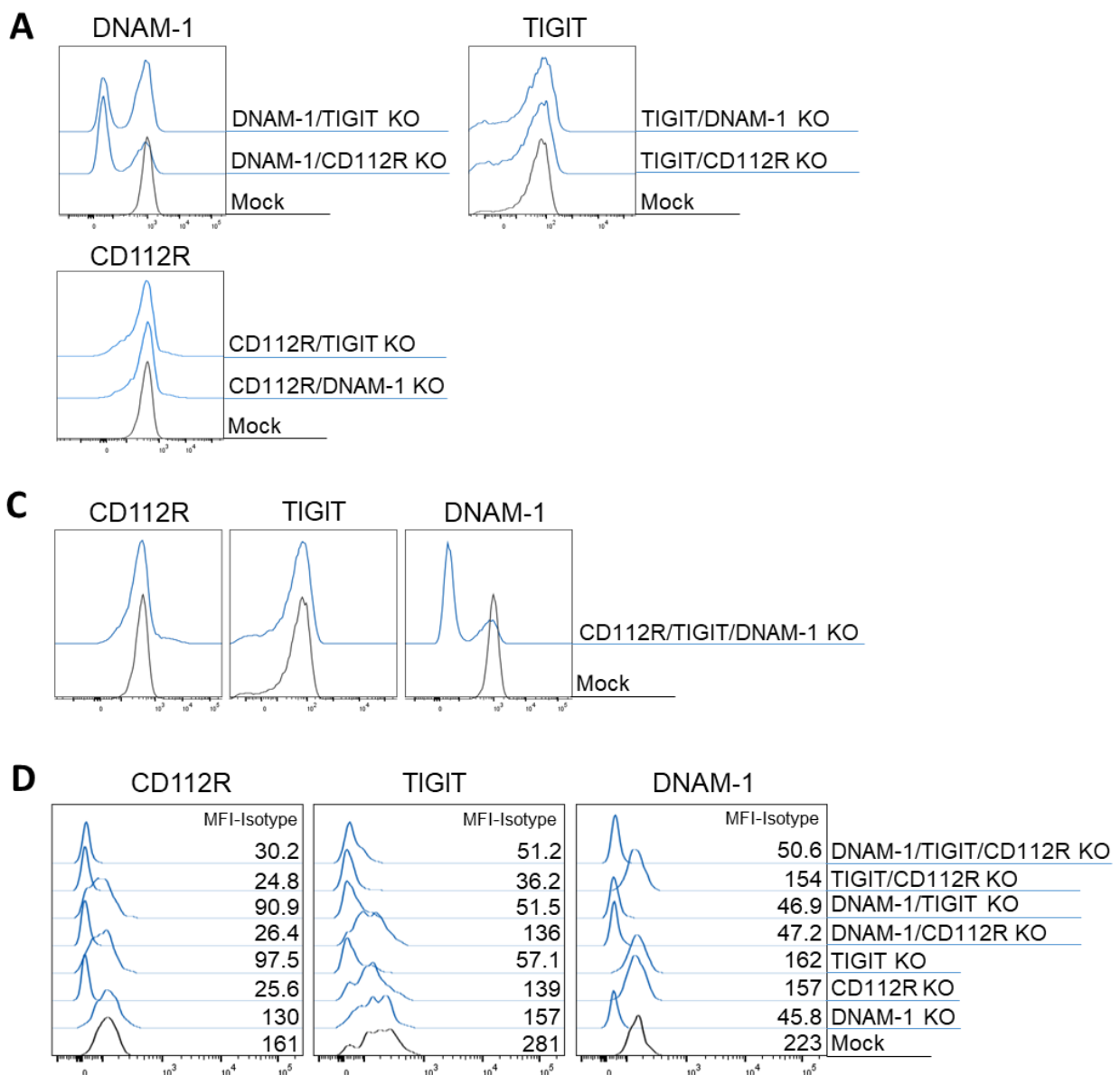


**Figure 8.31: Manufactured primary NK cells with double and triple KO of receptor recognizing nectin molecules maintain their genetic edition after sorting** (A) Histogram of surface expression of targeted proteins for double KO edition before sorting: DNAM-1/CD112R KO, DNAM-1/TIGIT KO and TIGIT/CD112R KO. (B) Histogram displaying a triple gene edition targeting DNAM-1/TIGIT/CD112R. (D) Protein expression of each double and triple KO combination 72h after sorting. p-value\* < 0.05; p-value\*\* < 0.01. Analysis done by Saphiro's normality test and paired t-test.

### 8.3.3 Functional evaluation of unsorted KO NK cells shows cell line and ligand dependency

To assess the functional relevance of the knockouts, I selected the K562 cell line (MHC-I negative) and the A375 cell line (MHC-I positive) for analysis of NK cells anti-tumor response. The co-culture with K562 showed a consistent degranulation detectable by CD107a marker between DNAM-1 KO and mock controls (43 % and 39 % respectively,  $p = 0.062$  compared to mock control). CD96 and TIGIT KO displayed a similar tendency of CD107a minor increase in frequency (52 %). Regarding IFN $\gamma$ , there were no significant differences but a trend of upregulation in TIGIT KO (21 % of frequency compared to 13.3 % in mock group) (Figure 4.31 A). A375 co-culture with targeted NK cells showed a tendency of reduction of CD107a in DNAM-1 targeted condition (9.2 % in comparison to 15.3 % in mock NK cells). In collaboration with Tomáš Hofman (Cerwenka's group), I used the generated CD155 KO A375 (CD155 is a common ligand for all the three receptors tested here), which showed a noticeable decrease of CD107a frequency in DNAM-1 targeted NK cells (17.3 %) in comparison to mock control NK cells (34 %). TIGIT targeting did not altered significantly altered the CD107a frequency, which remained at 27 %. CD96 targeting indicated a similar tendency as DNAM-1 in two tested donors (19 %) (Figure 8.31 B).

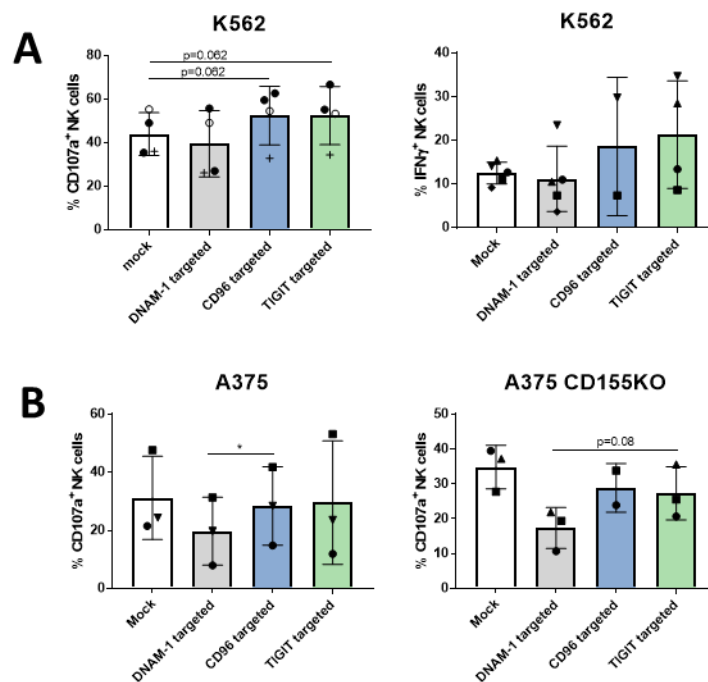


**Figure 8.32: Primary CD96 KO NK cells display a similar trend as TIGIT KO in coculture with K562 cells whereas A375 degranulation is mediated by DNAM-1** (A) CD107a frequency (left) and IFN $\gamma$  production (right) after 4h co-culture of K562 and gene edited NK cells (without sorting) for

CD96, TIGIT and DNAM-1 targeting. (B) CD107a frequency of NK cells co-cultured with A375 or A375 CD155 KO melanoma cell line. p-value\* < 0.05. Analysis done by Shapiro's normality test and one way ANOVA.

## 9 DISCUSSION

---

Oxygen is essential for human life. Nevertheless, a wide range of concentration percentages exists among biological compartments; approximately 5 % oxygen is found in the lung and liver, around 4 % in the brain, and 13 % in arterial blood (Carreau et al., 2011; Jagannathan et al., 2016). In addition to physiologically developed hypoxic niches, there is pathological hypoxia (oxygen concentration below physiological levels) as seen in the microenvironments of solid tumors as well as in certain lymphomas or leukemias in the bone marrow (Deynoux et al., 2016; Fiegl et al., 2009).

NK cells possess anti-tumor activity, and their infiltration into the tumor microenvironment has been associated with reduced cancer mortality (Nersesian et al., 2021). During this infiltration process, NK cells encounter hypoxia, which has been linked to various dysregulations in their activity. Gao et al. observed an intermediate ILC-1 conversion, displaying a subdued response to cancer cells driven by elevated TGF- $\beta$  secretion (Gao et al., 2017). NK cells exposed to hypoxia exhibited a downregulation of NKp44, NKp30, NKp46, and NKG2D, while ADCC remained unaffected (Balsamo et al., 2013). Parodi and collaborators documented increased CXCR4 expression and migration, accompanied by diminished cytokine production of human NK cells exposed to hypoxia (Parodi et al., 2018). The metabolism of NK cells exposed to hypoxia demonstrated a reduced ATP production due to OXPHOS arrest with microscopically detectible fragmentation of mitochondria (X. Zheng et al., 2019). The transcription factor HIF-1 $\alpha$  is the main driver of the transcriptional reprogramming induced by hypoxia, and its depletion in NK cells has been shown to improve tumour clearing by NK cells with enhanced NF $\kappa$ B pathway activation and IFN- $\gamma$  production (Ni et al., 2020). Another group described a role of HIF-1 $\alpha$  in murine NK cells, where its deletion in disrupted tumor angiogenesis, which is associated with promoting metastasis (Krzywinska et al., 2017). However, the role of HIF-1 $\alpha$  as a potential target for NK cell-based immunotherapy towards solid tumors remains unclear.

The study of *in vitro* tumor models has long been limited to the use of universal cell lines, however, biotechnology has advanced with the development of 3D “organoid” cultures, derived from patient samples (patient-derived organoids; PDOs) (Tuveson & Clevers, 2019). In this process, organoids generate a hypoxic environment, recapitulating both the genetic individuality of each patient and aspects of the tumor microenvironment (Betge et al., 2022; Okkelman et al., 2017; Z. Zhou et al., 2021). In my study, I investigate PDOs derived from colorectal cancer. In 2020, colorectal cancer had an incidence of 1.9 million cases and resulted in 0.9 million deaths worldwide, with 5.5 million people living with the disease. The predicted incidence for 2040 is 3.1 million cases (Xi & Xu, 2021). Therefore, both in the present and the future, colorectal cancer remains a highly prevalent cancer type worldwide, affecting numerous patients who are in need of innovative therapies (Myer et al., 2022).

The overarching goal of this study was to revert the impaired function of human NK cells exposed to hypoxia by counteracting HIF-1 $\alpha$ , and introduce chimeric antigen receptors in

order to develop efficient anti-tumor NK cells in the context of colorectal adenocarcinoma, using four PDO lines as targets (Figure 8.1 – Figure 8.26).

The maturation of NK cells by cytokines and surrounding immune cells is a frequent phenomenon in the tumor microenvironment, and this activation has been largely reproduced in cytokine induced memory-like NK cells (CML) NK cells (M. A. Cooper et al., 2009; Leong et al., 2014). CML NK cells display an enhanced response towards tumor and cytokines stimuli upon recall, leading to increased cytotoxicity and soluble factor production (Romee et al., 2016; Uppendahl et al., 2019). However, whether these CML NK cells retain enhanced recall responses after exposure to a hypoxic microenvironment has not yet been explored. For this reason, a secondary aim of this study is to describe the response of CML NK cells to tumor cells, cytokines and surface receptors expression after exposure to normoxia or hypoxia (Figure 8.27 and 8.28).

Human NK cells show resistance to different transduction methods (such as lentivirus) which severely limits targeting efficiency of CRISPR/Cas9 approaches (Bari et al., 2019). Overcoming this obstacle to genetically engineer primary NK cells was a major challenge, as it was a prerequisite to establish an efficient protocol using CRISPR/Cas9 technology to disrupt target genes, including HIF-1 $\alpha$  (main focus in the first aim) and cell surface receptors (Figure 4.29 to Figure 4.32).

## 9.1 OPTIMIZING IMMUNOTHERAPIES TARGETING HYPOXIC SOLID TUMORS THROUGH NK CELL MODULATION

In the first section of this study, I focused in the engineering of NK cells exposed to hypoxia to improve its effector activity against solid tumors.

### 9.1.1 Altered surface expression of human NK cell markers and receptors after seven days hypoxia

NK cells exposed to 7 days 1 % oxygen, showed a reduced FSC-A mean indicating a reduced size (Figure 4.1). The FSC-A reduction was not present in NK cells exposed to 6 hours of hypoxia, suggesting that 7 days of hypoxia exposure is affecting the size of NK cells. This would suggest that NK cells infiltrating the hypoxic tumor niche in a sustained timelapse (of at least 7 days), would have a reduced size.

PLEIOTROPIC EFFECT OF SEVEN DAYS HYPOXIA IN SURFACE MARKERS		
Surface receptors	Upregulation + Downregulation -	Function
CD38	--	Hydroxylates cyclic ADP from NAD residues and binds CD31 ligand to trigger activation of immune cells (Horenstein et al., 2018).
CD39	-	ATP transporter channel (Vijayan et al., 2017)
CD57	++	Related with NK cells maturations and activation (Björkström et al., 2010).
CD69	+	Activation marker of NK cells. Directly regulated by HIF-1 $\alpha$ in human and murine T cells (Labiano et al., 2017).
IL-18R	--	Receptor of IL-18 cytokine. Reported to be regulated by

NKG2A	---	HIF-1 $\alpha$ in murine NK cells (Ni et al., 2020). Inhibitory receptor binding to HLA-E. Increased in mature NK cell populations (Björkström et al., 2010).
NKp44	--	Associated with quiescent NK cells and activation (main ligand unknown) (Baychelier et al., 2013). Upregulation correlated with HIF-1 $\alpha$ gene editing in human NK cells (Lim et al., 2021).
TRAIL	-	Apoptosis-inducing ligand. Binds to DR4 and DR5 (LeBlanc & Ashkenazi, 2003).

**Table 9.1:** Summary of the altered surface markers and receptors of human NK cells exposed to seven days of hypoxia compared to normoxia. Up- and downregulation are stated by “+” and “-” symbols. Repetition of symbols represent the p-value significance (e. g \* for +, \*\* for ++).

Hypoxia exposure caused pleiotropic changes in NK cells, affecting the expression of receptors and surface markers such as; downregulation of metabolism related receptors (CD38, CD39), upregulation of activation markers (CD57, CD69), downregulation of cytokine receptor (IL-18R), reduced frequency of inhibitory receptor (NKG2A), downregulation of activation receptor NKp44 and diminished surface expression of death-cell receptor (TRAIL) (see Table 9.1).

Regarding the extracellular staining of ectoenzyme CD38 (hydroxylates cyclic ADP from NAD residues and binds CD31 ligand to trigger activation of immune cells) and CD39 (ATP transporter channel), both experienced reduced expression in NK cells pre-exposed to seven days of hypoxia. It has been observed that cytokine-induced memory-like NK cells exhibit elevated surface expression of CD38 and CD39 molecules (Horenstein et al., 2018; Tak et al., 2017; Vijayan et al., 2017). Cytokine-induced memory-like NK cells are highly reactive to tumor cells and IL-12/18. In contrast, I observed an overall reduction of soluble factor production upon exposure to tumor cells or IL-12/18 stimulation in hypoxia-exposed NK cells (see Figure 8.3). A potential hypothesis is that CD38 and CD39 expression correlates with NK cell activity, as showed by the reduction of both NK cell response to target and cytokines in hypoxia-exposed NK cells.

In general, an enrichment of CD57 frequency was observed after seven days of 1 % oxygen. CD57 antigen is an epitope associated with mature NK cells, correlating with NK cell proliferation or senescence status (Björkström et al., 2010). While no current literature directly associates the CD57 molecule with hypoxia, it is plausible that this upregulation is linked to the NK cells' limited proliferation capacity (see Figure 8.4). Concomitantly, the decrease in NKG2A expression (in the absence of target cells expressing HLA-E ligand) could signify a differentiation of NK cells toward a more mature phenotype (Björkström et al., 2010). This mature phenotype was described as low proliferative, with a reduced NKG2A expression independently of KIR distribution and diminished surface frequency of CXCR4, CXCR3, NKp46 and NKp30. In addition, mature CD57<sup>+</sup> NK cells showed a reduced degranulation towards K562 and IFN $\gamma$  production after IL-12/18 stimulation (Björkström et al., 2010; Poznanski & Ashkar, 2019). To confirm if hypoxia is inducing a similar “mature phenotype” as described, the expression of KIRs, CXCR4 and CXCR3 must be taken in consideration in future studies.

Another marker that exhibited an increased expression on NK cells upon hypoxia exposure was CD69, a well-established early activation marker which binds to galectin 1 (although unknown ligands are expected) (Cibrián & Sánchez-Madrid, 2017). In T cells, CD69 expression has been reported to be directly regulated by the HIF-1 $\alpha$  transcription factor, which binds to CD69 promoter (Labiano et al., 2017). A plausible explanation is that similar pathways might interconnect in NK cells, resulting in increased CD69 expression under hypoxic exposure due to HIF-1 $\alpha$  stabilization.

Furthermore, there was a decrease in the surface expression of IL-18R, suggesting reduced sensitivity to its cognate ligand, IL-18. The connection between HIF-1 $\alpha$  and IL-18R was reported in a murine model with conditional *HIF1A* knockout in NK cells. Tumor-infiltrating NK cells with HIF-1 $\alpha$  expression inhibited both IL-18R protein expression and transcription (Ni et al., 2020). However, in my study, I did not find decisive evidence supporting this conclusion, besides observing a reduction in the frequency of IL-18R in NK cells exposed to hypoxia.

The receptor NKp44, demonstrated a noticeable reduction in expression following hypoxia exposure. NKp44 is associated with quiescent NK cells and NK cell activation, however, the ligand for NKp44, has definitively not been identified (Baychelier et al., 2013). In the context of hypoxia, the downregulation of NKp44 expression has been correlated with the activation of HIF-1 $\alpha$  in human NK cells (Lim et al., 2021). However, the duration of hypoxia exposure in that study was up to 17 days in presence of feeder cells, which is inherently different to the culture method used in the present study (400 U/mL of rhIL-2).

The expression of the TNF-related apoptosis-inducing ligand (TRAIL) notably decreased upon NK cell exposure to hypoxia. This reduction implies a diminished capacity to induce apoptosis in tumor cells expressing DR4 or DR5 receptors, consequently affecting their susceptibility to lysis (LeBlanc & Ashkenazi, 2003). As TRAIL staining was performed in absence of a target cell, the relevance of TRAIL in hypoxia-exposed NK cells against target cells was not assessed in this study.

### 9.1.2 Reduced soluble factor production, proliferation and OXPHOS in NK cells exposed to hypoxia

The impact of hypoxia on NK cell activation was evaluated through stimulation with IL-12/18 or K562 target cells (refer to Figure 8.3). To explore the potential time-dependent effects of *in vitro* hypoxia exposure, NK cells were categorized into three groups: the control group (normoxia), NK cells exposed to hypoxia for six hours ("early infiltration into hypoxic niche"), and NK cells exposed to hypoxia for seven days (representing resident NK cells within the tumor's hypoxic niche) (depicted in Figure 8.3 A). The ability of NK cells to release soluble factors stored in granules (comprising granzymes and perforins), directly correlates with the surface exposure of the degranulation marker CD107a (LAMP-1), which serves as an immediate indicator of NK cell response to stimuli (Alter et al., 2004; Krzewski et al., 2013). Evaluation of CD107a staining in NK cells exposed to varying periods of hypoxia demonstrated that, following co-culture with K562 cells, NK cells exposed to seven days of hypoxia exhibited reduced granule production and/or proteins inside the granules in comparison to the six-hour hypoxia group or the normoxia control (see Figure 8.3 B and C).

Similarly, NK cell production of IFN $\gamma$  upon IL-12/18 stimulation was notably diminished following seven days of hypoxia exposure, contrasting with normoxia and six hours hypoxia exposure NK cells groups (refer to Figure 8.3 B-C). IFN $\gamma$  staining decreased in NK cells exposed to six hours of hypoxia. This suggests that a shorter hypoxia exposure is sufficient to impact IFN $\gamma$  production elicited by combined stimulation with IL-12 and IL-18. However, the shorter hypoxia exposure does not affect the degranulation response detected by CD107a following K562 co-culture. The observed decrease in IL-18R surface expression on NK cells exposed to hypoxia (Figure 8.2) suggests a plausible correlation with reduced sensitivity to IL-18 stimulation. This reduced sensitivity may contribute to the observed decrease in IFN $\gamma$  production. The reduction in degranulation was not dependent on the target, as evidenced by the similar decrease of CD107a staining observed under hypoxia in response to stimulation with A375 melanoma and HT-29 colorectal adenocarcinoma cell lines (Figure 8.3 D). Furthermore, there was a noticeable decrease in the fraction of NK cells with detectible surface CD107a expression under hypoxia following chemical stimulation with PMA/Ionomycin (Figure 8.3 D). The chemical stimulation with phorbol myristyl acetate (PMA) and ionomycin activates NF- $\kappa$ B and NFAT pathways, triggering degranulation and secretion of soluble factors (Frantz et al., 1994). Therefore, the reduction of detectable CD107a appears to be independent of receptor-ligand interactions. This data suggested that seven days of exposure to 1 % oxygen concentration was sufficient to impair the functional response of NK cells to cytokines, tumor cell lines and PMA/Ionomycin.

As previously stated, reducing cell proliferation under hypoxic conditions typically serves as a mechanism to mitigate the oxygen demand and consequent hypoxic stress arising from the generation of new progeny (Hubbi & Semenza, 2015). Human NK cells exposed to seven days of hypoxia exhibited a notable decrease in Ki67 expression and an increase in the labelling dye used or cell tracing CFSE (refer Figure 8.4). This observation suggests that NK cells exposed to hypoxia arrest proliferation and revert to a mitotically quiescent (Ki67) state. A study conducted by Zheng et al. suggests a critical role of mTOR as a key regulator in the hypoxia-induced proliferative arrest of NK cells (X. Zheng et al., 2019). However, there is not a definitive consensus regarding the precise pathway responsible for the proliferation arrest of NK cells under hypoxic conditions, nor was it further explored in this study. A potential approach to unravel the regulation of proliferation of hypoxia-exposed NK cells could be the specific inhibition of mTOR pathway upon hypoxia or normoxia exposure.

Oxygen supply is directly linked to metabolism, as oxygen is the final receiver of the electron transfer chain in the mitochondrial membrane. The OCR is intricately tied to ATP production by oxidative phosphorylation. The rate of oxygen consumption (OCR) was significantly decreased in NK cells pre-exposed to seven days of hypoxia, although the OCR measurement was performed uniquely at normoxic conditions (see figure 8.5). This data indicates that despite sufficient oxygen availability, NK cells previously exposed to hypoxia can no longer consume the available oxygen at the same rate.

The extracellular acidification rate (ECAR) serves as an indicator of glycolytic metabolism, producing two ATP molecules from a glucose molecule in the cytosol, as compared to 28-30

ATP typically generated by subsequent oxidative phosphorylation in mitochondria (Epstein et al., 2014; Schmidt et al., 2021).

Overall ATP production was nonetheless significantly diminished in NK cells exposed to hypoxia, alongside reductions in both maximal and basal respiration. These findings align with prior studies, supporting the observation that NK cells prioritize an inefficient metabolism under conditions of oxygen deprivation, leading to decreased ATP production for energy supply (Ni et al., 2020; X. Zheng et al., 2019). Such outcome correlates with the reduced CD39 surface staining, which evidences a decrease in ATP transport.

In line with compensating for reduced oxidative phosphorylation, NK cells exposed to hypoxia displayed an increase in baseline glycolysis (Figure 8.5). The elevation of glycolysis and reduction in OXPHOS metabolism is a known adaptation in eukaryotic cells. Oxygen serves as the primary energy source for cells; however, in its absence, cells transition from OXPHOS (which demands high electron input and efficiently produces 36 ATP molecules per glucose) to glycolysis (yielding 2 ATP molecules per glucose) (Eales et al., 2016). Therefore, it's plausible that NK cells encountering a hypoxic tumor environment shift their metabolic pathway toward glycolysis for ATP production. While HIF-1 $\alpha$  is thought to be involved in this metabolic switch, evidence suggests that HIF-2 $\alpha$  may also play a role (Ratcliffe, 2007). However, this study did not delve deeper into the primary regulator of human NK cell metabolism under hypoxia. Further exploration of this aspect could provide valuable insights into the biology of tumor-infiltrating NK cells.

Thus, I have observed negative effects of hypoxia in human NK cells at four different levels; reduced surface expression of activating receptors, reduced proliferation, reduced response to target cells and cytokines and diminished ATP turnover.

### 9.1.3 HIF-1 alpha targeted NK cells: A promising candidate for alleviating the effects of hypoxia exposure

Oxygen availability plays a crucial role in numerous cellular processes. Hypoxia-inducible factor 1alpha (HIF-1 $\alpha$ ) is the primary regulator of the cellular response to hypoxia. It can detect low oxygen levels and coordinate the necessary responses as a transcription factor (Covello & Simon, 2004; Loboda et al., 2010).

HIF-1 $\alpha$ 's significance extends to various aspects of NK cell function. In the context of bacterial infections, the absence of *HIF1A* in NK cells resulted in enhanced M2 macrophage turnover and reduced skin wound healing (Sobecki et al., 2021). In viral CMV infections, *HIF1A*-deficient NK cells failed to control the viral load and exhibited increased apoptosis (Victorino et al., 2021).

When it comes to the response to tumor cells, two studies involving murine NK cells demonstrated that conditional knockout of *HIF1A* correlated with reduced tumor control in RMAs and B16 tumor models (Krzywinska et al., 2017; Ni et al., 2020). Stockman's group suggested that the regulation of the tumor growth is mediated by non-productive angiogenesis, which reduces tumor burden but negatively affects the healthy vasculature through which immune cells infiltrate and drugs can be delivered to the tumor niche

(Krzywinska et al., 2017). Our group uncovered HIF-1 $\alpha$ -mediated inhibition of the NF $\kappa$ B pathway when analyzing the single-cell transcriptome of tumor-infiltrating NK cells. This NF $\kappa$ B inhibition correlated with reduced surface expression of IL-18R in tumor-infiltrating NK cells following IL-12/18 stimulation (pro-inflammatory cytokines often present in the tumor microenvironment) (Ni et al., 2020).

Additionally, a recent study highlighted the role of HIF-1 $\alpha$  in murine NK cells as a redox homeostatic regulator of resting NK cells. In summary, HIF-1 $\alpha$ -driven tryptophan/NAD<sup>+</sup> regulation enhanced glycolysis, which was found to be essential for the activation of resting NK cells (Pelletier et al., 2023). Although it was not tested in this study, the reduced ATP production and OXPHOS metabolism of hypoxia-exposed NK cells could be linked to HIF-1 $\alpha$  downstream effects, which would correlate with the mentioned study although the set up used in my study was of 7 days expanded NK cells in presence of IL-2 instead of homeostasis.

While the majority of HIF-1 $\alpha$  targeting research is focused on murine NK cells, an exception is found in the work conducted by Lim and colleagues, who employed siRNA transfection to manipulate human NK cells (Lim et al., 2021). The editing of HIF-1 $\alpha$  in human NK cells reported a higher cytotoxicity into tumor cell lines, mediated by reduced NKp44 surface expression and increased ERK signalling. The experimental set up of this study implied a seven days expansion of NK cells under normoxia, and a posterior hypoxia exposure of 17 days. In my study, I used maximum time-frame of seven days of hypoxia exposure of freshly isolated human NK cells. This fact might explain the lack this connection between NKp44 and HIF-1 $\alpha$ , which was not altered (data not shown).

In my study, a CRISPR/Cas9 ribonucleoprotein-based protocol was employed to genetically target HIF-1 $\alpha$  in human NK cells using ATTO-550 labelled sgRNA (see Figure 4.6). I optimized the protocol using readily detectible surface markers as targets for genetic disruption, which are further explained in the last section of this discussion (Figure 8.29 to 8.32).

Consistent with findings from our previous investigation utilizing a murine model featuring NKp46-HIF-1 $\alpha$ <sup>-/-</sup> NK cells, human NK cells with targeted HIF-1 $\alpha$  demonstrated increased IFN $\gamma$  production after 24 hours of preconditioning in hypoxia when co-cultured with target cells or upon stimulation with IL-12/18 (Ni et al., 2020) (as shown in Figures 8.7 and 8.8). However, NK cells subjected to seven days of 1 % oxygen exhibited a diminished response regardless of HIF-1 $\alpha$  targeting, implying a temporal window in which HIF-1 $\alpha$  targeting enhances the response to IL-12/18 stimulation (Figure 8.8).

The co-culture of HIF-1 $\alpha$  targeted NK cells with HT-29 cancer cells exposed to 24 and 48 hours of hypoxia resulted in a reduced percentage of tumor cells in confluency, suggesting the improved control of tumor growth by HIF-1 $\alpha$  targeted NK cells in comparison to mock NK cells after hypoxia exposure (see Figure 8.8 C). Thus, I hypothesized that HIF-1 $\alpha$  targeted NK cells might improve NK cell responses to cytokines and tumor cell lines, similarly as in the reported murine model (Ni et al., 2020).

The involvement of HIF-2 $\alpha$  cannot be dismissed, as targeting HIF-1 $\alpha$  might actually enhance the function of HIF-2 $\alpha$ . This occurs because all the targeted promoter sites remain

unoccupied by HIF-1 $\alpha$  (e. g. VEGF or EPO)(Loboda et al., 2010; Ratcliffe, 2007). A similar situation might arise concerning FIH and VHL function, where HIF-2 $\alpha$  becomes the sole target for inhibitors, potentially leading to increased degradation and inhibition of HIF-2 $\alpha$  in NK cells, reducing the targets of HIF-2 $\alpha$  (such as invasion-related genes MMP2 and PAI1). However, this study did not assess the potential importance of HIF-2 $\alpha$  as a transcription factor, which shares regulatory mechanisms and some targets with HIF-1 $\alpha$

Despite this, the observation that HIF-1 $\alpha$ -targeted NK cells survive under 1 % oxygen suggests that these cells adapt to hypoxic conditions to a certain extent. One hypothesis would be the fueling not only by glycolysis but also by fatty acid oxidation, which was recently described *in vivo*, where glucose and adiposity in tissues was reduced upon a hypoxia exposure of 3 hours to 3 weeks. Although it was described as a systemic effect, one hypothesis would be that NK cells under hypoxia get fueled by these pathways. In that regard, HIF-1 $\alpha$  is described as a key regulator of glycolysis, however, it is yet to be unraveled if NK cells can metabolically adjust to hypoxia in absence of HIF-1 $\alpha$ .

However, despite this, the observation that HIF-1 $\alpha$ -targeted NK cells survive under 1% oxygen implies an adaptive response to hypoxic conditions to some extent. One hypothesis is their potential utilization of not only glycolysis but also fatty acid oxidation, recently documented *in vivo*, where exposure to hypoxia for 3 hours to 3 weeks resulted in reduced glucose levels and tissue adiposity (Midha et al., 2023). While initially described as a systemic effect, it's posited that NK cells might also harness these pathways under hypoxic conditions.

In this context, although HIF-1 $\alpha$  is recognized as a critical regulator of glycolysis, it remains uncertain whether NK cells can adapt metabolically to hypoxia independently of HIF-1 $\alpha$ .

#### 9.1.4 HIF-1 $\alpha$ targeted NK Cells exhibit line-dependent efficacy against patient derived organoids

Patient-derived organoids (PDOs) have been established as a tumor model capable of replicating the hypoxic microenvironment found in solid tumors while maintaining patient-specific variations (Okkelman et al., 2017; Z. Zhou et al., 2021). PDOs serve as a living biobank, preserving patient-specific characteristics and uniqueness while allowing for *in vitro* experimentation with therapeutic approaches.

However, it's important to note that while PDO models offer numerous advantages, they lack several key elements necessary for understanding the tumor microenvironment. These include the absence of vasculature, which hinders the study of immune cell infiltration from the bloodstream into the tumor; the absence of other cells found within the tumor (such as dendritic cells, stromal cells, T cells, etc.); and the utilization of artificial materials (like BME), impacting the retention of soluble factors and the survival of immune cells introduced in co-cultures.

Moreover, it's essential to highlight the limitation concerning biological material. Patients eligible for PDO generation often have tumors from which biopsies provide insufficient material for donation. Consequently, certain tumors, such as pancreatic ductal

adenocarcinomas (challenging to biopsy), suppose a medical, technical and economical challenge for generating PDOs (Boj et al., 2015).

For this study, organoids were obtained from patients with colorectal adenocarcinoma in collaboration with Prof. Ebert, Dr. Betge, and Dr. Burgermeister, who produced the PDO lines (Betge et al., 2022). Four PDO lines were utilized in this study, each exhibiting microsatellite stability. Their molecular subtype was identified as CMS 2, with PDO7, 19, and 22 falling under the canonical subtype (37 % frequency), while PDO30 was categorized as CMS 3, defined as metabolically deregulated and present in 13 % of tumors (Guinney et al., 2015) (Figure 8.9). The biopsy location was heterogeneous, from rectum, sigma or colon ascendens. The PDOs collection provided a range of stages, varying from I-IV. Thus, the PDO collection used represents a diverse pool of colorectal adenocarcinoma samples, avoiding potential bias towards sensitive/resistant PDO cells.

The presence of less than 5 % oxygen in the four PDO lines was confirmed through staining with ImageIT Hypoxia Green dye and measuring it by imaging and flow cytometry (see in figure 8.10 and 8.11). Imaging revealed the presence of a hypoxic core under normoxic conditions, with the center of the organoids stained with the green dye, indicating the generation of spontaneous hypoxia within the 3D structure. Measurement of the green fluorescence unit (GCU) by IncuCyte demonstrated a significant increase in fluorescence in the PDOs cultured under 1% oxygen, confirming the dye's sensitivity to low oxygen concentrations (see Figure 8.10). Additionally, PDO 19 and 30 exhibited a similar trend in ImageIT Hypoxia Green dye staining, suggesting the presence of hypoxic cores in the lines used for this study (see Figure 8.10 C). Flow cytometry analysis revealed a heterogeneous spread of the dye in the PDO 22 line, whereas PDO 7 line had a homogeneous oxygen distribution in the core of the structure (Figure 8.11). There was no further imaging to assess the exact location of hypoxia staining, therefore the exact gradient and distribution of oxygen concentration within the organoids structures was not explored in this study.

Thus, I hypothesized that using PDOs to assess the effects of the hypoxic tumor microenvironment was a suitable approach to test HIF-1 $\alpha$  targeted NK cells with patient-derived materials. To co-culture the edited NK cells with the PDO lines, a large-scale NK cell expansion method was required. For this purpose, Prof. Wels provided engineered K562 feeder cells, which were modified to express membrane-bound IL-15, IL-21, as well as 41BB-L, and facilitate NK cell expansion (Oberoi et al., 2020) (see Figure 8.12). The overall expansion process demonstrated that feeder cells irradiated with 100 Grays led to a 10-fold expansion of NK cells after seven days of co-culture with the feeder cells (Figure 8.12). These expanded NK cells following electroporation were subsequently used for further analysis with the engineered NK cells.

HIF-1 $\alpha$  targeted and mock NK cells were cultured with PDO 7, 19, 22, and 30 lines for five days in the presence of CytotoxRed dye (used to stain dead cells). Images were captured at 10 x magnification, and the increased presence of red-stained cells indicated a higher number of dead cells (as seen in Figure 8.13). The images and quantification of the intensity of the CytotoxRed dye suggest that PDO 19 and 22 were more sensitive to HIF-1 $\alpha$  targeted NK cells, while PDO7 was not sensitive, displaying lower dead cell staining than in the mock control

(Figure 8.13 and 14). The differences in the kinetics observed in PDO 7 and 19 (which displayed rapid cell death staining in the first 24-48 hours) compared to PDO 22 and 30 (where it appeared from 72 hours onwards) were evident. This suggests that the pool of PDO lines used exhibited heterogeneity in response to NK cell-mediated killing indicating that the samples obtained were not biased towards resistance or sensitivity. The variations in the cytotoxicity time-course may be attributed to the fact that each PDO line was obtained from individual patients, implying that only specific PDO lines might be responsive to HIF-1 $\alpha$  targeted NK cells.

An important consideration is the fact that although HIF-1 $\alpha$  is primarily degraded under normoxic conditions, it's not completely eliminated. Since the co-culture with organoids was performed under ambient conditions (without artificial hypoxia of 1 % oxygen), it cannot be ruled out that HIF-1 $\alpha$  is active even in normoxia. Transcriptomic analysis of tumor cells revealed that HIF-1 $\alpha$  is expressed in normoxia, having a latent function (Cimmino et al., 2019). Among the findings, there's evidence of metabolic regulation in normoxia, while in hypoxia, HIF-1 $\alpha$  alters DNA methylation patterns in tumor cells.

Although NK cells differ from tumor cells, it's reasonable to speculate that HIF-1 $\alpha$  targeted NK cells, even when not in direct contact with the hypoxic core of PDOs, might exhibit distinct functional responses compared to mock NK cells. Ultimately, correlating all differences in cytotoxicity of HIF-1 $\alpha$  targeted NK cells solely to the presence of hypoxia is not conclusive, although PDO lines do present a hypoxic core of < 5% oxygen. To specifically discern the effect of HIF-1 $\alpha$  in hypoxia and normoxia, isolating infiltrating NK cells within organoids and those on the surface, and comparing HIF-1 $\alpha$  targeted and mock NK cells, would be necessary. Hence, this limitation underscores the study presented in this research

#### 9.1.5 HER-2 CAR NK cells efficacy is hampered by hypoxia exposure

The utilization of HER-2 CAR-based immune cells, such as T cells or NK cells, has been applied in the context of different solid tumors (Hegde et al., 2020; Nowakowska et al., 2018; Raj et al., 2019). However, there have been no studies assessing the effects of HER-2 CAR NK cells against colorectal adenocarcinoma tumor cells. The analysis of 348 patients of colorectal cancer from a database available online, revealed a marked variation of disease-specific and progression free survival depending on the *ERBB2* mRNA expression (refer to Figure 8.19 A) (Roelands et al., 2023). The survival months measured by disease-specific parameter (time to death with colorectal cancer) indicated that patients with higher *ERBB2* mean had less mortality linked to colorectal cancer. Same tendency was reported by the progression-free survival (time to detect colorectal cancer relapse or death since treatment), indicating a better recovery after treatment by these patients without a relapse (Figure 8.19) (Edler et al., 2000). This data suggested the potential benefit of HER-2 targeted therapies for certain colorectal cancer patients exhibiting high *ERBB2* expression. In this context, I hypothesized that HER-2 CAR NK cells would be a potential cytotoxic cell towards colorectal cancer cells.

In collaboration with Professor Wels, I employed a second-generation CAR plasmid based on the FRP5 antibody targeting the HER-2 molecule, with CD28 and CD3 $\zeta$  costimulatory domains (see Figure 4.16). Following transduction with lentivirus, I achieved an average

efficacy of 15-20 % CAR plasmid integration within 5 days post-infection, enabling the sorting of HER-2 CAR NK cells into positive and negative populations (see Figure 8.16).

The functionality of HER-2 CAR NK cells was confirmed after sorting, as demonstrated through co-culturing with melanoma cells expressing the HER-2 molecule (see Figure 8.17). Previously, the HER-2 CAR NK92 cell line was reported to maintain its efficiency even under hypoxic conditions (Nowakowska et al., 2018). However, the HER-2 CAR NK cells produced in our study exhibited a reduced capacity to control tumor growth, comparable to the non-transgenic group of NK cells (see Figure 8.17). Notably, significant differences exist between NK92 and human primary NK cells, ranging from surface ligands to their response to target cells, such as NKG2A (Kotzur et al., 2022). One plausible hypothesis is that the NK92 cell line responds differently to hypoxia compared to primary NK cells. This implies that the same CAR construct may elicit distinct responses in the NK92 cell line and primary NK cells.

The use of the HER-2 KO HT-29 cell line allowed me to discern varying responses to the presence of the ligand under hypoxic or normoxic conditions by HER-2 CAR NK cells (see Figure 8.18). HER-2 CAR NK cells exposed to hypoxia did not exhibit a preference for HER-2<sup>+</sup> HT-29 tumor cells. HER-2 surface expression was not altered after hypoxia exposure to HT-29 cells, indicating that the ligand to CAR NK cells was present in the hypoxic co-culture (refer Figure 8.18 D). This data suggested that HER-2 CAR NK cells pre-exposed to hypoxia reduced their cytotoxicity. Further research assessing the receptor-ligand recognition of HER-2 CAR NK cells and HER-2 bearing target cells would clarify whether there is an ineffective synapse or a reduction of the surface CAR molecule in NK cells exposed to hypoxia.

I postulated that the PDO lines 7, 19, 22 and 30 also express HER-2, in concordance, its surface expression was detectable in all the lines (Figure 8.19), allowing testing of HER-2 CAR NK cells with patient derived material. HER-2 CAR-NK cells co-cultured with PDO 22 line exhibited enhanced cytotoxicity, as deduced from the increased fluorescence intensity of the CytotoxRed dye (refer to Figure 8.20). This data implies the promising potential of HER-2 CAR NK cells as effective immune cells for targeting patient-derived samples from colorectal adenocarcinoma. To date, there is no evidence supporting the efficacy of HER-2 CAR NK cells against colorectal adenocarcinoma samples. While there are studies documenting the effectiveness of HER-2 CAR T cells in colorectal cancer, T cells face a significant limitation in terms of autologous generation. Often, these T cells are derived from already dysfunctional T cells in patients with cancer malignancies, which is added to the potential cytokine storm syndrome that results from the over-activation of CAR-T cells sustained in time (Sternier & Sternier, 2021). In contrast, CAR-NK cells are sourced from allogeneic donors, offering the advantage of TCR-independent activating receptors, such as DNAM-1 and TRAIL (Albinger et al., 2021). This characteristic broadens the spectrum of receptor-ligand interactions available.

Furthermore, the data obtained from the co-culture experiments indicated that CAR-NK cells had a rapid cytotoxicity, however, the increase of the ImageIT Hypoxia Green dye signal suggested an increase of PDO 22 hypoxic core at later time points that correlated with a decline in cytotoxicity (refer to Figure 8.20). Given these findings, I hypothesized that the efficacy of CARs could potentially be enhanced through the additional genetic modification involving HIF-1 $\alpha$ .

### 9.1.6 Targeting HIF-1 alpha to enhance HER-2 CAR NK cell cytotoxicity against PDO lines

Although CAR based therapies are promising and used in clinics towards B cell malignancies, there is still a major challenge regarding the therapy of solid tumors. In this regard, there are ongoing efforts to enhance CAR constructs, including the development of fourth-generation CARs, referred to as TRUCKs (T cells redirected for antigen-unrestricted cytokine-initiated killing). TRUCKs combine tumor antigen targeting with autologous cytokine production, creating a feedback loop of self-activation and paracrine stimulation of other immune cells (Chmielewski & Abken, 2020). Regarding hypoxia, Kosti and colleagues recently reported a mechanism for HypoxiCAR T cells, which incorporate nine hypoxia-responsive elements (HREs) within their sequence. These elements are under the transcriptional control of HIF-1 $\alpha$  in low oxygen concentrations, thereby preventing off-tumor reactivity (Kosti et al., 2021).

However, there have been no additional modifications to CAR NK cells specifically focused on the hypoxic microenvironment. CAR-T cells have the limitation of inducing graft-versus-host disease (GVHD) via the TCR-recognition. However, CAR NK cells are a powerful approach for allogeneic cell therapy (Daher & Rezvani, 2021). For this reason, combining HIF-1 $\alpha$  targeted NK cells with HER-2 CAR NK cells could introduce a new approach for implementing adoptive cell therapies targeting solid tumors.

All PDO lines (PDO 7, 19, 22, and 30) exhibited sensitivity to HER-2 CAR-NK cell-mediated killing due to their HER-2 expression (which was consistent across all lines, as shown in Figure 8.19). However, IncuCyte images captured during co-culture experiments with HER-2 CAR NK cells showed that PDO 30 exhibited a resistance to HER-2 CAR NK cell cytotoxicity, evidenced by a dimmer cell death staining (red) (Figure 8.21). PDO 7 and 19 showed a similar tendency, where CytotoxRed intensity was rapidly detected during the first six hours of co-culture, and dead cells remained present until 96 hours incubation. Finally, PDO 22, in contrast to the previous reported experiment where the CytotoxRed dye signal declined at later time points, showed a CytotoxRed dye intensity even after 48 hours. I hypothesized that the different effector to target ratio (from 1:1 to 0.5:1) induced a reduced HER-2 NK cell mediated killing of the PDO target cells, although the killing was detectable (Figure 8.21). Conversely, co-culturing HER-2 CAR HIF-1 $\alpha$  targeted NK cells with PDO lines prevented tumor growth by day 4 and maintained cytotoxicity until the end of the co-culture period (as observed in Figure 8.20). PDO 30 line cell death staining showed a rapid killing of HER-2 CAR HIF-1 $\alpha$  targeted NK cells, which was noticeable after the first 48 hours of co-culture. The images of PDO 7 and 19 displayed a similar tendency, with an intense CytotoxRed dye signal after 96 hours of co-culture. The cell death staining in PDO 22 was dimmer compared to the PDO 7, 19 or 30, but increased after 96 hours of co-culture with HER-2 HIF-1 $\alpha$  targeted NK cells compared to HER-2 CAR NK cells (Figure 8.21).

Analysis of total tumor growth showed that the area of PDO 22 was reduced in co-culture with HER-2 HIF-1 $\alpha$  targeted NK cells, which suggested an increased control of tumor burden. However, similar kinetics were observed in PDO 7, 19 and 30 between the CAR NK products regardless of HIF-1 $\alpha$  targeting (Figure 8.22). To note, the IncuCyte analysis is performed measuring the bright field mask, therefore, the measurement of the area does not discern

between alive organoid and NK cells aggregating to an organoid and exerting cytotoxicity. For this reason, it is crucial to analyse the intensity of CytotoxRed dye, which lead to a quantification of PDO cell death (Figure 8.22).

The quantification of CytotoxRed dye revealed an enhanced and sustained killing by HER-2 CAR HIF-1 $\alpha$  targeted NK cells in all PDO lines when compared to HER-2 CAR NK cells, with notable improvements observed in PDO 19 and 30 (see Figure 8.23). Killing of PDO 7 and 22 cells was increased in the HER-2 CAR HIF-1 $\alpha$  targeted NK cell group co-culture, but to a lower extent (Figure 8.21).

In contrast, when comparing HIF-1 $\alpha$  only targeted NK cells or mock co-culture with PDO lines, PDO 7 and PDO 30 did not display susceptibility to targeting by HIF-1 $\alpha$  targeted NK cells (Figure 8.14). However, this situation was reversed in the case of HER-2 CAR HIF-1 $\alpha$  targeted NK cells compared to HER-2 CAR NK cells, suggesting that the addition of HIF-1 $\alpha$  solely in NK cells is insufficient to enhance the killing of PDO 7 and 30 (see Figure 4.14 and 4.21). Conversely, PDO 22 and 19 exhibited enhanced killing by HIF-1 $\alpha$  targeted NK cells, and this effect was sustained by HER-2 CAR HIF-1 $\alpha$  targeted NK cells (Figure 8.14 and 8.22).

Biologically, several factors could contribute to the varying susceptibility of PDOs to killing by HER-2 CAR HIF-1 $\alpha$  targeted NK cells. One hypothesis is their genetic background, such as KRAS gene mutations (which dysfunction is related to poor outcome to therapies such as cetuximab), which are shared by PDO 30 and 19 but not by PDO 7 and 22 (Figure 8.9) (Betge et al., 2022). In summary, the double-edited HER-2 CAR HIF-1 $\alpha$  targeted NK cells efficiently killed all four PDO lines, regardless of their susceptibility to HIF-1 $\alpha$  targeted NK cells alone.

It's worth noting that targeting HIF-1 $\alpha$  to generate CAR cells isn't solely considered for NK cells. Johnson's group conducted a comparison between HIF-1 $\alpha$  and HIF-2 $\alpha$  ectopic expression, concluding that CD19 CAR T cells exhibiting ectopic expression of HIF-2 $\alpha$  exhibited improved tumor burden resolution in humanized mice (Veliça et al., 2021). This suggests that the depletion of HIF factors may not consistently correlate with enhanced immune reactivity against tumors. While this study focused on CRISPR/Cas9 targeting of HIF-1 $\alpha$  and did not explore ectopic expression, it's plausible that NK cells and CD8<sup>+</sup> T cells rely on HIF factors differently.

Soluble factors are often the drivers of the NK cell-mediated killing, for that reason an analysis of the media in the PDO 7 and 22 co-cultured with HER-2 CAR or HER-2 HIF-1 $\alpha$  targeted NK cells was performed. Analysis of IFN $\gamma$ , Granzyme B, Perforin and GM-CSF showed a prominent increase in the co-culture of PDO 7 with both groups of edited NK cells, which correlate with the rapid killing observed in the cytotoxicity kinetics. Although there was a minor increase of IFN $\gamma$  production, there were no noticeable differences between HER-2 CAR and HER-2 CAR HIF-1 $\alpha$  targeted NK cells (Figure 8.24). This might be due to the differences in receptor-ligand interactions, or the absorption of soluble factors by the basal membrane extract compound, which could retain the secreted soluble factors, diminishing the quantity in the medium. The timing of medium collection might be also of relevance, since 96 hours of co-culture is a prolonged time, and some of the relevant factors produced in the first 24-28 hours might be degraded. Further research would be required to conclude a

specific killing mechanism driving the increased killing by HER-2 CAR HIF-1 $\alpha$  targeted NK cells compared to HER-2 CAR NK cells, with a larger panel of soluble factor evaluation, surface marker staining and proliferation assays.

### 9.1.7 Enhanced infiltration of HER-2 CAR HIF-1 $\alpha$ targeted NK Cells into HT-29 spheroids

3D microscopy is a powerful technique for analyzing structures with vascularization or immune cell infiltration. However, the analysis of large samples, such as mouse embryos or organoids, has posed a significant challenge in accessing imaging capabilities. Currently, there are microscope models that facilitate this technology, including the Ultramicroscope Blaze (Karam et al., 2022; Ramos-Vega et al., 2022).

In collaboration with Dr. Möker's department at Miltenyi Biotech, we generated spheroids from HER-2<sup>+</sup>/KO HT-29 tumor cells for further imaging (see Figure 8.18 and 8.25). Although our primary interest was to use patient-derived organoids, ethical limitations associated with working with such samples necessitated the use of an alternative 3D model; spheroids. Similar to organoids, colorectal adenocarcinoma spheroids from HT-29 cell line exhibited positive staining with ImageIT Hypoxia Green dye. After 24 hours of co-culture, the 3D structure was disrupted by HER-2 CAR-NK cells, regardless of their HER-2 surface expression (Figure 8.25).

The effects are noticeable after 24 hours in spheroids, whereas in some PDO lines, such as PDO 22 and 30, the cytotoxicity exerted by NK cells become apparent after 48 hours (see Figure 8.19 and 8.25). While the HT-29 cell line originates from a colorectal adenocarcinoma patient, it inherently differs from PDO structures, where the stem-cell niche remains intact, resulting in heterogeneous growth (Betge et al., 2022). Spheroids were cultured in an agarose matrix, whereas organoids require a basement membrane extract (BME) scaffold. Hence, it is plausible that NK-mediated killing of spheroids occurs more rapidly than that of organoids.

To avoid complete disintegration of the 3D structure, 2-hour co-culture period was selected to analyse the infiltration of human NK cells into HT-29 spheroids. By embedding the co-cultured spheroids in agarose cubes, samples were prepared for acquiring stacked images using the Ultramicroscope Blaze. After counting and normalizing the number of spheroids/NK cells, a noticeable trend of increased infiltration in the group of HER-2 CAR HIF-1 $\alpha$  targeted NK cells co-cultured with HER-2<sup>+</sup> HT-29 spheroids was observed (Figure 8.25). The condition with the fewest CD45<sup>+</sup> stained cells (NK cells) was in the group of HER-2 CAR HIF-1 $\alpha$  targeted NK cells in combination with HER-2 KO HT-29 spheroids, whereas HER-2 CAR NK cells did not exhibit a preference for HER-2 surface presence for infiltration (Figure 8.24).

These imaging results support the hypothesis of ligand-independence between cancer cells and CAR-NK cells in the presence of hypoxia. On the other hand, HER-2 CAR HIF-1 $\alpha$  targeted NK cells displayed increased infiltration/recruitment only in the presence of HER-2, suggesting that HIF-1 $\alpha$  targeting alone may not be sufficient to efficiently target the hypoxic tumor niche, as observed previously by the cytotoxicity kinetics measured in PDO lines co-cultures (Figure 8.14).

However, this data was generated with a unique NK cell donor, for that reason, further investigation is warranted to prove this preliminary data, either through imaging or an *in vivo* model using humanized mice with injections of HER-2 CAR or HER-2 CAR HIF-1 $\alpha$  targeted NK cells, concomitant tumor extraction, and NK cell counting. If confirmed, it would prove that HER-2 CAR HIF-1 $\alpha$  targeted NK cells infiltrate hypoxic tumors efficiently, therefore displaying enhanced cytotoxicity.

Finally, it's important to highlight a potential limitation regarding the use of CAR HIF-1 $\alpha$  targeted NK cells, which might be beneficial specifically in colorectal cancer cases. Therefore, it cannot be definitively claimed that the same benefit might be observed in other tumors. For instance, targeting HIF-1 $\alpha$  in NK cells for highly hypoxic tumors, like glioblastoma, where healthy tissue already exhibits oxygen concentrations < 5%, might not be effective (Carreau et al., 2011). Adapting to the environment could be crucial for the proper functioning of NK cells. Consequently, targeting HIF-1 $\alpha$  might lead to the elimination of a necessary biological mechanism in certain tissues.

To validate this assumption, an extensive evaluation using *in vivo* models with different tumor locations would be necessary. This evaluation would involve assessing tumor resolution using both HIF-1 $\alpha$  targeted and mock CAR NK cells.

#### 9.1.8 Surface receptors, soluble factor production and proliferation alterations in hypoxia-exposed cytokine-induced memory-like NK Cells

Cytokine-induced memory-like NK (CML NK) cells are generated *in vitro* through initial exposure to IL-12/IL-18/IL-15/IL-2 followed by further expansion (Leong et al., 2014; Romee et al., 2016). This treatment results in the generation of highly efficient NK cells, replicating the 'educated' NK cells found within the tumor microenvironment, which are 'trained' to recognize and combat tumors. To date, there have been no reports on the impact of hypoxia exposure on CLM NK cells. Therefore, I assessed how seven days of hypoxia exposure would influence the activity of CML NK cells after hypoxia pre-exposure.

CML NK cells exhibit the capability to produce increased levels of IFN $\gamma$  upon encountering target cells, as previously demonstrated in co-culture with K562 cells (Romee et al., 2016). Unlike regular NK cells, CML NK cells exposed to hypoxia maintained their IFN $\gamma$  production after K562 co-culture (see Figure 8.27). However, CML NK cells pre-exposed to hypoxia exhibited a significant reduction in IFN $\gamma$  production after stimulation with IL-12/18, suggesting differential regulation pathways depending on the upstream trigger (Figure 8.27).

In contrast to regular NK cells isolated and cultured with IL-2/15, CML NK cells did not exhibit any reduction in CD107a or Ki67 expression (Figure 8.27). A plausible explanation may be the consistent expression of CD25 (IL-2Ra) by CML NK cells, even under hypoxia conditions (Figure 8.28). The sustained surface expression of CD25 suggests a continual activation of the STAT5 pathway in the presence of IL-2 (supplemented in the media), which has been shown to be pivotal for T cell and NK cell proliferation (Leong et al., 2014; Moriggl et al., 1999).

Expressions of NKG2A, TRAIL, and NKp80 were maintained after hypoxia exposure, as shown in Figure 8.26. However, NKp44, previously reported to be downregulated in CML NK cells, exhibited an upregulation under hypoxic conditions (Figure 8.29)(Romee et al., 2016). CD127 (IL7Ra), a well-established murine ILC marker, displayed a noticeable increase in both IL-2/15 control NK cells and CML NK cells, as demonstrated in Figure 8.26. Notably, there is no prior report of CD127 expression in human NK cells isolated from PBMCs; however, its presence has been associated with tissue-resident NK cells (Allan et al., 2017; Lopes et al., 2022).

The use of cytokine-induced memory-like NK cells as effector cells for adoptive cell therapy has been explored in pre-clinical studies for solid tumors, such as triple ovarian cancer and hepatocellular carcinoma (as well as B cell malignancies) (Dong et al., 2023; He et al., 2023; Uppendahl et al., 2019). The data obtained from my previous experiments suggest that, even though CML NK cells increase their IFN $\gamma$  production, this ability is compromised when exposed to 1 % oxygen. Therefore, engineered CML NK cells lacking HIF-1 $\alpha$  might be capable of maintaining IFN $\gamma$  production or cytotoxicity against solid targets, such as patient-derived organoids (PDOs). Unlike CARs, CML NK cells do not necessitate lentivirus transduction, which is preferable for complying with good manufacturing practice (GMP) guidelines (European Commission, 2017). Consequently, CML NK cells show promise as effector cells for further optimization in solid tumor therapy, but their efficiency may be hindered by the hypoxic microenvironment of tumors. Hence, ongoing research assessing CML NK cells under hypoxic conditions may illuminate an alternative avenue for NK cell-based immunotherapy.

## 9.2 ENHANCING CRISPR/CAS9-BASED GENE EDITING IN HUMAN PRIMARY NK CELLS

Ever since Nobel laureates Dr. Doudna and Dr. Charpentier introduced the groundbreaking biotechnology of genetic editing through the CRISPR/Cas9 system, a new frontier in gene editing emerged (Doudna & Charpentier, 2014; Mojica et al., 2005). CRISPR/Cas9 offers precision editing at specific sites, enabling targeted excision at desired genomic locations. However, eukaryotic cells do not naturally express the Cas9 enzyme, necessitating either transduction to induce Cas9 expression or the introduction of the protein itself.

While this technology is effective in a wide range of cell types, primary cells often pose challenges in terms of transfection. Notably, NK cells exhibit inherent resistance to viral transduction due to their sensitivity to TLRs or PAMPs and the low surface expression of the LDL receptor, which binds to the VSVG molecule commonly used in lentivirus envelopes (Bari et al., 2019). Consequently, achieving efficient knockout (KO) in human primary NK cells has proven to be a formidable challenge in recent years.

In the latter part of this study, I concentrated on developing a protocol for achieving highly efficient CRISPR/Cas9 editing in NK cells, with the aim of generating single, double, and triple knockouts (Figure 8.29 A).

### 9.2.1 CRISPR/Cas9 electroporation has high efficacy for single KOs

Primary NK cells were electroporated using the Neon Transfection System, employing CRISPR/Cas9 ribonucleoproteins to target multiple surface receptors. TRAIL, NKG2A, TIGIT,

and CD112R were successfully edited (Figure 8.29). Although there is variation in the editing percentages, it is anticipated that some of the less-expressed proteins may exhibit reduced accessibility to the DNA region, presenting a potential impediment to Cas9 binding and cleavage. DNAM-1 and NKG2A exhibited a high knockout (KO) percentage, which correlates with the abundance of these receptors in NK cells (Figure 8.29 and 8.30). The ability to edit even low-expressed receptors for subsequent sorting is of significant relevance in the NK cell field, given the diverse array of activating and inhibitory receptors within NK cell populations, which can hinder their overall activation or inhibition.

I hypothesized that the editing would be sufficient to enable the sorting of negative NK cells. To assess whether the editing was finely tuned to explore a specific pathway, I conducted experiments aimed at generating double and triple knockouts (KO) of the nectin pathway. The nectin pathway encompasses stress ligands present on tumor cells, such as CD112, CD111, CD155, and CD113, with their cognate receptors, including TIGIT, DNAM-1, CD112R, and CD96, competing for binding (Bottino et al., 2003; Fuchs et al., 2004). The nectin pathway is known for maintaining a delicate balance between activating (DNAM-1) and inhibitory receptors (TIGIT and CD112R). However, there has been limited investigation into the effects of an imbalance in this pathway, pushing it towards activation or inhibition. I specifically targeted the receptors binding to the CD112 ligand: CD112R, DNAM-1, and TIGIT, to explore how single, double, or triple KO would impact NK cell reactivity.

The edition of DNAM-1 exhibited the highest percentage of efficacy (60 %), followed by TIGIT (40 %) and CD112R (20 %) (Figure 4.31). Triple editing consistently yielded favourable results for DNAM-1 but to a lesser extent for TIGIT and CD112R. Nevertheless, through subsequent sorting and purification of each population, it was feasible to generate pure KO populations, encompassing single, double, and triple KOs (Figure 8.31).

To assess the effectiveness of edited NK cells, unsorted NK cells with modifications in CD96, DNAM-1, and TIGIT were employed. These edited NK cells were exposed to tumor cells bearing ligands, such as K562. Degranulation, quantified through CD107a, as previously discussed, exhibited a modest upward trend in NK cells with TIGIT and CD96 modifications, which correlated with the reduction of inhibitory receptors. However, DNAM-1 editing did not yield a noticeable alteration in the CD107a frequency. A similar pattern was observed with IFN $\gamma$  staining.

One plausible explanation for this outcome could be attributed to the absence of MHC-I molecules in the K562 cell line, which typically trigger a potent NK cell response (Sutherland et al., 1986). As such, the sole depletion of an activation receptor may not suffice to counterbalance the activation of other activating receptors. Consequently, it was hypothesized that a cell line less susceptible to NK cell-mediated cytotoxicity would be more appropriate for testing the edited NK cells. In collaboration with Tomáš Hofman, the melanoma cell line A375 was utilized, with the added modification of depleting the CD155 ligand shared by DNAM-1, CD96, and TIGIT receptors. The degranulation assay of NK cells revealed a reduction in DNAM-1-edited NK cells, whereas editing CD96 and TIGIT did not demonstrate a distinct trend in degranulation upon exposure to targets.

A reasonable hypothesis for these results is that the bulk NK cells might not be sufficiently homogeneous to detect the impact of the edited populations of CD96 and TIGIT, whereas DNAM-1 displayed 60 % edited NK cells in the bulk population. Subsequent repetitions with sorted NK cells would provide further insights into the functionality of each receptor within the nectin pathway. In summary, the methodology for generating singly, doubly, and triply targeted genes in human primary NK cells achieved successful modifications in all the surface-targeted molecules. This suggests that this technique is applicable to other genes of interest.

## 10 Conclusions

---

The study of the effect of environmental conditions on immune cells is becoming increasingly relevant for the development of new immunotherapies. In this study, I demonstrated the pleiotropic negative effects of hypoxia exposure on human NK cells compared to NK cells exposed to normoxia.

Overall, exposing NK cells to 1% oxygen induced a reduction in NK cell-mediated responses to different stimuli: tumor cells (K562, HT-29, A375), PMA/Ionomycin, and IL-12/18. This resulted in diminished degranulation and IFN $\gamma$  production. Additionally, human NK cells displayed reduced proliferation after exposure to hypoxia. I also showed a decrease in oxygen consumption rate and ATP production, which correlated with reduced surface expression of the ATP transporter CD39. In conclusion, NK cells exposed to hypoxia exhibit a unique repertoire of receptors and reduced proliferation and OXPHOS metabolism, which correlates with a reduced response to stimuli.

Furthermore, targeting HIF-1 $\alpha$  in human NK cells partially restored the hypoxia-induced phenotype, leading to the recovery of IFN $\gamma$  production after IL-12/18 stimulation. The co-culture of PDOs from colorectal adenocarcinoma patients showed a dependency on the PDO line for the cytotoxicity of HIF-1 $\alpha$  targeted NK cells against tumor cells. Based on these observations, HIF-1 $\alpha$  targeting alone is not sufficient to achieve sustained cytotoxicity against all four PDO lines. The combination of HER-2 CAR NK cells with HIF-1 $\alpha$  targeting resulted in enhanced cytotoxicity against the PDO lines, regardless of the specific PDO entity. In conclusion, PDO cultures with spontaneous hypoxic cores were efficiently targeted by HER-2 CAR HIF-1 $\alpha$  targeted NK cells, suggesting the potential use of double gene-edited NK cells for therapy against solid tumors.

Regarding cytokine-induced memory-like NK cells, hypoxia exposure reduced IFN $\gamma$  production in CML NK cells upon IL-12/18 stimulation, although degranulation toward K562 cells and proliferation were not affected. While no further studies were conducted in this study beyond a description of surface markers and responses to stimuli, this suggests that CML NK cells might benefit from HIF-1 $\alpha$  targeting to maintain their superior tumor response in hypoxic environments. The electroporation of human NK cells with CRISPR/Cas9 RNP was successful, resulting in single, double, and triple KOs, which may be further used in other immune cells or in NK cells targeting other proteins.

In conclusion, my study not only highlights the relevance of hypoxia's impact on human NK cells but also presents new approaches to counteract the NK cell-mediated response to tumors. This points to the combination of HER-2 CAR NK cells with HIF-1 $\alpha$  targeting as a new approach for colorectal adenocarcinoma therapy, with a potential enhancement of CML NK cells using CRISPR/Cas9 mediated gene edition for future research. Overall, understanding the impact of the hypoxic solid tumor microenvironment on NK cells will expand our comprehension of the factors contributing to failed NK cell-mediated tumor cytotoxicity, potentially paving the way for more effective future therapies.



## 11 REFERENCES

---

- Albinger, N., Hartmann, J., & Ullrich, E. (2021). Current status and perspective of CAR-T and CAR-NK cell therapy trials in Germany. In *Gene Therapy* (Vol. 28, Issue 9, pp. 513–527). Springer Nature. <https://doi.org/10.1038/s41434-021-00246-w>
- Allan, D. S. J., Cerdeira, A. S., Ranjan, A., Kirkham, C. L., Aguilar, O. A., Tanaka, M., Childs, R. W., Dunbar, C. E., Strominger, J. L., Kopcow, H. D., & Carlyle, J. R. (2017). Transcriptome analysis reveals similarities between human blood CD3<sup>+</sup> CD56<sup>bright</sup> cells and mouse CD127<sup>+</sup> innate lymphoid cells. *Scientific Reports*, 7(1). <https://doi.org/10.1038/s41598-017-03256-0>
- Allegra, C. J., Yothers, G., O'Connell, M. J., Sharif, S., Petrelli, N. J., Colangelo, L. H., Atkins, J. N., Seay, T. E., Fehrenbacher, L., Goldberg, R. M., O'Reilly, S., Chu, L., Azar, C. A., Lopa, S., & Wolmark, N. (2011). Phase III trial assessing bevacizumab in stages II and III carcinoma of the colon: Results of NSABP protocol C-08. *Journal of Clinical Oncology*, 29(1), 11–16. <https://doi.org/10.1200/JCO.2010.30.0855>
- Alter, G., Malenfant, J. M., & Altfeld, M. (2004). CD107a as a functional marker for the identification of natural killer cell activity. *Journal of Immunological Methods*, 294(1–2), 15–22. <https://doi.org/10.1016/j.jim.2004.08.008>
- Assoians, R. K., Komoriya, A., Meyers, C. A., Miller, D. M., & Sporn, M. B. (1983). Transforming Growth Factor- $\beta$  in Human Platelets. *The Journal of Biological Chemistry*, 258(11), 7155–7160.
- Balsamo, M., Manzini, C., Pietra, G., Raggi, F., Blengio, F., Mingari, M. C., Varesio, L., Moretta, L., Bosco, M. C., & Vitale, M. (2013). Hypoxia downregulates the expression of activating receptors involved in NK-cell-mediated target cell killing without affecting ADCC. *European Journal of Immunology*, 43(10), 2756–2764. <https://doi.org/10.1002/eji.201343448>
- Bargou, R., Leo, E., Zugmaier, G., Klinger, M., Goebeler, M., Knop, S., Noppeney, R., Viardot, A., Hess, G., Schuler, M., Einsele, H., Brandl, C., Wolf, A., Kirchinger, P., Klappers, P., Schmidt, M., Riethmüller, G., Reinhardt, C., Bauerle, P. A., & Kufer, P. (2008). Tumor regression in cancer patients by very low doses of a T cell-engaging antibody. *Science*, 321(5891), 970–974. <https://doi.org/10.1126/science.1159194>
- Bari, R., Granzin, M., Tsang, K. S., Roy, A., Krueger, W., Orentas, R., Pfeifer, R., Moeker, N., Verhoeyen, E., Dropulic, B., & Leung, W. (2019). A distinct subset of highly proliferative and lentiviral vector (LV)-transducible NK cells define a readily engineered subset for adoptive cellular therapy. *Frontiers in Immunology*, 10(AUG). <https://doi.org/10.3389/fimmu.2019.02001>
- Bartel, Y., Bauer, B., & Steinle, A. (2013). Modulation of NK cell function by genetically coupled C-type lectin-like receptor/ligand pairs encoded in the human natural killer

- gene complex. In *Frontiers in Immunology* (Vol. 4, Issue NOV). Frontiers Media SA. <https://doi.org/10.3389/fimmu.2013.00362>
- Barth, R. J., Mull, J. J., Spiess, P. J., & Rosenberg, S. A. (1991). Interferon  $\gamma$  and Tumor Necrosis Factor Have a Role in Tumor Regressions Mediated by Murine CD8<sup>+</sup> Tumor-infiltrating Lymphocytes. In *The Journal of Experimental Medicine* (Vol. 173). <http://rupress.org/jem/article-pdf/173/3/647/1101285/647.pdf>
- Basu, R., Whitlock, B. M., Husson, J., Le Floc'h, A., Jin, W., Oyler-Yaniv, A., Dotiwala, F., Giannone, G., Hivroz, C., Biais, N., Lieberman, J., Kam, L. C., & Huse, M. (2016). Cytotoxic T Cells Use Mechanical Force to Potentiate Target Cell Killing. *Cell*, 165(1), 100–110. <https://doi.org/10.1016/j.cell.2016.01.021>
- Bauer, S., Groh, V., Wu, J., Steinle, A., Phillips, J. H., Lanier, L. L., & Spies, T. (1998). Activation of NK Cells and T Cells by NKG2D, a Receptor for Stress-Inducible MICA. 27. *R. M. Corfield, Earth Sci. Rev*, 113(15), 27–34. [www.sciencemag.org](http://www.sciencemag.org)
- Baychelier, F., Sennepin, A., Ermonval, M., Dorgham, K., Debré, P., Debré, D., & Vieillard, V. (2013). Identification of a cellular ligand for the natural cytotoxicity receptor NKp44. *Blood*, 122(17), 2935–2942. <https://doi.org/10.1182/blood-2013-03>
- Behring, E. von. (1890). Untersuchungen ueber das Zustandekommen der Diphtherie-Immunität bei Thieren. *Deutsche Medizinische Wochenschrift*, 5, 1–14.
- Behring, E. von, & Kitasato, S. (1890). Ueber das Zustandekommen der Diphtherie-Immunität und der Tetanus-Immunität bei Thieren. *Deutsche Medizinische Wochenschrift*, 49, 1–8. <https://doi.org/10.17192/eb2013.0164>
- Bellone, G., Aste-Amezaga, M., Trinchieri, G., & Rodeck, U. (1995). Regulation of NK cell functions by TGF- $\beta$  1. *The Journal of Immunology*, 155(3), 1066–1073. <https://doi.org/10.4049/jimmunol.155.3.1066>
- Berón, W., Alvarez-Dominguez, C., Mayorga, L., & Stahl, P. D. (1995). Membrane trafficking along the phagocytic pathway. *Trends in Cell Biology*, 5, 100–104.
- Betge, J., Rindtorff, N., Sauer, J., Rauscher, B., Dingert, C., Gaitantzi, H., Herweck, F., Srour-Mhanna, K., Miersch, T., Valentini, E., Boonekamp, K. E., Hauber, V., Gutting, T., Frank, L., Belle, S., Gaiser, T., Buchholz, I., Jesenofsky, R., Härtel, N., ... Boutros, M. (2022). The drug-induced phenotypic landscape of colorectal cancer organoids. *Nature Communications*, 13(1). <https://doi.org/10.1038/s41467-022-30722-9>
- Bjorkman, P. J., Saper, M. A., Samraoui, B., Bennett, W. S., Strominger, J. L., & Wiley, D. C. (1987). Structure of the human class I histocompatibility antigen, HLA-A2. *Nature*, 329, 506–512.
- Björkström, N. K., Riese, P., Heuts, F., Andersson, S., Fauriat, C., Ivarsson, M. A., Björklund, A. T., Flodström-Tullberg, M., Michaëlsson, J., Rottenberg, M. E., Guzmán, C. A., Ljunggren, H. G., & Malmberg, K. J. (2010). Expression patterns of NKG2A, KIR, and

- CD57 define a process of CD56 dim NK-cell differentiation uncoupled from NK-cell education. *Blood*, 116(19), 3853–3864. <https://doi.org/10.1182/blood-2010-04-281675>
- Blake, S. J., Stannard, K., Liu, J., Allen, S., Yong, M. C. R., Mittal, D., Aguilera, A. R., Miles, J. J., Lutzky, V. P., de Andrade, L. F., Martinet, L., Colonna, M., Takeda, K., Kühnel, F., Gurlevik, E., Bernhardt, G., Teng, M. W. L., & Smyth, M. J. (2016). Suppression of metastases using a new lymphocyte checkpoint target for cancer immunotherapy. *Cancer Discovery*, 6(4), 446–459. <https://doi.org/10.1158/2159-8290.CD-15-0944>
- Boix-Perales, H., Borregaard, J., Jensen, K. B., Ersbøll, J., Galluzzo, S., Giuliani, R., Ciceroni, C., Melchiorri, D., Salmonson, T., Bergh, J., Schellens, J. H., & Pignatti, F. (2014). The European Medicines Agency Review of Pertuzumab for the Treatment of Adult Patients With HER2-Positive Metastatic or Locally Recurrent Unresectable Breast Cancer: Summary of the Scientific Assessment of the Committee for Medicinal Products for Human Use. *The Oncologist*, 19(7), 766–773. <https://doi.org/10.1634/theoncologist.2013-0348>
- Boj, S. F., Hwang, C. Il, Baker, L. A., Chio, I. I. C., Engle, D. D., Corbo, V., Jager, M., Ponz-Sarvisé, M., Tiriác, H., Spector, M. S., Gracanin, A., Oni, T., Yu, K. H., Van Boxtel, R., Huch, M., Rivera, K. D., Wilson, J. P., Feigin, M. E., Öhlund, D., ... Tuveson, D. A. (2015). Organoid models of human and mouse ductal pancreatic cancer. *Cell*, 160(1–2), 324–338. <https://doi.org/10.1016/j.cell.2014.12.021>
- Bottino, C., Castriconi, R., Pende, D., Rivera, P., Nanni, M., Carnemolla, B., Cantoni, C., Grassi, J., Marcenaro, S., Reymond, N., Vitale, M., Moretta, L., Lopez, M., & Moretta, A. (2003). Identification of PVR (CD155) and Nectin-2 (CD112) as cell surface ligands for the human DNAM-1 (CD226) activating molecule. *Journal of Experimental Medicine*, 198(4), 557–567. <https://doi.org/10.1084/jem.20030788>
- Braumüller, H., Wieder, T., Brenner, E., Aßmann, S., Hahn, M., Alkhaled, M., Schilbach, K., Essmann, F., Kneilling, M., Griessinger, C., Ranta, F., Ullrich, S., Mocikat, R., Braungart, K., Mehra, T., Fehrenbacher, B., Berdel, J., Niessner, H., Meier, F., ... Röcken, M. (2013). T-helper-1-cell cytokines drive cancer into senescence. *Nature*, 494(7437), 361–365. <https://doi.org/10.1038/nature11824>
- Brischwein, K., Schlereth, B., Guller, B., Steiger, C., Wolf, A., Lutterbuese, R., Offner, S., Locher, M., Urbig, T., Raum, T., Kleindienst, P., Wimberger, P., Kimmig, R., Fichtner, I., Kufer, P., Hofmeister, R., Da Silva, A. J., & Baeuerle, P. A. (2006). MT110: A novel bispecific single-chain antibody construct with high efficacy in eradicating established tumors. *Molecular Immunology*, 43(8), 1129–1143. <https://doi.org/10.1016/j.molimm.2005.07.034>
- Brubaker, D. B., & Whiteside, T. L. (1977). Localization of Human T Lymphocytes in Tissue Sections by a Rosetting Technique. *American Journal of Pathology*, 323–343.
- Cantor, H., & Boyse, E. A. (1975). Functional subclasses of T lymphocytes bearing different Ly antigens. *The Journal of Experimental Medicine*, 14, 1390–1399. <http://rupress.org/jem/article-pdf/141/6/1390/1657157/1390.pdf>

- Carayannopoulos, L. N., Naidenko, O. V, Fremont, D. H., & Yokoyama, W. M. (2002). Cutting Edge: Murine UL16-Binding Protein-Like Transcript 1: A Newly Described Transcript Encoding a High-Affinity Ligand for Murine NKG2D 1. *The Journal of Immunology*, *169*, 4079–4083. <http://journals.aai.org/jimmunol/article-pdf/169/8/4079/1158753/4079.pdf>
- Carreau, A., Hafny-Rahbi, B. El, Matejuk, A., Grillon, C., & Kieda, C. (2011). Why is the partial oxygen pressure of human tissues a crucial parameter? Small molecules and hypoxia. *Journal of Cellular and Molecular Medicine*, *15*(6), 1239–1253. <https://doi.org/10.1111/j.1582-4934.2011.01258.x>
- Carroll, M. C. (2004). The complement system in B cell regulation. *Molecular Immunology*, *41*(2–3), 141–146. <https://doi.org/10.1016/j.molimm.2004.03.017>
- Carson, W. E., Giri, J. G., Lindemann, M. J., Linett, M. L., Ahdieh, M., Paxton, R., Anderson, D., Eisenmann, J., Grabstein, K., & Caligiuri, M. A. (1994). Interleukin (IL) 15 Is a Novel Cytokine That Activates Human Natural Killer Cells via Components of the IL-2 Receptor. *Journal of Experimental Medicine*, *180*, 1395–1403. <http://rupress.org/jem/article-pdf/180/4/1395/1105678/1395.pdf>
- Carswell, E. A., Old, L. J., Kassel, R. L., Green, S., Fiore, N., & Williamson, B. (1975). An endotoxin-induced serum factor that causes necrosis of tumors. *Proceedings of the National Academy of Sciences*, *72*(9), 3666–3670. <https://www.pnas.org>
- Cerwenka, A., Alexander, †, Bakker, B. H., Mcclanahan, T., Wagner, J., Wu, J., Phillips, J. H., & Lanier, L. L. (2000). Retinoic Acid Early Inducible Genes Define a Ligand Family for the Activating NKG2D Receptor in Mice. *Immunity*, *12*, 721–727.
- Chames, P., & Baty, D. (2009). Bispecific antibodies for cancer therapy: The light at the end of the tunnel? In *mAbs* (Vol. 1, Issue 6, pp. 539–547). <https://doi.org/10.4161/mabs.1.6.10015>
- Chen, G. Y., Tang, J., Zheng, P., & Liu, Y. (2009). CD24 and siglec-10 selectively repress tissue damage - Induced immune responses. *Science*, *323*(5922), 1722–1725. <https://doi.org/10.1126/science.1168988>
- Chen, K., Magri, G., Grasset, E. K., & Cerutti, A. (2020). Rethinking mucosal antibody responses: IgM, IgG and IgD join IgA. In *Nature Reviews Immunology* (Vol. 20, Issue 7, pp. 427–441). Nature Research. <https://doi.org/10.1038/s41577-019-0261-1>
- Cheng, J., Kang, X., Zhang, S., & Yeh, E. T. H. (2007). SUMO-Specific Protease 1 Is Essential for Stabilization of HIF1 $\alpha$  during Hypoxia. *Cell*, *131*(3), 584–595. <https://doi.org/10.1016/j.cell.2007.08.045>
- Chiossone, L., Dumas, P. Y., Vienne, M., & Vivier, E. (2018). Natural killer cells and other innate lymphoid cells in cancer. In *Nature Reviews Immunology* (Vol. 18, Issue 11, pp. 671–688). Nature Publishing Group. <https://doi.org/10.1038/s41577-018-0061-z>
- Chmielewski, M., & Abken, H. (2020). TRUCKS, the fourth-generation CAR T cells: Current developments and clinical translation. *ADVANCES IN CELL AND GENE THERAPY*, *3*(3). <https://doi.org/10.1002/acg2.84>

- Cibrián, D., & Sánchez-Madrid, F. (2017). CD69: from activation marker to metabolic gatekeeper. In *European Journal of Immunology* (Vol. 47, Issue 6, pp. 946–953). Wiley-VCH Verlag. <https://doi.org/10.1002/eji.201646837>
- Cimmino, F., Avitabile, M., Lasorsa, V. A., Montella, A., Pezone, L., Cantalupo, S., Visconte, F., Corrias, M. V., Iolascon, A., & Capasso, M. (2019). HIF-1 transcription activity: HIF1A driven response in normoxia and in hypoxia. *BMC Medical Genetics*, 20(1). <https://doi.org/10.1186/s12881-019-0767-1>
- Clynes, R. A., Towers, T. L., Presta, L. G., & Ravetch, J. V. (2000). Inhibitory Fc receptors modulate in vivo cytotoxicity against tumor targets. *Nature Medicine*, 6, 443–446.
- Coley, W. B. (1909). The Treatment of Inoperable Sarcoma by Bacterial Toxins (the Mixed Toxins of the Streptococcus erysipelas and the Bacillus prodigiosus). In *Mr. J. WARRINGTON HAWARD*.
- Colomar-Carando, N., Gauthier, L., Merli, P., Loiacono, F., Canevali, P., Falco, M., Galaverna, F., Rossi, B., Bosco, F., Caratini, M., Mingari, M. C., Locatelli, F., Vivier, E., Meazza, R., & Pende, D. (2022). Exploiting Natural Killer Cell Engagers to Control Pediatric B-cell Precursor Acute Lymphoblastic Leukemia. *Cancer Immunology Research*, 10(3), 291–302. <https://doi.org/10.1158/2326-6066.CIR-21-0843>
- Committee for Medicinal Products for Human Use. (2022). *Carvykti*.
- Cooper, M. A., Elliott, J. M., Keyel, P. A., Yang, L., Carrero, J. A., & Yokoyama, W. M. (2009). Cytokine-induced memory-like natural killer cells. *Proceedings of the National Academy of Sciences*, 106(6), 1915–1919. <https://doi.org/10.1073/pnas.0813192106>
- Cooper, M. A., Fehniger, T. A., & Caligiuri, M. A. (2001). The biology of human natural killer-cell subsets. *Trends in Immunology*, 22(10), 633–640. [https://doi.org/10.1016/S1471-4906\(01\)02060-9](https://doi.org/10.1016/S1471-4906(01)02060-9)
- Cooper, M. D. (2015). The early history of B cells. *Nature Reviews Immunology*, 15(3), 191–197. <https://doi.org/10.1038/nri3801>
- Cooper, M. D., Peterson, R. D. A., & Good, R. A. (1965). Delineation of the thymic and bursal lymphoid systems in the chicken. *Nature*, 205, 143–146.
- Cosgrove, D., Gray, D., Dierich, A., Kaufman, J., Lemeur, M., Benoist, C., & Mathis, D. (1991). Mice Lacking MHC Class II Molecules. In *Cell* (Vol. 66).
- Cosman, D., Jü Rgen Mü, ‡, Sutherland, C. L., Chin, W., Armitage, R., Fanslow, W., Kubin, M., & Chalupny, N. J. (2001). ULBPs, Novel MHC Class I–Related Molecules, Bind to CMV Glycoprotein UL16 and Stimulate NK Cytotoxicity through the NKG2D Receptor. *Immunity*, 14, 123–133.
- Covello, K. L., & Simon, M. C. (2004). *HIFs, Hypoxia, and Vascular Development*.
- Daher, M., Basar, R., Gokdemir, E., Baran, N., Uprety, N., Karen, A., Cortes, N., Mendt, M., Kerbauy, L. N., Banerjee, P. P., Shanley, M., Imahashi, N., Li, L., Wei, F. L., Lim, I., Fathi,

- M., Rezvan, A., Mohanty, V., Shen, Y., ... Rezvani, K. (2021). Targeting a cytokine checkpoint enhances the fitness of armored cord blood CAR-NK cells. *Blood*, 137(5), 624–636. <http://ashpublications.org/blood/article-pdf/137/5/624/1798880/bloodbld2020007748.pdf>
- Daher, M., & Rezvani, K. (2021). Outlook for new car-based therapies with a focus on car nk cells: What lies beyond car-engineered t cells in the race against cancer. In *Cancer Discovery* (Vol. 11, Issue 1, pp. 45–58). American Association for Cancer Research Inc. <https://doi.org/10.1158/2159-8290.CD-20-0556>
- Daniels, B. F., Karlhofer, F. M., Seaman, W. E., & Yokoyama, W. M. (1994). A Natural Killer Cell Receptor Specific for a Major Histocompatibility Complex Class I Molecule. *The Journal of Experimental Medicine*, 180(2), 687–692. <https://doi.org/10.1084/jem.180.2.687>
- De Vries, J. E. (1995). Immunosuppressive and anti-inflammatory properties of interleukin 10. *Annals of Medicine*, 27(5), 537–541. <https://doi.org/10.3109/07853899509002465>
- Dejean, A. S., Beisner, D. R., Ch'en, I. L., Kerdiles, Y. M., Babour, A., Arden, K. C., Castrillon, D. H., DePinho, R. A., & Hedrick, S. M. (2009). Transcription factor Foxo3 controls the magnitude of T cell immune responses by modulating the function of dendritic cells. *Nature Immunology*, 10(5), 504–513. <https://doi.org/10.1038/ni.1729>
- Demaria, O., Gauthier, L., Debroas, G., & Vivier, E. (2021). Natural killer cell engagers in cancer immunotherapy: Next generation of immuno-oncology treatments. In *European Journal of Immunology* (Vol. 51, Issue 8, pp. 1934–1942). John Wiley and Sons Inc. <https://doi.org/10.1002/eji.202048953>
- Demaria, O., Gauthier, L., Vetizou, M., Blanchard Alvarez, A., Vagne, C., Habif, G., Batista, L., Baron, W., Belaïd, N., Girard-Madoux, M., Cesari, C., Caratini, M., Bosco, F., Benac, O., Lopez, J., Fenis, A., Galluso, J., Trichard, S., Carrette, B., ... Vivier, E. (2022). Antitumor immunity induced by antibody-based natural killer cell engager therapeutics armed with not-alpha IL-2 variant. *Cell Reports Medicine*, 3(10). <https://doi.org/10.1016/j.xcrm.2022.100783>
- Deynoux, M., Sunter, N., Héroult, O., & Mazurier, F. (2016). Hypoxia and hypoxia-inducible factors in leukemias. In *Frontiers in Oncology* (Vol. 6, Issue FEB). Frontiers Media S.A. <https://doi.org/10.3389/fonc.2016.00041>
- Diefenbach, A., Hsia, J. K., Hsiung, M. Y. B., & Raulet, D. H. (2003). A novel ligand for the NKG2D receptor activates NK cells and macrophages and induces tumor immunity. *European Journal of Immunology*, 33(2), 381–391. <https://doi.org/10.1002/immu.200310012>
- Divakaruni, A. S., Paradyse, A., Ferrick, D. A., Murphy, A. N., & Jastroch, M. (2014). Analysis and interpretation of microplate-based oxygen consumption and pH data. In *Methods in Enzymology* (Vol. 547, Issue C, pp. 309–354). Academic Press Inc. <https://doi.org/10.1016/B978-0-12-801415-8.00016-3>

- Dong, Y., Hung, Y., Zhang, Z., Chen, A., Li, L., Tian, M., Shen, J., & Shao, J. (2023). iRGD-modified memory-like NK cells exhibit potent responses to hepatocellular carcinoma. *Journal of Translational Medicine*, 21(1). <https://doi.org/10.1186/s12967-023-04024-7>
- Doudna, J. A., & Charpentier, E. (2014). The new frontier of genome engineering with CRISPR-Cas9. *Science*, 345(6213), 1077–1093. <https://www.science.org>
- Dreier, T., Baeuerle, P. A., Fichtner, I., Grü, M., Schlereth, B., Lorenczewski, G., Kufer, P., Lutterbü, R., Riethmü, G., Gjørstrup, P., & Bargou, R. C. (2003). T Cell Costimulus-Independent and Very Efficacious Inhibition of Tumor Growth in Mice Bearing Subcutaneous or Leukemic Human B Cell Lymphoma Xenografts by a CD19-/CD3-Bispecific Single-Chain Antibody Construct 1. In *The Journal of Immunology* (Vol. 170). <http://journals.aai.org/jimmunol/article-pdf/170/8/4397/1165790/4397.pdf>
- Eales, K. L., Hollinshead, K. E. R., & Tennant, D. A. (2016). Hypoxia and metabolic adaptation of cancer cells. In *Oncogenesis* (Vol. 5, Issue 1). Springer Nature. <https://doi.org/10.1038/ONCSIS.2015.50>
- Edler, D., Kressner, U., Ragnhammar, P., Johnston, P. G., Magnusson, I., Glimelius, B., Pählman, L., Lindmark, G., & Blomgren, H. (2000). Immunohistochemically Detected Thymidylate Synthase in Colorectal Cancer: An Independent Prognostic Factor of Survival. *Clinical Cancer Research*, 6, 488–492. <http://aacrjournals.org/clincancerres/article-pdf/6/2/488/2073831/df020000488.pdf>
- Ehrlich, E. S., Wang, T., Luo, K., Xiao, Z., Niewiadomska, A. M., Martinez, T., Xu, W., Neckers, L., & Yu, X.-F. (2008). Regulation of Hsp90 client proteins by a Cullin5-RING E3 ubiquitin ligase. *Proceedings of the National Academy of Sciences*, 106(48), 20330–20335. [www.pnas.org/cgi/content/full/](http://www.pnas.org/cgi/content/full/)
- Ennis S Lamon, D. J., Rian Eyland -j Ones, B. L., Teven Hak, S. S., Ank Uchs, H. F., Irginia Aton, V. P., Harm, P. D., Lex Ajamonde, A. B., Homas Leming, T. F., Olfgang Iermann, W. E., Anet Olter, J. W., Ark Egram, M. P., Ose Aselga, J. B., & Arry Orton, L. N. (2001). Use of chemotherapy plus a monoclonal antibody against HER2 for metastatic breast cancer that overexpresses HER2. *New England Journal of Medicine*, 344(11), 783–792. [www.nejm.org](http://www.nejm.org)
- Epstein, T., Xu, L., Gillies, R. J., & Gatenby, R. A. (2014). Separation of metabolic supply and demand: aerobic glycolysis as a normal physiological response to fluctuating energetic demands in the membrane. *Cancer & Metabolism*, 2(1). <https://doi.org/10.1186/2049-3002-2-7>
- Eshhar, Z., Waks, T., Grosst, G., & Schindler, D. G. (1993). Specific activation and targeting of cytotoxic lymphocytes through chimeric single chains consisting of antibody-binding domains and the y or C subunits of the immunoglobulin and T-cell receptors. *Proceedings of the National Academy of Sciences*, 90, 720–724. <https://www.pnas.org>
- European Cancer Patient Coalition. (2022). *CAR-T cell therapy white paper*.

- European Commission. (2017). *Eudralex-The rules governing medicinal products in the European Union, Volume 4 Good Manufacturing Practice (GMP) guidelines*. [https://health.ec.europa.eu/medicinal-products/eudralex/eudralex-volume-4\\_en](https://health.ec.europa.eu/medicinal-products/eudralex/eudralex-volume-4_en)
- European Medicines Agency. (2021a). *Abecma*.
- European Medicines Agency. (2021b). *Tecartus*.
- Fagraeus, A. (1947). Plasma Cellular Reaction and its Relation to the Formation of Antibodies in vitro. *Nature*, 404, 499–499. <https://doi.org/https://doi.org/10.1038/159499a0>
- Fiegl, M., Samudio, I., Clise-Dwyer, K., Burks, J. K., Mnjoyan, Z., & Andreeff, M. (2009). CXCR4 expression and biologic activity in acute myeloid leukemia are dependent on oxygen partial pressure. *Blood*, 113(7), 1504–1512. <https://doi.org/10.1182/blood-2008-06-161539>
- Fiorentino, D. F., Zlotnik, A., Vieira, P., Mosmann, T. R., Howard, M., Moore, K. W., & O'garra, A. (1991). *IL-10 acts on the antigen-presenting cell to inhibit cytokine production by Th1 cells* (Vol. 146, Issue 10). <http://journals.aai.org/jimmunol/article-pdf/146/10/3444/1050909/3444.pdf>
- Fisher, D. T., Appenheimer, M. M., & Evans, S. S. (2014). The two faces of IL-6 in the tumor microenvironment. In *Seminars in Immunology* (Vol. 26, Issue 1, pp. 38–47). Academic Press. <https://doi.org/10.1016/j.smim.2014.01.008>
- Florentino, D. F., Zlotnik, A., Mosmann, T. R., Howard, M., & Anne O'garra, A. N. D. (1991). IL-10 inhibits cytokine production by activated macrophages. In *THE JOURNAL OF IMMUNOLOGY* (Vol. 147, Issue 11). <http://journals.aai.org/jimmunol/article-pdf/147/11/3815/1053392/3815.pdf>
- Florido, R., Smith, K. L., Cuomo, K. K., & Russell, S. D. (2017). Cardiotoxicity From Human Epidermal Growth Factor Receptor-2 (HER2) Targeted Therapies. *Journal of the American Heart Association*, 6(9). <https://doi.org/10.1161/JAHA.117.006915>
- Folkman, J. (1972). Anti-Angiogenesis: New Concept for Therapy of Solid Tumors. *Annals of Surgery*, 175(3), 409–416.
- Foltz, J. A., Moseman, J. E., Thakkar, A., Chakravarti, N., & Lee, D. A. (2018). Tgfβ imprinting during activation promotes natural killer cell cytokine hypersecretion. *Cancers*, 10(11). <https://doi.org/10.3390/cancers10110423>
- Franklin, M. C., Carey, K. D., Vajdos, F. F., Leahy, D. J., De Vos, A. M., & Sliwkowski, M. X. (2004). Insights into ErbB signaling from the structure of the ErbB2-pertuzumab complex. *Cancer Cell*, 5, 317–328.
- Frantz, B., Nordby, E. C., Bren, G., Steffan, N., Paya, C. V., Kincaid, R. L., Tocci, M. J., O'Keefe, S. J., & O'Neill, E. A. (1994). Calcineurin acts in synergy with PMA to inactivate IκB/MAD3 an inhibitor of NF-κB. *EMBO Journal*, 13(4), 861–870. <https://doi.org/10.1002/j.1460-2075.1994.tb06329.x>

- Freeman, G. J., Long, A. J., Iwai, Y., Bourque, K., Chernova, T., Nishimura, H., Fitz, L. J., Malenkovich, N., Okazaki, T., Byrne, M. C., Horton, H. F., Fouser, L., Carter, L., Ling, V., Bowman, M. R., Carreno, B. M., Collins, M., Wood, C. R., & Honjo, T. (2000). Engagement of the PD-1 Immunoinhibitory Receptor by a Novel B7 Family Member Leads to Negative Regulation of Lymphocyte Activation. In *J. Exp. Med* (Vol. 192, Issue 7). <http://www.jem.org/cgi/content/full/192/7/1027>
- Friedmann-Morvinski, D., Bendavid, A., Waks, T., Schindler, D., & Eshhar, Z. (2005). Redirected primary T cells harboring a chimeric receptor require costimulation for their antigen-specific activation. *Gene Therapy*, 105(8), 3087–3093. <https://doi.org/10.1182/blood>
- Fu, Q., Fu, T. M., Cruz, A. C., Sengupta, P., Thomas, S. K., Wang, S., Siegel, R. M., Wu, H., & Chou, J. J. (2016). Structural Basis and Functional Role of Intramembrane Trimerization of the Fas/CD95 Death Receptor. *Molecular Cell*, 61(4), 602–613. <https://doi.org/10.1016/j.molcel.2016.01.009>
- Fuchs, A., Cella, M., Giurisato, E., Shaw, A. S., & Colonna, M. (2004). Cutting Edge: CD96 (Tactile) Promotes NK Cell-Target Cell Adhesion by Interacting with the Poliovirus Receptor (CD155). *The Journal of Immunology*, 172(7), 3994–3998. <https://doi.org/10.4049/jimmunol.172.7.3994>
- Fulgenzi, C. A. M., Cheon, J., D'Alessio, A., Nishida, N., Ang, C., Marron, T. U., Wu, L., Saeed, A., Wietharn, B., Cammarota, A., Pressiani, T., Personeni, N., Pinter, M., Scheiner, B., Balcar, L., Napolitano, A., Huang, Y. H., Phen, S., Naqash, A. R., ... Pinato, D. J. (2022). Reproducible safety and efficacy of atezolizumab plus bevacizumab for HCC in clinical practice: Results of the AB-real study. *European Journal of Cancer*, 175, 204–213. <https://doi.org/10.1016/j.ejca.2022.08.024>
- Gao, Y., Souza-Fonseca-Guimaraes, F., Bald, T., Ng, S. S., Young, A., Ngiow, S. F., Rautela, J., Straube, J., Waddell, N., Blake, S. J., Yan, J., Bartholin, L., Lee, J. S., Vivier, E., Takeda, K., Messaoudene, M., Zitvogel, L., Teng, M. W. L., Belz, G. T., ... Smyth, M. J. (2017). Tumor immunoevasion by the conversion of effector NK cells into type 1 innate lymphoid cells. *Nature Immunology*, 18(9), 1004–1015. <https://doi.org/10.1038/ni.3800>
- Garcés-Lázaro, I., Kotzur, R., Cerwenka, A., & Mandelboim, O. (2022). NK Cells Under Hypoxia: The Two Faces of Vascularization in Tumor and Pregnancy. In *Frontiers in Immunology* (Vol. 13). Frontiers Media S.A. <https://doi.org/10.3389/fimmu.2022.924775>
- Gasteiger, G., Fan, X., Dikiy, S., Lee, S. Y., & Rudensky, A. Y. (2015). Tissue residency of innate lymphoid cells in lymphoid and nonlymphoid organs. *Science*, 350(6263), 981–958. <https://doi.org/10.1126/science.aad3346>
- Gauthier, L., Morel, A., Anceriz, N., Rossi, B., Blanchard-Alvarez, A., Grondin, G., Trichard, S., Cesari, C., Sapet, M., Bosco, F., Rispaud-Blanc, H., Guillot, F., Cornen, S., Roussel, A., Amigues, B., Habif, G., Caraguel, F., Arrufat, S., Remark, R., ... Vivier, E. (2019). Multifunctional Natural Killer Cell Engagers Targeting Nkp46 Trigger Protective Tumor Immunity. *Cell*, 177(7), 1701–1713.e16. <https://doi.org/10.1016/j.cell.2019.04.041>

- Gauthier, L., Virone-Oddos, A., Beninga, J., Rossi, B., Nicolazzi, C., Amara, C., Blanchard-Alvarez, A., Gourdin, N., Courta, J., Basset, A., Agnel, M., Guillot, F., Grondin, G., Bonnevaux, H., Bauchet, A. L., Morel, A., Morel, Y., Chiron, M., & Vivier, E. (2023). Control of acute myeloid leukemia by a trifunctional Nkp46-CD16a-NK cell engager targeting CD123. *Nature Biotechnology*, *41*(9), 1296–1306. <https://doi.org/10.1038/s41587-022-01626-2>
- Gleason, M. K., Ross, J. A., Warlick, E. D., Lund, T. C., Verneris, M. R., Wiernik, A., Spellman, S., Haagenson, M. D., Lenvik, A. J., Litzow, M. R., Epling-Burnette, P. K., Blazar, B. R., Weiner, L. M., Weisdorf, D. J., Vallera, D. A., & Miller, J. S. (2014). CD16xCD33 bispecific killer cell engager (BiKE) activates NK cells against primary MDS and MDSC CD33 targets. *Blood*, *123*, 3016–3026. <https://doi.org/10.1182/blood-2013>
- Gleason, M. K., Verneris, M. R., Todhunter, D. A., Zhang, B., McCullar, V., Zhou, S. X., Panoskaltsis-Mortari, A., Weiner, L. M., Vallera, D. A., & Miller, J. S. (2012). Bispecific and trispecific killer cell engagers directly activate human NK cells through CD16 signaling and induce cytotoxicity and cytokine production. *Molecular Cancer Therapeutics*, *11*(12), 2674–2684. <https://doi.org/10.1158/1535-7163.MCT-12-0692>
- Goodnow, C. C., Crosbie, J., Jorgensen, H., Brink, R. A., & Basten, A. (1989). *Induction of self-tolerance in mature peripheral B lymphocytes*.
- Groenen, L. C., Nice, E. C., & Burgess, A. W. (1994). Structure-function relationships for the EGF/TGF- $\alpha$  family of mitogens. In *Growth Factors* (Vol. 11, Issue 4, pp. 235–257). Informa Healthcare. <https://doi.org/10.3109/08977199409010997>
- Gross, G., & Eshhar, Z. (2016). Therapeutic Potential of T Cell Chimeric Antigen Receptors (CARs) in Cancer Treatment: Counteracting Off-Tumor Toxicities for Safe CAR T Cell Therapy. *Annual Review of Pharmacology and Toxicology*, *56*, 59–83. <https://doi.org/10.1146/annurev-pharmtox-010814-124844>
- Gross, G., Waks, T., & Eshhar, Z. (1989). Expression of immunoglobulin-T-cell receptor chimeric molecules as functional receptors with antibody-type specificity. *Proceedings of the National Academy of Sciences*, *86*, 10024–10028. <https://www.pnas.org>
- Guerra, N., Tan, Y. X., Joncker, N. T., Choy, A., Gallardo, F., Xiong, N., Knoblaugh, S., Cado, D., Greenberg, N. R., & Raulet, D. H. (2008). NKG2D-Deficient Mice Are Defective in Tumor Surveillance in Models of Spontaneous Malignancy. *Immunity*, *28*(4), 571–580. <https://doi.org/10.1016/j.immuni.2008.02.016>
- Guinney, J., Dienstmann, R., Wang, X., De Reyniès, A., Schlicker, A., Soneson, C., Marisa, L., Roepman, P., Nyamundanda, G., Angelino, P., Bot, B. M., Morris, J. S., Simon, I. M., Gerster, S., Fessler, E., De Sousa, E. Melo, F., Missiaglia, E., Ramay, H., Barras, D., ... Tejpar, S. (2015). The consensus molecular subtypes of colorectal cancer. *Nature Medicine*, *21*(11), 1350–1356. <https://doi.org/10.1038/nm.3967>
- H Allen, L.-A., & Aderem, A. (1996). Mechanisms of phagocytosis. *Current Opinion in Immunology*, *8*, 36–40.

- Hammers, H., Plimack, E. R., Infante, J. R., Ernstoff, M., Rini, B. I., McDermott, D. F., Razak, A., Pal, S. K., Voss, M., Sharma, P., Kollmannsberger, C. K., Heng, D., Shen, Y., Kurland, J., Spratlin, J., Gagnier, P., & Amin, A. (2014). Phase I Study of Nivolumab in Combination with Ipilimumab in Metastatic Renal Cell Carcinoma (Mrcc). *Annals of Oncology*, 25, iv361. <https://doi.org/10.1093/annonc/mdu342.3>
- Harrington, L. E., Hatton, R. D., Mangan, P. R., Turner, H., Murphy, T. L., Murphy, K. M., & Weaver, C. T. (2005). Interleukin 17-producing CD4<sup>+</sup> effector T cells develop via a lineage distinct from the T helper type 1 and 2 lineages. *Nature Immunology*, 6(11), 1123–1132. <https://doi.org/10.1038/ni1254>
- He, B., Mai, Q., Pang, Y., Deng, S., He, Y., Xue, R., Xu, N., Zhou, H., Liu, X., Xuan, L., Li, C., & Liu, Q. (2023). Cytokines induced memory-like NK cells engineered to express CD19 CAR exhibit enhanced responses against B cell malignancies. *Frontiers in Immunology*, 14. <https://doi.org/10.3389/fimmu.2023.1130442>
- Hedrick, S. M., Cohen, D. I., Nielsen, E. A., & Davis, M. M. (1982). Isolation of cDNA clones encoding T cell-specific membrane-associated proteins. In 22. *Parnes. I. R. et al. Proc. natl. Acad. Sci. u.s.A* (Vol. 71).
- Heeger, P. S., Lalli, P. N., Lin, F., Valujskikh, A., Liu, J., Muqim, N., Xu, Y., & Medof, M. E. (2005). Decay-accelerating factor modulates induction of T cell immunity. *Journal of Experimental Medicine*, 201(10), 1523–1530. <https://doi.org/10.1084/jem.20041967>
- Hegde, M., Joseph, S. K., Pashankar, F., DeRenzo, C., Sanber, K., Navai, S., Byrd, T. T., Hicks, J., Xu, M. L., Gerken, C., Kalra, M., Robertson, C., Zhang, H., Shree, A., Mehta, B., Dakhova, O., Salsman, V. S., Grilley, B., Gee, A., ... Ahmed, N. (2020). Tumor response and endogenous immune reactivity after administration of HER2 CAR T cells in a child with metastatic rhabdomyosarcoma. *Nature Communications*, 11(1). <https://doi.org/10.1038/s41467-020-17175-8>
- Hersh, E. M., Mavligit, G. M., Gutterman, J. U., & Barsales, P. B. (1976). Mononuclear cell content of human solid tumors. *Medical and Pediatric Oncology*, 2(1), 1–9. <https://doi.org/10.1002/mpo.2950020102>
- Hewitson, K. S., McNeill, L. A., Riordan, M. V., Tian, Y. M., Bullock, A. N., Welford, R. W., Elkins, J. M., Oldham, N. J., Bhattacharya, S., Gleadle, J. M., Ratcliffe, P. J., Pugh, C. W., & Schofield, C. J. (2002). Hypoxia-inducible factor (HIF) asparagine hydroxylase is identical to factor inhibiting HIF (FIH) and is related to the cupin structural family. *Journal of Biological Chemistry*, 277(29), 26351–26355. <https://doi.org/10.1074/jbc.C200273200>
- Hoh, J. H., Werbin, J. L., & Heinz, W. F. (2018). Restricted exchange microenvironments for cell culture. *BioTechniques*, 64(3), 101–109. <https://doi.org/10.4155/btn-2017-0110>
- Hon, W.-C., Wilson, M. I., Harlos, K., Claridgek, T. D. W., Schofieldk, C. J., Pugh, C. W., Maxwell, P. H., Ratcliffe, P. J., Stuart, D. I., & Jones, E. Y. (2002). *Structural basis for the recognition of hydroxyproline in HIF-1α by pVHL*. [www.nature.com/nature](http://www.nature.com/nature)

- Horenstein, A. L., Chillemi, A., Zini, R., Quarona, V., Bianchi, N., Manfredini, R., Gambari, R., Malavasi, F., & Ferrari, D. (2018). Cytokine-induced killer cells express CD39, CD38, CD203a, CD73 ectoenzymes and P1 adenosinergic receptors. *Frontiers in Pharmacology*, 9(APR). <https://doi.org/10.3389/fphar.2018.00196>
- Houchins, J. P., Yabe, T., Mcsherry, C., & Bach, F. H. (1991). DNA sequence analysis of NKG2, a family of related cDNA clones encoding type II Integral membrane proteins on human Natural Killer cells. *Journal of Experimental Medicine*, 1017–1020. <http://rupress.org/jem/article-pdf/173/4/1017/1101475/1017.pdf>
- Hubbi, M. E., & Semenza, G. L. (2015). Regulation of cell proliferation by hypoxia-inducible factors. In *American Journal of Physiology - Cell Physiology* (Vol. 309, Issue 12, pp. C775–C782). American Physiological Society. <https://doi.org/10.1152/ajpcell.00279.2015>
- Hutchings, M., Morschhauser, F., Iacoboni, G., Carlo-Stella, C., Fritz, ;, Offner, C., Sureda, A., Salles, G., Joaquín Martínez-Lopez, ;, Crump, M., Thomas, D. N., Peter, ;, Morcos, N., Ferlini, C., Ann-Marie, ;, Bröske, E., Bröske, B., Belousov, A., Bacac, ; Marina, ... Dickinson, M. J. (2021). Glofitamab, a Novel, Bivalent CD20-Targeting T-Cell-Engaging Bispecific Antibody, Induces Durable Complete Remissions in Relapsed or Refractory B-Cell Lymphoma: A Phase I Trial. *Communications J Clin Oncol*, 39, 1959–1970. <https://doi.org/10.1200/JCO.20>
- Imai, C., Mihara, K., Andreansky, M., Nicholson, I. C., Pui, C. H., Geiger, T. L., & Campana, D. (2004). Chimeric receptors with 4-1BB signaling capacity provoke potent cytotoxicity against acute lymphoblastic leukemia. *Leukemia*, 18(4), 676–684. <https://doi.org/10.1038/sj.leu.2403302>
- Ishida, Y., Agata, Y., Shibahara, K., & Honjo, T. (1992). Induced expression of PD-1, a novel member of the immunoglobulin gene superfamily, upon programmed cell death. *EMBO Journal*, 11(11), 3887–3895. <https://doi.org/10.1002/j.1460-2075.1992.tb05481.x>
- Ivan MKondo, K., Yang H, Kim, W., Valiando, J., Ohh, M., Salic, A., Asara JM, Lane, W., & Kaelin, W. Jr. (2001). HIFalpha targeted for VHL-mediated destruction by proline hydroxylation: implications for O2 sensing. *Science*, 292(5516), 464–468.
- Jagannathan, L., Cuddapah, S., & Costa, M. (2016). Oxidative Stress Under Ambient and Physiological Oxygen Tension in Tissue Culture. In *Current Pharmacology Reports* (Vol. 2, Issue 2, pp. 64–72). Springer International Publishing. <https://doi.org/10.1007/s40495-016-0050-5>
- Jenkinson, E. J., Anderson, G., & Owen, J. J. T. (1992). Studies on T Cell Maturation on Defined Thymic Stromal Cell Populations In Vitro. *Journal of Experimental Medicine*, 176, 845–853. <https://doi.org/https://doi.org/10.1084/jem.176.3.845>
- Kaminski, M. F., Bendzick, L., Hopps, R., Kauffman, M., Kodal, B., Soignier, Y., Hinderlie, P., Walker, J. T., Lenvik, T. R., Geller, M. A., Miller, J. S., & Felices, M. (2022). TEM8 Tri-specific Killer Engager binds both tumor and tumor stroma to specifically engage natural

- killer cell anti-tumor activity. *Journal for ImmunoTherapy of Cancer*, 10(9).  
<https://doi.org/10.1136/jitc-2022-004725>
- Kaplan, D. H., Shankaran, V., Dighe, A. S., Stockert, E., Aguet, M., Old, L. J., & Schreiber, R. D. (1998). Demonstration of an interferon-dependent tumor surveillance system in immunocompetent mice. In *Immunology* (Vol. 95). [www.pnas.org](http://www.pnas.org).
- Karam, M., Janbon, H., Malkinson, G., & Brunet, I. (2022). Heterogeneity and developmental dynamics of LYVE-1 perivascular macrophages distribution in the mouse brain. *Journal of Cerebral Blood Flow and Metabolism*, 42(10), 1797–1812.  
<https://doi.org/10.1177/0271678X221101643>
- Karikó, K., Buckstein, M., Ni, H., & Weissman, D. (2005). Suppression of RNA recognition by Toll-like receptors: The impact of nucleoside modification and the evolutionary origin of RNA. *Immunity*, 23(2), 165–175. <https://doi.org/10.1016/j.immuni.2005.06.008>
- Karikó, K., Muramatsu, H., Welsh, F. A., Ludwig, J., Kato, H., Akira, S., & Weissman, D. (2008). Incorporation of pseudouridine into mRNA yields superior nonimmunogenic vector with increased translational capacity and biological stability. *Molecular Therapy*, 16(11), 1833–1840. <https://doi.org/10.1038/mt.2008.200>
- Kashii, Y., Giorda, R., Herberman, R. B., Whiteside, T. L., & Vujanovic, N. L. (1999). Constitutive Expression and Role of the TNF Family Ligands in Apoptotic Killing of Tumor Cells by Human NK Cells 1. In *The Journal of Immunology* (Vol. 163).  
<http://journals.aai.org/jimmunol/article-pdf/163/10/5358/1104564/im229905358p.pdf>
- Kaufmann, S. H. E. (2008). Immunology's foundation: the 100-year anniversary of the Nobel Prize to Paul Ehrlich and Elie Metchnikoff. *Nature Immunology*, 9, 705–712.
- Kaufmann, S. H. E. (2019). Immunology's coming of age. In *Frontiers in Immunology* (Vol. 10, Issue APR). Frontiers Media S.A. <https://doi.org/10.3389/fimmu.2019.00684>
- Kawai, T., & Akira, S. (2009). The roles of TLRs, RLRs and NLRs in pathogen recognition. In *International Immunology* (Vol. 21, Issue 4, pp. 317–337).  
<https://doi.org/10.1093/intimm/dxp017>
- Kebenko, M., Goebeler, M. E., Wolf, M., Hasenburg, A., Seggewiss-Bernhardt, R., Ritter, B., Rautenberg, B., Atanackovic, D., Kratzer, A., Rottman, J. B., Friedrich, M., Vieser, E., Elm, S., Patzak, I., Wessiepe, D., Stienen, S., & Fiedler, W. (2018). A multicenter phase 1 study of solitomab (MT110, AMG 110), a bispecific EpCAM/CD3 T-cell engager (BiTE®) antibody construct, in patients with refractory solid tumors. *OncoImmunology*, 7(8).  
<https://doi.org/10.1080/2162402X.2018.1450710>
- Kennedy, P. R., Vallera, D. A., Etestad, B., Hallstrom, C., Kodal, B., Todhunter, D. A., Bendzick, L., Hinderlie, P., Walker, J. T., Pulkrabek, B., Pastan, I., Kratzke, R. A., Fujioka, N., Miller, J. S., & Felices, M. (2023). A tri-specific killer engager against mesothelin targets NK cells towards lung cancer. *Frontiers in Immunology*, 14.  
<https://doi.org/10.3389/fimmu.2023.1060905>

- Kiessling, R., Klein, E., Pross, H., & Wigzell, H. (1975). „Natural” killer cells in the mouse. II. Cytotoxic cells with specificity for mouse Moloney leukemia cells. Characteristics of the killer cell. *European Journal of Immunology*, 5(2), 117–121. <https://doi.org/10.1002/eji.1830050209>
- Kiessling, R., Klein, E., & Wigzell, H. (1975). „Natural” killer cells in the mouse. I. Cytotoxic cells with specificity for mouse Moloney leukemia cells. Specificity and distribution according to genotype. *European Journal of Immunology*, 5(2), 112–117. <https://doi.org/10.1002/eji.1830050208>
- Kishimoto, T. (1989). The Biology of Interleukin-6. *Blood*, 74(1), 1–10.
- Klein, G. O., Klein, G., Kiessling, R., & K-irre, K. (1978). Immunogenetics H-2-Associated Control of Natural Cytotoxicity and Hybrid Resistance Against RBL-5. *Immunogenetics*, 6, 561–569.
- Koebel, C. M., Vermi, W., Swann, J. B., Zerafa, N., Rodig, S. J., Old, L. J., Smyth, M. J., & Schreiber, R. D. (2007). Adaptive immunity maintains occult cancer in an equilibrium state. *Nature*, 450(7171), 903–907. <https://doi.org/10.1038/nature06309>
- Kosti, P., Opzoomer, J. W., Larios-Martinez, K. I., Henley-Smith, R., Scudamore, C. L., Okesola, M., Taher, M. Y. M., Davies, D. M., Muliaditan, T., Larcombe-Young, D., Woodman, N., Gillett, C. E., Thavaraj, S., Maher, J., & Arnold, J. N. (2021). Hypoxia-sensing CAR T cells provide safety and efficacy in treating solid tumors. *Cell Reports Medicine*, 2(4). <https://doi.org/10.1016/j.xcrm.2021.100227>
- Kotzur, R., Duev-Cohen, A., Kol, I., Reches, A., Mandelboim, O., & Stein, N. (2022). NK-92 cells retain vitality and functionality when grown in standard cell culture conditions. *PLoS ONE*, 17(3 March). <https://doi.org/10.1371/journal.pone.0264897>
- Kowolik, C. M., Topp, M. S., Gonzalez, S., Pfeiffer, T., Olivares, S., Gonzalez, N., Smith, D. D., Forman, S. J., Jensen, M. C., & Cooper, L. J. N. (2006). CD28 costimulation provided through a CD19-specific chimeric antigen receptor enhances in vivo persistence and antitumor efficacy of adoptively transferred T cells. *Cancer Research*, 66(22), 10995–11004. <https://doi.org/10.1158/0008-5472.CAN-06-0160>
- Kruse, P. H., Matta, J., Ugolini, S., & Vivier, E. (2014). Natural cytotoxicity receptors and their ligands. In *Immunology and Cell Biology* (Vol. 92, Issue 3, pp. 221–229). Nature Publishing Group. <https://doi.org/10.1038/icb.2013.98>
- Krzewski, K., Gil-Krzewska, A., Nguyen, V., Peruzzi, G., & Coligan, J. E. (2013). LAMP1/CD107a is required for efficient perforin delivery to lytic granules and NK-cell cytotoxicity. *Blood*, 121(23), 4672–4683. <https://doi.org/10.1182/blood-2012-08>
- Krzywinska, E., Kantari-Mimoun, C., Kerdiles, Y., Sobecki, M., Isagawa, T., Gotthardt, D., Castells, M., Haubold, J., Millien, C., Viel, T., Tavitian, B., Takeda, N., Fandrey, J., Vivier, E., Sendl, V., & Stockmann, C. (2017). Loss of HIF-1 $\alpha$  in natural killer cells inhibits tumour growth by stimulating non-productive angiogenesis. *Nature Communications*, 8(1). <https://doi.org/10.1038/s41467-017-01599-w>

- Labiano, S., Meléndez-Rodríguez, F., Palazón, A., Teijeira, Á., Garasa, S., Etxeberria, I., Aznar, M. Á., Sánchez-Paulete, A. R., Azpilikueta, A., Bolaños, E., Molina, C., de la Fuente, H., Maiso, P., Sánchez-Madrid, F., de Landázuri, M. O., Aragonés, J., & Melero, I. (2017). CD69 is a direct HIF-1 $\alpha$  target gene in hypoxia as a mechanism enhancing expression on tumor-infiltrating T lymphocytes. *OncImmunity*, 6(4).  
<https://doi.org/10.1080/2162402X.2017.1283468>
- Langley, R. R., & Fidler, I. J. (2011). The seed and soil hypothesis revisited-The role of tumor-stroma interactions in metastasis to different organs. *International Journal of Cancer*, 128(11), 2527–2535. <https://doi.org/10.1002/ijc.26031>
- Lanier, L. L., Corliss, B., Wu, J., & Phillips, J. H. (1998). Association of DAP12 with Activating CD94/NKG2C NK Cell Receptors domain (designated KIR2DL and KIR3DL) recruit SHP-1 and prevent NK cell effector function (Burshtyn et al Olcese et. *Immunity*, 8, 693–701.
- Lanier, L. L., Le, A. M., Civin, C. I., Loken, M. R., & Phillips, J. H. (1986). The relationship of CD16 (Leu-11) and Leu-19 (NKH-1) antigen expression on human peripheral blood NK cells and cytotoxic T lymphocytes. *The Journal of Immunology*, 136(12), 4480–4486.  
<https://doi.org/10.4049/jimmunol.136.12.4480>
- Lanier, L. L., & Phillips, J. H. (1996). Inhibitory MHC class I receptors on NK cells and T cells. *Immunology Today*, 17(2), 86–91. [https://doi.org/10.1016/0167-5699\(96\)80585-8](https://doi.org/10.1016/0167-5699(96)80585-8)
- Lanier, L. L., Ruitenberg, J. J., & Phillips, J. H. (1988). Functional and biochemical analysis of CD16 antigen on natural killer cells and granulocytes. *The Journal of Immunology*, 141(10), 3478–3485. <https://doi.org/10.4049/jimmunol.141.10.3478>
- Larson, C., Oronsky, B., Carter, C. A., Oronsky, A., Knox, S. J., Sher, D., & Reid, T. R. (2020). TGF-beta: a master immune regulator. In *Expert Opinion on Therapeutic Targets* (Vol. 24, Issue 5, pp. 427–438). Taylor and Francis Ltd.  
<https://doi.org/10.1080/14728222.2020.1744568>
- Lazarevic, V., Chen, X., Shim, J. H., Hwang, E. S., Jang, E., Bolm, A. N., Oukka, M., Kuchroo, V. K., & Glimcher, L. H. (2011). T-bet represses TH 17 differentiation by preventing Runx1-mediated activation of the gene encoding ROR $\gamma$ t. *Nature Immunology*, 12(1), 96–104.  
<https://doi.org/10.1038/ni.1969>
- Lazetic, S., Chang, C., Houchins, J. P., Lanier, L. L., & Phillips, J. H. (1996). Human natural killer cell receptors involved in MHC class I recognition are disulfide-linked heterodimers of CD94 and NKG2 subunits. *The Journal of Immunology*, 157(11), 4741–4745. <https://doi.org/10.4049/jimmunol.157.11.4741>
- Leach, D. R., Krummel, M. F., & Allison, J. P. (1996). *Enhancement of Antitumor Immunity by CTLA-4 Blockade*. <https://www.science.org>
- LeBlanc, H. N., & Ashkenazi, A. (2003). Apo2L/TRAIL and its death and decoy receptors. In *Cell Death and Differentiation* (Vol. 10, Issue 1, pp. 66–75).  
<https://doi.org/10.1038/sj.cdd.4401187>

- Lee, N. I., Llano, M., Carretero, M., Ishitani, A., Navarro, F., Lo 'pezlo 'pez-Botet, M., & Geraghty, D. E. (1998). HLA-E is a major ligand for the natural killer inhibitory receptor CD94NKG2A. In *Immunology* (Vol. 95). www.pnas.org.
- Leong, W. J., Chase, J. M., Romee, R., Scheider, S. E., Sullivan, R. P., Cooper, M. A., & Fehniger, T. A. (2014). Preactivation with IL-12, IL-15, and IL-18 Induces CD25 and a Functional High-Affinity IL-2 Receptor on Human Cytokine-Induced Memory-like Natural Killer cells. *Biology of Blood and Marrow Transplantation*, 20(4), 463–473.
- Li, J., Whelan, S., Kotturi, M. F., Meyran, D., D'Souza, C., Hansen, K., Liang, S., Hunter, J., Trapani, J. A., & Neeson, P. J. (2021). PVRIG is a novel natural killer cell immune checkpoint receptor in acute myeloid leukemia. *Haematologica*, 106(12), 3115–3124. <https://doi.org/10.3324/haematol.2020.258574>
- Li, Y., Zhang, Y., Cao, G., Zheng, X., Sun, C., Wei, H., Tian, Z., Xiao, W., Sun, R., & Sun, H. (2021). Blockade of checkpoint receptor PVRIG unleashes anti-tumor immunity of NK cells in murine and human solid tumors. *Journal of Hematology and Oncology*, 14(1). <https://doi.org/10.1186/s13045-021-01112-3>
- Lim, S. A., Moon, Y., Shin, M. H., Kim, T. J., Chae, S., Yee, C., Hwang, D., Park, H., & Lee, K. M. (2021). Hypoxia-driven hif-1 $\alpha$  activation reprograms pre-activated nk cells towards highly potent effector phenotypes via erk/stat3 pathways. *Cancers*, 13(8). <https://doi.org/10.3390/cancers13081904>
- Litman, G. W., Cannon, J. P., & Dishaw, L. J. (2005). Reconstructing immune phylogeny: New perspectives. In *Nature Reviews Immunology* (Vol. 5, Issue 11, pp. 866–879). <https://doi.org/10.1038/nri1712>
- Ljunggren, H.-G., & Kärre, K. (1990). In search of the “missing self”: MHC molecules and NK cell recognition. *Immunology Today*, 11, 237–244. [https://doi.org/10.1016/0167-5699\(90\)90097-S](https://doi.org/10.1016/0167-5699(90)90097-S)
- Loboda, A., Jozkowicz, A., & Dulak, J. (2010). HIF-1 and HIF-2 transcription factors--similar but not identical. In *Molecules and cells* (Vol. 29, Issue 5, pp. 435–442). <https://doi.org/10.1007/s10059-010-0067-2>
- Lopes, N., Galluso, J., Escalière, B., Carpentier, S., Kerdiles, Y. M., & Vivier, E. (2022). Tissue-specific transcriptional profiles and heterogeneity of natural killer cells and group 1 innate lymphoid cells. *Cell Reports Medicine*, 3(11). <https://doi.org/10.1016/j.xcrm.2022.100812>
- Lucas, JR. (1979). Wilberforce and Huxley: a Legendary Encounter . *The Historical Journal*, 313–330.
- M. Braud, V., S. J. Allan, D., A. O'Callaghan, C., Söderström, K., D'Andrea, A., I. Bell, J., H. Phillips, J., Lanier, L. L., & McMichael, A. J. (1998). HLA-E binds to natural killer cell receptors CD94/NKG2A, B and C. *Nature*, 391, 795–799.

- Mack, M., Riethmuller, G., & Kufer, P. (1995). A small bispecific antibody construct expressed as a functional single-chain molecule with high tumor cell cytotoxicity. *Proceedings of the National Academy of Sciences*, 92, 7021–7025. <https://www.pnas.org>
- Mahon, P. C., Hirota, K., & Semenza, G. L. (2001). FIH-1: A novel protein that interacts with HIF-1 $\alpha$  and VHL to mediate repression of HIF-1 transcriptional activity. *Genes and Development*, 15(20), 2675–2686. <https://doi.org/10.1101/gad.924501>
- Masoud, G. N., & Li, W. (2015). HIF-1 $\alpha$  pathway: Role, regulation and intervention for cancer therapy. In *Acta Pharmaceutica Sinica B* (Vol. 5, Issue 5, pp. 378–389). Chinese Academy of Medical Sciences. <https://doi.org/10.1016/j.apsb.2015.05.007>
- Matsushita, M. (1996). The Lectin Pathway of the Complement System. *Microbiol. Immunol*, 40(12), 887–893.
- Mayer, M. M. (1973). The complement system. *Scientific American*, 229(5), 54–69. <https://doi.org/10.2307/24923243>
- McDermott, D. F., Huseni, M. A., Atkins, M. B., Motzer, R. J., Rini, B. I., Escudier, B., Fong, L., Joseph, R. W., Pal, S. K., Reeves, J. A., Sznol, M., Hainsworth, J., Rathmell, W. K., Stadler, W. M., Hutson, T., Gore, M. E., Ravaud, A., Bracarda, S., Suárez, C., ... Powles, T. (2018). Clinical activity and molecular correlates of response to atezolizumab alone or in combination with bevacizumab versus sunitinib in renal cell carcinoma. *Nature Medicine*, 24(6), 749–757. <https://doi.org/10.1038/s41591-018-0053-3>
- Mchedlidze, T., Waldner, M., Zopf, S., Walker, J., Rankin, A. L., Schuchmann, M., Voehringer, D., McKenzie, A. N. J., Neurath, M. F., Pflanz, S., & Wirtz, S. (2013). Interleukin-33-dependent innate lymphoid cells mediate hepatic fibrosis. *Immunity*, 39(2), 357–371. <https://doi.org/10.1016/j.immuni.2013.07.018>
- Michiko Kobayashi, B., Fitz, L., Ryan, M., Hewick, R. M., Clark, S. C., Chan, S., Loudon, R., Sherman, F., Bice Perussia, I., & Trinchier, G. (1989). Identification and purification of natural killer cell stimulatory factor (NKSF), a cytokine with multiple biologic effects on human. *Journal of Experimental Medicine*, 170, 827–845. <http://rupress.org/jem/article-pdf/170/3/827/1099552/827.pdf>
- Midha, A. D., Zhou, Y., Queliconi, B. B., Barrios, A. M., Haribowo, A. G., Chew, B. T. L., Fong, C. O. Y., Blecha, J. E., VanBrocklin, H., Seo, Y., & Jain, I. H. (2023). Organ-specific fuel rewiring in acute and chronic hypoxia redistributes glucose and fatty acid metabolism. *Cell Metabolism*, 35(3), 504–516.e5. <https://doi.org/10.1016/j.cmet.2023.02.007>
- Miller, J. F. A. P. (1962). Effect of Neonatal Thymectomy on the Immunological. *Proceedings of the Royal Society of London*, 156, 415–428.
- Miller, J. S., Zorko, N., Merino, A., Phung, G., Khaw, M., Howard, P., Hamsher, H., Davis, Z., Cichocki, F., Berk, G. I., & Felices, M. (2022). B7H3-targeted tri-specific killer engagers deliver IL-15 to NK cells but not T-cells, and specifically target solid tumors as a pan-tumor antigen strategy mediated through NK cells. *Annals of Oncology*, 33(S7), S889–S889. <https://doi.org/10.1016/j.annonc.2022.07.880>

- Miska, J., Lee-Chang, C., Rashidi, A., Muroski, M. E., Chang, A. L., Lopez-Rosas, A., Zhang, P., Panek, W. K., Cordero, A., Han, Y., Ahmed, A. U., Chandel, N. S., & Lesniak, M. S. (2019). HIF-1 $\alpha$  Is a Metabolic Switch between Glycolytic-Driven Migration and Oxidative Phosphorylation-Driven Immunosuppression of Tregs in Glioblastoma. *Cell Reports*, 27(1), 226-237.e4. <https://doi.org/10.1016/j.celrep.2019.03.029>
- Mojica, F. J. M., Díez-Villaseñor, C., García-Martínez, J., & Soria, E. (2005). Intervening sequences of regularly spaced prokaryotic repeats derive from foreign genetic elements. *Journal of Molecular Evolution*, 60(2), 174-182. <https://doi.org/10.1007/s00239-004-0046-3>
- Molina, M. A., Codony-Servat, J., Albanell, J., Rojo, F., Arribas, J., & Baselga, J. (2001). Trastuzumab (Herceptin), a humanized anti-HER2 receptor monoclonal antibody, inhibits basal and activated HER2 ectodomain cleavage in breast cancer cells. *Cancer Research*, 61, 4744-4749. <http://aacrjournals.org/cancerres/article-pdf/61/12/4744/2485678/4744.pdf>
- Moore, K., & Moore, M. (1979). Systemic and in-situ natural killer activity in tumour-bearing rats. *British Journal of Cancer*, 39, 636-347.
- Moo-Young, T. A., Larson, J. W., Belt, B. A., Tan, M. C., Hawkins, W. G., Eberlein, T. J., Goedegebuure, P. S., & Linehan, D. C. (2009). Tumor-derived TGF- $\beta$  mediates conversion of CD4+Foxp3+ regulatory T cells in a murine model of pancreas cancer. *Journal of Immunotherapy*, 32(1), 12-21. <https://doi.org/10.1097/CJI.0b013e318189f13c>
- Moriggl, R., Topham, D. J., Teglund, S., Sexl, V., McKay, C., Wang, D., Hoffmeyer, A., Van Deursen, J., Sangster, M. Y., Bunting, K. D., Grosveld, G. C., & Ihle, J. N. (1999). Stat5 Is Required for IL-2-Induced Cell Cycle Progression of Peripheral T Cells. *Immunity*, 10, 249-259.
- Mosmann, T. R., Cherwinski, H., Bond, M. W., Giedlin, M. A., & Coffman, R. L. (1986). Two types of murine helper T cell clone. I. Definition according to profiles of lymphokine activities and secreted proteins. *The Journal of Immunology*, 136(7), 2348-2357. <https://doi.org/10.4049/jimmunol.136.7.2348>
- Murphy, K. M., & Reiner, S. L. (2002). The lineage decisions of helper T cells. In *Nature Reviews Immunology* (Vol. 2, Issue 12, pp. 933-944). <https://doi.org/10.1038/nri954>
- Myer, P. A., Lee, J. K., Madison, R. W., Pradhan, K., Newberg, J. Y., Isasi, C. R., Klempner, S. J., Frampton, G. M., Ross, J. S., Venstrom, J. M., Schrock, A. B., Das, S., Augenlicht, L., Verma, A., Grealley, J. M., Raj, S. M., Goel, S., & Ali, S. M. (2022). The Genomics of Colorectal Cancer in Populations with African and European Ancestry. *Cancer Discovery*, OF1-OF17. <https://doi.org/10.1158/2159-8290.CD-21-0813/3110692/cd-21-0813.pdf>
- Nausch, N., & Cerwenka, A. (2008). NKG2D ligands in tumor immunity. In *Oncogene* (Vol. 27, Issue 45, pp. 5944-5958). <https://doi.org/10.1038/onc.2008.272>
- Nersesian, S., Schwartz, S. L., Grantham, S. R., MacLean, L. K., Lee, S. N., Pugh-Toole, M., & Boudreau, J. E. (2021). NK cell infiltration is associated with improved overall survival in

- solid cancers: A systematic review and meta-analysis. *Translational Oncology*, 14(1).  
<https://doi.org/10.1016/j.tranon.2020.100930>
- Nesargikar, P., Spiller, B., & Chavez, R. (2012). The complement system: History, pathways, cascade and inhibitors. *European Journal of Microbiology and Immunology*, 2(2), 103–111.  
<https://doi.org/10.1556/eujmi.2.2012.2.2>
- Ni, J., Wang, X., Stojanovic, A., Zhang, Q., Wincher, M., Bühler, L., Arnold, A., Correia, M. P., Winkler, M., Koch, P. S., Sexl, V., Höfer, T., & Cerwenka, A. (2020). Single-Cell RNA Sequencing of Tumor-Infiltrating NK Cells Reveals that Inhibition of Transcription Factor HIF-1 $\alpha$  Unleashes NK Cell Activity. *Immunity*, 52(6), 1075-1087.e8.  
<https://doi.org/10.1016/j.immuni.2020.05.001>
- Nowakowska, P., Romanski, A., Miller, N., Odendahl, M., Bonig, H., Zhang, C., Seifried, E., Wels, W. S., & Tonn, T. (2018). Clinical grade manufacturing of genetically modified, CAR-expressing NK-92 cells for the treatment of ErbB2-positive malignancies. *Cancer Immunology, Immunotherapy*, 67(1), 25–38. <https://doi.org/10.1007/s00262-017-2055-2>
- Nürnberg, T., Brunner, F., Kemmerling, B., & Piater, L. (2004). Innate immunity in plants and animals: striking similarities and obvious differences. *Immunological Reviews*, 198, 249–266.
- Oberoi, P., Kamenjarin, K., Ossa, J. F. V., Uherek, B., Bönig, H., & Wels, W. S. (2020). Directed Differentiation of Mobilized Hematopoietic Stem and Progenitor Cells into Functional NK cells with Enhanced Antitumor Activity. *Cells*, 9(4).  
<https://doi.org/10.3390/cells9040811>
- Oelsner, S., Waldmann, A., Billmeier, A., Röder, J., Lindner, A., Ullrich, E., Marschalek, R., Dotti, G., Jung, G., Große-Hovest, L., Oberoi, P., Bader, P., & Wels, W. S. (2019). Genetically engineered CAR NK cells display selective cytotoxicity against FLT3-positive B-ALL and inhibit in vivo leukemia growth. *International Journal of Cancer*, 145(7), 1935–1945. <https://doi.org/10.1002/ijc.32269>
- Ogasawara, K., Hida, S., Azimi, N., Tagaya, Y., Sato, T., Yokochi-Fukuda, T., Waldmann, T. A., Taniguchi, T., & Taki, S. (1998). Requirement for IRF-1 in the microenvironment supporting development of natural killer cells. *Nature*, 391, 700–703.  
<https://www.nature.com/articles/35636>
- Okamura, H., Tsutsui, H., Kashiwamura, S.-I., Yoshimoto, T., & Nakanishi, K. (1998). *Interleukin-18: A Novel Cytokine That Augments Both Innate and Acquired Immunity* (pp. 281–312). [https://doi.org/10.1016/S0065-2776\(08\)60389-2](https://doi.org/10.1016/S0065-2776(08)60389-2)
- Okkelman, I. A., Foley, T., Papkovsky, D. B., & Dmitriev, R. I. (2017). Live cell imaging of mouse intestinal organoids reveals heterogeneity in their oxygenation. *Biomaterials*, 146, 86–96. <https://doi.org/10.1016/j.biomaterials.2017.08.043>
- Ooft, S. N., Weeber, F., Dijkstra, K. K., Mclean, C. M., Kaing, S., Van Werkhoven, E., Schipper, L., Hoes, L., Vis, D. J., Van De Haar, J., Prevoo, W., Snaebjornsson, P., Van Der Velden, D., Klein, M., Chalabi, M., Boot, H., Van Leerdam, M., Bloemendal, H. J., Beerepoot, L. V.,

- ... Voest, E. E. (2019). Patient-derived organoids can predict response to chemotherapy in metastatic colorectal cancer patients. In *Sci. Transl. Med* (Vol. 11).  
<https://www.science.org>
- Orange, J. S., & Biron, C. A. (1996). Characterization of Early IL-12, IFN-alpha beta, and TNF Effects on Antiviral State and NK Cell Responses During Murine Cytomegalovirus Infection. *The Journal of Immunology*, 156(12), 4746–4756.  
<https://doi.org/10.4049/jimmunol.156.12.4746>
- Orange, J. S., Wang, B., Cox Terhorst, ~, & Biron, C. A. (1995). Requirement For Natural Killer Cell-produced Interferon gama in Defense against Murine Cytomegalovirus Infection and Enhancement of This Defense Pathway by Interleukin 12 Administration. *Journal of Experimental Medicine*, 182, 1045–1056. <http://rupress.org/jem/article-pdf/182/4/1045/1107145/1045.pdf>
- Paget, S. (1889). The distribution of secondary growths in cancer of the breast. *The Lancet*, 133, 571–573.
- Palazon, A., Tyrakis, P. A., Macias, D., Veliça, P., Rundqvist, H., Fitzpatrick, S., Vojnovic, N., Phan, A. T., Loman, N., Hedenfalk, I., Hatschek, T., Lövrot, J., Foukakis, T., Goldrath, A. W., Bergh, J., & Johnson, R. S. (2017). An HIF-1 $\alpha$ /VEGF-A Axis in Cytotoxic T Cells Regulates Tumor Progression. *Cancer Cell*, 32(5), 669–683.e5.  
<https://doi.org/10.1016/j.ccell.2017.10.003>
- Papavramidou, N., Papavramidis, T., & Demetriou, T. (2010). Ancient greek and greco-Roman methods in modern surgical treatment of cancer. In *Annals of Surgical Oncology* (Vol. 17, Issue 3, pp. 665–667). <https://doi.org/10.1245/s10434-009-0886-6>
- Parkin, D. M., & Parkin, M. (2001). Global cancer statistics in the year 2000. In *THE LANCET Oncology*. <http://www.dep.iarc.fr/dataava/globocan/who.htm>
- Parodi, M., Raggi, F., Cangelosi, D., Manzini, C., Balsamo, M., Blengio, F., Eva, A., Varesio, L., Pietra, G., Moretta, L., Mingari, M. C., Vitale, M., & Bosco, M. C. (2018). Hypoxia modifies the transcriptome of human NK cells, modulates their immunoregulatory profile, and influences NK cell subset migration. *Frontiers in Immunology*, 9(OCT).  
<https://doi.org/10.3389/fimmu.2018.02358>
- Pedersen, L., Idorn, M., Olofsson, G. H., Lauenborg, B., Nookaew, I., Hansen, R. H., Johannesen, H. H., Becker, J. C., Pedersen, K. S., Dethlefsen, C., Nielsen, J., Gehl, J., Pedersen, B. K., Thor Straten, P., & Hojman, P. (2016). Voluntary running suppresses tumor growth through epinephrine- and IL-6-dependent NK cell mobilization and redistribution. *Cell Metabolism*, 23(3), 554–562. <https://doi.org/10.1016/j.cmet.2016.01.011>
- Pelletier, A., Nelius, E., Fan, Z., Khatchatourova, E., Alvarado-Diaz, A., He, J., Krzywinska, E., Sobocki, M., Nagarajan, S., Kerdiles, Y., Fandrey, J., Gotthardt, D., Sexl, V., de Bock, K., & Stockmann, C. (2023). Resting natural killer cell homeostasis relies on tryptophan/ NAD + metabolism and HIF -1 $\alpha$  . *EMBO Reports*, 24(6).  
<https://doi.org/10.15252/embr.202256156>

- Pende, D., Parolini, S., Pessino, A., Sivori, S., Augugliaro, R., Morelli, L., Marcenaro, E., Accame, L., Malaspina, A., Biassoni, R., Bottino, C., Moretta, L., & Moretta, A. (1999). Identification and Molecular Characterization of NKP30, a Novel Triggering Receptor Involved in Natural Cytotoxicity Mediated by Human Natural Killer Cells. In *J. Exp. Med* (Vol. 190, Issue 10). <http://www.jem.org>
- Perez, P., Hoffman, R. W., Shaw, S., Bluestone, J. A., & Segal, D. M. (1985). Specific targeting of cytotoxic T cells by anti-T3 linked to anti-target cell antibody. *Nature*, 316, 354–356.
- Perussia, B., Trinchieri, G., Jackson, A., Warner, N. L., Faust, J., Rumpold, H., Kraft, D., & Lanier, L. L. (1984). The Fc receptor for IgG on human natural killer cells: phenotypic, functional, and comparative studies with monoclonal antibodies. *The Journal of Immunology*, 133(1), 180–189. <https://doi.org/10.4049/jimmunol.133.1.180>
- Pessino, A., Sivori, S., Bottino, C., Malaspina, A., Morelli, L., Moretta, L., Biassoni, R., & Moretta, A. (1998). Molecular Cloning of NKP46: A Novel Member of the Immunoglobulin Superfamily Involved in Triggering of Natural Cytotoxicity. In *J. Exp. Med* (Vol. 188, Issue 5). <http://www.jem.org>
- Poznanski, S. M., & Ashkar, A. A. (2019). What defines NK cell functional fate: Phenotype or metabolism? In *Frontiers in Immunology* (Vol. 10, Issue JUN). Frontiers Media S.A. <https://doi.org/10.3389/fimmu.2019.01414>
- Raj, D., Yang, M. H., Rodgers, D., Hampton, E. N., Begum, J., Mustafa, A., Lorizio, D., Garces, I., Propper, D., Kench, J. G., Kocher, H. M., Young, T. S., Aicher, A., & Heeschen, C. (2019). Switchable CAR-T cells mediate remission in metastatic pancreatic ductal adenocarcinoma. *Gut*, 68(6), 1052–1064. <https://doi.org/10.1136/gutjnl-2018-316595>
- Ramos-Vega, M., Kjellman, P., Todorov, M. I., Kylkilahti, T. M., Bäckström, B. T., Ertürk, A., Madsen, C. D., & Lundgaard, I. (2022). Mapping of neuroinflammation-induced hypoxia in the spinal cord using optoacoustic imaging. *Acta Neuropathologica Communications*, 10(1). <https://doi.org/10.1186/s40478-022-01337-4>
- Ran, M., Klein, G., & Witz, I. P. (1976). Tumor-bound immunoglobulins. Evidence for the in vivo coating of tumor cells by potentially cytotoxic anti-tumor antibodies. *International Journal of Cancer*, 17, 90–97.
- Ran, M., & Witz, I. P. (1972). Tumor-associated immunoglobulins. enhancement of syngeneic tumors by igg2-containing tumor eluates. *International Journal of Cancer*, 9(1), 242–247. <https://doi.org/10.1002/ijc.2910090126>
- Raskov, H., Orhan, A., Christensen, J. P., & Gögenur, I. (2021). Cytotoxic CD8+ T cells in cancer and cancer immunotherapy. In *British Journal of Cancer* (Vol. 124, Issue 2, pp. 359–367). Springer Nature. <https://doi.org/10.1038/s41416-020-01048-4>
- Rataj, F., Jacobi, S. J., Stoiber, S., Asang, F., Ogonek, J., Tokarew, N., Cadilha, B. L., van Puijenbroek, E., Heise, C., Duester, P., Endres, S., Klein, C., & Kobold, S. (2019). High-affinity CD16-polymorphism and Fc-engineered antibodies enable activity of CD16-

- chimeric antigen receptor-modified T cells for cancer therapy. *British Journal of Cancer*, 120(1), 79–87. <https://doi.org/10.1038/s41416-018-0341-1>
- Ratcliffe, P. J. (2007). HIF-1 and HIF-2: Working alone or together in hypoxia? In *Journal of Clinical Investigation* (Vol. 117, Issue 4, pp. 862–865). <https://doi.org/10.1172/JCI31750>
- Rebouissou, S., Amessou, M., Couchy, G., Poussin, K., Imbeaud, S., Pilati, C., Izard, T., Balabaud, C., Bioulac-Sage, P., & Zucman-Rossi, J. (2009). Frequent in-frame somatic deletions activate gp130 in inflammatory hepatocellular tumours. *Nature*, 457(7226), 200–204. <https://doi.org/10.1038/nature07475>
- Reiner, S. L. (2007). Development in Motion: Helper T Cells at Work. In *Cell* (Vol. 129, Issue 1, pp. 33–36). Elsevier B.V. <https://doi.org/10.1016/j.cell.2007.03.019>
- Roberts, G. W., & Palade, G. E. (1997). Neovasculature Induced by Vascular Endothelial Growth Factor Is Fenestrated. *Cancer Research*, 57, 765–772.
- Roelands, J., Kuppen, P. J. K., Ahmed, E. I., Mall, R., Masoodi, T., Singh, P., Monaco, G., Raynaud, C., de Miranda, N. F. C. C., Ferraro, L., Carneiro-Lobo, T. C., Syed, N., Rawat, A., Awad, A., Decock, J., Mifsud, W., Miller, L. D., Sherif, S., Mohamed, M. G., ... Bedognetti, D. (2023). An integrated tumor, immune and microbiome atlas of colon cancer. *Nature Medicine*, 29(5), 1273–1286. <https://doi.org/10.1038/s41591-023-02324-5>
- Romee, R., Foley, B., Lenvik, T., Wang, Y., Zhang, B., Ankarlo, D., Luo, X., Cooley, S., Verneris, M., Walcheck, B., & Miller, J. (2013). NK cell CD16 surface expression and function is regulated by a disintegrin and metalloprotease-17 (ADAM17). *Blood*, 121(18), 3599–3608. <https://doi.org/10.1182/blood-2012-04>
- Romee, R., Rosario, M., Berrien-Elliott, M. M., Wagner, J. A., Jewell, B. A., Schappe, T., Leong, J. W., Abdel-Latif, S., Schneider, S. E., Willey, S., Neal, C. C., Yu, L., Oh, S. T., Lee, Y.-S., Mulder, A., Claas, F., Cooper, M. A., & Fehniger, T. A. (2016). Cytokine-induced memory-like natural killer cells exhibit enhanced responses against myeloid leukemia. *Science Translational Medicine*, 8(357), 1–12. <https://www.science.org>
- Sakaguchi, S., Sakaguchi, N., Asano, M., Itoh, M., & Toda, M. (1995). *Immunologic Self-Tolerance Maintained by Activated T Cells Expressing 11-2 Receptor  $\alpha$ -Chains (CD25) Breakdown of a Single Mechanism of Self-Tolerance Causes Various Autoimmune Diseases*. <http://journals.aai.org/jimmunol/article-pdf/155/3/1151/1070324/1151.pdf>
- Sakano, H., Maki, R., Kurosawa, Y., Roeder, W., & Tonegawa, S. (1980). Two types of somatic recombination are necessary for the generation of complete immunoglobulin heavy-chain genes Identification of J DNA for MOPC<sub>141</sub>. In *Nature* (Vol. 286).
- Santana Carrero, R. M., Beceren-Braun, F., Rivas, S. C., Hegde, S. M., Gangadharan, A., Plote, D., Pham, G., Anthony, S. M., & Schluns, K. S. (2019). IL-15 is a component of the inflammatory milieu in the tumor microenvironment promoting antitumor responses. *Proceedings of the National Academy of Sciences of the United States of America*, 116(2), 599–608. <https://doi.org/10.1073/pnas.1814642116>

- Sarma, J. V., & Ward, P. A. (2011). The complement system. In *Cell and Tissue Research* (Vol. 343, Issue 1, pp. 227–235). <https://doi.org/10.1007/s00441-010-1034-0>
- Sarria, G. J., Saria, G. R., & Pinillos, L. V. (2018). The Inca Trail to the Present: The Development of Radiation Therapy in Peru. In *International Journal of Radiation Oncology Biology Physics* (Vol. 101, Issue 2, pp. 244–249). Elsevier Inc. <https://doi.org/10.1016/j.ijrobp.2018.01.115>
- Sato, T., Stange, D. E., Ferrante, M., Vries, R. G. J., Van Es, J. H., Van Den Brink, S., Van Houdt, W. J., Pronk, A., Van Gorp, J., Siersema, P. D., & Clevers, H. (2011). Long-term expansion of epithelial organoids from human colon, adenoma, adenocarcinoma, and Barrett's epithelium. *Gastroenterology*, 141(5), 1762–1772. <https://doi.org/10.1053/j.gastro.2011.07.050>
- Schlereth, B., Fichtner, I., Lorenczewski, G., Kleindienst, P., Brischwein, K., Da Silva, A., Kufer, P., Lutterbuese, R., Junghahn, I., Kasimir-Bauer, S., Wimberger, P., Kimmig, R., & Baeuerle, P. A. (2005). Eradication of Tumors from a Human Colon Cancer Cell Line and from Ovarian Cancer Metastases in Immunodeficient Mice by a Single-Chain Ep-CAM-/CD3-Bispecific Antibody Construct. *Cancer Research*, 65, 2882–2889. [www.aacrjournals.org](http://www.aacrjournals.org)
- Schmidt, C. A., Fisher-Wellman, K. H., & Darrell Neuffer, P. (2021). From OCR and ECAR to energy: Perspectives on the design and interpretation of bioenergetics studies. In *Journal of Biological Chemistry* (Vol. 297, Issue 4). American Society for Biochemistry and Molecular Biology Inc. <https://doi.org/10.1016/j.jbc.2021.10.1140>
- Semenza, G. L. (2000). *HIF-1: mediator of physiological and pathophysiological responses to hypoxia*. <http://www.jap.org>
- Shibuya, A., Campbell, D., Hannum, C., Yssel, H., Franz-Bacon, K., Mcclanahan, T., Kitamura, T., Nicholl, J., Sutherland, G. R., Lanier, L. L., & Phillips, J. H. (1996). DNAM-1, A Novel Adhesion Molecule Involved in the Cytolytic Function of T Lymphocytes. In *Immunity* (Vol. 4).
- Shiku, H., Kisielow, P., Bean, M. A., Takahashi, T., Boyse, E. A., Oettgen, H. F., & Old, L. J. (1975). Expression of T-cell differentiation antigens on effector cells in cell-mediated cytotoxicity in vitro. *The Journal of Experimental Medicine*, 141, 227–241. <http://rupress.org/jem/article-pdf/141/1/227/1656736/227.pdf>
- Siegler, J. J., Correia, M. P., Hofman, T., Prager, I., Birgin, E., Rahbari, N. N., Watzl, C., Stojanovic, A., & Cerwenka, A. (2022). Human ILC3 Exert TRAIL-Mediated Cytotoxicity Towards Cancer Cells. *Frontiers in Immunology*, 13. <https://doi.org/10.3389/fimmu.2022.742571>
- Sivori, S., Pende, D., Bottino, C., Marcenaro, E., Pessino, A., Biassoni, R., Moretta, L., & Moretta, A. (1999). Nkp46 is the major triggering receptor involved in the natural cytotoxicity of fresh or cultured human NK cells. Correlation between surface density of Nkp46 and natural cytotoxicity against autologous, allogeneic or xenogeneic target cells.

- European Journal of Immunology*, 29(5), 1656–1666. [https://doi.org/10.1002/\(SICI\)1521-4141\(199905\)29:05<1656::AID-IMMU1656>3.0.CO;2-1](https://doi.org/10.1002/(SICI)1521-4141(199905)29:05<1656::AID-IMMU1656>3.0.CO;2-1)
- Slamon, D. J., Clark, G. M., Wong, S. G., Levin, W. J., Ullrich, A., & Mcguire, W. L. (1987). Human Breast Cancer: Correlation of Relapse and Survival with Amplification of the HER-2neu Oncogene. *Science*, 177–182. <https://www.science.org>
- Sobecki, M., Krzywinska, E., Nagarajan, S., Audigé, A., Huynh, K., Zacharjasz, J., Debbache, J., Kerdiles, Y., Gotthardt, D., Takeda, N., Fandrey, J., Sommer, L., Sexl, V., & Stockmann, C. (2021). NK cells in hypoxic skin mediate a trade-off between wound healing and antibacterial defence. *Nature Communications*, 12(1). <https://doi.org/10.1038/s41467-021-25065-w>
- Spits, H., Artis, D., Colonna, M., Diefenbach, A., Di Santo, J. P., Eberl, G., Koyasu, S., Locksley, R. M., McKenzie, A. N. J., Mebius, R. E., Powrie, F., & Vivier, E. (2013). Innate lymphoid cells—a proposal for uniform nomenclature. *Nature Reviews Immunology*, 13(2), 145–149. <https://doi.org/10.1038/nri3365>
- Staerz, U. D., Kanagawa, O., & Bevan, M. J. (1985). Hybrid antibodies can target sites for attack by T cells. *Nature*, 314, 628–631.
- Stanietsky, N., Simic, H., Arapovic, J., Toporik, A., Levy, O., Novik, A., Levine, Z., Beiman, M., Dassa, L., Achdout, H., Stern-Ginossar, N., Tsukerman, P., Jonjic, S., & Mandelboim, O. (2009). *The interaction of TIGIT with PVR and PVRL2 inhibits human NK cell cytotoxicity* (Vol. 106).
- Stasi, A. Di, Tey, S.-K., Dotti, G., Fujita, Y., Kennedy-Nasser, A., Martinez, C., Straathof, K., Liu, E., Durett, A. G., Grilley, B., Liu, H., Cruz, C. R., Savoldo, B., Gee, A. P., Schindler, J., Krance, R. A., Heslop, H. E., Spencer, D. M., Rooney, C. M., & Brenner, M. K. (2011). Inducible Apoptosis as a Safety Switch for Adoptive Cell Therapy. *N Engl J Med*, 365, 1673–1683.
- Stebbins, C. E., Kaelin, W. G., & Pavletich, N. P. (1999). Structure of the VHL-ElonginC-ElonginB Complex: Implications for VHL Tumor Suppressor Function. *Science*, 284, 455–461. <https://www.science.org>
- Sterner, R. C., & Sterner, R. M. (2021). CAR-T cell therapy: current limitations and potential strategies. In *Blood Cancer Journal* (Vol. 11, Issue 4). Springer Nature. <https://doi.org/10.1038/s41408-021-00459-7>
- Storkus, W. J., Alexander, J., Payne, J. A., Dawson, J. R., Cresswell, P., Ways, J., & Parham, P. (1989). Reversal of natural killing susceptibility in target cells expressing transfected class I HLA genes (natural killing/target structure/class I antigens). *PNAS*, 86, 2361–2364. <https://www.pnas.org>
- Sullivan, K. M., Jiang, X., Guha, P., Lausted, C., Carter, J. A., Hsu, C., Labadie, K. P., Kohli, K., Kenerson, H. L., Daniel, S. K., Yan, X., Meng, C., Abbasi, A., Chan, M., Seo, Y. D., Park, J. O., Crispe, I. N., Yeung, R. S., Kim, T. S., ... Pillarisetty, V. G. (2023). Blockade of

- interleukin 10 potentiates antitumour immune function in human colorectal cancer liver metastases. *Gut*, 72(2), 325–337. <https://doi.org/10.1136/gutjnl-2021-325808>
- Sutherland, J. A., Turner, R. A., Mannoni, P. M., Locksley E., & Turc, J.-M. (1986). Differentiation of K562 Leukemia Cells Along Erythroid, Macrophage, and Megakaryocyte Lineages. *Journal of Biological Response Modifiers*, 250–262.
- Swain, S. M., Baselga, J., Kim, S.-B., Ro, J., Semiglazov, V., Campone, M., Ciruelos, E., Ferrero, J.-M., Schneeweiss, A., Heeson, S., Clark, E., Ross, G., Benyunes, M. C., & Cortés, J. (2015). Pertuzumab, Trastuzumab, and Docetaxel in HER2-Positive Metastatic Breast Cancer. *New England Journal of Medicine*, 372(8), 724–734. <https://doi.org/10.1056/nejmoa1413513>
- Tak, E., Jung, D. H., Kim, S. H., Park, G. C., Jun, D. Y., Lee, J., Jung, B. hyun, Kirchner, V. A., Hwang, S., Song, G. W., & Lee, S. G. (2017). Protective role of hypoxia-inducible factor-1 $\alpha$ -dependent CD39 and CD73 in fulminant acute liver failure. *Toxicology and Applied Pharmacology*, 314, 72–81. <https://doi.org/10.1016/j.taap.2016.11.016>
- Tang, D., Kang, R., Coyne, C. B., Zeh, H. J., & Lotze, M. T. (2012). PAMPs and DAMPs: signal os that spur autophagy and immunity.
- Terrén, I., Orrantia, A., Vitallé, J., Zenarruzabeitia, O., & Borrego, F. (2019). NK cell metabolism and tumor microenvironment. In *Frontiers in Immunology* (Vol. 10, Issue SEP). Frontiers Media S.A. <https://doi.org/10.3389/fimmu.2019.02278>
- Thomas, D. A., & Massagué, J. (2005). TGF- $\beta$  directly targets cytotoxic T cell functions during tumor evasion of immune surveillance. *Cancer Cell*, 8(5), 369–380. <https://doi.org/10.1016/j.ccr.2005.10.012>
- Tiselius, A. B., & Kabat, E. A. (1938). An electrophoretic study of immune sera and purified antibody preparations. *Journal of Experimental Medicine*, 69, 119–139.
- Turner, J. R. (2009). Intestinal mucosal barrier function in health and disease. In *Nature Reviews Immunology* (Vol. 9, Issue 11, pp. 799–809). <https://doi.org/10.1038/nri2653>
- Tuveson, D., & Clevers, H. (2019). Cancer modeling meets human organoid technology. *Science*, 364, 952–955. <https://ocg.cancer.gov/programs/HCFI>
- Uppendahl, L. D., Felices, M., Bendzick, L., Ryan, C., Kodal, B., Hinderlie, P., Boylan, K. L. M., Skubitz, A. P. N., Miller, J. S., & Geller, M. A. (2019). Cytokine-induced memory-like natural killer cells have enhanced function, proliferation, and in vivo expansion against ovarian cancer cells. *Gynecologic Oncology*, 153(1), 149–157. <https://doi.org/10.1016/j.ygyno.2019.01.006>
- Urteaga B., O., & Pack, G. T. (1966). On the antiquity of melanoma. *Cancer*, 19(5), 607–610. [https://doi.org/10.1002/1097-0142\(196605\)19:5<607::AID-CNCR2820190502>3.0.CO;2-8](https://doi.org/10.1002/1097-0142(196605)19:5<607::AID-CNCR2820190502>3.0.CO;2-8)
- Veliça, P., Cunha, P. P., Vojnovic, N., Foskolou, I. P., Bargiela, D., Gojkovic, M., Rundqvist, H., & Johnson, R. S. (2021). Modified hypoxia-inducible factor expression in CD8 $\beta$  T cells increases antitumor efficacy. *Cancer Immunology Research*, 9(4), 401–414. <https://doi.org/10.1158/2326-6066.CIR-20-0561>

- Victorino, F., Bigley, T. M., Park, E., Yao, C.-H., Benoit, J., Yang, L.-P., Piersma, S. J., Lauron, E. J., Davidson, R. M., Patti, G. J., & Yokoyama, W. M. (2021). HIF1 $\alpha$  is required for NK cell metabolic adaptation during virus infection. *ELife*, 1–20. <https://doi.org/10.7554/eLife>
- Vijayan, D., Young, A., Teng, M. W. L., & Smyth, M. J. (2017). Targeting immunosuppressive adenosine in cancer. In *Nature Reviews Cancer* (Vol. 17, Issue 12, pp. 709–724). Nature Publishing Group. <https://doi.org/10.1038/nrc.2017.86>
- Vitale, M., Falco, M., Castriconi, R., Parolini, S., Zambello, R., Semenzato, G., Biassoni, R., Bottino, C., Moretta, L., & Moretta, A. (2001). Identification of NKp80, a novel triggering molecule expressed by human NK cells. *European Journal of Immunology*, 31(1), 233–242. [https://doi.org/10.1002/1521-4141\(200101\)31:1<233::AID-IMMU233>3.0.CO;2-4](https://doi.org/10.1002/1521-4141(200101)31:1<233::AID-IMMU233>3.0.CO;2-4)
- Vivier, E., Artis, D., Colonna, M., Diefenbach, A., Di Santo, J. P., Eberl, G., Koyasu, S., Locksley, R. M., McKenzie, A. N. J., Mebius, R. E., Powrie, F., & Spits, H. (2018). Innate Lymphoid Cells: 10 Years On. In *Cell* (Vol. 174, Issue 5, pp. 1054–1066). Cell Press. <https://doi.org/10.1016/j.cell.2018.07.017>
- Vose, B. M., Vánky, F., Argov, S., & Klein, E. (1977). Natural cytotoxicity in man: activity of lymph node and tumor-infiltrating lymphocytes. *European Journal of Immunology*, 7(11), 753–757. <https://doi.org/10.1002/eji.1830071102>
- Wagtmann, N., Biassoni, R., Cantoni, C., Verdiani, S., Malnati, M. S., Vitale, M., Bottino, C., Moretta, L., Moretta, A., & Long, E. O. (1995). Molecular clones of the p58 NK cell receptor reveal immunoglobulin-related molecules with diversity in both the extra- and intracellular domains. *Immunity*, 2(5), 439–449. [https://doi.org/10.1016/1074-7613\(95\)90025-X](https://doi.org/10.1016/1074-7613(95)90025-X)
- Wagtmann, N., Rajagopalan, S., Winter, C. C., Peruui, M., & Long, E. O. (1995). Killer cell inhibitory receptors specific for HLA-C and HLA-B identified by direct binding and by functional transfer. *Immunity*, 3(6), 801–809. [https://doi.org/10.1016/1074-7613\(95\)90069-1](https://doi.org/10.1016/1074-7613(95)90069-1)
- Wang, G. L., & Semenzas, G. L. (1993). Characterization of Hypoxia-inducible Factor 1 and Regulation of DNA Binding Activity by Hypoxia. In *THE JOURNAL OF BIOLOGICAL CHEMISTRY* (Vol. 268, Issue 29).
- Wang, P. L., O'Farrell, S., Clayberger, C., & Krensky, A. M. (1992). Identification and molecular cloning of tactile. A novel human T cell activation antigen that is a member of the Ig gene superfamily. *The Journal of Immunology*, 148(8), 2600–2608. <https://doi.org/10.4049/jimmunol.148.8.2600>
- Weber, J. S., Del Vecchio, M., Mandala, M., Gogas, H., Arance, A. M., Dalle, S., Cowey, C. L., Schenker, M., Grob, J. J., Chiarion-Sileni, V., Marquez-Rodas, I., Butler, M. O., Maio, M., Middleton, M. R., Tang, T., Saci, A., De Pril, V., Lobo, M., Larkin, J. M. G., & Ascierto, P. A. (2019). Adjuvant nivolumab (NIVO) versus ipilimumab (IPI) in resected stage III/IV melanoma: 3-year efficacy and biomarker results from the phase III CheckMate 238 trial. *Annals of Oncology*, 30, v533–v534. <https://doi.org/10.1093/annonc/mdz255>

- Weeber, F., Van De Wetering, M., Hoogstraat, M., Dijkstra, K. K., Krijgsman, O., Kuilman, T., Gadellaa-Van Hooijdonk, C. G. M., Van Der Velden, D. L., Peeper, D. S., Cuppen, E. P. J. G., Vries, R. G., Clevers, H., & Voest, E. E. (2015). Preserved genetic diversity in organoids cultured from biopsies of human colorectal cancer metastases. *Proceedings of the National Academy of Sciences of the United States of America*, *112*(43), 13308–13311. <https://doi.org/10.1073/pnas.1516689112>
- Wetsel, R. A. (1995). Expression of the complement C5a anaphylatoxin receptor (C5aR) on non-myeloid cells. In *immunology Letters* (Vol. 44).
- Wheelock, E. F. (1965). Interferon-like virus-inhibitor induced in Human Leukocytes by Phytohemagglutinin. *Science*, *149*, 310–311.
- Wiernik, A., Foley, B., Zhang, B., Verneris, M. R., Warlick, E., Gleason, M. K., Ross, J. A., Luo, X., Weisdorf, D. J., Walcheck, B., Vallera, D. A., & Miller, J. S. (2013). Targeting natural killer cells to acute myeloid leukemia in vitro with a CD16×33 bispecific killer cell engager and ADAM17 inhibition. *Clinical Cancer Research*, *19*(14), 3844–3855. <https://doi.org/10.1158/1078-0432.CCR-13-0505>
- Witz, I. P. (2009). The tumor microenvironment: The making of a paradigm. *Cancer Microenvironment*, *2*(SUPPL. 1). <https://doi.org/10.1007/s12307-009-0025-8>
- Wolf, S. F., Temple, P. A., Kobayashi, M., Young, D., Dicig, M., Lowe, L., Dzialo, R., Fitz, L., Ferenz, C., & Hewick, R. M. (1991). Cloning of cDNA for natural killer cell stimulatory factor, a heterodimeric cytokine with multiple biologic effects on T and natural killer cells. *The Journal of Immunology*, *146*(9), 3074–3081. <https://doi.org/10.4049/jimmunol.146.9.3074>
- Wu, J., Song, Y., Bakker, A. B. H., Bauer, S., Spies, T., Lanier, L. L., & Phillips, J. H. (1999). An activating immunoreceptor complex formed by NKG2D and DAP10. *Science*, 730–732. [www.sciencemag.org/feature/](http://www.sciencemag.org/feature/)
- Xi, Y., & Xu, P. (2021). Global colorectal cancer burden in 2020 and projections to 2040. In *Translational Oncology* (Vol. 14, Issue 10). Neoplasia Press, Inc. <https://doi.org/10.1016/j.tranon.2021.101174>
- Yeh, E. T. H. (2009). SUMOylation and De-SUMOylation: Wrestling with life's processes. In *Journal of Biological Chemistry* (Vol. 284, Issue 13, pp. 8223–8227). <https://doi.org/10.1074/jbc.R800050200>
- Ying, Z., He, T., Wang, X., Zheng, W., Lin, N., Tu, M., Xie, Y., Ping, L., Zhang, C., Liu, W., Deng, L., Qi, F., Ding, Y., Lu, X. an, Song, Y., & Zhu, J. (2019). Parallel Comparison of 4-1BB or CD28 Co-stimulated CD19-Targeted CAR-T Cells for B Cell Non-Hodgkin's Lymphoma. *Molecular Therapy - Oncolytics*, *15*, 60–68. <https://doi.org/10.1016/j.omto.2019.08.002>
- Young, H. A., & Hardy, K. J. (1995). Role of interferon-γ in immune cell regulation. In *Journal of Leukocyte Biology* (Vol. 58, Issue 4, pp. 373–381). Federation of American Societies for Experimental Biology. <https://doi.org/10.1002/jlb.58.4.373>

- Yu, X., Harden, K., Gonzalez, L. C., Francesco, M., Chiang, E., Irving, B., Tom, I., Ivelja, S., Refino, C. J., Clark, H., Eaton, D., & Grogan, J. L. (2009). The surface protein TIGIT suppresses T cell activation by promoting the generation of mature immunoregulatory dendritic cells. *Nature Immunology*, *10*(1), 48–57. <https://doi.org/10.1038/ni.1674>
- Zhang, Z., Wu, N., Lu, Y., Davidson, D., Colonna, M., & Veillette, A. (2015). DNAM-1 controls NK cell activation via an ITT-like motif. *Journal of Experimental Medicine*, *212*(12), 2165–2182. <https://doi.org/10.1084/jem.20150792>
- Zheng, W., & Flavell, R. A. (1995). The Transcription Factor GATA-3 Is Necessary and Sufficient for Th2 Cytokine Gene Expression in CD4 T cells. *Cell*, *89*, 587–596. [https://doi.org/10.1016/S0092-8674\(00\)80240-8](https://doi.org/10.1016/S0092-8674(00)80240-8)
- Zheng, X., Qian, Y., Fu, B., Jiao, D., Jiang, Y., Chen, P., Shen, Y., Zhang, H., Sun, R., Tian, Z., & Wei, H. (2019). Mitochondrial fragmentation limits NK cell-based tumor immunosurveillance. *Nature Immunology*, *20*(12), 1656–1667. <https://doi.org/10.1038/s41590-019-0511-1>
- Zhou, X., Tu, S., Wang, C., Huang, R., Deng, L., Song, C., Yue, C., He, Y., Yang, J., Liang, Z., Wu, A., Li, M., Zhou, W., Du, J., Guo, Z., Li, Y., Jiao, C., Liu, Y., Chang, L. J., & Li, Y. (2020). Phase I Trial of Fourth-Generation Anti-CD19 Chimeric Antigen Receptor T Cells Against Relapsed or Refractory B Cell Non-Hodgkin Lymphomas. *Frontiers in Immunology*, *11*. <https://doi.org/10.3389/fimmu.2020.564099>
- Zhou, Z., Van der Jeught, K., Fang, Y., Yu, T., Li, Y., Ao, Z., Liu, S., Zhang, L., Yang, Y., Eyvani, H., Cox, M. L., Wang, X., He, X., Ji, G., Schneider, B. P., Guo, F., Wan, J., Zhang, X., & Lu, X. (2021). An organoid-based screen for epigenetic inhibitors that stimulate antigen presentation and potentiate T-cell-mediated cytotoxicity. *Nature Biomedical Engineering*, *5*(11), 1320–1335. <https://doi.org/10.1038/s41551-021-00805-x>
- Zhu, H., Blum, R. H., Bjordahl, R., Gaidarova, S., Rogers, P., Lee, T. T., Abujarour, R., Bonello, G. B., Wu, J., Tsai, P.-F., Miller, J. S., Walcheck, B., Valamehr, B., & Kaufman, D. S. (2020). *Pluripotent stem cell-derived NK cells with high-affinity noncleavable CD16a mediate improved antitumor activity*. <https://doi.org/10.1182/blood.2019000621>
- Zhu, Y., Paniccia, A., Schulick, A. C., Chen, W., Koenig, M. R., Byers, J. T., Yao, S., Bevers, S., & Edil, B. H. (2016). Identification of CD112R as a novel checkpoint for human T cells. *Journal of Experimental Medicine*, *213*(2), 167–176. <https://doi.org/10.1084/jem.20150785>
- Zinkernagel, R. M., & Doherty, P. C. (1979). MHC-restricted cytotoxic T cells: studies on the biological role of polymorphic major transplantation antigens determining T-cell restriction-specificity, function, and responsiveness. *Advances in Immunology*, *27*, 51–177.



## 12 Abbreviations

---

7AAD	7-aminoactinomycin D
AMO	Adenosine monophosphate
APCs	Antigen-presenting cells
ATP	Adenosine triphosphate
BCR	B cell receptor
BM	Basement membrane
BSA	Bovine serum albumin
CD	Cluster of differentiation
CILP	Common ILC progenitor
CHILP	Common helper-like ILC progenitor
CLP	Common lymphoid progenitor
CLRs	C-type lectin receptors
CML	Cytokine-induced memory-like
CRISPR	Clustered Regularly Interspaced Short Palindromic Repeats
CRISPR/Cas9	CRISPR-associated protein 9
CXCR4	C-X-C chemokine receptor type 4
DAMPs	Damage-associated molecular patterns
DCs	Dendritic cells
DKO	Double knockout
DMEM	Dulbecco's modified Eagle Medium
DMSO	Dimethylsulphoxide
DNAM-1	DNAX accessory molecule-1
DR	Death receptor
Eomes	Eomesodermin
FACS	Fluorescence-activated cell sorting
FasL	Fas ligand
FIH	Factor inhibiting HIFs
FoxP3	Forkhead box P3
GATA3	GATA binding protein 3
GATA4	GATA binding protein 4
GM-CSF	Granulocyte-macrophage colony-stimulating factor
GzmB	Granzyme B
HIF-1 $\alpha$	Hypoxia inducible factor 1 alpha
HIF-1 $\beta$	Hypoxia inducible factor 1 beta
HIF-2 $\alpha$	Hypoxia inducible factor 2 alpha
HIF-3 $\alpha$	Hypoxia inducible factor 3 alpha
IFN $\gamma$	Interferon gamma
Ig	Immunoglobulin
IL	Interleukin
IL-18R	Interleukin-18 receptor
ILCs	Innate lymphoid cells
ILCP	Innate lymphoid cell progenitor
ITAM	Immunoreceptor tyrosine-based activation motif
ITIM	Immunoreceptor tyrosine-based inhibitory motif

KIRs	Killer Ig-like receptors
KO	Knockout
MHC	Major histocompatibility complex
NCR	Natural cytotoxicity receptor
NFAT	Nuclear factor of activated T-cells
NFκB	Nuclear factor kappa-light-chain-enhancer of activated B cells
NK cells	Natural killer cells
PDO	Patient derived organoid
scRNA seq	Single-cell RNA sequencing
STAT	Signal transducer and activator of transcription
Tbet	T-box expressed in T cells
TCR	T cell receptor
Th1 cells	Type 1 helper T cell
Th2 cells	Type 2 helper T cell
Th17 cells	Type 17 helper T cell
TIGIT	T cell immunoreceptor with immunoglobulin and ITIM domain
TLR	Toll-like receptors
TGF-β	Transforming growth factor-β
TNF	Tumor necrosis factor
TNFSF	Tumor necrosis factor super family
TRAIL	TNF-related apoptosis-inducing ligand
Treg	Regulatory T cells
VEGF	Vascular endothelial growth factor
VHL	Von Hippel Lindau protein
WT	Wild type

## 13 Acknowledgments

---

I would like to thank my supervisor Adelheid Cerwenka, who gave me the opportunity of joining to her group and conducting my PhD studies. Her mentorship was crucial to grow professionally and finish my PhD project with success (despite all my lab-language fight).

Special mention to the MATURE-NK consortium, to all the 13 labs involved that made the meetings and activities highly interesting and fruitful. In concrete, I thank Rebecca Kotzur for a great collaboration for writing a review combining our topics, being partners in crime in science and laughs (master of memes and gifs that apparently only us enjoyed). Natalia Colomar, also PhD fellow of the consortium who also helped me out in having a blast in our MATURE-NK meetings, special mention to sharing the room in the NK-meetings, where our tiredness was never a problem to enjoy our time. Jonathan Cruge, for welcoming me in my secondment at Miltenyi, where the whole department of NK cells and  $\gamma\delta$ T cells hosted me and made my stay the most comfortable. The managing team of the department, Nina Möker, and Congcong Zhang and Jose Alberto Villacorta, who made possible the collaboration between Mannheim-Miltenyi, and also guided me through my PhD. Of course, to the rest of PhD fellows, which I truly believe we made a great team, having always a good ambiance and without unhealthy competition but rather camaraderie.

From AG Cerwenka, the post-doc core of the lab, Ana Stojanovic, hypoxia-expert and senior scientist, who despite of not being my direct supervisor inspired me to perform my research and helped out with the process of generating a manuscript. I cannot forget about Indra Shatiël, who corrected the present thesis document, and despite the short overlap of our time in the group, really helped and guided me. I absolutely must mention Sina Schwam, the only administrative person I have ever met that always copes with the documents with a smile, comfort words and pushes for everyone's best interest. I enjoyed my time together with you, Sina, I won't forget about our emails and laughs.

But if I must thank someone, is my partner in crime in AG Cerwenka, Tomato Hofman, who was my PhD sibling and next to who I was struggling, celebrating and learning which beer is the good one (of course czcheck beer!). I was very lucky of having such a kind hearted and (crazy!) smart PhD friend, if I finished with any hair left on my head is because of your support and inspiration. Sophia Papaio(a)nnou, how would I not thank you, my favourite half german/greek person, sharing tea-breaks, puzzles and jokes has been a super important part of the PhD journey. Francesco Cortopassi, best Fortnite player and meme sharer, I really cherish our laughs and time together, what HIF-1 $\alpha$  brought together, it shall never be tore apart. Mingeum Jeong, the person who showed me how to endure and never give up, you inspired me to keep going and I will forever remember your laugh and your hugs. Jia Xiang, senior PhD since first year of PhD, I will carry with me the good memories of sharing beer and chess games. Andi, for joining the team of this scientific story to carry it until we have a nice manuscript, which I really appreciate, and for sharing your precious gym advices. Bianca and Helen, the girl german team, thank you for the organoid work and for having a nice

environment in the office, I promise I will try the good german bread and respect your culture. To Seba, who I bothered to ask all the questions related to plants and insects, I appreciate your calm and spirit to always help. To Erika, my dear Indonesian friend with high resistance to spicy and none to bier, I cherish the time we spent together, sleeping on my couch as a burrito and dancing, it is indeed part of my PhD.

Cómo olvidar a la potra mexicana, Silvina. No tengo palabras para agradecer tu amistad y tu apoyo, por compartir juntas salseos, cervezas y ser dos gymrats como dos titanas. Me llevo nuestros momentos para siempre, escucharme y ayudarme, este doctorado también es gracias a ti. A Gustavo y Adriana, qué os voy a decir, si habéis sufrido conmigo todo este proceso, creo que ya sabéis lo importantes que habéis sido (y sois), realmente mi familia en Alemania, aunque me gradúe, no os vais a librar tan fácilmente de mí. Por supuesto a Sara, con quien me llevo recuerdos de Paquita Salas y aunque empañados por la pandemia, tengo en mi memoria las risas y las excursiones en bici. A Diego, la única persona que tiene un ojo marrón y uno asulado, por todos los memontos compartidos entre cervezas, risas y algo de llanto.

A mi familia española, mi hermana María, mi otra mitad que me guía y me apoya en las duras y maduras. Gracias por venir a visitarme tantas veces, aunque eso me obligase a encender la calefacción. A mis padres, por educarme en la resiliencia y siempre apoyarme independientemente del camino elegido, sé que normalmente se espera que unos padres estén orgullosos de su hija (que espero que lo estéis), pero estoy especialmente orgullosa de vosotros, por tener la mente abierta, por permanecer fuertes y por haber superado múltiples enfermedades. Mamá, espero poder desarrollar terapias que ayuden a otras personas a superar el cáncer, eres una inspiración constante. Papá, aunque no sé si llegaré a ser profesora en la universidad, quiero que sepas que este doctorado en parte se debe a tu apoyo y por siempre creer en mí. A todas mis amigas, las que han venido y las que no, las de Montemolín, las del Pablo Serrano, las del Tomás Alvira, las de la universidad, no os puedo mencionar a todas porque sería más largo este apartado que los resultados, pero habéis sido una parte fundamental de sentirme acompañada, muchísimas gracias por venir hasta aquí a verme y a apoyarme.

Finalment, a la meva companya de l'ànima, Alejandra. Amor, ets tot el que està bé en aquest món, m'has acompanyat i acceptat malgrat traslladar-me fins a Alemanya, la millor companya que podia haver desitjat o imaginat. Ets la meva millor amiga, m'has ajudat a acabar el doctorat sempre empenyent-me cap endavant. Aquests quilòmetres de distància només ens han fet més fortes, no puc esperar a ser doctora i la teva dona. To the hell and back, always.